

# The Evolution of Star Formation Rates in High-Redshift Galaxies

by

Andrew H. Marquis

A Thesis Submitted to Saint Mary's University, Halifax, Nova Scotia in Partial Fulfillment of the Requirements for the Degree of

MASTER OF SCIENCE

in

Astronomy

(Department of Astronomy and Physics)

September 22, 2010, Halifax, Nova Scotia

© Andrew H. Marquis, 2010

Approved:

Dr. M. Sawicki  
Supervisor

Approved:

Dr. R.J. Thacker  
Examiner

Approved:

Dr. D.B. Guenther  
Examiner

Date: September 22, 2010



Library and Archives  
Canada

Published Heritage  
Branch

395 Wellington Street  
Ottawa ON K1A 0N4  
Canada

Bibliothèque et  
Archives Canada

Direction du  
Patrimoine de l'édition

395, rue Wellington  
Ottawa ON K1A 0N4  
Canada

*Your file Votre référence*  
*ISBN: 978-0-494-71810-0*  
*Our file Notre référence*  
*ISBN: 978-0-494-71810-0*

#### NOTICE:

The author has granted a non-exclusive license allowing Library and Archives Canada to reproduce, publish, archive, preserve, conserve, communicate to the public by telecommunication or on the Internet, loan, distribute and sell theses worldwide, for commercial or non-commercial purposes, in microform, paper, electronic and/or any other formats.

The author retains copyright ownership and moral rights in this thesis. Neither the thesis nor substantial extracts from it may be printed or otherwise reproduced without the author's permission.

In compliance with the Canadian Privacy Act some supporting forms may have been removed from this thesis.

While these forms may be included in the document page count, their removal does not represent any loss of content from the thesis.

#### AVIS:

L'auteur a accordé une licence non exclusive permettant à la Bibliothèque et Archives Canada de reproduire, publier, archiver, sauvegarder, conserver, transmettre au public par télécommunication ou par l'Internet, prêter, distribuer et vendre des thèses partout dans le monde, à des fins commerciales ou autres, sur support microforme, papier, électronique et/ou autres formats.

L'auteur conserve la propriété du droit d'auteur et des droits moraux qui protège cette thèse. Ni la thèse ni des extraits substantiels de celle-ci ne doivent être imprimés ou autrement reproduits sans son autorisation.

Conformément à la loi canadienne sur la protection de la vie privée, quelques formulaires secondaires ont été enlevés de cette thèse.

Bien que ces formulaires aient inclus dans la pagination, il n'y aura aucun contenu manquant.

■\*■  
**Canada**

# Contents

<b>Contents</b> . . . . .	ii
<b>List of Figures</b> . . . . .	v
<b>List of Tables</b> . . . . .	xii
<b>Acknowledgements</b> . . . . .	ii
<b>Abstract</b> . . . . .	1
<b>1 Introduction</b> . . . . .	2
1.1 Motivation . . . . .	2
1.2 Theory . . . . .	4
1.3 The Lyman Break Selection Technique . . . . .	6
<b>2 Data</b> . . . . .	8
2.1 $z \sim 3$ . . . . .	8
2.1.1 Observations . . . . .	8
2.1.2 Data Reduction . . . . .	10
2.1.3 Object Detection and Photometry . . . . .	10
2.1.4 Selection Criteria . . . . .	11
2.2 $z \sim 2$ . . . . .	14
2.2.1 The Observations . . . . .	14
2.2.2 Data Reduction, Object Detection, and Photometry . . . . .	16

---

2.2.3	Selection Criteria . . . . .	16
2.2.4	Initial Modeling . . . . .	17
2.3	Comparison Data Sets . . . . .	18
2.3.1	The Need for Comparison Data Sets . . . . .	18
2.3.2	$z \sim 5$ (Yabe et al. 2009) . . . . .	19
2.3.3	$z \sim 2$ (Shapley et al. 2005) . . . . .	19
<b>3</b>	<b>Model-fitting . . . . .</b>	<b>29</b>
3.1	SEDfit . . . . .	29
3.1.1	The Software . . . . .	29
3.1.2	The Parameters . . . . .	30
3.2	$z \sim 3$ . . . . .	31
3.2.1	Assuming Constant Star Formation . . . . .	31
3.2.2	Assuming Exponential Star Formation . . . . .	32
3.3	$z \sim 2$ . . . . .	36
3.3.1	Assuming Exponential Star Formation . . . . .	36
3.4	Age Considerations . . . . .	39
<b>4</b>	<b>Analysis . . . . .</b>	<b>41</b>
4.1	The Stellar Mass-Star Formation Rate Relation . . . . .	41
4.1.1	For Constant Star Formation . . . . .	41
4.1.2	For Exponential Star Formation . . . . .	45
4.2	Dust . . . . .	55
4.2.1	For Constant Star Formation . . . . .	55
4.2.2	For Exponential Star Formation . . . . .	59
<b>5</b>	<b>Summary and Conclusions . . . . .</b>	<b>61</b>

<b>Bibliography</b>	64
<b>A <math>z \sim 3</math> Best-fit SEDfit Parameters</b>	67
<b>B <math>z \sim 2</math> Best-fit SEDfit Parameters</b>	92

# List of Figures

1.1	Star formation rate density versus redshift. The SFR density of the universe is seen to peak at approximately $z \sim 2$ . The data points are compiled from a number of surveys and scaled to the SalA IMF for illustrative purposes. The solid black lines are best-fit parameterizations of the data. For details, see Hopkins & Beacom (2006).	3
2.1	Filter transmission curves for WFPC2 ( $U_{300}$ , $B_{450}$ , $V_{606}$ , $I_{814}$ ) aboard <i>HST</i> and ISAAC ( $J_s$ , $H$ , $K_s$ ) at the VLT. We use observations through these filters to select and model-fit a population of $z \sim 3$ galaxies from the HDF-S. A $z \sim 3$ model spectrum is overlaid in red.	9
2.2	Histogram of synthetic $\mathcal{R}_{VI}$ magnitudes in the HDF-S. The vertical dotted line corresponds to $\mathcal{R}_{VI} = 26.6$ , the first peak in the distribution and the faint-end limit of our galaxy sample.	13
2.3	Color-color plot displaying objects detected in the HDF-S and their relationship to the $z \sim 3$ selection criteria of Steidel et al. (1996). Objects detected at all wavelengths are shown as asterisks, while objects undetected in $U_{300}$ but detected in all other bands are represented by upward pointing triangles. We select all asterisks and triangles above and to the left of the solid red line, resulting in 242 total $z \sim 3$ galaxy candidates.	14
2.4	Filter transmission curves for WFPC2 ( $U_{300}$ , $B_{450}$ , $V_{606}$ , $I_{814}$ ) and NICMOS ( $J_{110}$ , $H_{160}$ ) aboard <i>HST</i> . Observations through these filters are used to select and model-fit a population of $z \sim 2$ galaxies from the HDF. A $z \sim 2$ model spectrum is overlaid in red.	15



---

3.3 Number counts for best-fit ages output by SEDfit for $z_{phot} \sim 2$ galaxies in the HDF assuming constant, exponentially increasing ( $\tau = 700$ Myr), and exponentially decreasing ( $\tau = -700$ Myr) star formation. The median best-fit age is given in each plot. The 3.22 Gyr age of the universe at $z \sim 2$ is represented by $t_0$ . . . . .	37
3.4 Example plots of best-fit model spectra determined by SEDfit assuming 3 different star formation histories. Left to right, the columns assume a constant SFR, an exponentially increasing ( $\tau = 700$ Myr) SFR, and an exponentially decreasing ( $\tau = -700$ Myr) SFR. The spectra are overlaid with the corresponding real-world photometry of $z \sim 2$ galaxies from the HDF. Solid red circles indicate a detection, while open circles represent upper limits. The horizontal wavelength uncertainties are indicative of the FWHM of that filter's transmission curve. Uncertainties of the magnitudes themselves are mostly on the order of 0.01 or smaller. Best-fit parameters for each LBG are listed in the panels. Photometry courtesy Sawicki. . . . .	38
4.1 Stellar masses versus constant star formation rates. The three leftmost vertical panels display the complete data set(s) at each redshift. Uncertainties are plotted in light grey for all objects $\sim 30$ Myr $\leq$ age $\leq t_0$ . The top right panel shows these intermediate aged objects and their corresponding lines of best-fit. The best-fit slope is calculated from the combined $z \sim 2$ data sets of Sawicki et al. (2007) and Shapley et al. (2005). That slope is then assumed for the $z \sim 3$ and $z \sim 5$ populations. The bottom right panel displays the residual offsets for all data relative to the $z \sim 2$ line of best-fit. We use these offsets to calculate the $\delta$ -term for each redshift in Equation 4.1. . . . .	43

- 
- 4.2 Stellar masses versus constant star formation rates. The black line is the evolutionary track of a toy galaxy evolved from  $z \sim 5$  to  $z \sim 2$ . The open circles mark the location of the toy without accounting for mass loss, while the diamonds correct for mass loss. The  $z \sim 5$ ,  $\sim 3$ , and  $\sim 2$  best-fit lines are displayed in green, blue, and red, respectively. The light green, light blue, and pink lines enclose each redshift group's region of acceptable agreement (see Eqs. 4.4 and 4.5). At  $z \sim 3$ , the toy galaxy is  $4.02 \times 10^8 M_{\odot}$ , or  $\sim 70\%$ , more massive than the upper limit acceptable mass. At  $z \sim 2$ , the toy is  $1.14 \times 10^9 M_{\odot}$ , or  $\sim 120\%$ , more massive than the acceptable upper limit. . . . .
- 44
- 4.3 Stellar masses versus exponentially increasing star formation rates ( $\tau = 700$  Myr). The two leftmost vertical panels display the complete data set at each redshift. Uncertainties are plotted in light grey for all objects  $\sim 30$  Myr  $\leq$  age  $\leq t_0$ . The top right panel shows these intermediate aged objects and their corresponding lines of best-fit. The best-fit slope is calculated from the Sawicki et al. (2007)  $z \sim 2$  data set. That slope is then assumed for the  $z \sim 3$  population. The bottom right panel displays the residual offsets for all data relative to the  $z \sim 2$  line of best-fit. We use these offsets to calculate the  $\delta$ -term for each redshift in Equation 4.7. . . . .
- 47
- 4.4 Stellar masses versus exponentially increasing star formation rates ( $\tau = 700$  Myr). The black line is the evolutionary track of a toy galaxy evolved from  $z \sim 5$  to  $z \sim 2$ . The open circles mark the evolution of toy with no correction for mass loss. The diamonds mark its evolution as adjusted for mass loss. The  $z \sim 2$  and  $\sim 3$  best-fit lines are shown in red and blue, respectively. The pink and light blue lines outline each redshift group's region of acceptable agreement. At  $z \sim 3$ , the toy galaxy is  $\sim 58\%$  more massive than the spread in observational data allows. By  $z \sim 2$ , the toy has evolved into a  $1.45 \times 10^{10} M_{\odot}$  object forming stars at  $21.88 M_{\odot} \text{ yr}^{-1}$ . These values lie within the  $z \sim 2$  region of acceptable agreement. . . . .
- 48

---

4.5 Stellar masses versus exponentially increasing star formation rates ( $\tau = 500$ Myr). The two leftmost vertical panels display the complete data set at each redshift. Uncertainties are not calculated for these model-fits but are assumed to be similar to the 700 Myr e-folding model. The top right panel shows these intermediate aged objects and their corresponding lines of best-fit. The best-fit slope is calculated from the Sawicki et al. (2007) $z \sim 2$ data set. That slope is then assumed for the $z \sim 3$ population. The bottom right panel displays the residual offsets for all data relative to the $z \sim 2$ line of best-fit. We use these offsets to calculate the $\delta$ -term for each redshift in Equation 4.10 . . . . .	50
4.6 Stellar mass versus exponentially increasing star formation rates ( $\tau = 500$ Myr). The black line is the evolutionary track of a toy galaxy evolved from $z \sim 5$ to $z \sim 2$ . The open circles mark the evolution of toy with no correction for mass loss. The diamonds mark its evolution as adjusted for mass loss. The $z \sim 2$ and $\sim 3$ best-fit lines are shown in red and blue, respectively. The pink and light blue lines outline each redshift group's region of acceptable agreement. At $z \sim 3$ , the mass of the toy overshoots the upper limit acceptable mass $\sim 15\%$ . Correcting for mass loss does not bring the toy galaxy into agreement with the data. At $z \sim 2$ , the toy's evolution is consistent with the data spread, and no correction for mass loss is necessary. . . . .	51
4.7 Stellar masses versus star formation rates, assuming exponential star formation ( $\tau = -700$ Myr). The two leftmost vertical panels display the complete data set at each redshift. Uncertainties are plotted in light grey for all objects $\sim 30$ Myr $\leq$ age $\leq t_0$ . The top right panel shows these intermediate aged objects and their corresponding lines of best-fit. The best-fit slope is calculated from Sawicki's $z \sim 2$ data set. That slope is then assumed for the $z \sim 3$ population. The bottom right panel displays the residual offsets for both data sets relative to the $z \sim 2$ line of best-fit. We use these offsets to calculate the $\delta$ -term for each redshift in Equation 4.13. . . . .	53

---

4.8 Stellar masses versus exponentially decreasing star formation rates ( $\tau = -700$ Myr). The black line is the evolutionary track of a toy galaxy evolved from $z \sim 5$ to $z \sim 2$ . The best-fit lines for the $z \sim 2$ and $\sim 3$ populations are displayed in red and blue, respectively. The pink and light blue lines enclose the region of acceptable agreement at each redshift. At $z \sim 3$ , the stellar mass of the toy galaxy is $\sim 250\%$ too large for its SFR. The agreement worsens at $z \sim 2$ where its stellar mass ( $5.89 \times 10^8 M_\odot$ ) is $\sim 1000\%$ larger than the acceptable upper limit. . . . .	54
4.9 Color excess versus rest-frame UV magnitude for galaxies model-fit with constant star formation. The left panel shows all data regardless of magnitude or age. The right panel is limited to magnitudes where the samples at each redshift have significant overlap and presents only data for objects with ages greater than $\sim 30$ Myr but less than the age of the universe. The red and dotted blue lines show median $E(B - V)$ values for magnitude bins -19 to -20 and -20 to -21. Across the fainter bin, we find $E(B - V)_{med.} = 0.12$ for both $z \sim 2$ and $z \sim 3$ . Across the brighter bin, we find $E(B - V)_{med.} = 0.16$ for $z \sim 2$ and $E(B - V)_{med.} = 0.18$ for $z \sim 3$ . Shapley et al. (2005) provide no uncertainties for their data here. . . . .	56
4.10 Stellar mass versus rest-frame UV magnitude for galaxies model-fit with constant star formation. The left panel shows all data regardless of age. The right panel presents the $z \sim 2$ to $z \sim 3$ population offset for those objects with ages greater than $\sim 30$ Myr but less than the age of the universe. . . . .	57

---

4.11 Color excess versus rest-frame UV magnitude for galaxies model-fit with exponential star formation ( $\tau = 700$ Myr). The left panel shows all data regardless of magnitude or age. The right panel is limited to magnitudes where the samples at each redshift display overlap and presents only data for objects with ages greater than $\sim 30$ Myr but less than the age of the universe. The red and dotted blue lines show median color excesses for the data binned according to UV magnitude. Across the fainter bin, we find median color excesses of 0.19 and 0.14 for $z \sim 2$ and $z \sim 3$ galaxies, respectively. Across the brighter bin, objects at $z \sim 3$ are found to have a median color excess of 0.18.	58
4.12 Stellar mass versus rest-frame UV magnitude for galaxies model-fit with exponential star formation ( $\tau = 700$ Myr). The left panel shows all data regardless of age. The right panel presents the $z \sim 2$ to $z \sim 3$ population offset for those objects with ages greater than $\sim 30$ Myr but less than the age of the universe.	60

# List of Tables

2.1	HDF-S Photometric Catalog. An uncertainty of 99.00 means the reported magnitude is a $3\sigma$ upper limit. . . . .	21
2.1	HDF-S Photometric Catalog. An uncertainty of 99.00 means the reported magnitude is a $3\sigma$ upper limit. . . . .	22
2.1	HDF-S Photometric Catalog. An uncertainty of 99.00 means the reported magnitude is a $3\sigma$ upper limit. . . . .	23
2.1	HDF-S Photometric Catalog. An uncertainty of 99.00 means the reported magnitude is a $3\sigma$ upper limit. . . . .	24
2.1	HDF-S Photometric Catalog. An uncertainty of 99.00 means the reported magnitude is a $3\sigma$ upper limit. . . . .	25
2.1	HDF-S Photometric Catalog. An uncertainty of 99.00 means the reported magnitude is a $3\sigma$ upper limit. . . . .	26
2.2	HDF catalog of Sawicki et al. (2007). An uncertainty of 99.00 means the magnitude value is a $3\sigma$ upper limit. . . . .	27
2.2	HDF catalog of Sawicki et al. (2007). An uncertainty of 99.00 means the magnitude value is a $3\sigma$ upper limit. . . . .	28
4.1	Median color excess and $V$ -band extinction values for galaxies model-fit assuming constant star formation and binned according to rest-frame UV magnitude. . . . .	57

---

4.2 Median color excess and $V$ -band extinction values for galaxies model-fit assuming exponential star formation ( $\tau = 700$ Myr) and binned according to rest-frame UV magnitude. . . . .	59
A.1 Best-fit parameters for this work's HDF-S catalog, constant SFR. . . . .	67
A.1 Best-fit parameters for this work's HDF-S catalog, constant SFR. . . . .	68
A.1 Best-fit parameters for this work's HDF-S catalog, constant SFR. . . . .	69
A.1 Best-fit parameters for this work's HDF-S catalog, constant SFR. . . . .	70
A.1 Best-fit parameters for this work's HDF-S catalog, constant SFR. . . . .	71
A.2 Best-fit parameters for this work's HDF-S catalog, 700 Myr e-folding exponential SFR. .	72
A.2 Best-fit parameters for this work's HDF-S catalog, 700 Myr e-folding exponential SFR. .	73
A.2 Best-fit parameters for this work's HDF-S catalog, 700 Myr e-folding exponential SFR. .	74
A.2 Best-fit parameters for this work's HDF-S catalog, 700 Myr e-folding exponential SFR. .	75
A.3 Best-fit parameters for this work's HDF-S catalog, 500 Myr e-folding exponential SFR. .	76
A.3 Best-fit parameters for this work's HDF-S catalog, 500 Myr e-folding exponential SFR. .	77
A.3 Best-fit parameters for this work's HDF-S catalog, 500 Myr e-folding exponential SFR. .	78
A.3 Best-fit parameters for this work's HDF-S catalog, 500 Myr e-folding exponential SFR. .	79
A.4 Best-fit parameters for this work's HDF-S catalog, 350 Myr e-folding exponential SFR. .	80
A.4 Best-fit parameters for this work's HDF-S catalog, 350 Myr e-folding exponential SFR. .	81
A.4 Best-fit parameters for this work's HDF-S catalog, 350 Myr e-folding exponential SFR. .	82
A.4 Best-fit parameters for this work's HDF-S catalog, 350 Myr e-folding exponential SFR. .	83
A.5 Best-fit parameters for this work's HDF-S catalog, 250 Myr e-folding exponential SFR. .	84
A.5 Best-fit parameters for this work's HDF-S catalog, 250 Myr e-folding exponential SFR. .	85
A.5 Best-fit parameters for this work's HDF-S catalog, 250 Myr e-folding exponential SFR. .	86
A.5 Best-fit parameters for this work's HDF-S catalog, 250 Myr e-folding exponential SFR. .	87

---

A.6 Best-fit parameters for this work's HDF-S catalog, $-700$ Myr e-folding exponential SFR . . . . .	88
A.6 Best-fit parameters for this work's HDF-S catalog, $-700$ Myr e-folding exponential SFR . . . . .	89
A.6 Best-fit parameters for this work's HDF-S catalog, $-700$ Myr e-folding exponential SFR . . . . .	90
A.6 Best-fit parameters for this work's HDF-S catalog, $-700$ Myr e-folding exponential SFR . . . . .	91
B.1 Best-fit parameters for Sawicki et al. (2007) HDF catalog, $700$ Myr e-folding exponential SFR . . . . .	92
B.1 Best-fit parameters for Sawicki et al. (2007) HDF catalog, $700$ Myr e-folding exponential SFR . . . . .	93
B.1 Best-fit parameters for Sawicki et al. (2007) HDF catalog, $700$ Myr e-folding exponential SFR . . . . .	94
B.1 Best-fit parameters for Sawicki et al. (2007) HDF catalog, $700$ Myr e-folding exponential SFR . . . . .	95
B.2 Best-fit parameters for Sawicki et al. (2007) HDF catalog, $500$ Myr e-folding exponential SFR . . . . .	96
B.2 Best-fit parameters for Sawicki et al. (2007) HDF catalog, $500$ Myr e-folding exponential SFR . . . . .	97
B.2 Best-fit parameters for Sawicki et al. (2007) HDF catalog, $500$ Myr e-folding exponential SFR . . . . .	98
B.3 Best-fit parameters for Sawicki et al. (2007) HDF catalog, $350$ Myr e-folding exponential SFR . . . . .	99

---

B.3 Best-fit parameters for Sawicki et al. (2007) HDF catalog, 350 Myr e-folding exponential SFR. . . . .	100
B.3 Best-fit parameters for Sawicki et al. (2007) HDF catalog, 350 Myr e-folding exponential SFR. . . . .	101
B.4 Best-fit parameters for Sawicki et al. (2007) HDF catalog, 250 Myr e-folding exponential SFR. . . . .	102
B.4 Best-fit parameters for Sawicki et al. (2007) HDF catalog, 250 Myr e-folding exponential SFR. . . . .	103
B.4 Best-fit parameters for Sawicki et al. (2007) HDF catalog, 250 Myr e-folding exponential SFR. . . . .	104
B.5 Best-fit parameters for Sawicki et al. (2007) HDF catalog, -700 Myr e-folding exponential SFR. . . . .	105
B.5 Best-fit parameters for Sawicki et al. (2007) HDF catalog, -700 Myr e-folding exponential SFR. . . . .	106
B.5 Best-fit parameters for Sawicki et al. (2007) HDF catalog, -700 Myr e-folding exponential SFR. . . . .	107

# Acknowledgements

First, thank you to Dr. Marcin Sawicki for the opportunity, knowledge, and patience. Thank you, as well, to Drs. Rob Thacker and David Guenther for their committee participation.

To Kathleen, Jon, James, Dave, Chris, Liz, Larkin, Pascal, and all four Michaels, whose friendship and experience I relied upon. To Larry, Amy, Laena, Shannon, and Kylene, who made Halifax both livable and lovable.

To my parents, Randy and Wendy, and my sister, Valerie, for everything.

# Abstract

## The Evolution of Star Formation Rates in High-Redshift Galaxies

by Andrew H. Marquis

We use photometric galaxy samples and spectral synthesis models to investigate the ability of three dramatically divergent star formation histories (SFHs) to describe the build-up of stellar mass in galaxy populations between  $z \sim 5$  and  $z \sim 2$ . The SFHs in question assume constant, exponentially increasing, and exponentially decreasing star formation rates (SFRs). For each considered SFH, we use a broadband spectral energy distribution model-fitting technique to parameterize the galaxy samples according to photometric redshift, color excess, age, stellar mass, and SFR. Starting at  $z \sim 5$ , we then evolve the stellar mass and SFR of a toy galaxy across the epochs in question and quantify its agreement with the model-fit observations at  $z \sim 3$  and  $z \sim 2$ . This is done for each assumed SFH. We find the exponentially increasing SFH with a 500 Myr e-folding agrees best with the model-fit observations, while the exponentially decreasing SFH shows the worst agreement. We further analyze the model-fit data for trends in color excess versus rest-frame UV magnitude and identify that, for  $z \sim 3$  galaxies fit for constant star formation, UV-brighter objects are more highly obscured by dust than the UV-faint. This dependence is not identified in the other data sets.

September 22, 2010

# Chapter 1

## Introduction

### 1.1 Motivation

During the epoch immediately following the Big Bang, the universe was hot, dense, and relatively featureless. Some 13.5 billion years later, we observe structure across an immense range of scales. The evolution of structure in the universe is intimately linked to the evolution of galaxies across cosmological timescales and, more specifically, how structure evolves within galaxies. Structural evolution within a galaxy is governed by its gravitational potential. This determines the star formation history (SFH), or how stellar mass builds up. A galaxy’s SFH describes how its star formation rate (SFR) changes with time.

The star formation rate density (SFR per unit volume) in the universe peaks at approximately redshift 2 (Hopkins & Beacom 2006; see Fig. 1.1). (When noting redshift, we will often use the standard redshift abbreviation  $z$ .) Therefore, an understanding of how galaxies built up their stellar masses in the epochs preceding  $z \sim 2$  is crucial to our picture high-redshift galaxy evolution. As yet, a clear, qualitative picture of the SFHs of high-redshift galaxies has not been established. Via the technique of model-fitting galaxies’ broadband spectral energy distributions (SEDs; see Chapter 3), this work seeks to identify an SFH that both realistically model-fits observational data at  $z \sim 5$ ,  $\sim 3$ , and  $\sim 2$  and evolves a galaxy across those epochs in a manner consistent with the model-fit observations.

Previous studies that model-fit galaxies according to their broadband SED properties adopted exponentially decreasing SFHs, which assume galaxies exist in closed boxes. Any given galaxy has a certain amount of gas to transform into stars. As stars are created, the gas reservoir depletes,

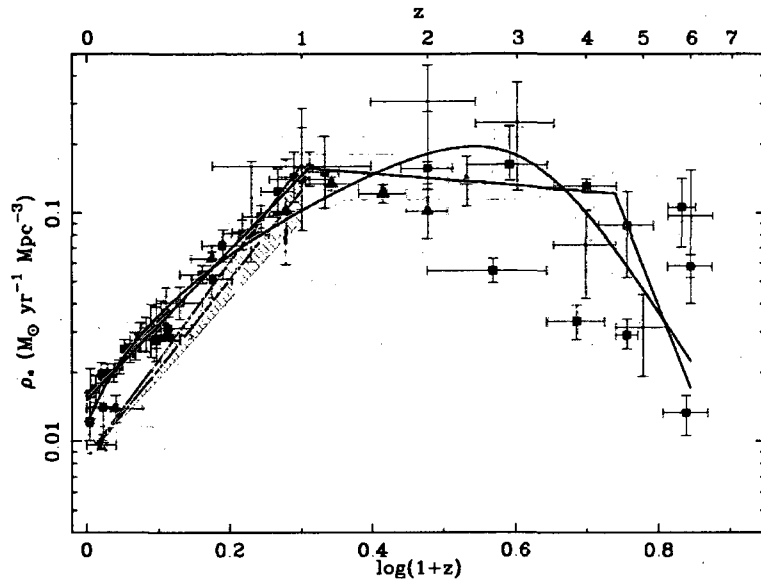


Figure 1.1: Star formation rate density versus redshift. The SFR density of the universe is seen to peak at approximately  $z \sim 2$ . The data points are compiled from a number of surveys and scaled to the SalA IMF for illustrative purposes. The solid black lines are best-fit parameterizations of the data. For details, see Hopkins & Beacom (2006).

and the SFR decreases. These model SFHs come in three varieties. First, the explicitly decreasing exponential SFH takes the form  $\text{SFR}(t) \propto \exp(-t/\tau)$ . The second and third varieties are the limiting cases of the explicit exponential: the single stellar population (SSP) model and the constant star formation (CSF) model. The SSP model assumes an instantaneous starburst, and no star formation occurs at later epochs, which mimics a sharply declining exponential. The CSF model assumes that a galaxy begins forming stars at some rate and continues to do so for the duration of the starburst episode, which mimics a slowly declining exponential.

Sawicki & Yee (1998) utilize SSP and CSF models to study the extinctions, star formation rates, ages, and masses of  $z > 2$  galaxies in the Hubble Deep Field. Shapley et al. (2001) use the CSF model in their investigation of the  $z \sim 3$  rest-frame luminosity function, while Shapley et al. (2004; 2005) employ both the CSF model and the explicit exponential in their studies of stellar masses at  $z \sim 2$ . Stellar masses are also analyzed by Papovich et al. (2001), who use the SSP and explicit exponential SFHs to model galaxies at redshifts  $2.0 \lesssim z \lesssim 3.5$  in the Hubble Deep Field North.

Yabe et al. (2009) explore many of these parameters for objects at  $z \sim 5$ . It is key to note that these groups' investigations treated galaxies at specific redshifts in isolation from the rest of cosmological time, with no focused effort on determining how a galaxy at, say,  $z \sim 5$  evolves to become a galaxy at  $z \sim 2$ . In Chapter 4, we show that the explicitly decreasing exponential and CSF models fail to plausibly describe this evolution.

Contrary to the assumptions these models make, we know galaxies do not exist in complete isolation but in environments with which they interact. Furthermore, the star formation activity within a galaxy must not solely draw from some initial reservoir of baryonic gas because galaxies routinely acquire more via the smooth accretion and merger mechanisms (Mihos & Hernquist 1996).

Recent interpretations of observational data suggest the SFHs of high-redshift galaxies are best described by SFRs that increase with passing time. For instance, if it were true that high-redshift galaxies had either constant or decreasing SFRs, then it would follow that their progenitors would be characterized by higher specific SFRs (SFR per unit stellar mass). This proposition is contradicted by Stark et al. (2009), who observe no evolution in the specific SFRs of UV-selected galaxies at redshifts  $4 \lesssim z \lesssim 6$ . Additionally, Finkelstein et al. (2010) determine that, as cosmological time progresses from  $z \sim 8$  to  $z \sim 3$ , the characteristic luminosity of the UV luminosity function,  $L_{UV}^*$  (Schechter 1976), increases, as do the stellar masses of galaxies at  $L_{UV}^*$ . The simplest explanation for this trend is that these galaxies' SFRs increase with time.

## 1.2 Theory

To make sense of these new interpretations, we turn to a theory of stellar mass build-up provided by Kouji Ohta (private communication, 2009). Ohta begins with the assumption that a galaxy's SFR is proportional to the rate at which it accretes gas.

$$\text{SFR}(t) = \frac{dM_*}{dt} = c_1 \frac{dM_{gas}}{dt} \quad (1.1)$$

For this derivation, all constants of proportionality are called  $c_i$  and indexed with numbers  $i$  to distinguish them from one another. Next, he supposes that a galaxy accretes both gas and dark matter at a rate proportional to the mass of its dark matter halo.

$$\frac{dM_{gas}}{dt} = c_2 M_{DH} \quad (1.2)$$

$$\frac{dM_{DH}}{dt} = c_3 M_{DH} \quad (1.3)$$

Equation 1.3 is then rearranged to isolate the dark matter terms on the left hand side.

$$\frac{dM_{DH}}{M_{DH}} = c_3 dt \quad (1.4)$$

Integrating this differential and applying an exponential to both sides yields

$$M_{DH}(t) = M_0 e^{c_3 t}, \quad (1.5)$$

where  $M_0$  is the initial mass of the dark matter halo. The mass evolution of the dark matter halo (Eq. 1.5) is related back to the star formation rate via equation 1.2. These substitutions reveal a time-dependent exponentially increasing SFR of the form

$$SFR(t) = c_1 c_2 e^{c_3 t}, \quad (1.6)$$

which we rewrite as

$$SFR(t) = SFR_0 e^{t/\tau}, \quad (1.7)$$

where  $SFR_0$  is the star formation rate at  $t = 0$  and  $\tau$  is the e-folding time measured in years. We will henceforth refer to this exponentially increasing SFR as the positive  $\tau$  model and the exponentially decreasing SFR as the negative  $\tau$  model. Using these model SFRs, we fit observational data at  $z \sim 3$

and  $\sim 2$ . For the positive  $\tau$  model, we use 700, 500, 350, and 250 Myr e-foldings (see section 3.2.2). For the negative  $\tau$  model, we use a 700 Myr e-folding. We also model-fit the  $z \sim 3$  data according to the CSF model to compare along side the model-fit catalogs of Sawicki (in preparation;  $z \sim 2$ ), Shapley et al. (2005;  $z \sim 2$ ), and Yabe et al. (2009;  $z \sim 5$ ).

### 1.3 The Lyman Break Selection Technique

All galaxy catalogs employed in this work are selected using the Lyman break technique, which culls galaxies based on their rest-frame ultraviolet (UV) colors. The Lyman break is a spectral discontinuity that occurs at rest-frame 912 Å and originates from the ionization of hydrogen in the atmospheres of massive stars. The discontinuity is enhanced by the photoelectric absorption of both interstellar and intergalactic HI gas (Steidel et al. 1995, 1999; Madau 1995).

For distant galaxies, the Lyman break spectral feature redshifts along with the rest of the light according to

$$1 + z = \frac{\lambda_{obs.}}{\lambda_{r.f.}}, \quad (1.8)$$

where  $z$  is the redshift,  $\lambda_{obs.}$  is the observed wavelength, and  $\lambda_{r.f.}$  is the rest-frame wavelength. To then select galaxies at a specific redshift, we need only measure the flux ratios of filters on either side of the break. This task requires that the initial observations be taken with a filter set appropriate to the redshift of interest. However, if this condition is met, objects may be selected by a suitably chosen color-color criteria (see sections 2.1.4 and 2.2.3). Galaxies selected via this technique are often referred to as Lyman Break Galaxies (LBGs).

We note here that, by selecting galaxies according to their rest-frame UV properties alone, the Lyman break technique culls only actively star-forming galaxies. While ignoring quiescent objects may be a potentially damaging bias, every data set we utilize is biased in an identical way. We therefore assert our data are representative of high-redshift starbursting galaxies, if not the entire high-redshift population.

This thesis is organized as follows. In Chapter 2, we discuss the origins and qualities of the data we use. We describe the SED model-fitting process and its results in Chapter 3. (Appendix 1 and Appendix 2 contain tables listing the best-fit parameters for  $z \sim 3$  and  $\sim 2$ , respectively.) In Chapter 4, we analyze the stellar mass-SFR relations of the model-fit observational data and briefly discuss the dust qualities of the CSF and 700 Myr e-folding model-fits. We present our conclusions in Chapter 5.

Throughout this work, we make casual use of Ned Wright's Cosmological Calculator (Wright 2006). We adopt the cosmology  $(\Omega_M, \Omega_\Lambda, H_0) = (0.3, 0.7, 70 \text{ km s}^{-1} \text{ Mpc}^{-1})$ . For this cosmology, the ages of the universe at redshifts 5, 3, and 2 are 1.15, 2.11, and 3.22 Gyr, respectively. We use the PerlDL software language (Glazebrook & Economou 1997) to analyze and plot all data. We report magnitudes in the Absolute Magnitude (AB) system.

# Chapter 2

# Data

## 2.1 $z \sim 3$

While past studies concerned themselves with galaxy populations at a single epoch, our interest lies in connecting these epochs together to form a single picture of high-redshift galaxy evolution. Previous works by Shapley et al. (2005), Sawicki et al. (2007), and Yabe et al. (2009) provide us with either suitable photometric or model-fit catalogs at  $z \sim 2$  and  $z \sim 5$ . However, with no appropriate catalog to bridge these two epochs, we must consequently generate our own  $z \sim 3$  data set.

### 2.1.1 Observations

To create a sample of  $z \sim 3$  galaxies, this work uses publicly available image mosaics of the Hubble Deep Field South (HDF-S), a field whose existence is predicated upon its ability to constrain cosmological and galaxy evolution models. Ultra-deep optical ( $U_{300}$ ,  $B_{450}$ ,  $V_{606}$ ,  $I_{814}$ ) data are provided by the Wide Field and Planetary Camera 2 (WFPC2) on the *Hubble Space Telescope* (*HST*). The WFPC2/*HST* data covers an area of  $\sim 5.05$  arcmin $^2$  centered at  $\alpha = 22^h 32^m 56^s.22$ ,  $\delta = -60^\circ 33' 02''.69$  (J2000.0). These data probe down to magnitudes of 26.8 in  $U_{300}$ , 27.7 in  $B_{450}$ , 28.3 in  $V_{606}$ , and 27.7 in  $I_{814}$  (10 $\sigma$  limit for an object 0.2 arcsec $^2$  in area). The point-spread functions (PSFs) of these bands are best-fit by Gaussians with full-width half-maximums (FWHMs) of 0''.163, 0''.139, 0''.126, and 0''.143, respectively (Casertano et al. 2000).

The WFPC2/*HST* data are supplemented by the wide-field NIR  $J_s$ -,  $H$ -, and  $K_s$ -band data of the Faint Infrared Extragalactic Survey (FIRE; Franx et al. 2000) conducted with the Infrared Spectrometer and Array Camera (ISAAC) on the Very Large Telescope (VLT). The FIRE images

capture a  $\sim 6.25$  arcmin $^2$  field of view approximately centered upon the HDF-S main field imaged by WFPC2. Limiting magnitudes ( $3\sigma$  for point sources) are 25.9 in  $J_s$ , 24.8 in  $H$ , and 24.4 in  $K_s$  (Labbé et al. 2002). The median Gaussian PSFs of these bands have FWHMs of 0''.45, 0''.48, and 0''.46, respectively (Labbé et al. 2003). That these ISAAC PSFs stand in stark contrast to the significantly narrower PSFs of the WFPC2 can be attributed to the VLT's station as an earth-bound observatory, whereas *HST*'s loftier position in low Earth orbit places it above the influence of atmospheric turbulence.

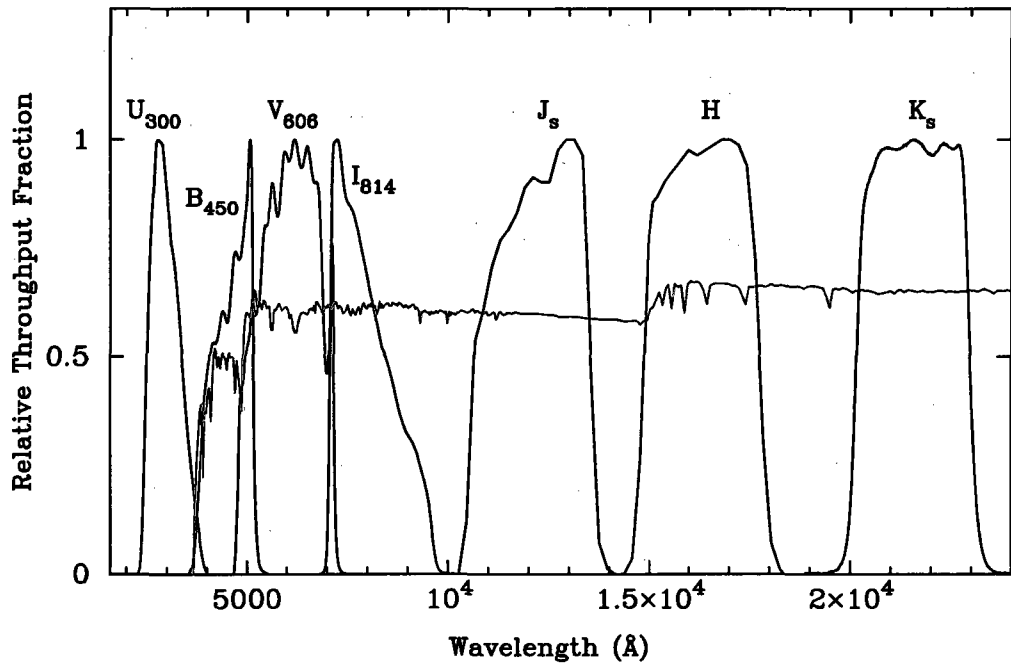


Figure 2.1: Filter transmission curves for WFPC2 ( $U_{300}$ ,  $B_{450}$ ,  $V_{606}$ ,  $I_{814}$ ) aboard *HST* and ISAAC ( $J_s$ ,  $H$ ,  $K_s$ ) at the VLT. We use observations through these filters to select and model-fit a population of  $z \sim 3$  galaxies from the HDF-S. A  $z \sim 3$  model spectrum is overlaid in red.

Crucially, both spectroscopic features essential to selecting and model-fitting  $z \sim 3$  galaxies are contained within these seven passbands. The Lyman break, observed in the rest-frame at 912 Å, appears in  $z \sim 3$  galaxies at 3600 Å. This placement identifies the relevant  $z \sim 3$  population as  $U_{300}$  dropouts. Meanwhile, the 4000 Å break, a metallicity indicator required to estimate a galaxy's age, shifts to  $1.6 \times 10^4$  Å, which locates it near the central wavelength of the ISAAC/VLT  $H$ -filter.

Figure 2.1 shows transmission curves for all seven passbands as well as an overlaid  $z \sim 3$  model spectrum.

### 2.1.2 Data Reduction

We employ the image convolutions of Labb   et al. (2003) to procure photometry in all seven bands. The ISAAC/VLT NIR PSFs are found to be symmetric and invariable across the field. The  $J_s$  and  $K_s$  images are convolved with the  $H$ -band kernel, in accordance with its standing as the lowest quality image ( $\text{FWHM} \simeq 0''.48$ ). Because of the consistency of the NIR PSF, an excellent match is achieved with simple Gaussian smoothing. However, the WFPC2 PSF structure demands a more complicated kernel, which Labb   et al. (2003) construct by way of a deconvolution process. The resultant kernel is then applied to the  $U_{300}$ ,  $B_{450}$ ,  $V_{606}$ , and  $I_{814}$  images.

To check the fit of their convolutions, Labb   et al. (2003) divide the stellar growth curves of the six convolved images by the unsmoothed  $H$ -band growth curve. This analysis reveals, for radii  $r \leq 0''.35$ , the images' fractional enclosed fluxes agree to within 3%. Such a result ensures comparable aperture photometry among the different passbands.

### 2.1.3 Object Detection and Photometry

We employ SExtractor version 2.3.2 in dual-image mode to perform object detection and photometry (Bertin & Arnouts 1996). In this mode, SExtractor detects an object in one image, called the detection image, and then performs photometry at the same location in a second image, called the measure image.

Being the deepest among the seven bands, the unsmoothed  $V_{606}$  image acts as the detection image. This work considers a detection to be a collection of 5 or more pixels brighter than the  $1.5\sigma$  sky background. The application of these criteria to the unsmoothed  $V_{606}$  image produces an initial yield of 3919 detected objects. Then, administering an aperture 50 pixels ( $\sim 2''.0$ ) in diameter, we obtain photometry at corresponding coordinates in the measure images: the convolved  $U_{300}$ ,  $B_{450}$ ,

$V_{606}$ ,  $I_{814}$ ,  $J_s$ , and  $K_s$  images, as well as the unsmoothed  $H$ -band.

SExtractor is designed to measure fluxes, flux uncertainties, magnitudes, and magnitude uncertainties where it is possible, but it does not detect every object in every passband. For these undetected objects, it is vital we construct their magnitude upper-limits based upon the noise level at the site of the non-detection. All magnitude upper-limits are calculated from unsmoothed images to  $3\sigma$  confidence according to the formula

$$m_{u.l.} = -2.5 \log(3\sigma \cdot df_{ap}) + ZP_{AB} \quad (2.1)$$

where  $df_{ap}$  is the aperture flux uncertainty and  $ZP_{AB}$  is that passband's zero-point in absolute magnitude. Magnitude upper-limits may become relevant when using color-color plots to select high- $z$  galaxy candidates, as discussed in the next section.

#### 2.1.4 Selection Criteria

We begin with a master sample of 3919 objects detected in the HDF-S and their complementing UV, optical, and NIR photometry. Because our sample is determined by HDF-S *HST* data, we rely upon the Hubble Deep Field (HDF) color-color selection criteria of Steidel et al. (1996) to select  $z \sim 3$  galaxy candidates and narrow the sample. These selection cuts require  $R$ -band data, which the WFPC2 is not equipped to provide. As per the example of Steidel et al. (1996), we average the  $V_{606}$  and  $I_{814}$  fluxes to create our own synthetic  $R$ -band photometry for each galaxy in the sample:

$$\mathcal{R}_{VI} = -2.5 \log\left(\frac{10^{-0.4V_{606}} + 10^{-0.4I_{814}}}{2}\right). \quad (2.2)$$

With the  $\mathcal{R}_{VI}$  magnitudes in place, we then limit our sample to galaxies within the magnitude range

$$23 < \mathcal{R}_{VI} < 26.6. \quad (2.3)$$

The bright-end limit exists to protect our sample from the possibility of contamination by aberrant, suspiciously luminous objects, while the faint-end limit is crafted to expel objects with large photometric uncertainties. These too-uncertain data produce both dubious object selections and problematically generous uncertainties in the parameter-spaces of models, therefore supplying uselessly ambiguous model fits.

A concern for the completeness of the sample also informs our  $\mathcal{R}_{VI} < 26.6$  faint-end cut. If the cut is made too deep, we forfeit the desired near completeness of our sample. However, if the cut is made too shallow, we sacrifice usable data. With this in mind, we construct a histogram of the  $\mathcal{R}_{VI}$  magnitudes and restrict our sample to objects brighter than the magnitude, 26.6, that corresponds to the first peak in the distribution (see Figure 2.2). This cut eliminates 2807 objects from inclusion in our final sample, leaving 1112 objects.

Having now limited our sample for data quality and completeness, we apply the  $z \sim 3$  color-color selection criteria of Steidel et al. (1996) to objects detected in all seven passbands. Selected galaxies must satisfy two conditions, the “spectral curvature” condition,

$$U_{300} - B_{450} > 1.2 + (B_{450} - \mathcal{R}_{VI}), \quad (2.4)$$

and the “blueness” condition,

$$B_{450} - \mathcal{R}_{VI} < 1.2. \quad (2.5)$$

The spectral curvature condition mandates the discontinuity across the  $U_{300}$  and  $B_{450}$  passbands must be greater than three times the gradient across the  $B_{450}$  and  $\mathcal{R}_{VI}$  passbands. The blueness condition reflects the Steidel group’s expectation that high-redshift galaxies (up to  $z \sim 3.5$ ) will exhibit very blue continua. Of the 714 objects detected in all filters, 104 meet both criteria, and it is noteworthy that the majority of objects that satisfy the spectral curvature condition also satisfy the blueness condition. This is qualitatively consistent with the HDF results of Steidel et al. (1996).

We then apply the spectral curvature and blueness conditions to objects undetected in  $U_{300}$  but

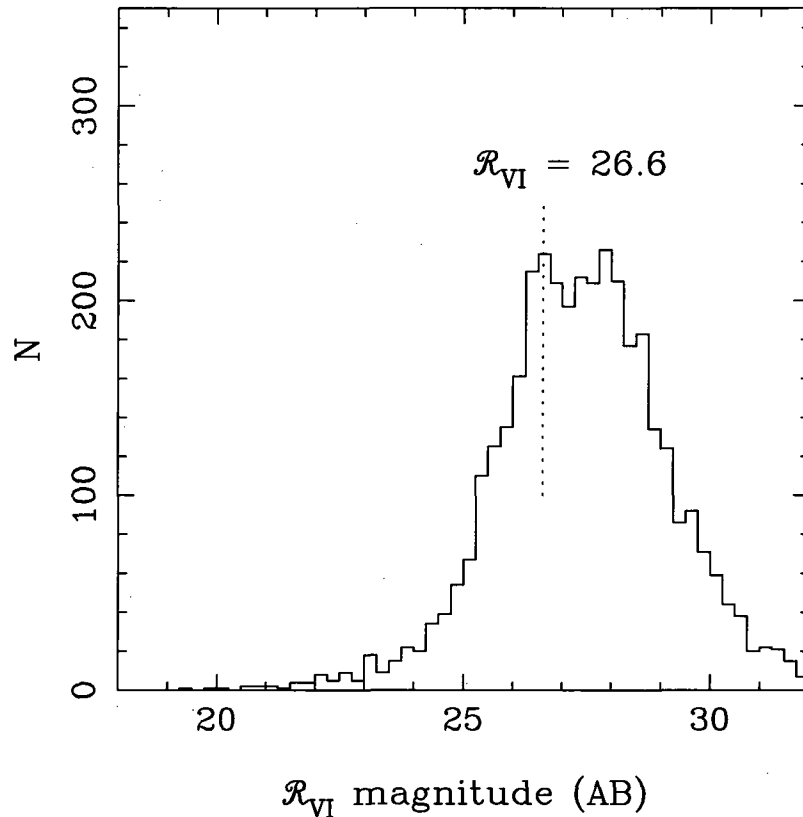


Figure 2.2: Histogram of synthetic  $R_{VI}$  magnitudes in the HDF-S. The vertical dotted line corresponds to  $R_{VI} = 26.6$ , the first peak in the distribution and the faint-end limit of our galaxy sample.

detected at all other wavelengths. For these objects, the  $U_{300}$   $3\sigma$  magnitude upper-limit stands in place for the absent  $U_{300}$  aperture magnitude. 138 such objects are selected.

We initially detect 3919 objects in the HDF-S. After limiting our sample based on data quality, completeness, spectral curvature, and blueness, we model-fit a catalog of 242  $z \sim 3$  LBG candidates (see Figure 2.3 for color-color selection plot). Table 2.1 contains the photometry for our entire color-color selected HDF-S catalog. Once model-fit, the catalog is further defined by a photometric redshift cut to excise any lower redshift interlopers (see section 3.2.1).

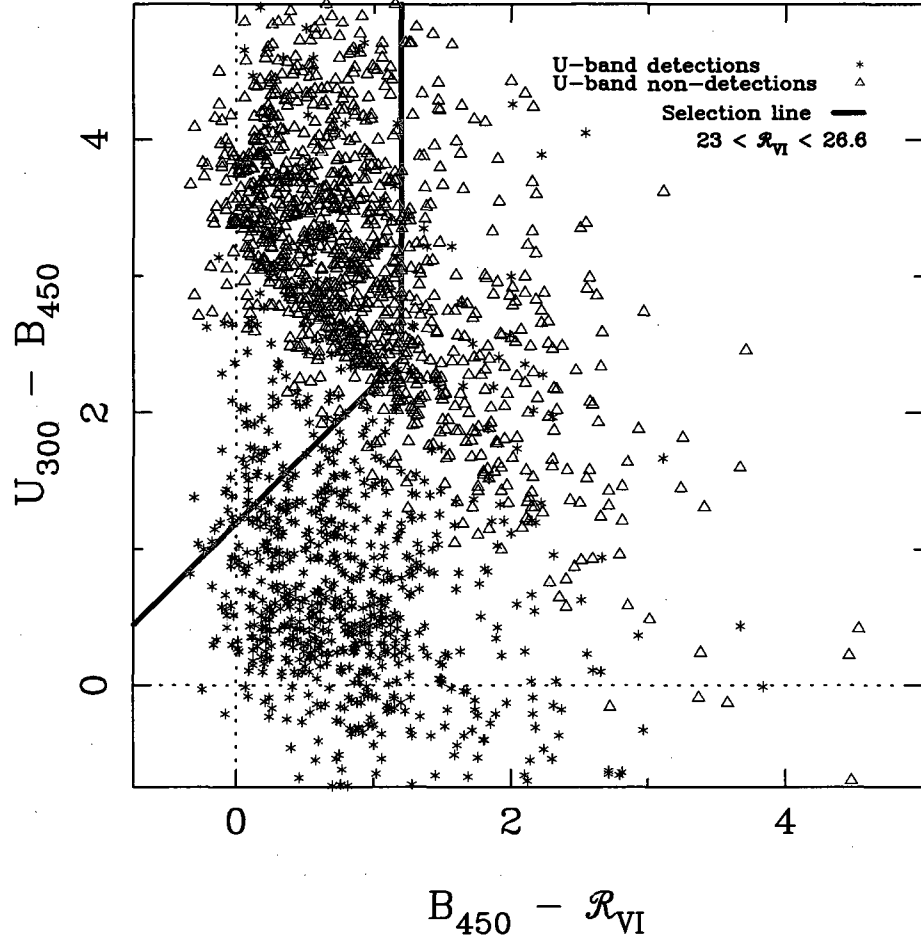


Figure 2.3: Color-color plot displaying objects detected in the HDF-S and their relationship to the  $z \sim 3$  selection criteria of Steidel et al. (1996). Objects detected at all wavelengths are shown as asterisks, while objects undetected in  $U_{300}$  but detected in all other bands are represented by upward pointing triangles. We select all asterisks and triangles above and to the left of the solid red line, resulting in 242 total  $z \sim 3$  galaxy candidates.

## 2.2 $z \sim 2$

### 2.2.1 The Observations

We complement our  $z \sim 3$  HDF-S data with a catalog of UV-selected galaxies culled from the original Hubble Deep Field (HDF; Williams et al. 1996). Taken from Sawicki et al. (2007), the catalog contains optical ( $U_{300}$ ,  $B_{450}$ ,  $V_{606}$ ,  $I_{814}$ ) and NIR ( $J_{110}$ ,  $H_{160}$ ) photometry measured from publicly available image mosaics taken by WFPC2 and the Near Infrared Camera and Multi-Object

Spectrometer (NICMOS), both on board *HST*. The uncommonly deep  $U_{300}$  imaging in the HDF distinguishes it as a dataset particularly suited to studying galaxies at  $z \sim 2$ . Limiting magnitudes for the WFPC2 observations are 27.0 in  $U_{300}$ , 27.9 in  $B_{450}$ , 28.2 in  $V_{606}$ , and 27.6 in  $I_{814}$ . The NICMOS filters each have a limiting magnitude of 26.5. For both instruments, these limits are  $10\sigma$  in a  $0.2 \text{ arcsec}^2$  aperture (Papovich et al. 2001). The HDF covers an area of  $\sim 5.3 \text{ arcmin}^2$  centered at  $\alpha = 12^h 36^m 49^s.4$ ,  $\delta = +62^\circ 12' 58''$  (J2000.0).

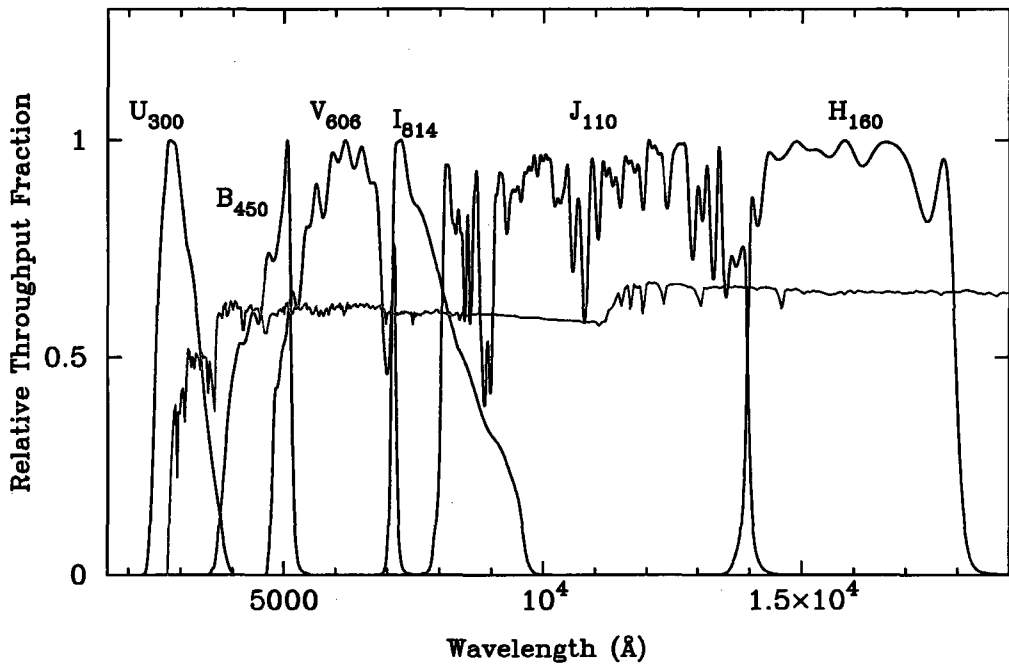


Figure 2.4: Filter transmission curves for WFPC2 ( $U_{300}$ ,  $B_{450}$ ,  $V_{606}$ ,  $I_{814}$ ) and NICMOS ( $J_{110}$ ,  $H_{160}$ ) aboard *HST*. Observations through these filters are used to select and model-fit a population of  $z \sim 2$  galaxies from the HDF. A  $z \sim 2$  model spectrum is overlaid in red.

It is once again critical to note that both features pertinent to selecting and model-fitting our galaxies-of-interest (this time at  $z \sim 2$ ) are captured within these six passbands. In  $z \sim 2$  galaxies, the Lyman break is observed at  $\sim 2700 \text{ \AA}$ , which identifies relevant objects as  $U_{300}$ -band dropouts. (Recall the Lyman break in  $z \sim 3$  LBGs also falls within the  $U_{300}$  filter.) The  $4000 \text{ \AA}$  break, our age/metallicity indicator, shifts to  $1.2 \times 10^4 \text{ \AA}$ , placing it within the NICMOS  $J_{110}$ -band. Figure 2.4 shows transmission curves for all six filters as well as an overlaid  $z \sim 2$  model spectrum.

### 2.2.2 Data Reduction, Object Detection, and Photometry

Sawicki et al. (2007) convolve the  $U_{300}$ ,  $B_{450}$ ,  $V_{606}$ ,  $I_{814}$ , and  $H_{160}$  images with Gaussian kernels to match the  $0''.22$  seeing of the NICMOS  $J_{110}$ -band, the lowest resolution image. Thusly, the flux ratio for any given object is conserved image to image. They then perform object detection and photometry with SExtractor 2.3.2 in dual-image mode. The unsmoothed  $V_{606}$ -band serves as the detection image while the smoothed  $U_{300}$ ,  $B_{450}$ ,  $V_{606}$ ,  $I_{814}$ , and  $H_{160}$  images are measured using fixed, circular apertures  $\sim 0''.5$  in diameter. The Sawicki group next procures photometry from the unsmoothed  $V_{606}$  image, which yields total  $V_{606}$  magnitudes. Total magnitudes for the other filters are then calculated according to the following formula:

$$m_{tot} = m_{ap} + (V_{606,tot} - V_{606,ap}). \quad (2.6)$$

The  $m_{tot}$  and  $m_{ap}$  refer to the  $U_{300}$ ,  $B_{450}$ ,  $I_{814}$ ,  $J_{110}$ , and  $H_{160}$  total and aperture magnitudes, respectively.

### 2.2.3 Selection Criteria

Sawicki and company then apply the color-color criteria of Steidel et al. (1996) to their calculated total magnitudes to define the high-redshift ( $z > 1.7$ ) sample (see Fig. 2.5 for this color-color plot). Recall we employ these same criteria to select LBGs at  $z \sim 3$  in the HDF-S. Section 2.1.4 contains the inequalities for spectral curvature (Eq. 2.4) and blueness (Eq. 2.5) that characterize the Steidel group's criteria. In addition to the color-color criteria, the Sawicki group limit their sample with the magnitude cut

$$23 < \mathcal{R}_{VI} < 28. \quad (2.7)$$

Doing so protects the sample against any infrequent, aberrant bright-end objects while, at the same time, excising those faint-end objects with large photometric uncertainties. Again, such faint-end

objects are best restricted from the sample because their locations in the color-color scheme are ambiguous, and their inclusion only produces problematically large uncertainties in the model-fit parameters. Sawicki's catalog is virtually complete up to  $\mathcal{R}_{VI} \leq 27$ , with meaningful incompleteness exhibited solely in its final two magnitude bins (see Fig. 2.5 for  $\mathcal{R}_{VI}$ -band number counts). Administering these color-color and magnitude cuts generates a sample of 284 objects in the HDF.

#### 2.2.4 Initial Modeling

Assuming a constant star formation history for each, Sawicki et al. (2007) then model-fit the 284 objects for photometric redshift, dust, stellar mass, SFR, and age (see Chapter 3). Uncertainties in the best-fit parameters are to 68% confidence. They define their  $z \sim 2$  sample according to the following photometric redshift cut:

$$1.8 \leq z_{phot} \leq 2.6. \quad (2.8)$$

Requiring the  $z \sim 2$  population to be model-fit for  $z_{phot} \geq 1.8$  prevents lower redshift interlopers from contaminating the analysis, and 87 objects are so eliminated. Meanwhile, filter availability in the HDF necessitates the upper limit cut. Objects at  $z \geq 2.6$  do not have sufficient rest-frame spectral coverage to be accurately model-fit. With no filter redder than the WFPC2  $H_{160}$ , the 4000 Å break cannot be constrained. This technological limitation reduces the sample by another 106 objects, leaving a subsample of 91  $z_{phot} \sim 2$  UV-selected galaxies. The right panel inset of Fig. 2.5 displays the photometric redshift distribution for all 284 model-fit objects.

In our analysis of high redshift galaxies model-fit assuming constant SFRs, we place the Sawicki et al. (2007)  $z_{phot} \sim 2$  model-fits along side those from Shapley et al. (2005;  $z \sim 2$ ), Yabe et al. (2009;  $z \sim 5$ ), and our own  $z \sim 3$  HDF-S sample. Having been granted access to Sawicki's photometry, we also refit the potentially relevant subset of his catalog ( $1.1 \leq z_{phot} \leq 2.9$ , 171 objects) under the assumptions of both an exponentially increasing and an exponentially decreasing star formation history. Photometry for the 171 objects we refit may be found in Table 2.2.

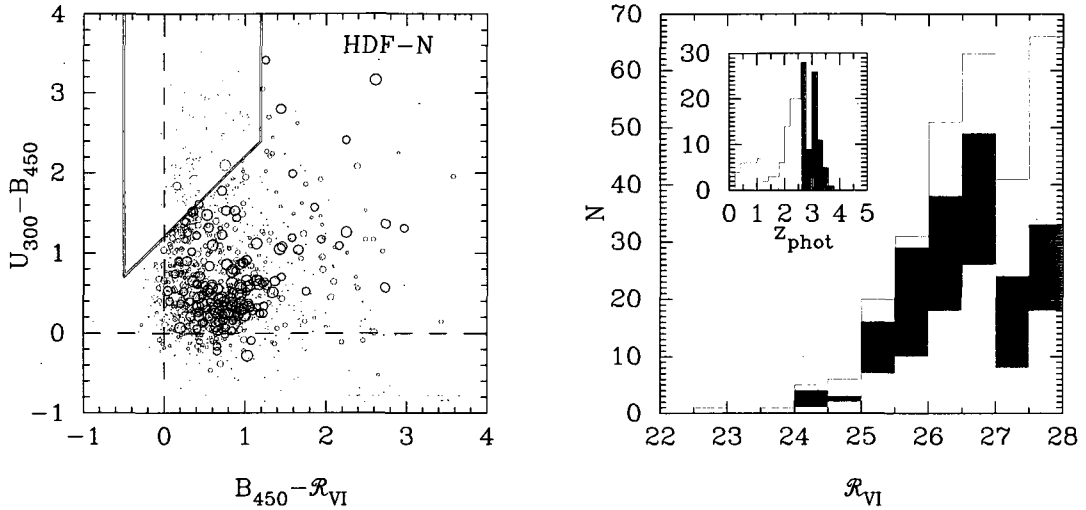


Figure 2.5: Sample selection for  $z \sim 2$  objects in the HDF. The left panel shows the  $U_{300} - B_{450} - \mathcal{R}_{VI}$  color-color selection criteria Sawicki employs to define his sample. The symbol sizes are scaled to indicate their relative brightnesses. All objects shown are  $23 \leq \mathcal{R}_{VI} \leq 28$ . The selection region (Steidel et al. 1996) is outlined in red. Selected objects are color-coded according to their model-fit photometric redshifts. The right panel inset displays the photometric redshift distribution. Objects satisfying Eq. 2.8 are colored orange, while blue objects lie at  $z_{phot} > 2.6$  and cyan objects at  $z_{phot} < 1.8$ . The right panel further shows the  $\mathcal{R}_{VI}$  number counts for selected objects. These histograms are stacked and do not overlap. Figures courtesy Sawicki (in preparation).

## 2.3 Comparison Data Sets

### 2.3.1 The Need for Comparison Data Sets

This project seeks to understand how UV-selected galaxies, as characterized by certain parameters (see Chapter 3), evolve over time. We produce information describing objects at redshifts  $\sim 3$  and  $\sim 2$ , but where possible a broader context is desired. Consequently, we place our results alongside studies at redshifts  $\sim 5$  (Yabe et al. 2009) and  $\sim 2$  (Shapley et al. 2005). The results of Yabe et al. (2009) provide a key high-redshift base to our analysis of the evolution of constant SFRs, while the Shapley group's findings reinforce and extend Sawicki's  $z \sim 2$  work. The utilization of these additional studies allows us to better track the evolution of LBG parameters as the universe ages from  $\sim 1.2$  to  $\sim 3.2$  billion years old.

### 2.3.2 $z \sim 5$ (Yabe et al. 2009)

Yabe et al. (2009) extract their  $z \sim 5$  LBG sample from the GOODS-N region and its associated flanking fields (GOODS-FF). Subaru Suprime-Cam provides their optical  $V$ ,  $I_c$ , and  $z'$  data. These data, originally reported in Iwata et al. (2007), cover 508.5 arcmin<sup>2</sup> and are magnitude limited ( $3\sigma$ , 1''.6 diameter aperture) at 28.1, 26.8, and 26.6, respectively. The reduced data are characterized by FWHMs of  $\sim 1''.1$ .

*Spitzer's* publicly available Data Release 1 and Data Release 2 furnish Yabe et al. (2009) with GOODS-N MIR IRAC images at 3.6, 4.5, 5.8, and 8.0  $\mu\text{m}$ . The Yabe group also procure new IRAC observations blanketing  $\sim 400$  arcmin<sup>2</sup> in the GOODS-FF. Here limiting magnitudes ( $3\sigma$ , 2''.4 diameter aperture) are 24.8, 24.1, 22.2, and 22.3, respectively. In lieu of smoothing their MIR data, Yabe et al. (2009) apply a filter-specific aperture correction factor to obtain their final magnitudes.

Object detection and photometry are performed with SExtractor. Those objects determined to be at  $z \sim 5$  according to a  $V - I_c - z'$  color-color criteria are then visually inspected for photometric contamination by near neighbors. All isolated objects are model-fit in the manner described in Chapter 3, section 3.1.1. Uncertainties for the Yabe et al. (2009) best-fit model parameters are to 90% confidence.

### 2.3.3 $z \sim 2$ (Shapley et al. 2005)

Shapley et al. (2005) model-fit a sample of 72 UV-selected galaxies situated in a 72 arcmin<sup>2</sup> tract centered about the bright background quasi-stellar object HS 1700+643. All 72 objects in the sample are spectroscopically confirmed to lie at  $z = 2.0 \pm 0.3$ . Optical data ( $U_n$ ,  $G$ ,  $R$ ) come from the William Herschel 4.2 m telescope's Prime Focus Imager. NIR  $K_s$  data are the product of observations with the Wide Field Infrared Camera on the Palomar 5.1 m Hale telescope. The Shapley group's catalog is then completed by MIR IRAC/*Spitzer* images at 3.6, 4.5, 5.8, and 8.0  $\mu\text{m}$ . Limiting magnitudes ( $5\sigma$ , 2'' diameter aperture) for these data are 26.4 ( $U_n$ ), 26.5 ( $G$ ), 25.7

( $R$ ), 24.0 ( $K_s$ ), 24.6 (3.5  $\mu\text{m}$ ), 24.3 (4.5  $\mu\text{m}$ ), 23.0 (5.8  $\mu\text{m}$ ), and 22.8 (8.0  $\mu\text{m}$ ). Object detection, photometry, and model-fitting processes are similar to those of Sawicki, Yabe et al. (2009), and this work.

Table 2.1: HDF-S Photometric Catalog. An uncertainty of 99.00 means the reported magnitude is a  $3\sigma$  upper limit.

ID	RA(J2000.0)	Dec(2000.0)	$U_{300}$	$B_{450}$	$V_{606}$	$I_{814}$	$H_{160}$	$K_s$
3	649.873	348.668	27.78 ± 0.09	26.45 ± 0.01	26.26 ± 0.01	26.49 ± 0.01	26.36 ± 0.07	27.19 ± 0.33
147	2528.670	573.725	26.56 ± 0.03	23.90 ± 0.00	23.22 ± 0.00	22.85 ± 0.00	22.68 ± 0.00	23.13 ± 0.01
156	671.568	569.715	29.03 ± 0.18	25.38 ± 0.00	25.28 ± 0.00	25.23 ± 0.00	24.69 ± 0.01	24.42 ± 0.02
172	3802.951	586.048	28.81 ± 0.26	25.83 ± 0.01	25.49 ± 0.00	25.03 ± 0.00	23.86 ± 0.01	23.18 ± 0.01
177	2673.885	592.230	26.74 ± 0.03	25.45 ± 0.00	25.48 ± 0.00	25.54 ± 0.01	25.36 ± 0.02	25.11 ± 0.04
201	2918.725	608.209	28.17 ± 0.11	26.64 ± 0.01	26.37 ± 0.01	26.42 ± 0.01	26.17 ± 0.05	25.53 ± 0.05
356	1309.749	780.919	27.61 ± 0.04	25.13 ± 0.00	24.78 ± 0.00	24.09 ± 0.00	22.91 ± 0.00	22.54 ± 0.00
401	1124.201	771.280	27.93 ± 0.06	26.21 ± 0.01	26.13 ± 0.00	25.88 ± 0.01	25.15 ± 0.02	24.96 ± 0.03
428	1459.148	760.711	29.32 ± 0.22	26.67 ± 0.01	26.07 ± 0.00	25.74 ± 0.01	25.46 ± 0.02	26.18 ± 0.08
430	1375.951	759.470	29.36 ± 0.22	26.25 ± 0.01	26.14 ± 0.00	26.03 ± 0.01	26.47 ± 0.06	27.47 ± 0.31
447	2515.662	792.243	26.70 ± 0.02	25.55 ± 0.00	25.72 ± 0.00	25.69 ± 0.01	25.45 ± 0.02	26.05 ± 0.09
462	1934.582	771.182	29.65 ± 0.30	26.54 ± 0.01	26.31 ± 0.00	25.75 ± 0.01	25.52 ± 0.02	25.83 ± 0.07
472	3470.557	779.177	28.82 ± 0.16	26.87 ± 0.01	26.55 ± 0.01	25.86 ± 0.01	24.94 ± 0.01	24.96 ± 0.03
475	3475.316	780.107	29.46 ± 0.29	27.12 ± 0.02	26.70 ± 0.01	26.00 ± 0.01	25.08 ± 0.02	25.47 ± 0.04
481	2521.508	800.471	27.39 ± 0.04	25.86 ± 0.01	25.95 ± 0.00	25.85 ± 0.01	25.28 ± 0.02	26.03 ± 0.08
526	1889.508	823.484	28.50 ± 0.10	26.01 ± 0.01	25.47 ± 0.00	24.91 ± 0.00	24.68 ± 0.01	24.75 ± 0.03
650	2414.232	903.477	29.03 ± 0.19	26.52 ± 0.01	26.36 ± 0.01	26.20 ± 0.01	26.59 ± 0.06	25.22 ± 0.04
715	3125.174	984.592	27.71 ± 0.05	25.13 ± 0.00	24.50 ± 0.00	24.11 ± 0.00	24.05 ± 0.01	23.46 ± 0.01
720	2441.115	966.361	28.19 ± 0.09	26.28 ± 0.01	26.31 ± 0.00	26.11 ± 0.01	25.82 ± 0.03	25.78 ± 0.07
726	776.049	970.150	27.51 ± 0.04	25.36 ± 0.00	25.10 ± 0.00	24.77 ± 0.00	23.87 ± 0.01	23.55 ± 0.01
779	565.710	1025.748	27.77 ± 0.05	25.69 ± 0.00	25.50 ± 0.00	25.29 ± 0.00	24.29 ± 0.01	23.87 ± 0.01
797	600.784	1018.846	27.77 ± 0.05	26.04 ± 0.01	26.07 ± 0.00	26.24 ± 0.01	25.84 ± 0.03	25.37 ± 0.01
818	3309.787	1036.668	27.68 ± 0.05	26.17 ± 0.01	26.12 ± 0.00	26.03 ± 0.01	25.28 ± 0.02	26.01 ± 0.07
824	592.990	1025.646	27.80 ± 0.05	25.88 ± 0.00	25.72 ± 0.00	25.79 ± 0.01	25.48 ± 0.02	24.70 ± 0.03
876	1456.188	1076.114	28.67 ± 0.12	26.01 ± 0.01	26.03 ± 0.00	26.17 ± 0.01	25.95 ± 0.04	26.46 ± 0.11
878	2351.010	1147.531	29.48 ± 0.28	26.06 ± 0.01	25.07 ± 0.00	24.83 ± 0.00	24.64 ± 0.01	24.01 ± 0.01
901	1565.964	1101.056	29.01 ± 0.16	26.00 ± 0.01	25.63 ± 0.00	24.67 ± 0.00	23.95 ± 0.01	23.87 ± 0.01
1029	1401.119	1215.825	28.71 ± 0.13	25.83 ± 0.00	25.72 ± 0.00	25.59 ± 0.00	25.05 ± 0.02	24.73 ± 0.03
1089	3882.917	1287.241	28.32 ± 0.10	25.45 ± 0.00	25.17 ± 0.00	25.02 ± 0.00	24.21 ± 0.01	23.94 ± 0.01
1102	1362.437	280.470	28.48 ± 0.11	25.55 ± 0.00	24.75 ± 0.00	24.65 ± 0.00	24.51 ± 0.02	24.25 ± 0.03
1159	1138.190	1336.697	28.73 ± 0.12	26.10 ± 0.01	26.31 ± 0.00	26.32 ± 0.01	25.73 ± 0.03	26.20 ± 0.10
1191	2233.1973	1358.994	28.62 ± 0.13	25.48 ± 0.00	25.63 ± 0.00	25.59 ± 0.00	26.01 ± 0.04	26.32 ± 0.11
1195	3598.523	1367.513	27.54 ± 0.05	25.78 ± 0.00	25.55 ± 0.00	25.43 ± 0.00	25.42 ± 0.02	25.31 ± 0.04
1228	1135.531	1425.712	27.45 ± 0.04	25.21 ± 0.00	25.06 ± 0.00	24.84 ± 0.00	24.05 ± 0.02	24.85 ± 0.03
1239	3775.311	1388.452	29.09 ± 0.19	27.01 ± 0.01	26.65 ± 0.01	26.52 ± 0.01	26.11 ± 0.04	27.10 ± 0.22
1267	1636.649	1484.515	26.77 ± 0.02	24.28 ± 0.00	23.59 ± 0.00	23.14 ± 0.00	22.99 ± 0.00	23.01 ± 0.01
1366	976.116	1618.243	28.41 ± 0.09	25.54 ± 0.00	25.20 ± 0.00	24.70 ± 0.00	23.35 ± 0.00	23.08 ± 0.01
1384	1623.066	1503.178	28.63 ± 0.11	26.19 ± 0.01	25.47 ± 0.00	25.06 ± 0.00	25.05 ± 0.02	25.31 ± 0.04
1441	955.069	1613.618	28.87 ± 0.14	26.31 ± 0.01	25.98 ± 0.00	25.41 ± 0.00	24.13 ± 0.01	24.07 ± 0.01
1451	646.576	1587.893	27.40 ± 0.04	25.79 ± 0.00	25.59 ± 0.00	25.31 ± 0.00	24.81 ± 0.01	24.61 ± 0.02
1467	381.001	1662.547	29.74 ± 0.33	24.59 ± 0.00	24.35 ± 0.00	24.26 ± 0.00	24.11 ± 0.01	23.55 ± 0.01
1478	941.927	1628.647	29.02 ± 0.16	26.59 ± 0.01	26.15 ± 0.00	25.69 ± 0.00	24.68 ± 0.01	24.53 ± 0.02
1482	3015.909	1702.893	27.71 ± 0.05	24.76 ± 0.00	24.41 ± 0.00	23.12 ± 0.00	22.90 ± 0.00	22.67 ± 0.00
1484	953.728	1636.515	29.15 ± 0.18	25.81 ± 0.00	25.36 ± 0.00	24.92 ± 0.00	23.51 ± 0.00	23.19 ± 0.01
1498	694.636	1684.869	26.12 ± 0.01	24.01 ± 0.00	23.67 ± 0.00	23.33 ± 0.00	22.41 ± 0.00	22.22 ± 0.00

Table 2.1: HDF-S Photometric Catalog. An uncertainty of 99.00 means the reported magnitude is a  $3\sigma$  upper limit.

ID	RA(J2000.0)	Dec(2000.0)	$U_{300}$	$B_{450}$	$V_{606}$	$I_{814}$	$J_s$	$H_{160}$	$K_s$
1521	477.713	1644.995	28.99 ± 0.16	26.65 ± 0.01	26.09 ± 0.00	25.53 ± 0.00	25.15 ± 0.02	25.70 ± 0.07	26.56 ± 0.13
1533	972.485	1667.295	28.98 ± 0.15	26.91 ± 0.01	26.54 ± 0.01	26.27 ± 0.01	24.89 ± 0.01	24.53 ± 0.02	24.87 ± 0.03
1565	3011.660	1688.476	27.94 ± 0.04	26.10 ± 0.00	25.71 ± 0.00	25.39 ± 0.00	24.36 ± 0.00	24.03 ± 0.01	23.78 ± 0.01
1576	455.442	1691.479	27.10 ± 0.03	25.90 ± 0.00	26.02 ± 0.00	26.02 ± 0.01	25.90 ± 0.04	25.92 ± 0.09	25.47 ± 0.05
1598	1750.966	1766.932	28.02 ± 0.06	25.93 ± 0.00	25.41 ± 0.00	25.12 ± 0.00	25.01 ± 0.01	24.62 ± 0.02	25.49 ± 0.04
1604	1705.304	1713.935	28.11 ± 0.07	26.08 ± 0.01	26.13 ± 0.00	25.97 ± 0.01	25.96 ± 0.04	24.99 ± 0.03	26.33 ± 0.10
1634	478.703	1810.185	28.12 ± 0.07	25.80 ± 0.00	25.16 ± 0.00	24.94 ± 0.00	24.67 ± 0.01	24.20 ± 0.02	24.03 ± 0.01
1695	1354.877	1786.556	28.76 ± 0.13	26.31 ± 0.01	26.27 ± 0.00	26.19 ± 0.01	26.15 ± 0.02	25.27 ± 0.04	25.39 ± 0.04
1817	3047.482	1957.326	29.51 ± 0.28	27.02 ± 0.01	26.61 ± 0.01	25.85 ± 0.01	25.38 ± 0.02	25.46 ± 0.05	25.45 ± 0.04
1933	564.799	2082.604	27.01 ± 0.03	24.96 ± 0.00	24.61 ± 0.00	24.41 ± 0.00	23.92 ± 0.01	23.50 ± 0.01	23.15 ± 0.01
1973	1550.894	2151.201	27.42 ± 0.04	25.85 ± 0.01	25.76 ± 0.00	25.62 ± 0.01	24.82 ± 0.01	25.05 ± 0.03	24.99 ± 0.03
1985	2890.613	2044.663	28.41 ± 0.10	26.71 ± 0.01	26.44 ± 0.01	26.68 ± 0.01	27.05 ± 0.10	26.23 ± 0.10	26.15 ± 0.08
2005	3724.809	2086.688	28.24 ± 0.09	25.95 ± 0.01	26.02 ± 0.00	26.10 ± 0.01	25.90 ± 0.03	26.05 ± 0.08	25.11 ± 0.03
2033	3727.261	2106.245	28.71 ± 0.14	26.34 ± 0.01	26.40 ± 0.01	26.31 ± 0.01	25.87 ± 0.03	25.33 ± 0.04	25.56 ± 0.05
2042	3723.067	2095.802	28.12 ± 0.08	26.03 ± 0.01	26.07 ± 0.00	26.04 ± 0.01	25.58 ± 0.02	25.39 ± 0.04	24.91 ± 0.02
2050	3261.672	2122.854	29.65 ± 0.32	26.42 ± 0.01	27.01 ± 0.00	25.65 ± 0.03	25.65 ± 0.03	25.79 ± 0.07	25.26 ± 0.04
2192	988.672	2267.939	28.31 ± 0.15	26.56 ± 0.02	26.45 ± 0.01	26.48 ± 0.02	26.90 ± 0.08	25.76 ± 0.07	26.59 ± 0.12
2207	3210.374	2332.104	27.00 ± 0.03	25.07 ± 0.00	25.03 ± 0.00	24.96 ± 0.00	24.84 ± 0.01	24.22 ± 0.02	24.49 ± 0.02
2306	2339.180	2442.354	28.40 ± 0.12	26.13 ± 0.01	25.84 ± 0.00	25.70 ± 0.01	25.69 ± 0.03	24.86 ± 0.03	25.41 ± 0.04
2361	2353.332	2475.457	27.17 ± 0.04	25.43 ± 0.00	25.28 ± 0.00	25.31 ± 0.00	24.45 ± 0.02	24.92 ± 0.03	25.13 ± 0.03
2367	2340.903	2471.840	28.68 ± 0.16	25.91 ± 0.01	25.73 ± 0.00	25.70 ± 0.01	25.66 ± 0.03	25.12 ± 0.04	25.45 ± 0.04
2389	2010.222	2497.914	27.56 ± 0.14	24.80 ± 0.00	24.23 ± 0.00	23.83 ± 0.00	23.39 ± 0.00	23.44 ± 0.01	23.49 ± 0.01
2560	1234.283	2678.259	28.88 ± 0.32	26.23 ± 0.01	26.16 ± 0.01	26.01 ± 0.01	25.74 ± 0.03	25.70 ± 0.06	25.68 ± 0.05
2575	2289.916	2716.151	27.69 ± 0.05	26.02 ± 0.01	25.86 ± 0.00	25.95 ± 0.01	25.38 ± 0.02	25.23 ± 0.04	25.26 ± 0.04
2597	2765.087	2728.628	28.18 ± 0.08	26.63 ± 0.01	26.44 ± 0.01	26.69 ± 0.01	26.94 ± 0.03	27.30 ± 0.27	27.39 ± 0.25
2661	1920.233	2770.688	27.53 ± 0.09	26.15 ± 0.01	26.54 ± 0.01	26.39 ± 0.01	25.70 ± 0.03	25.87 ± 0.07	26.68 ± 0.13
2728	1787.856	2877.697	26.66 ± 0.04	24.79 ± 0.00	24.67 ± 0.00	24.46 ± 0.00	23.73 ± 0.00	23.74 ± 0.01	23.51 ± 0.01
2747	3508.538	2851.543	29.73 ± 0.34	27.01 ± 0.01	26.73 ± 0.01	26.31 ± 0.01	25.77 ± 0.03	25.88 ± 0.07	26.38 ± 0.10
2763	3640.979	2895.399	27.27 ± 0.04	25.88 ± 0.00	25.98 ± 0.00	25.84 ± 0.01	25.28 ± 0.02	26.82 ± 0.17	25.42 ± 0.04
2765	3739.512	2894.196	27.81 ± 0.06	26.45 ± 0.01	26.46 ± 0.01	26.27 ± 0.01	26.09 ± 0.04	26.08 ± 0.09	26.00 ± 0.07
2784	1815.115	2881.088	26.67 ± 0.04	25.61 ± 0.01	25.91 ± 0.00	25.69 ± 0.01	25.13 ± 0.02	24.62 ± 0.02	24.80 ± 0.02
2799	1842.128	2905.962	27.35 ± 0.08	26.31 ± 0.01	27.01 ± 0.01	26.29 ± 0.01	26.63 ± 0.07	26.26 ± 0.10	25.52 ± 0.05
2958	2675.847	2940.169	29.76 ± 0.20	26.53 ± 0.01	26.00 ± 0.00	26.04 ± 0.01	25.80 ± 0.01	25.67 ± 0.03	26.10 ± 0.08
2837	3400.468	2981.986	28.76 ± 0.13	25.68 ± 0.00	25.43 ± 0.00	25.38 ± 0.00	24.94 ± 0.01	24.87 ± 0.03	24.88 ± 0.03
2849	2739.478	2983.953	28.52 ± 0.10	25.59 ± 0.01	25.24 ± 0.00	25.07 ± 0.00	24.69 ± 0.01	23.97 ± 0.01	24.04 ± 0.01
2889	3350.144	3021.707	28.80 ± 0.14	25.49 ± 0.00	25.25 ± 0.00	25.17 ± 0.00	25.18 ± 0.02	24.95 ± 0.03	25.16 ± 0.03
2913	3304.073	3260.790	28.51 ± 0.10	23.98 ± 0.00	23.35 ± 0.00	23.35 ± 0.00	23.13 ± 0.00	22.70 ± 0.00	22.69 ± 0.00
2958	2689.735	3095.440	27.66 ± 0.05	26.86 ± 0.01	25.84 ± 0.00	25.80 ± 0.01	25.70 ± 0.03	24.93 ± 0.03	25.05 ± 0.03
3043	3264.175	3253.996	27.47 ± 0.04	23.62 ± 0.00	23.18 ± 0.00	23.00 ± 0.00	22.88 ± 0.00	22.78 ± 0.00	22.73 ± 0.00
3098	3326.658	3248.114	28.21 ± 0.08	26.09 ± 0.01	25.92 ± 0.00	25.74 ± 0.01	25.52 ± 0.02	25.56 ± 0.05	25.62 ± 0.05
3127	3561.665	3419.115	27.61 ± 0.05	25.08 ± 0.00	24.70 ± 0.00	24.32 ± 0.00	23.24 ± 0.00	22.91 ± 0.00	22.63 ± 0.00
3166	3296.689	3292.694	28.26 ± 0.08	25.90 ± 0.00	25.72 ± 0.00	25.47 ± 0.00	24.83 ± 0.01	24.50 ± 0.02	24.64 ± 0.02
3169	3227.206	3295.887	28.43 ± 0.10	26.86 ± 0.01	26.59 ± 0.01	26.46 ± 0.01	25.96 ± 0.04	26.96 ± 0.20	25.92 ± 0.07
3217	3468.804	3413.116	28.90 ± 0.15	26.85 ± 0.01	26.50 ± 0.01	26.69 ± 0.01	25.39 ± 0.04	26.18 ± 0.10	25.59 ± 0.05
3321	2562.344	3522.984	28.92 ± 0.15	26.96 ± 0.01	26.48 ± 0.01	26.14 ± 0.01	25.88 ± 0.03	26.00 ± 0.08	25.98 ± 0.07
3330	3531.600	3548.944	28.10 ± 0.07	26.38 ± 0.01	26.47 ± 0.01	25.94 ± 0.01	25.50 ± 0.02	24.83 ± 0.03	25.15 ± 0.03

Table 2.1: HDF-S Photometric Catalog. An uncertainty of 99.00 means the reported magnitude is a  $3\sigma$  upper limit.

ID	RA(J2000.0)	Dec(2000.0)	$U_{300}$	$B_{450}$	$V_{606}$	$I_{814}$	$J_s$	$H_{160}$	$K_s$
3397	3050.417	3730.565	29.31 ± 0.22	26.66 ± 0.01	26.60 ± 0.01	26.54 ± 0.01	25.95 ± 0.04	25.82 ± 0.07	26.20 ± 0.08
3407	3328.932	3795.278	28.63 ± 0.12	26.26 ± 0.01	26.12 ± 0.00	25.81 ± 0.01	25.60 ± 0.03	25.71 ± 0.06	25.09 ± 0.03
3419	2570.686	4044.583	27.74 ± 0.05	26.20 ± 0.01	26.16 ± 0.00	25.95 ± 0.01	25.20 ± 0.03	24.92 ± 0.04	24.75 ± 0.03
3554	2378.105	3787.095	27.81 ± 0.05	26.39 ± 0.01	26.54 ± 0.01	26.41 ± 0.01	26.04 ± 0.04	25.91 ± 0.07	26.72 ± 0.14
3560	2820.692	4121.754	27.12 ± 0.03	25.93 ± 0.01	26.01 ± 0.00	25.89 ± 0.01	25.17 ± 0.02	25.10 ± 0.04	25.21 ± 0.04
3625	3778.317	3678.652	29.14 ± 0.35	27.02 ± 0.02	26.62 ± 0.01	26.02 ± 0.01	25.15 ± 0.02	25.33 ± 0.05	25.14 ± 0.04
3639	3379.672	4074.863	28.51 ± 0.10	26.22 ± 0.01	25.25 ± 0.00	25.02 ± 0.00	24.81 ± 0.01	23.88 ± 0.01	23.69 ± 0.01
3666	2591.548	4051.707	27.64 ± 0.05	25.98 ± 0.01	25.94 ± 0.00	25.92 ± 0.01	25.30 ± 0.02	25.27 ± 0.05	25.59 ± 0.06
3689	2442.234	4337.217	28.95 ± 0.24	26.27 ± 0.01	26.36 ± 0.01	25.99 ± 0.01	26.09 ± 0.10	24.95 ± 0.07	26.37 ± 0.25
3782	3221.708	4436.387	26.96 ± 0.04	25.52 ± 0.01	25.50 ± 0.00	25.36 ± 0.01	24.76 ± 0.03	24.26 ± 0.04	25.28 ± 0.11
3789	2771.316	3798.776	28.10 ± 0.07	26.49 ± 0.01	26.57 ± 0.01	26.28 ± 0.01	25.80 ± 0.03	25.57 ± 0.05	26.54 ± 0.12
3795	2358.761	3880.387	29.85 ± 0.36	26.57 ± 0.01	26.13 ± 0.00	25.79 ± 0.01	25.63 ± 0.03	26.68 ± 0.16	25.04 ± 0.03
3808	3298.800	4288.436	29.01 ± 0.21	25.81 ± 0.01	24.91 ± 0.00	24.67 ± 0.00	24.28 ± 0.01	23.68 ± 0.01	23.36 ± 0.01
8	727.362	331.963	29.27 ± 99.00	29.93 ± 0.02	30.29 ± 0.01	29.87 ± 0.01	28.19 ± 0.02	27.33 ± 0.04	27.49 ± 0.03
59	1900.733	497.954	29.54 ± 99.00	30.30 ± 0.01	30.69 ± 0.00	30.19 ± 0.01	28.28 ± 0.04	27.42 ± 0.06	27.58 ± 0.08
69	2284.570	446.620	29.08 ± 99.00	29.81 ± 0.01	30.21 ± 0.01	29.79 ± 0.01	28.15 ± 0.02	27.27 ± 0.17	27.44 ± 0.05
73	1770.971	469.119	29.50 ± 99.00	30.28 ± 0.01	30.66 ± 0.01	30.15 ± 0.01	28.26 ± 0.07	27.40 ± 0.19	27.57 ± 0.09
100	2842.045	480.016	29.14 ± 99.00	29.87 ± 0.02	30.27 ± 0.01	29.82 ± 0.01	28.11 ± 0.03	27.23 ± 0.11	27.40 ± 0.09
160	3774.426	546.761	29.10 ± 73.06	29.86 ± 0.01	30.25 ± 0.00	29.80 ± 0.00	28.06 ± 0.02	27.17 ± 0.08	27.35 ± 0.15
161	3825.990	546.501	29.08 ± 99.00	29.84 ± 0.01	30.22 ± 0.01	29.77 ± 0.01	28.05 ± 0.03	27.16 ± 0.09	27.34 ± 0.18
171	3812.673	558.198	29.11 ± 0.62	29.86 ± 0.01	30.24 ± 0.01	29.85 ± 0.01	28.08 ± 0.03	27.18 ± 0.06	27.36 ± 0.04
190	659.994	572.883	28.82 ± 99.00	30.57 ± 0.01	30.99 ± 0.00	30.36 ± 0.00	28.42 ± 0.02	27.55 ± 0.08	27.71 ± 0.03
203	1986.847	619.884	28.80 ± 99.00	30.51 ± 0.01	30.92 ± 0.00	30.32 ± 0.01	28.42 ± 0.02	27.55 ± 0.03	27.72 ± 0.03
207	3798.406	595.663	29.18 ± 7.53	29.94 ± 0.01	30.40 ± 0.00	29.93 ± 0.00	28.15 ± 0.01	27.27 ± 0.01	27.44 ± 0.01
242	1992.282	617.731	29.81 ± 99.00	30.52 ± 0.01	30.92 ± 0.00	30.32 ± 0.01	28.43 ± 0.02	27.56 ± 0.03	27.72 ± 0.03
288	3528.036	679.507	29.46 ± 99.00	30.24 ± 0.01	30.71 ± 0.00	30.15 ± 0.00	28.30 ± 0.01	27.44 ± 0.02	27.61 ± 0.02
296	1780.859	705.549	29.85 ± 99.00	30.58 ± 0.01	31.00 ± 0.00	30.36 ± 0.00	28.47 ± 0.03	27.61 ± 0.08	27.77 ± 0.32
310	1843.624	674.989	29.84 ± 99.00	30.58 ± 0.00	31.00 ± 0.01	30.36 ± 0.01	28.46 ± 0.08	27.60 ± 0.10	27.76 ± 0.13
313	3706.568	708.017	29.47 ± 0.82	30.25 ± 0.01	30.71 ± 0.00	30.14 ± 0.01	28.32 ± 0.02	27.46 ± 0.02	27.62 ± 0.04
328	1840.422	684.772	29.86 ± 99.00	30.60 ± 0.00	31.02 ± 0.00	30.38 ± 0.00	28.49 ± 0.04	27.63 ± 0.06	27.78 ± 0.11
339	1839.409	693.295	29.84 ± 99.00	30.58 ± 0.00	31.00 ± 0.00	30.36 ± 0.00	28.48 ± 0.02	27.61 ± 0.05	27.76 ± 0.07
344	1793.904	695.347	29.83 ± 99.00	30.58 ± 0.01	31.00 ± 0.00	30.36 ± 0.00	28.47 ± 0.03	27.61 ± 0.08	27.77 ± 0.16
348	1799.449	701.098	29.84 ± 99.00	30.58 ± 0.01	31.00 ± 0.00	30.36 ± 0.00	28.48 ± 0.02	27.61 ± 0.05	27.77 ± 0.07
448	1441.155	783.202	29.86 ± 99.00	30.58 ± 0.01	31.01 ± 0.00	30.35 ± 0.00	28.49 ± 0.02	27.62 ± 0.03	27.78 ± 0.02
453	1912.339	763.758	29.84 ± 99.00	30.58 ± 0.01	31.00 ± 0.00	30.36 ± 0.00	28.49 ± 0.04	27.62 ± 0.04	27.78 ± 0.06
464	3820.306	798.055	29.66 ± 99.00	30.47 ± 0.01	30.88 ± 0.00	30.30 ± 0.00	28.48 ± 0.02	27.61 ± 0.02	27.78 ± 0.02
466	1919.805	774.197	29.85 ± 99.00	30.58 ± 0.01	31.00 ± 0.00	30.36 ± 0.00	28.49 ± 0.02	27.62 ± 0.04	27.78 ± 0.06
470	1458.320	783.278	29.88 ± 99.00	30.59 ± 0.01	31.01 ± 0.00	30.36 ± 0.01	28.49 ± 0.02	27.62 ± 0.05	27.78 ± 0.05
473	1912.311	779.407	29.85 ± 10.28	30.58 ± 0.01	31.00 ± 0.00	30.36 ± 0.00	28.49 ± 0.02	27.62 ± 0.03	27.78 ± 0.06
480	3832.355	802.846	29.62 ± 99.00	30.42 ± 0.01	30.83 ± 0.00	30.24 ± 0.01	28.43 ± 0.04	27.55 ± 0.03	27.72 ± 0.03
519	1909.995	815.863	29.88 ± 1.44	30.59 ± 0.01	31.02 ± 0.00	30.36 ± 0.00	28.49 ± 0.02	27.63 ± 0.05	27.78 ± 0.11
520	1916.397	816.724	29.87 ± 2.51	30.59 ± 0.01	31.02 ± 0.01	30.36 ± 0.01	28.48 ± 0.03	27.62 ± 0.07	27.78 ± 0.14
533	1905.160	829.895	29.88 ± 99.00	30.60 ± 0.01	31.03 ± 0.00	30.37 ± 0.00	28.49 ± 0.02	27.63 ± 0.04	27.79 ± 0.06
534	1902.024	826.758	29.89 ± 0.54	30.61 ± 0.01	31.04 ± 0.00	30.38 ± 0.00	28.50 ± 0.01	27.64 ± 0.03	27.79 ± 0.04

Table 2.1: HDF-S Photometric Catalog. An uncertainty of 99.00 means the reported magnitude is a  $3\sigma$  upper limit.

ID	RA(J2000.0)	Dec(J2000.0)	$U_{300}$	$B_{450}$	$V_{606}$	$I_{814}$	$J_s$	$H_{160}$	$K_s$
542	1910.276	832.481	29.88 $\pm$ 99.00	30.59 $\pm$ 0.01	31.03 $\pm$ 0.01	30.36 $\pm$ 0.01	28.49 $\pm$ 0.02	27.63 $\pm$ 0.06	27.78 $\pm$ 0.07
544	1915.552	836.236	29.87 $\pm$ 99.00	30.58 $\pm$ 0.01	31.02 $\pm$ 0.01	30.36 $\pm$ 0.01	28.49 $\pm$ 0.03	27.62 $\pm$ 0.11	27.78 $\pm$ 0.11
570	1907.792	846.716	29.88 $\pm$ 99.00	30.59 $\pm$ 0.01	31.02 $\pm$ 0.01	30.36 $\pm$ 0.01	28.49 $\pm$ 0.04	27.62 $\pm$ 0.06	27.78 $\pm$ 0.19
572	1803.282	847.811	29.88 $\pm$ 99.00	30.60 $\pm$ 0.01	31.03 $\pm$ 0.00	30.37 $\pm$ 0.00	28.48 $\pm$ 0.01	27.62 $\pm$ 0.04	27.78 $\pm$ 0.05
579	1845.613	852.399	29.88 $\pm$ 99.00	30.59 $\pm$ 0.01	31.02 $\pm$ 0.00	30.37 $\pm$ 0.00	28.48 $\pm$ 0.01	27.62 $\pm$ 0.03	27.78 $\pm$ 0.04
590	1808.814	857.609	29.88 $\pm$ 99.00	30.60 $\pm$ 0.01	31.03 $\pm$ 0.01	30.37 $\pm$ 0.01	28.48 $\pm$ 0.02	27.62 $\pm$ 0.07	27.78 $\pm$ 0.06
639	2693.558	886.159	29.76 $\pm$ 99.00	30.52 $\pm$ 0.02	30.98 $\pm$ 0.00	30.32 $\pm$ 0.01	28.49 $\pm$ 0.02	27.63 $\pm$ 0.03	27.78 $\pm$ 0.03
649	749.263	902.964	29.88 $\pm$ 99.00	30.60 $\pm$ 0.01	31.04 $\pm$ 0.01	30.36 $\pm$ 0.01	28.48 $\pm$ 0.05	27.62 $\pm$ 0.08	27.78 $\pm$ 0.04
665	2701.871	897.737	29.77 $\pm$ 99.00	30.53 $\pm$ 0.01	31.00 $\pm$ 0.00	30.33 $\pm$ 0.00	28.50 $\pm$ 0.01	27.64 $\pm$ 0.02	27.79 $\pm$ 0.02
673	2700.987	902.733	29.77 $\pm$ 99.00	30.53 $\pm$ 0.01	30.99 $\pm$ 0.00	30.33 $\pm$ 0.00	28.49 $\pm$ 0.02	27.63 $\pm$ 0.03	27.79 $\pm$ 0.02
692	772.736	959.118	29.90 $\pm$ 99.00	30.61 $\pm$ 0.00	31.05 $\pm$ 0.00	30.37 $\pm$ 0.00	28.48 $\pm$ 0.01	27.62 $\pm$ 0.01	27.78 $\pm$ 0.01
721	735.251	965.105	29.89 $\pm$ 99.00	30.60 $\pm$ 0.01	31.03 $\pm$ 0.00	30.36 $\pm$ 0.00	28.48 $\pm$ 0.02	27.62 $\pm$ 0.02	27.78 $\pm$ 0.01
746	2674.570	971.645	29.77 $\pm$ 99.00	30.53 $\pm$ 0.02	31.00 $\pm$ 0.01	30.33 $\pm$ 0.01	28.49 $\pm$ 0.02	27.63 $\pm$ 0.05	27.78 $\pm$ 0.03
848	726.081	1082.719	29.89 $\pm$ 99.00	30.61 $\pm$ 0.01	31.04 $\pm$ 0.00	30.37 $\pm$ 0.00	28.48 $\pm$ 0.01	27.62 $\pm$ 0.01	27.78 $\pm$ 0.01
871	2335.606	1102.777	29.76 $\pm$ 99.00	30.53 $\pm$ 0.01	30.99 $\pm$ 0.00	30.32 $\pm$ 0.00	28.50 $\pm$ 0.02	27.63 $\pm$ 0.02	27.79 $\pm$ 0.02
972	3279.945	1169.706	29.79 $\pm$ 1.25	30.55 $\pm$ 0.01	31.01 $\pm$ 0.01	30.33 $\pm$ 0.01	28.49 $\pm$ 0.04	27.62 $\pm$ 0.05	27.78 $\pm$ 0.05
1047	2212.658	1213.340	29.64 $\pm$ 99.00	30.37 $\pm$ 0.01	30.89 $\pm$ 0.00	30.21 $\pm$ 0.01	28.48 $\pm$ 0.11	27.62 $\pm$ 0.03	27.78 $\pm$ 0.20
1106	3618.822	1297.586	29.79 $\pm$ 99.00	30.55 $\pm$ 0.02	31.00 $\pm$ 0.01	30.34 $\pm$ 0.01	28.49 $\pm$ 0.02	27.62 $\pm$ 0.03	27.78 $\pm$ 0.02
1108	2758.722	1343.835	29.80 $\pm$ 99.00	30.56 $\pm$ 0.00	31.02 $\pm$ 0.00	30.34 $\pm$ 0.00	28.49 $\pm$ 0.01	27.62 $\pm$ 0.02	27.78 $\pm$ 0.01
1124	2266.537	1294.901	29.76 $\pm$ 99.00	30.52 $\pm$ 0.01	30.99 $\pm$ 0.01	30.31 $\pm$ 0.01	28.48 $\pm$ 0.04	27.62 $\pm$ 0.04	27.78 $\pm$ 0.10
1140	2269.129	1288.354	29.76 $\pm$ 99.00	30.52 $\pm$ 0.01	30.99 $\pm$ 0.01	30.32 $\pm$ 0.01	28.49 $\pm$ 0.03	27.63 $\pm$ 0.05	27.78 $\pm$ 0.19
1225	2770.030	1366.619	29.80 $\pm$ 99.00	30.56 $\pm$ 0.01	31.01 $\pm$ 0.01	30.34 $\pm$ 0.01	28.49 $\pm$ 0.11	27.62 $\pm$ 0.22	27.78 $\pm$ 0.20
1273	3120.332	1443.937	29.80 $\pm$ 99.00	30.56 $\pm$ 0.01	31.02 $\pm$ 0.00	30.34 $\pm$ 0.01	28.49 $\pm$ 0.02	27.63 $\pm$ 0.20	27.78 $\pm$ 0.02
1403	1612.254	1518.481	29.88 $\pm$ 99.00	30.62 $\pm$ 0.02	31.04 $\pm$ 0.01	30.37 $\pm$ 0.01	28.48 $\pm$ 0.04	27.62 $\pm$ 0.17	27.78 $\pm$ 0.05
1471	628.498	1581.015	29.85 $\pm$ 99.00	30.60 $\pm$ 0.01	31.02 $\pm$ 0.01	30.35 $\pm$ 0.01	28.48 $\pm$ 0.04	27.62 $\pm$ 0.04	27.77 $\pm$ 0.04
1473	983.064	1645.727	29.90 $\pm$ 0.41	30.63 $\pm$ 0.01	31.05 $\pm$ 0.00	30.38 $\pm$ 0.00	28.48 $\pm$ 0.01	27.62 $\pm$ 0.02	27.78 $\pm$ 0.01
1501	3446.440	1609.919	29.80 $\pm$ 99.00	30.55 $\pm$ 0.02	31.01 $\pm$ 0.00	30.33 $\pm$ 0.01	28.49 $\pm$ 0.02	27.62 $\pm$ 0.09	27.78 $\pm$ 0.03
1523	488.644	1668.703	29.85 $\pm$ 99.00	30.60 $\pm$ 0.01	31.02 $\pm$ 0.00	30.35 $\pm$ 0.01	28.35 $\pm$ 0.02	27.50 $\pm$ 0.06	27.66 $\pm$ 0.07
1527	361.841	1641.740	29.84 $\pm$ 99.00	30.58 $\pm$ 0.01	31.01 $\pm$ 0.01	30.33 $\pm$ 0.01	28.48 $\pm$ 0.07	27.32 $\pm$ 0.04	27.47 $\pm$ 0.06
1540	900.344	1693.728	29.89 $\pm$ 99.00	30.60 $\pm$ 0.01	31.05 $\pm$ 0.00	30.38 $\pm$ 0.01	28.48 $\pm$ 0.01	27.62 $\pm$ 0.03	27.78 $\pm$ 0.01
1543	1603.752	1694.299	29.89 $\pm$ 99.00	30.62 $\pm$ 0.00	31.03 $\pm$ 0.00	30.37 $\pm$ 0.00	28.49 $\pm$ 0.01	27.62 $\pm$ 0.01	27.78 $\pm$ 0.01
1551	942.724	1663.504	29.90 $\pm$ 0.63	30.63 $\pm$ 0.02	31.05 $\pm$ 0.01	30.38 $\pm$ 0.01	28.48 $\pm$ 0.02	27.62 $\pm$ 0.02	27.78 $\pm$ 0.02
1572	1586.512	1677.595	29.88 $\pm$ 99.00	30.62 $\pm$ 0.01	31.04 $\pm$ 0.00	30.37 $\pm$ 0.01	28.49 $\pm$ 0.02	27.62 $\pm$ 0.03	27.78 $\pm$ 0.04
1585	1785.070	1699.979	29.89 $\pm$ 1.74	30.62 $\pm$ 0.01	31.05 $\pm$ 0.01	30.38 $\pm$ 0.01	28.49 $\pm$ 0.02	27.62 $\pm$ 0.03	27.78 $\pm$ 0.04
1590	1589.613	1690.311	29.90 $\pm$ 99.00	30.64 $\pm$ 0.01	31.02 $\pm$ 0.01	30.39 $\pm$ 0.01	28.48 $\pm$ 0.03	27.62 $\pm$ 0.15	27.78 $\pm$ 0.06
1593	2228.863	1709.418	29.77 $\pm$ 99.00	30.51 $\pm$ 0.01	30.99 $\pm$ 0.00	30.31 $\pm$ 0.00	28.49 $\pm$ 0.01	27.62 $\pm$ 0.02	27.78 $\pm$ 0.01
1647	1361.556	1779.715	29.85 $\pm$ 99.00	30.60 $\pm$ 0.00	31.01 $\pm$ 0.00	30.35 $\pm$ 0.00	28.49 $\pm$ 0.01	27.63 $\pm$ 0.02	27.78 $\pm$ 0.02
1676	1379.816	1790.182	29.89 $\pm$ 99.00	30.62 $\pm$ 0.01	31.04 $\pm$ 0.01	30.38 $\pm$ 0.01	28.49 $\pm$ 0.02	27.62 $\pm$ 0.04	27.78 $\pm$ 0.03
1686	1798.389	1787.107	29.88 $\pm$ 99.00	30.62 $\pm$ 0.01	31.04 $\pm$ 0.01	30.38 $\pm$ 0.01	28.49 $\pm$ 0.05	27.62 $\pm$ 0.06	27.78 $\pm$ 0.06
1699	2701.704	1808.327	29.79 $\pm$ 99.00	30.56 $\pm$ 0.02	31.02 $\pm$ 0.01	30.34 $\pm$ 0.01	28.48 $\pm$ 0.03	27.62 $\pm$ 0.15	27.78 $\pm$ 0.06
1739	2605.547	1868.321	29.79 $\pm$ 99.00	30.55 $\pm$ 0.00	31.01 $\pm$ 0.00	30.34 $\pm$ 0.00	28.49 $\pm$ 0.01	27.62 $\pm$ 0.02	27.78 $\pm$ 0.01
1863	3507.966	2171.561	29.77 $\pm$ 0.65	30.53 $\pm$ 0.00	31.01 $\pm$ 0.00	30.32 $\pm$ 0.00	28.49 $\pm$ 0.01	27.62 $\pm$ 0.01	27.78 $\pm$ 0.01
1881	2874.599	2036.550	29.79 $\pm$ 99.00	30.53 $\pm$ 0.00	31.01 $\pm$ 0.00	30.34 $\pm$ 0.00	28.49 $\pm$ 0.01	27.62 $\pm$ 0.02	27.78 $\pm$ 0.01
1908	913.031	1980.341	29.84 $\pm$ 99.00	30.57 $\pm$ 0.01	31.01 $\pm$ 0.01	30.36 $\pm$ 0.01	28.48 $\pm$ 0.03	27.62 $\pm$ 0.05	27.78 $\pm$ 0.03
1915	2332.194	2017.799	29.75 $\pm$ 0.37	30.51 $\pm$ 0.01	31.00 $\pm$ 0.01	30.31 $\pm$ 0.01	28.48 $\pm$ 0.12	27.62 $\pm$ 0.11	27.77 $\pm$ 0.06

Table 2.1: HDF-S Photometric Catalog. An uncertainty of 99.00 means the reported magnitude is a  $3\sigma$  upper limit.

ID	RA(J2000.0)	Dec(2000.0)	$U_{300}$	$B_{450}$	$V_{606}$	$I_{814}$	$J_s$	$H_{160}$	$K_s$
1926	363.782	2036.971	29.74 ± 99.00	30.49 ± 0.01	30.93 ± 0.00	30.27 ± 0.00	28.23 ± 0.02	27.38 ± 0.02	27.54 ± 0.01
1954	2856.973	2035.260	29.79 ± 0.40	30.54 ± 0.01	31.02 ± 0.01	30.35 ± 0.01	28.49 ± 0.03	27.63 ± 0.04	27.79 ± 0.03
1960	570.101	2042.880	29.76 ± 0.88	30.51 ± 0.01	30.95 ± 0.01	30.28 ± 0.01	28.47 ± 0.03	27.61 ± 0.06	27.77 ± 0.04
2021	1771.362	2087.166	29.80 ± 99.00	30.55 ± 0.02	30.99 ± 0.01	30.33 ± 0.01	28.49 ± 0.04	27.62 ± 0.04	27.78 ± 0.15
2025	929.826	2114.499	29.71 ± 99.00	30.45 ± 0.01	30.92 ± 0.01	30.17 ± 0.00	28.48 ± 0.01	27.62 ± 0.02	27.78 ± 0.02
2030	3089.316	2123.113	29.78 ± 99.00	30.54 ± 0.01	31.01 ± 0.00	30.33 ± 0.00	28.48 ± 0.03	27.62 ± 0.05	27.78 ± 0.05
2052	3095.248	2113.957	29.78 ± 99.00	30.54 ± 0.01	31.01 ± 0.00	30.33 ± 0.01	28.48 ± 0.05	27.62 ± 0.18	27.78 ± 0.26
2071	2498.961	2174.486	29.76 ± 99.00	30.53 ± 0.01	30.99 ± 0.00	30.31 ± 0.00	28.48 ± 0.02	27.62 ± 0.02	27.77 ± 0.02
2188	930.013	2280.484	29.29 ± 99.00	29.98 ± 0.02	30.50 ± 0.01	29.49 ± 0.01	28.48 ± 0.03	27.62 ± 0.05	27.77 ± 0.02
2219	2461.808	2380.419	29.64 ± 99.00	30.40 ± 0.02	30.86 ± 0.01	30.13 ± 0.01	28.48 ± 0.01	27.62 ± 0.02	27.77 ± 0.01
2257	1209.112	2333.357	29.00 ± 99.00	29.82 ± 0.02	30.50 ± 0.01	29.71 ± 0.02	28.49 ± 0.01	27.62 ± 0.01	27.78 ± 0.01
2266	1206.690	2413.822	29.01 ± 99.00	29.81 ± 0.01	30.49 ± 0.00	29.71 ± 0.01	28.49 ± 0.01	27.62 ± 0.01	27.78 ± 0.00
2300	2699.938	2402.249	29.66 ± 99.00	30.42 ± 0.01	30.89 ± 0.00	30.15 ± 0.00	28.49 ± 0.02	27.63 ± 0.05	27.78 ± 0.02
2315	2093.187	2431.990	29.42 ± 99.00	30.08 ± 0.02	30.65 ± 0.01	30.02 ± 0.01	28.48 ± 0.03	27.62 ± 0.04	27.77 ± 0.04
2329	2331.009	2429.535	29.60 ± 1.37	30.36 ± 0.01	30.83 ± 0.01	30.16 ± 0.01	28.50 ± 0.04	27.64 ± 0.03	27.79 ± 0.04
2356	3720.698	2487.343	29.62 ± 0.46	30.38 ± 0.01	30.85 ± 0.00	30.13 ± 0.00	28.49 ± 0.01	27.62 ± 0.02	27.78 ± 0.02
2427	3736.681	2547.566	29.60 ± 31.42	30.36 ± 0.02	30.84 ± 0.01	30.16 ± 0.01	28.49 ± 0.03	27.62 ± 0.06	27.78 ± 0.08
2429	3087.653	2536.805	29.65 ± 99.00	30.42 ± 0.01	30.89 ± 0.01	30.24 ± 0.01	28.49 ± 0.04	27.62 ± 0.06	27.78 ± 0.09
2529	1893.146	2723.298	29.02 ± 99.00	29.99 ± 0.02	30.71 ± 0.01	29.99 ± 0.01	28.48 ± 0.02	27.62 ± 0.04	27.78 ± 0.03
2545	3617.478	2689.072	29.62 ± 99.00	30.44 ± 0.01	30.86 ± 0.00	30.23 ± 0.01	28.49 ± 0.02	27.62 ± 0.02	27.78 ± 0.02
2553	1229.556	2657.316	29.01 ± 99.00	29.94 ± 0.03	30.68 ± 0.01	29.93 ± 0.01	28.49 ± 0.07	27.62 ± 0.13	27.78 ± 0.08
2561	3581.439	2678.121	29.61 ± 99.00	30.42 ± 0.02	30.86 ± 0.01	30.23 ± 0.01	28.49 ± 0.03	27.62 ± 0.06	27.78 ± 0.08
2568	1221.186	2675.067	29.01 ± 99.00	29.87 ± 0.02	30.65 ± 0.01	29.89 ± 0.01	28.49 ± 0.03	27.62 ± 0.04	27.78 ± 0.04
2652	1920.631	2778.004	29.00 ± 99.00	29.95 ± 0.01	30.65 ± 0.01	29.94 ± 0.01	28.48 ± 0.02	27.62 ± 0.04	27.78 ± 0.04
2684	2318.718	2790.258	29.84 ± 3.16	30.60 ± 0.02	31.03 ± 0.01	30.37 ± 0.01	28.49 ± 0.05	27.62 ± 0.31	27.78 ± 0.06
2698	3161.605	2838.305	29.83 ± 99.00	30.59 ± 0.02	31.01 ± 0.01	30.36 ± 0.01	28.48 ± 0.03	27.62 ± 0.04	27.78 ± 0.02
2722	3287.178	2843.431	29.81 ± 99.00	30.42 ± 0.02	30.86 ± 0.01	30.23 ± 0.01	28.49 ± 0.04	27.62 ± 0.04	27.78 ± 0.06
2751	3279.099	2854.003	29.82 ± 99.00	30.59 ± 0.01	31.01 ± 0.00	30.36 ± 0.01	28.48 ± 0.10	27.62 ± 0.04	27.78 ± 0.04
2754	3499.665	2863.109	29.80 ± 99.00	30.58 ± 0.01	31.01 ± 0.01	30.35 ± 0.01	28.49 ± 0.03	27.62 ± 0.13	27.78 ± 0.07
2759	2307.658	2887.107	29.86 ± 99.00	30.61 ± 0.01	31.04 ± 0.00	30.38 ± 0.01	28.49 ± 0.04	27.62 ± 0.05	27.78 ± 0.02
2854	2494.469	2964.736	29.87 ± 99.00	30.62 ± 0.01	31.03 ± 0.00	30.39 ± 0.00	28.49 ± 0.01	27.62 ± 0.02	27.78 ± 0.01
2946	3458.222	3082.852	29.85 ± 99.00	30.60 ± 0.01	31.03 ± 0.00	30.37 ± 0.01	28.48 ± 0.03	27.62 ± 0.03	27.78 ± 0.03
2955	2071.214	3105.806	29.86 ± 99.00	30.57 ± 0.00	31.03 ± 0.00	30.36 ± 0.00	28.48 ± 0.01	27.62 ± 0.01	27.78 ± 0.01
2989	3771.244	3115.628	29.79 ± 99.00	30.50 ± 0.02	30.92 ± 0.01	30.29 ± 0.01	28.42 ± 0.02	27.55 ± 0.05	27.71 ± 0.20
3145	3286.009	3274.633	29.85 ± 99.00	30.63 ± 0.00	31.08 ± 0.00	30.40 ± 0.00	28.50 ± 0.01	27.64 ± 0.02	27.79 ± 0.02
3163	2771.068	3301.214	29.89 ± 99.00	30.64 ± 0.01	31.07 ± 0.00	30.40 ± 0.01	28.50 ± 0.02	27.63 ± 0.03	27.79 ± 0.02
3258	2454.472	3452.679	29.88 ± 99.00	30.62 ± 0.01	31.06 ± 0.01	30.39 ± 0.01	28.49 ± 0.16	27.62 ± 0.09	27.78 ± 0.06
3275	2031.409	3449.329	29.85 ± 99.00	30.55 ± 0.02	31.03 ± 0.01	30.35 ± 0.01	28.49 ± 0.10	27.62 ± 0.22	27.78 ± 0.08
3294	2672.584	3528.601	29.89 ± 99.00	30.62 ± 0.01	31.06 ± 0.00	30.39 ± 0.00	28.49 ± 0.00	27.62 ± 0.01	27.78 ± 0.00
3349	3548.728	3556.202	29.85 ± 99.00	30.60 ± 0.01	31.04 ± 0.01	30.36 ± 0.01	28.49 ± 0.04	27.62 ± 0.06	27.78 ± 0.04
3389	2044.041	3678.236	29.87 ± 99.00	30.58 ± 0.02	31.02 ± 0.01	30.35 ± 0.01	28.48 ± 0.03	27.62 ± 0.07	27.78 ± 0.03
3411	3094.591	3788.728	29.88 ± 0.64	30.61 ± 0.01	31.04 ± 0.00	30.38 ± 0.00	28.49 ± 0.02	27.62 ± 0.04	27.78 ± 0.03
3420	3127.912	3754.424	29.86 ± 99.00	30.60 ± 0.01	31.04 ± 0.01	30.37 ± 0.01	28.49 ± 0.03	27.62 ± 0.04	27.78 ± 0.06
3445	3033.404	3718.362	29.86 ± 99.00	30.61 ± 0.01	31.02 ± 0.01	30.37 ± 0.01	28.49 ± 0.06	27.62 ± 0.07	27.78 ± 0.05
3480	2796.097	3995.679	29.84 ± 99.00	30.57 ± 0.01	31.02 ± 0.01	30.36 ± 0.01	28.40 ± 0.02	27.54 ± 0.06	27.68 ± 0.05

Table 2.1: HDF-S Photometric Catalog. An uncertainty of 99.00 means the reported magnitude is a  $3\sigma$  upper limit.

ID	RA(J2000.0)	Dec(2000.0)	$U_{300}$	$B_{450}$	$V_{606}$	$I_{814}$	$J_s$	$H_{160}$	$K_s$
3485	3059.527	3723.460	29.87 $\pm$ 99.00	30.61 $\pm$ 0.01	31.04 $\pm$ 0.00	30.37 $\pm$ 0.01	28.48 $\pm$ 0.03	27.62 $\pm$ 0.08	27.78 $\pm$ 0.07
3491	3048.244	3713.056	29.87 $\pm$ 1.19	30.61 $\pm$ 0.01	31.04 $\pm$ 0.00	30.37 $\pm$ 0.01	28.49 $\pm$ 0.03	27.62 $\pm$ 0.08	27.78 $\pm$ 0.04
3503	3255.390	3860.542	29.86 $\pm$ 99.00	30.59 $\pm$ 0.00	31.04 $\pm$ 0.00	30.37 $\pm$ 0.00	28.49 $\pm$ 0.02	27.62 $\pm$ 0.05	27.78 $\pm$ 0.07
3511	3138.367	3748.706	29.86 $\pm$ 99.00	30.60 $\pm$ 0.00	31.04 $\pm$ 0.00	30.36 $\pm$ 0.00	28.48 $\pm$ 0.02	27.62 $\pm$ 0.03	27.78 $\pm$ 0.03
3542	2003.739	3687.892	29.84 $\pm$ 99.00	30.53 $\pm$ 0.01	31.00 $\pm$ 0.00	30.33 $\pm$ 0.00	28.49 $\pm$ 0.00	27.62 $\pm$ 0.01	27.78 $\pm$ 0.01
3548	3773.460	3625.988	29.45 $\pm$ 1.64	30.36 $\pm$ 0.02	30.70 $\pm$ 0.00	30.04 $\pm$ 0.01	28.35 $\pm$ 0.02	27.48 $\pm$ 0.04	27.64 $\pm$ 0.05
3563	2808.686	3764.366	29.87 $\pm$ 99.00	30.62 $\pm$ 0.00	31.04 $\pm$ 0.00	30.37 $\pm$ 0.00	28.49 $\pm$ 0.01	27.62 $\pm$ 0.01	27.78 $\pm$ 0.01
3578	2052.299	3671.002	29.87 $\pm$ 1.00	30.58 $\pm$ 0.02	31.03 $\pm$ 0.01	30.36 $\pm$ 0.01	28.48 $\pm$ 0.02	27.62 $\pm$ 0.05	27.78 $\pm$ 0.03
3635	3374.297	4054.934	29.83 $\pm$ 99.00	30.57 $\pm$ 0.00	31.02 $\pm$ 0.00	30.36 $\pm$ 0.01	28.40 $\pm$ 0.01	27.55 $\pm$ 0.01	27.69 $\pm$ 0.03
3641	201.037	3677.715	29.85 $\pm$ 99.00	30.55 $\pm$ 0.01	31.01 $\pm$ 0.01	30.34 $\pm$ 0.01	28.48 $\pm$ 0.01	27.62 $\pm$ 0.02	27.78 $\pm$ 0.01
3646	2445.774	4069.728	29.84 $\pm$ 99.00	30.56 $\pm$ 0.01	31.02 $\pm$ 0.00	30.37 $\pm$ 0.00	28.26 $\pm$ 0.05	27.41 $\pm$ 0.06	27.54 $\pm$ 0.08
3687	2489.990	4250.810	29.62 $\pm$ 0.50	30.37 $\pm$ 0.02	30.83 $\pm$ 0.01	29.97 $\pm$ 0.01	27.91 $\pm$ 0.09	27.03 $\pm$ 0.08	27.17 $\pm$ 0.09
3767	3568.128	3976.335	29.80 $\pm$ 99.00	30.54 $\pm$ 0.02	31.00 $\pm$ 0.01	30.33 $\pm$ 0.01	28.46 $\pm$ 0.03	27.60 $\pm$ 0.05	27.75 $\pm$ 0.12
3779	2637.433	4004.585	29.85 $\pm$ 1.21	30.58 $\pm$ 0.02	31.02 $\pm$ 0.01	30.38 $\pm$ 0.01	28.37 $\pm$ 0.04	27.52 $\pm$ 0.10	27.66 $\pm$ 0.06
3797	2568.312	4032.788	29.83 $\pm$ 99.00	30.55 $\pm$ 0.01	31.02 $\pm$ 0.01	30.36 $\pm$ 0.01	28.32 $\pm$ 0.03	27.46 $\pm$ 0.05	27.61 $\pm$ 0.04
3867	3209.050	4445.883	29.31 $\pm$ 99.00	29.97 $\pm$ 0.01	30.49 $\pm$ 0.01	29.51 $\pm$ 0.01	27.26 $\pm$ 0.07	26.48 $\pm$ 0.08	26.54 $\pm$ 0.09
3897	2915.408	4050.864	29.85 $\pm$ 99.00	30.56 $\pm$ 0.01	31.02 $\pm$ 0.01	30.36 $\pm$ 0.01	28.35 $\pm$ 0.02	27.48 $\pm$ 0.05	27.63 $\pm$ 0.06

Table 2.2: HDF catalog of Sawicki et al. (2007). An uncertainty of 99.00 means the magnitude value is a  $3\sigma$  upper limit.

ID	RA(J2000.0)	Dec(2000.0)	$U_{300}$	$B_{450}$	$V_{606}$	$I_{814}$	$J_{110}$	$H_{160}$
3	189.216	62.199	29.49 ± 99.00	25.19 ± 0.00	24.33 ± 0.00	23.84 ± 0.00	23.98 ± 0.01	23.73 ± 0.01
12	189.201	62.196	29.49 ± 99.00	25.85 ± 0.01	25.25 ± 0.00	25.05 ± 0.00	24.97 ± 0.02	24.51 ± 0.01
60	189.228	62.201	29.49 ± 99.00	26.99 ± 0.01	26.54 ± 0.01	26.56 ± 0.01	26.07 ± 0.03	25.28 ± 0.02
88	189.217	62.199	29.49 ± 99.00	27.01 ± 0.01	26.30 ± 0.00	26.25 ± 0.01	26.66 ± 0.05	26.20 ± 0.04
96	189.228	62.201	29.49 ± 99.00	27.13 ± 0.01	27.04 ± 0.01	26.93 ± 0.01	26.98 ± 0.05	25.98 ± 0.03
97	189.212	62.198	29.49 ± 99.00	27.55 ± 0.01	27.56 ± 0.01	27.59 ± 0.01	28.16 ± 0.12	27.04 ± 0.05
182	189.243	62.205	28.78 ± 0.12	26.05 ± 0.00	25.70 ± 0.00	25.45 ± 0.00	24.80 ± 0.01	24.05 ± 0.01
196	189.254	62.207	29.49 ± 99.00	26.92 ± 0.02	26.41 ± 0.01	26.23 ± 0.01	26.17 ± 0.05	25.76 ± 0.04
210	189.194	62.194	30.34 ± 0.28	27.59 ± 0.01	27.49 ± 0.01	27.53 ± 0.01	27.51 ± 0.06	27.48 ± 0.07
215	189.250	62.206	31.51 ± 1.26	27.45 ± 0.01	27.05 ± 0.01	27.05 ± 0.01	26.60 ± 0.04	25.66 ± 0.02
242	189.254	62.207	29.49 ± 99.00	27.15 ± 0.01	26.81 ± 0.01	26.60 ± 0.01	26.64 ± 0.05	26.58 ± 0.06
248	189.216	62.199	30.74 ± 0.74	26.31 ± 0.01	26.24 ± 0.00	26.31 ± 0.01	26.75 ± 0.06	26.00 ± 0.03
284	189.190	62.195	29.49 ± 99.00	27.11 ± 0.02	26.90 ± 0.01	26.70 ± 0.01	28.88 ± 0.48	26.64 ± 0.08
317	189.194	62.196	28.22 ± 0.08	26.14 ± 0.01	26.00 ± 0.00	25.91 ± 0.01	26.28 ± 0.04	25.52 ± 0.03
323	189.186	62.194	29.42 ± 0.14	26.72 ± 0.01	26.72 ± 0.00	26.75 ± 0.01	26.84 ± 0.04	26.86 ± 0.05
325	189.208	62.199	29.49 ± 99.00	26.85 ± 0.01	26.19 ± 0.00	26.04 ± 0.01	26.20 ± 0.03	25.59 ± 0.02
336	189.189	62.195	29.49 ± 99.00	27.33 ± 0.02	27.32 ± 0.01	27.23 ± 0.02	27.68 ± 0.15	28.07 ± 99.00
338	189.227	62.203	28.57 ± 0.11	26.96 ± 0.01	26.99 ± 0.01	26.99 ± 0.02	27.45 ± 0.12	26.32 ± 0.05
364	189.193	62.196	29.45 ± 0.20	27.67 ± 0.02	27.95 ± 0.02	27.84 ± 0.03	29.29 ± 0.52	26.96 ± 0.07
390	189.200	62.198	29.49 ± 99.00	27.43 ± 0.01	27.15 ± 0.01	27.13 ± 0.01	27.26 ± 0.07	26.65 ± 0.05
411	189.232	62.205	29.49 ± 99.00	27.68 ± 0.02	27.51 ± 0.01	27.62 ± 0.02	26.68 ± 0.05	27.50 ± 0.12
425	189.189	62.197	28.67 ± 0.09	26.85 ± 0.01	26.52 ± 0.00	26.23 ± 0.01	25.49 ± 0.01	24.65 ± 0.01
442	189.189	62.198	28.86 ± 0.05	24.76 ± 0.00	24.13 ± 0.00	23.86 ± 0.00	23.84 ± 0.01	23.17 ± 0.01
452	189.206	62.201	28.99 ± 0.13	27.16 ± 0.01	26.73 ± 0.01	26.65 ± 0.01	26.51 ± 0.04	25.81 ± 0.03
454	189.210	62.201	29.49 ± 99.00	26.78 ± 0.01	26.36 ± 0.00	26.17 ± 0.01	26.22 ± 0.04	25.61 ± 0.03
463	189.219	62.203	30.12 ± 0.31	26.92 ± 0.01	26.63 ± 0.00	26.61 ± 0.01	27.17 ± 0.06	26.30 ± 0.03
470	189.250	62.210	28.79 ± 0.10	26.61 ± 0.01	26.30 ± 0.00	26.16 ± 0.01	26.11 ± 0.03	25.26 ± 0.01
478	189.189	62.198	29.49 ± 99.00	25.26 ± 0.00	24.43 ± 0.00	24.02 ± 0.00	23.85 ± 0.01	23.01 ± 0.00
510	189.232	62.207	27.84 ± 0.04	26.43 ± 0.00	26.47 ± 0.00	26.46 ± 0.01	26.55 ± 0.03	25.66 ± 0.02
552	189.231	62.208	28.07 ± 0.06	26.53 ± 0.01	26.41 ± 0.00	26.45 ± 0.01	26.25 ± 0.04	26.21 ± 0.04
578	189.186	62.198	28.59 ± 0.13	26.72 ± 0.01	26.55 ± 0.01	26.64 ± 0.01	26.35 ± 0.05	25.75 ± 0.04
592	189.191	62.199	29.00 ± 0.12	26.28 ± 0.00	26.00 ± 0.00	25.87 ± 0.00	26.21 ± 0.03	25.25 ± 0.01
604	189.186	62.198	29.41 ± 0.17	27.48 ± 0.01	27.34 ± 0.01	27.36 ± 0.01	27.40 ± 0.08	26.74 ± 0.05
610	189.215	62.205	28.33 ± 0.10	26.10 ± 0.01	25.72 ± 0.00	25.28 ± 0.00	24.69 ± 0.01	23.98 ± 0.01
621	189.209	62.203	29.75 ± 0.20	27.62 ± 0.01	27.56 ± 0.01	27.65 ± 0.02	27.58 ± 0.08	27.92 ± 0.14
653	189.215	62.205	29.24 ± 0.16	26.85 ± 0.01	26.45 ± 0.00	26.06 ± 0.01	25.65 ± 0.02	24.93 ± 0.01
668	189.207	62.204	27.00 ± 0.02	25.57 ± 0.00	25.39 ± 0.00	25.31 ± 0.00	25.03 ± 0.01	24.43 ± 0.01
673	189.176	62.197	27.84 ± 0.08	26.23 ± 0.01	26.28 ± 0.01	26.39 ± 0.01	25.84 ± 0.04	25.35 ± 0.03
709	189.236	62.210	31.05 ± 0.55	27.73 ± 0.01	27.74 ± 0.01	27.58 ± 0.01	27.86 ± 0.09	26.77 ± 0.04
712	189.199	62.202	29.06 ± 0.09	27.73 ± 0.01	27.85 ± 0.01	28.04 ± 0.02	27.78 ± 0.09	27.35 ± 0.07
751	189.215	62.206	28.50 ± 0.15	26.66 ± 0.01	26.70 ± 0.01	26.80 ± 0.02	26.40 ± 0.07	25.85 ± 0.05
762	189.216	62.207	28.24 ± 0.10	26.43 ± 0.01	26.10 ± 0.00	25.75 ± 0.01	25.07 ± 0.02	24.27 ± 0.01
766	189.235	62.210	29.44 ± 0.20	27.70 ± 0.02	27.48 ± 0.01	27.48 ± 0.02	27.23 ± 0.08	27.43 ± 0.12
789	189.170	62.197	29.38 ± 0.15	26.82 ± 0.01	26.79 ± 0.00	26.73 ± 0.01	27.01 ± 0.05	26.12 ± 0.03
790	189.203	62.204	29.04 ± 0.15	26.30 ± 0.01	25.64 ± 0.00	24.82 ± 0.00	23.64 ± 0.00	22.54 ± 0.00
797	189.207	62.205	28.56 ± 0.12	25.56 ± 0.00	25.32 ± 0.00	25.22 ± 0.00	25.31 ± 0.02	24.62 ± 0.01
801	189.223	62.208	29.06 ± 0.15	27.67 ± 0.02	27.82 ± 0.02	27.99 ± 0.03	27.12 ± 0.08	27.50 ± 0.13
879	189.206	62.206	29.49 ± 99.00	27.56 ± 0.02	27.60 ± 0.01	27.57 ± 0.02	28.28 ± 0.23	27.00 ± 0.09
880	189.197	62.204	29.86 ± 0.18	27.36 ± 0.01	27.40 ± 0.01	27.39 ± 0.01	28.81 ± 0.21	27.68 ± 0.09
891	189.208	62.207	30.49 ± 0.33	27.62 ± 0.01	28.00 ± 0.01	27.88 ± 0.02	27.46 ± 0.06	27.11 ± 0.05
892	189.179	62.201	28.30 ± 0.05	26.95 ± 0.01	26.87 ± 0.00	26.75 ± 0.01	26.86 ± 0.04	26.04 ± 0.02
893	189.240	62.214	28.74 ± 0.09	26.73 ± 0.01	26.64 ± 0.00	26.55 ± 0.01	26.45 ± 0.03	25.44 ± 0.02
896	189.240	62.214	27.96 ± 0.05	26.46 ± 0.01	26.60 ± 0.00	26.68 ± 0.01	26.75 ± 0.05	25.67 ± 0.02
921	189.208	62.208	28.91 ± 0.12	26.92 ± 0.01	26.86 ± 0.01	26.64 ± 0.01	26.33 ± 0.03	25.75 ± 0.02
933	189.176	62.201	29.49 ± 99.00	26.77 ± 0.02	26.00 ± 0.01	25.54 ± 0.01	25.60 ± 0.03	25.34 ± 0.03
954	189.210	62.208	30.87 ± 0.53	27.89 ± 0.02	27.78 ± 0.01	27.73 ± 0.02	27.48 ± 0.07	27.02 ± 0.06
994	189.179	62.203	27.81 ± 0.05	26.06 ± 0.01	26.00 ± 0.00	26.02 ± 0.01	25.99 ± 0.03	25.48 ± 0.02
1006	189.234	62.214	29.49 ± 99.00	27.69 ± 0.02	27.68 ± 0.01	27.57 ± 0.02	27.53 ± 0.09	26.99 ± 0.07
1007	189.169	62.201	29.63 ± 0.22	28.12 ± 0.03	27.87 ± 0.01	27.76 ± 0.02	28.44 ± 0.22	27.64 ± 0.13
1026	189.186	62.204	29.43 ± 0.34	26.82 ± 0.02	26.57 ± 0.01	25.68 ± 0.01	24.43 ± 0.01	23.33 ± 0.00
1048	189.241	62.216	29.66 ± 0.40	26.92 ± 0.02	26.35 ± 0.01	26.31 ± 0.01	26.34 ± 0.06	25.48 ± 0.03
1062	189.177	62.203	29.93 ± 0.30	27.98 ± 0.02	27.42 ± 0.01	27.10 ± 0.01	27.55 ± 0.10	27.02 ± 0.08
1073	189.196	62.207	28.81 ± 0.11	26.00 ± 0.00	25.77 ± 0.00	25.72 ± 0.00	25.91 ± 0.02	25.65 ± 0.02
1074	189.195	62.207	30.91 ± 0.74	26.08 ± 0.00	25.99 ± 0.00	26.06 ± 0.01	26.18 ± 0.03	26.01 ± 0.03
1083	189.193	62.207	28.86 ± 0.11	27.11 ± 0.01	26.96 ± 0.01	26.78 ± 0.01	26.60 ± 0.04	25.75 ± 0.02
1095	189.192	62.207	29.49 ± 99.00	27.83 ± 0.02	27.66 ± 0.01	27.66 ± 0.02	28.81 ± 0.25	27.26 ± 0.08
1099	189.215	62.211	29.49 ± 99.00	27.89 ± 0.02	27.67 ± 0.01	27.58 ± 0.02	28.08 ± 0.15	27.43 ± 0.10
1106	189.181	62.204	29.49 ± 99.00	27.72 ± 0.02	27.78 ± 0.01	27.76 ± 0.02	28.73 ± 0.24	27.28 ± 0.08
1112	189.217	62.212	29.73 ± 0.28	27.74 ± 0.02	27.82 ± 0.02	27.64 ± 0.02	28.95 ± 0.40	26.38 ± 0.05
1129	189.180	62.205	28.76 ± 0.11	26.39 ± 0.01	26.13 ± 0.00	25.91 ± 0.00	25.51 ± 0.02	24.81 ± 0.01
1131	189.190	62.207	29.49 ± 99.00	26.71 ± 0.01	26.49 ± 0.00	26.50 ± 0.01	27.08 ± 0.07	26.15 ± 0.04
1158	189.180	62.205	28.98 ± 0.11	26.66 ± 0.01	26.42 ± 0.00	26.41 ± 0.01	26.83 ± 0.05	25.73 ± 0.02
1190	189.184	62.206	28.49 ± 0.08	27.31 ± 0.01	27.46 ± 0.01	27.28 ± 0.02	27.49 ± 0.10	26.34 ± 0.04
1191	189.187	62.207	29.49 ± 99.00	27.29 ± 0.02	27.15 ± 0.01	26.68 ± 0.01	25.51 ± 0.02	25.10 ± 0.02
1226	189.238	62.218	29.49 ± 99.00	27.59 ± 0.02	27.69 ± 0.01	27.66 ± 0.02	28.20 ± 0.17	26.67 ± 0.05
1236	189.163	62.203	29.49 ± 99.00	26.90 ± 0.01	26.56 ± 0.01	26.38 ± 0.01	25.89 ± 0.03	25.90 ± 0.04
1241	189.218	62.214	29.16 ± 0.17	26.60 ± 0.01	26.21 ± 0.00	25.97 ± 0.01	25.95 ± 0.03	25.07 ± 0.01
1264	189.207	62.212	28.77 ± 0.12	26.47 ± 0.01	26.46 ± 0.00	26.42 ± 0.01	26.82 ± 0.06	25.77 ± 0.03
1290	189.213	62.214	29.49 ± 99.00	27.44 ± 0.02	27.29 ± 0.01	27.56 ± 0.02	29.50 ± 0.65	26.77 ± 0.07
1294	189.198	62.211	27.51 ± 0.03	26.30 ± 0.00	26.37 ± 0.00	26.41 ± 0.01	26.63 ± 0.04	26.03 ± 0.03
1295	189.189	62.209	28.33 ± 0.09	26.50 ± 0.01	26.27 ± 0.00	25.97 ± 0.01	25.13 ± 0.01	24.38 ± 0.01
1296	189.236	62.219	29.16 ± 0.16	26.97 ± 0.01	26.91 ± 0.01	26.89 ± 0.01	26.	

Table 2.2: HDF catalog of Sawicki et al. (2007). An uncertainty of 99.00 means the magnitude value is a  $3\sigma$  upper limit.

ID	RA(J2000.0)	Dec(2000.0)	$U_{300}$	$B_{450}$	$V_{606}$	$I_{814}$	$J_{110}$	$H_{160}$
1501	189.173	62.209	30.16 ± 0.35	27.70 ± 0.02	27.70 ± 0.01	27.85 ± 0.02	28.30 ± 99.00	27.92 ± 0.17
1503	189.171	62.208	29.02 ± 0.16	26.97 ± 0.01	26.86 ± 0.01	26.49 ± 0.01	25.65 ± 0.02	25.56 ± 0.03
1516	189.220	62.219	27.93 ± 0.07	26.28 ± 0.01	26.12 ± 0.00	26.08 ± 0.01	26.08 ± 0.04	25.85 ± 0.04
1519	189.180	62.211	29.77 ± 0.49	26.09 ± 0.01	25.97 ± 0.00	26.03 ± 0.01	25.62 ± 0.03	24.90 ± 0.02
1525	189.195	62.214	27.86 ± 0.07	26.70 ± 0.01	26.74 ± 0.01	26.84 ± 0.02	26.89 ± 0.09	26.04 ± 0.05
1528	189.233	62.221	29.07 ± 0.15	27.31 ± 0.01	27.17 ± 0.01	27.18 ± 0.02	27.53 ± 0.11	26.26 ± 0.04
1531	189.188	62.212	29.49 ± 99.00	27.28 ± 0.01	26.98 ± 0.01	26.85 ± 0.01	26.63 ± 0.04	26.12 ± 0.03
1535	189.180	62.211	27.79 ± 0.05	25.43 ± 0.00	25.33 ± 0.00	25.28 ± 0.00	25.25 ± 0.01	24.49 ± 0.01
1539	189.220	62.219	29.32 ± 0.17	27.14 ± 0.01	26.83 ± 0.01	26.91 ± 0.01	26.21 ± 0.03	26.31 ± 0.04
1556	189.180	62.211	29.79 ± 0.17	26.98 ± 0.01	26.70 ± 0.00	26.64 ± 0.01	26.57 ± 0.03	25.47 ± 0.01
1561	189.181	62.211	28.80 ± 0.10	26.95 ± 0.01	26.80 ± 0.01	26.76 ± 0.01	27.32 ± 0.07	25.92 ± 0.03
1592	189.203	62.216	29.74 ± 0.19	27.54 ± 0.01	27.16 ± 0.01	27.05 ± 0.01	27.32 ± 0.06	26.45 ± 0.08
1606	189.237	62.223	28.21 ± 0.06	26.86 ± 0.01	26.84 ± 0.01	26.76 ± 0.01	27.02 ± 0.06	25.89 ± 0.03
1610	189.237	62.223	28.40 ± 0.09	26.60 ± 0.01	26.41 ± 0.00	26.37 ± 0.01	26.19 ± 0.04	25.16 ± 0.02
1611	189.237	62.224	31.68 ± 2.90	26.44 ± 0.01	26.41 ± 0.01	26.41 ± 0.01	25.98 ± 0.05	25.30 ± 0.03
1621	189.188	62.214	26.38 ± 0.03	25.02 ± 0.00	24.96 ± 0.00	24.79 ± 0.00	24.20 ± 0.01	24.04 ± 0.01
1654	189.174	62.212	30.43 ± 1.25	25.86 ± 0.01	25.35 ± 0.00	25.19 ± 0.01	24.52 ± 0.02	23.72 ± 0.01
1662	189.223	62.222	29.49 ± 99.00	26.23 ± 0.00	26.16 ± 0.00	26.23 ± 0.00	26.30 ± 0.03	26.08 ± 0.03
1700	189.190	62.215	28.62 ± 0.10	27.00 ± 0.01	27.13 ± 0.01	27.21 ± 0.02	26.58 ± 0.05	26.63 ± 0.06
1709	189.161	62.210	29.49 ± 99.00	26.49 ± 0.01	26.41 ± 0.01	26.39 ± 0.01	26.56 ± 0.06	25.83 ± 0.04
1734	189.193	62.216	29.34 ± 0.20	27.70 ± 0.02	27.29 ± 0.01	27.72 ± 0.03	29.41 ± 0.64	26.38 ± 0.05
1747	189.167	62.211	29.49 ± 99.00	27.16 ± 0.02	27.07 ± 0.01	27.02 ± 0.02	27.04 ± 0.09	26.68 ± 0.08
1777	189.222	62.223	28.44 ± 0.09	25.44 ± 0.00	25.09 ± 0.00	24.93 ± 0.00	24.90 ± 0.01	24.08 ± 0.01
1903	189.207	62.220	30.03 ± 0.38	27.65 ± 0.02	26.94 ± 0.01	26.55 ± 0.01	26.29 ± 0.04	26.00 ± 0.03
2006	189.191	62.218	29.49 ± 99.00	27.13 ± 0.01	27.06 ± 0.01	26.72 ± 0.01	26.34 ± 0.03	25.65 ± 0.02
2060	189.219	62.225	31.72 ± 1.51	28.29 ± 0.03	27.84 ± 0.01	27.68 ± 0.02	27.90 ± 0.13	27.25 ± 0.09
2066	189.228	62.226	29.49 ± 99.00	27.36 ± 0.01	27.18 ± 0.01	27.06 ± 0.01	27.65 ± 0.09	26.36 ± 0.04
2073	189.235	62.228	29.49 ± 99.00	27.70 ± 0.02	27.65 ± 0.01	27.96 ± 0.03	27.67 ± 0.13	27.19 ± 0.10
2079	189.227	62.226	30.58 ± 0.61	27.27 ± 0.01	27.12 ± 0.01	26.85 ± 0.01	26.76 ± 0.05	26.07 ± 0.04
2095	189.231	62.228	29.63 ± 0.28	26.72 ± 0.01	26.62 ± 0.01	26.49 ± 0.01	26.80 ± 0.06	26.13 ± 0.04
2106	189.187	62.219	30.86 ± 0.60	26.02 ± 0.00	25.90 ± 0.00	25.86 ± 0.00	25.91 ± 0.02	25.29 ± 0.01
2111	189.226	62.227	28.07 ± 0.05	26.33 ± 0.00	26.56 ± 0.00	26.59 ± 0.01	26.75 ± 0.04	25.66 ± 0.02
2169	189.235	62.229	30.06 ± 0.34	28.08 ± 0.03	27.93 ± 0.02	27.86 ± 0.03	30.39 ± 1.38	27.96 ± 0.18
2171	189.228	62.228	27.76 ± 0.05	25.67 ± 0.00	25.56 ± 0.00	25.54 ± 0.00	25.71 ± 0.02	24.98 ± 0.01
2188	189.225	62.227	29.39 ± 0.11	27.08 ± 0.01	27.33 ± 0.01	27.31 ± 0.01	27.36 ± 0.05	26.73 ± 0.04
2206	189.227	62.228	28.28 ± 0.06	26.53 ± 0.01	26.54 ± 0.00	26.58 ± 0.01	26.92 ± 0.05	25.85 ± 0.02
2208	189.214	62.226	29.58 ± 0.22	26.83 ± 0.01	26.65 ± 0.00	26.52 ± 0.01	26.46 ± 0.04	25.68 ± 0.02
2221	189.197	62.222	30.21 ± 0.32	27.99 ± 0.02	27.92 ± 0.01	27.95 ± 0.02	27.89 ± 0.11	27.89 ± 0.14
2228	189.176	62.218	29.44 ± 0.20	26.19 ± 0.00	25.96 ± 0.00	25.53 ± 0.00	24.88 ± 0.01	24.15 ± 0.01
2255	189.209	62.225	28.99 ± 0.14	27.10 ± 0.01	27.36 ± 0.01	27.18 ± 0.02	26.50 ± 0.04	25.79 ± 0.03
2260	189.183	62.220	29.65 ± 0.22	26.89 ± 0.01	26.23 ± 0.00	25.97 ± 0.00	25.90 ± 0.02	24.96 ± 0.01
2282	189.229	62.230	26.63 ± 0.02	24.79 ± 0.00	24.66 ± 0.00	24.59 ± 0.00	24.63 ± 0.01	23.98 ± 0.01
2300	189.227	62.229	28.95 ± 0.11	27.16 ± 0.01	26.74 ± 0.00	26.57 ± 0.01	26.47 ± 0.03	25.70 ± 0.02
2306	189.230	62.230	27.58 ± 0.05	25.85 ± 0.00	25.51 ± 0.00	25.34 ± 0.00	25.26 ± 0.02	24.50 ± 0.01
2342	189.221	62.228	30.03 ± 0.31	27.82 ± 0.02	27.93 ± 0.01	27.77 ± 0.02	27.48 ± 0.09	26.66 ± 0.05
2366	189.184	62.221	29.10 ± 0.15	27.07 ± 0.01	26.67 ± 0.01	26.21 ± 0.01	25.53 ± 0.02	24.35 ± 0.01
2404	189.233	62.232	31.18 ± 0.67	27.97 ± 0.02	27.73 ± 0.01	27.78 ± 0.02	27.29 ± 0.06	26.93 ± 0.05
2409	189.222	62.229	30.73 ± 0.94	27.10 ± 0.02	26.92 ± 0.01	26.89 ± 0.02	26.47 ± 0.06	25.67 ± 0.03
2490	189.225	62.231	29.02 ± 0.07	26.86 ± 0.00	27.00 ± 0.00	27.05 ± 0.01	27.16 ± 0.04	26.13 ± 0.02
2501	189.214	62.229	28.09 ± 0.06	26.13 ± 0.00	26.03 ± 0.00	25.93 ± 0.00	25.85 ± 0.02	25.23 ± 0.01
2560	189.208	62.229	31.55 ± 1.75	26.57 ± 0.01	26.41 ± 0.01	26.32 ± 0.01	25.94 ± 0.03	25.40 ± 0.02
2616	189.213	62.230	28.87 ± 0.14	26.26 ± 0.01	25.70 ± 0.00	25.46 ± 0.00	25.32 ± 0.02	24.53 ± 0.01
2625	189.213	62.230	30.93 ± 0.66	26.88 ± 0.01	26.67 ± 0.00	26.62 ± 0.01	26.51 ± 0.03	26.17 ± 0.03
2702	189.227	62.234	28.11 ± 0.07	26.07 ± 0.01	25.79 ± 0.00	25.66 ± 0.00	25.71 ± 0.02	24.99 ± 0.01
2710	189.208	62.231	26.56 ± 0.02	25.20 ± 0.00	25.12 ± 0.00	24.99 ± 0.00	24.86 ± 0.01	24.12 ± 0.01
2808	189.214	62.232	30.53 ± 0.45	28.34 ± 0.03	27.89 ± 0.01	27.61 ± 0.02	27.83 ± 0.11	27.42 ± 0.10
2832	189.226	62.235	30.91 ± 0.66	27.10 ± 0.01	26.72 ± 0.00	26.66 ± 0.01	26.98 ± 0.05	25.81 ± 0.02
2835	189.228	62.235	31.15 ± 1.06	28.05 ± 0.03	27.68 ± 0.01	27.67 ± 0.03	28.11 ± 0.19	26.93 ± 0.08
2848	189.198	62.238	29.07 ± 0.11	27.61 ± 0.01	27.77 ± 0.01	27.84 ± 0.02	27.95 ± 0.12	27.20 ± 0.08
2849	189.198	62.234	28.22 ± 0.06	26.01 ± 0.00	25.67 ± 0.00	25.52 ± 0.00	25.49 ± 0.01	24.60 ± 0.01
2853	189.191	62.237	27.39 ± 0.05	25.44 ± 0.00	25.26 ± 0.00	25.18 ± 0.00	25.17 ± 0.02	24.57 ± 0.01
2876	189.227	62.236	26.81 ± 0.02	25.69 ± 0.00	25.79 ± 0.00	25.83 ± 0.00	25.91 ± 0.03	25.39 ± 0.02
2894	189.192	62.234	29.28 ± 0.21	27.38 ± 0.02	27.12 ± 0.01	27.21 ± 0.02	27.08 ± 0.08	26.66 ± 0.07
2967	189.190	62.235	29.49 ± 99.00	27.08 ± 0.01	26.80 ± 0.01	26.80 ± 0.01	26.00 ± 0.03	25.61 ± 0.03
3025	189.190	62.231	29.49 ± 99.00	27.37 ± 0.01	26.99 ± 0.01	26.95 ± 0.01	27.18 ± 0.07	26.57 ± 0.05
3036	189.217	62.235	30.31 ± 0.36	27.73 ± 0.02	27.51 ± 0.01	27.61 ± 0.02	27.84 ± 0.11	27.04 ± 0.07
3042	189.202	62.234	29.49 ± 99.00	27.24 ± 0.01	27.24 ± 0.01	27.18 ± 0.01	26.84 ± 0.05	27.20 ± 0.09
3048	189.209	62.234	27.21 ± 0.05	25.06 ± 0.00	24.83 ± 0.00	24.65 ± 0.00	24.32 ± 0.01	23.64 ± 0.01
3083	189.189	62.231	27.24 ± 0.03	25.83 ± 0.00	25.71 ± 0.00	25.59 ± 0.00	25.18 ± 0.01	24.59 ± 0.01
3087	189.217	62.235	28.36 ± 0.10	26.78 ± 0.01	26.49 ± 0.01	26.43 ± 0.01	26.57 ± 0.06	26.23 ± 0.05
3111	189.184	62.236	26.47 ± 0.02	24.67 ± 0.00	24.63 ± 0.00	24.59 ± 0.00	24.53 ± 0.01	24.02 ± 0.01
3115	189.192	62.236	27.51 ± 0.08	25.81 ± 0.01	25.40 ± 0.00	25.41 ± 0.01	25.00 ± 0.02	24.53 ± 0.02
3134	189.181	62.236	28.91 ± 0.15	25.51 ± 0.00	25.12 ± 0.00	25.06 ± 0.00	24.78 ± 0.01	24.04 ± 0.01
3176	189.217	62.243	27.82 ± 0.05	26.05 ± 0.01	25.95 ± 0.00	25.78 ± 0.00	25.61 ± 0.02	25.06 ± 0.02
3189	189.199	62.240	28.47 ± 0.14	26.27 ± 0.01	26.07 ± 0.01	26.41 ± 0.01	25.97 ± 0.04	25.56 ± 0.04
3201	189.228	62.236	30.49 ± 0.68	27.59 ± 0.02	27.22 ± 0.01	27.10 ± 0.02	26.59 ± 0.06	26.28 ± 0.05
3250	189.185	62.234	28.76 ± 0.09	27.28 ± 0.01	27.14 ± 0.01	27.15 ± 0.01	27.34 ± 0.07	27.06 ± 0.07
3255	189.209	62.233	29.49 ± 99.00	27.35 ± 0.01	26.84 ± 0.00	26.63 ± 0.01	27.02 ± 0.04	25.95 ± 0.02
3256	189.218	62.242	29.49 ± 99.00	27.34 ± 0.01	26.99 ± 0.01	26.81 ± 0.01	26.69 ± 0.04	26.61 ± 0.05
3263	189.210	62.233	30.96 ± 0.70	28.08 ± 0.02	27.60 ± 0.01	27.54 ± 0.02	26.90 ± 0.05	26.29 ± 0.04
3264	189.201	62.238	25.95 ± 0.01	24.04 ± 0.00	23.81 ± 0.00	23.50 ± 0.00	23.25 ± 0.00	22.61 ± 0.00
3269	189.191	62.237	29.19 ± 0.17	2				

# Chapter 3

## Model-fitting

### 3.1 SEDfit

#### 3.1.1 The Software

We model-fit selected LBGs using SEDfit, a broadband spectral energy distribution (SED) fitting software package. Now a standard high-redshift galaxy-analysis implement, Sawicki & Yee (1998) pioneered the technique studying  $z > 2$  objects in the HDF. SEDfit quantitatively compares a galaxy's photometry to a cast of models parametrized by redshift, dust content ( $E(B - V)$ ), age, stellar mass, SFR, and photometric magnitudes. A maximum likelihood test ( $\chi^2$ -fit) is the method of comparison. Once the fit is completed for all LBGs in the catalog, SEDfit outputs the best-fitting parameters and associated uncertainties for each object. To calculate the parameter uncertainties, SEDfit perturbs the photometry within its uncertainties and recalculates the best-fit parameters accordingly (Sawicki & Yee 1998). Parameter uncertainties in this work are calculated to 68% confidence using 300 perturbations per object.

The stellar synthesis models of Bruzual & Charlot (2003) provide the underlying spectra used to create our cast of models. We build into these models an assumed solar metallicity, the stellar initial mass function (IMF) of Salpeter (1955), and a star formation history of our choosing. First, the spectra are reddened by the Calzetti et al. (2000) starburst extinction curve. This reddening is quantized in the output as the color excess  $E(B - V)$ . The wavelengths and intensities of the newly reddened spectra are then transposed according to their appointed redshifts and our adopted cosmology,  $(\Omega_M, \Omega_\Lambda, H_0) = (0.3, 0.7, 70 \text{ km s}^{-1} \text{ Mpc}^{-1})$ . Next, the spectra are attenuated below

1216 Å according to the instruction of Madau (1995). This simulates neutral Hydrogen along the line of sight absorbing UV photons emitted by the galaxy. The final step is the integration of these spectra through the instrument-specific filter transmission curves, which generates the cast of model magnitudes SEDfit compares against the real-world photometry (Sawicki & Yee 1998).

The specific best-fit parameter values output by SEDfit are critically dependent upon the details of the assumptions built into the models. For instance, Papovich et al. (2001) use SEDfit to remodel many  $z>2$  HDF objects previously fit by Sawicki & Yee (1998), yet the two teams report differing best-fit parameter values for these galaxies. This discrepancy is attributed to the Papovich group's employment of the Calzetti et al. (2000) extinction law rather than the Calzetti (1997) law adopted by Sawicki & Yee (1998). We therefore note that all model-fit data reported and analyzed in this work assume the stellar IMF of Salpeter (1955), the Calzetti et al. (2000) dust law, and the intergalactic attenuation prescription of Madau (1995). Sawicki et al. (2007), Shapley et al. (2005), and this work all assume solar metallicity, while Yabe et al. (2009) assume 0.2  $Z_{\odot}$ . During our preliminary work, we fit our  $z\sim3$  HDF-S sample with both solar and 0.2  $Z_{\odot}$  metallicities and find no qualitative change in the data's trends. This consistency insures data from the handful of surveys here employed combine to form a coherent picture.

### 3.1.2 The Parameters

The architecture of the model-generating software requires us to define the limits of the parameter spaces that SEDfit will then explore with the input photometry. The age parameter, which measures the time elapsed since the onset of the current episode of star formation, ranges between 5.1 and 10.3 log years with a 0.1 step size between values. We must also delimit the potential values of  $E(B - V)$ . Given the abundant dust in many high-redshift UV-selected galaxies, we provide a generous 0.00 to 1.00 range of possible  $E(B - V)$  fits, although a majority of objects will likely be best-fit with  $E(B - V) < 0.30$ . A step size of 0.02 is chosen to guarantee the necessary detail for later analysis. The final parameter we must constrain to generate the cast of models is the redshift itself.

Each catalog of model SEDs we fit to data allows for redshifts  $0.00 \leq z \leq 5.00$ , with a 0.05 step size. SED fitting cannot reliably determine photometric redshifts any more precisely.

Though these parameter arrays are built into the model catalogs, SEDfit conveniently gives its users the option to further restrict parameters. In fitting our samples, we use this feature to limit the redshifts to a range consistent with our color-color selection criteria. Doing so saves computation time.

The stellar mass and SFR parameters must undergo a scaling process before SEDfit outputs their ultimate best-fit values. To explain, the model magnitudes to which the data are fit are initially scaled to be compatible with a generic, hypothetical galaxy with an equally generic and hypothetical stellar mass and SFR. The real world photometry, on the other hand, originate from sources whose masses and SFRs can vary across orders of magnitude. SEDfit matches the data to a model according to the characteristic shape of the SED and then flux-scales the model magnitudes to values consistent with the data. As the magnitudes are flux-scaled, so are the stellar mass and SFR parameters. Note also that SEDfit automatically corrects its output SFRs for dust attenuation.

Using the Bruzual & Charlot (2003) source code, star formation histories of arbitrary complexity may be constructed. Indeed, exploring the consequences of alternate star formation histories is the central concern of this work. We model-fit our UV-selected  $z\sim 2$  and  $z\sim 3$  galaxies under the assumptions of constant, exponentially increasing, and exponentially decreasing SFHs. The  $U_{300}$ -band is not used to model-fit galaxies at either redshift because the shape of spectrum across that filter is critically dependent upon the specific line-of-sight to individual galaxies.

## 3.2 $z\sim 3$

### 3.2.1 Assuming Constant Star Formation

We first model-fit our sample of 242  $z\sim 3$  LBG candidates from the HDF-S assuming a constant star formation history. Here, the cast of models begin with an unscaled SFR of  $1.0 M_\odot \text{ yr}^{-1}$ . Given that

our  $U_{300}-B_{450}-\mathcal{R}_{VI}$  color-color selection criteria culls objects down to  $z \sim 1.7$ , we allow LBGs in our sample to be fit for redshifts  $1.5 \leq z \leq 3.7$ . To define the subsample of  $z \sim 3$  galaxies, we apply the following photometric redshift cut:

$$2.6 < z_{phot} \leq 3.5. \quad (3.1)$$

Sawicki's  $z \sim 2$  upper limit photo- $z$  cut ( $z_{phot} \leq 2.6$ ; see Eq 2.8) informs our chosen asymmetric  $z \sim 3$  lower limit.

SEDfit places 167 objects at  $z_{phot} \leq 2.6$  and one at a  $z_{phot} > 3.5$ . In total, 62 galaxies are model-fit as genuine  $z \sim 3$  objects according to equation 3.1. Three of these LBGs are best-fit by ages that exceed 2.11 Gyr, the age of the universe at  $z \sim 3$ , while 24 are fit by ages less than 30 Myr (see left panel, Fig. 3.2). When an object is best-fit by an age greater than that of the universe, it indicates the assumed SFH is incorrect and an SFH that generates less stellar mass would be appropriate. The existence of such objects poses no threat to a reliable analysis so long as their number is low, as it is for the CSF model-fits. We discuss age and the treatment of these old and young outliers in the last section of this chapter.

The best-fit parameters for galaxies fit for CSF are listed in Appendix A in Table A.1. We employ no  $\chi^2$ -based criteria for selecting objects. The best-fit spectra and corresponding photometry for four of these galaxies may be inspected in the first column of Figure 3.1. We note the horizontal uncertainties are not uncertainties in the strictest sense. Rather, they signify the FWHM of that filter's transmission curve. This wavelength range is the region across which both the real world and model fluxes are integrated to produce broadband magnitudes.

### 3.2.2 Assuming Exponential Star Formation

#### The Positive $\tau$ Models

We next fit the  $z \sim 3$  catalog assuming an exponentially increasing star formation history. Appropriate models are constructed using the Bruzual & Charlot (2003) source code. Here we equip each model

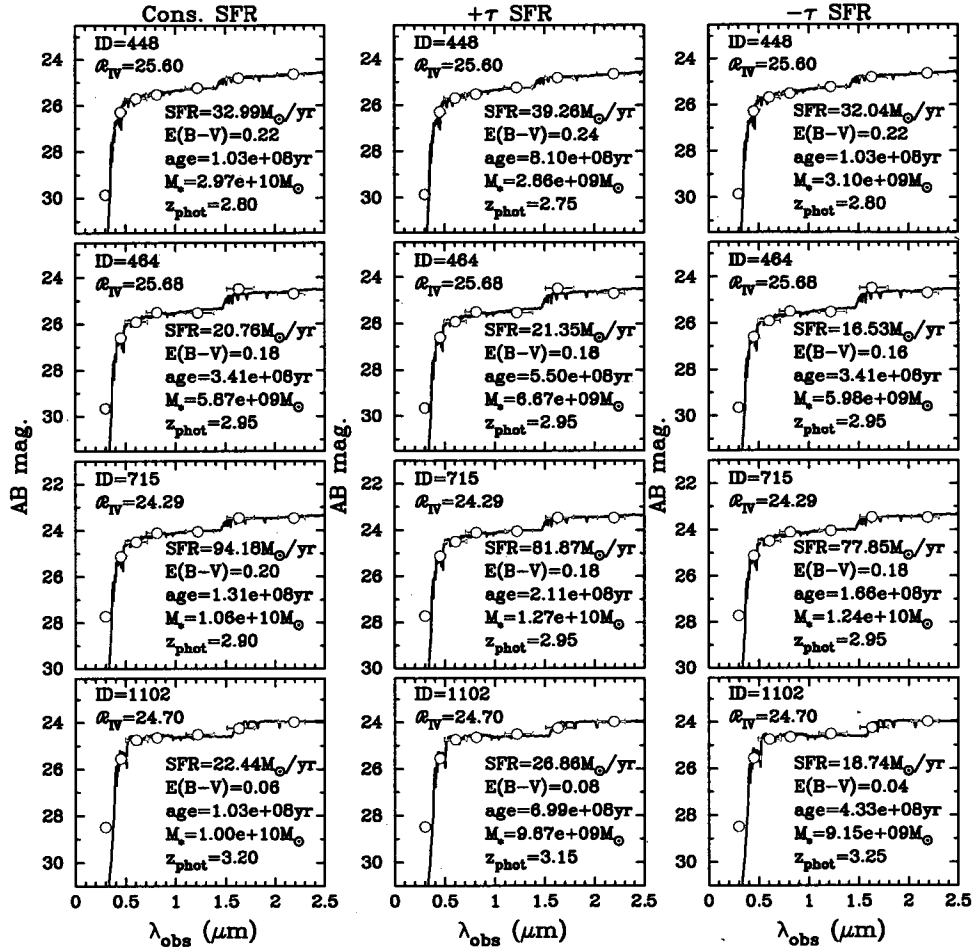


Figure 3.1: Example plots of best-fit model spectra determined by SEDfit assuming 3 different star formation histories. Left to right, the columns assume a constant SFR, an exponentially increasing ( $\tau = 700$  Myr) SFR, and an exponentially decreasing ( $\tau = -700$  Myr) SFR. The spectra are overlaid with the corresponding real-world photometry of  $z \sim 3$  galaxies from the HDF-S. Solid blue circles indicate a detection, while open circles represent upper limits. The horizontal wavelength uncertainties are indicative of the FWHM of that filter's transmission curve. Uncertainties of the magnitudes themselves are on the order of 0.01 or smaller. Best-fit parameters for each LBG are listed in the panels.

with a generic star formation history such that

$$\text{SFR}(t) = \text{SFR}_0 e^{t/\tau}, \quad (3.2)$$

where  $SFR_0 = 1.0 M_{\odot} \text{ yr}^{-1}$ ,  $t$  is the age parameter in units of years, and  $\tau$  is the e-folding, also measured in years. We model-fit our  $z \sim 3$  LBGs for  $\tau$  values of 700, 500, 350, and 250 Myr. The adoption of  $\tau = 700$  Myr is recommended by the good agreement between the evolutionary track of a toy galaxy (with a  $\tau = 700$  Myr SFR function) and data fit under the presumption of constant star formation (see Fig. 4.2). A 900 Myr e-folding evolutionary track was also tested in this way, but its agreement with the model-fit data was found to be qualitatively worse than the 700 Myr track's. Though admittedly inconsistent, this exercise proved instructive in selecting a reasonable  $\tau$ , 700 Myr, to begin our investigation. The 500, 350, and 250 Myr  $\tau$  values represent our efforts to better match the toy galaxy's evolutionary track to the model-fit data. We note here that SED fitting is unable to uniquely constrain  $\tau$  (Papovich et al. 2001; Shapley et al. 2001), and so it cannot be made a free parameter for each galaxy.

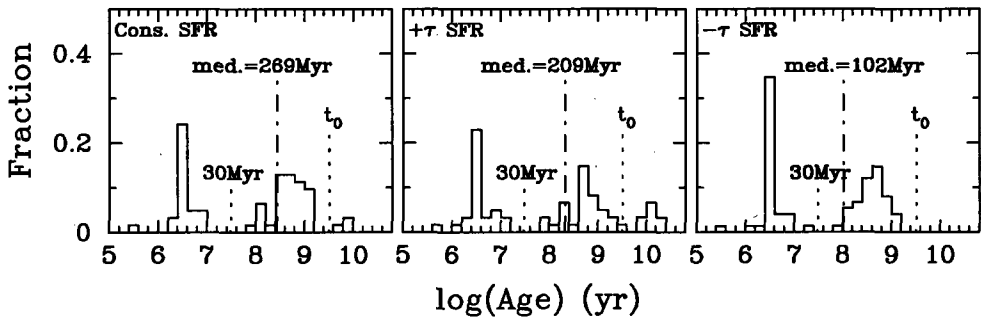


Figure 3.2: Number counts for best-fit ages output by SEDfit for  $z_{phot} \sim 3$  galaxies in the HDF-S assuming constant, exponentially increasing ( $\tau = 700$  Myr), and exponentially decreasing ( $\tau = -700$  Myr) star formation. The median best-fit age is given in each plot. The 2.11 Gyr age of the universe at  $z \sim 3$  is represented by  $t_0$ .

For  $\tau = 700$  Myr, applying the photometric redshift cut of equation 3.1 to the model-fit data identifies 168 objects at  $z_{phot} \leq 2.6$  and one object at a  $z_{phot} > 3.5$ . In total, 61 galaxies are fit as  $z_{phot} \sim 3$  LBGs. Ten of these objects are best-fit by ages older than the  $z \sim 3$  universe, and 25 are younger than 30 Myr (see middle panel, Fig. 3.2). The middle column of Figure 3.1 shows the model spectra and corresponding photometry for four galaxies fit assuming  $\tau = 700$  Myr exponentially increasing SFRs. The best-fit parameters for these objects are listed in Appendix A in Table A.2.

For  $\tau = 500$  Myr, 169 objects are fit for  $z_{phot} \leq 2.6$ , and two are fit for  $z_{phot} > 3.5$ . Altogether, SEDfit identifies 59 galaxies as  $z_{phot} \sim 3$  LBGs. Among these, 14 are best-fit with ages greater than 2.11 Gyr. Twenty-three are younger than 30 Myr. The best-fit parameters for these objects are listed in Appendix A in Table A.3.

For  $\tau = 350$  Myr, 167 objects are fit for  $z_{phot} \leq 2.6$ , and two are fit for  $z_{phot} > 3.5$ . In all, SEDfit classifies 61 galaxies as  $z_{phot} \sim 3$  LBGs. Among these, 23 are best-fit with ages greater than 2.11 Gyr. Twenty-five are younger than 30 Myr. The best-fit parameters for these objects are listed in Appendix A in Table A.4.

For  $\tau = 250$  Myr, 133 objects are fit for  $z_{phot} \leq 2.6$ . None are fit for  $z_{phot} > 3.5$ . Altogether, SEDfit identifies 44 galaxies as  $z_{phot} \sim 3$  LBGs. Among these, 15 are best-fit with ages greater than 2.11 Gyr. Eighteen are younger than 30 Myr. Here we note an unexpected peculiarity. Fifty-four galaxies are best-fit with an age of 20 Gyr. For these objects, SEDfit returns no stellar mass, SFR, flux normalization, or  $\chi^2$  value. We do not count these objects in the tallies presented here. The best-fit parameters for these objects are listed in Appendix A in Table A.5.

### The Negative $\tau$ Model

Having model-fit the  $z \sim 3$  catalog for positive values of  $\tau$ , we subsequently perform the operation again for a token negative  $\tau$  value,  $\tau = -700$  Myr. In sharp contrast with its positive counterpart, the compelling suggestion of a viable  $-\tau$  model is absent from our preliminary evolutionary track experiments. Indeed, the agreement is strikingly poor (see Fig. 4.2). Nonetheless, in the interests of rigor and symmetry, we refit the  $z \sim 3$  LBGs assuming an exponentially decreasing star formation history. Here, SEDfit places 166 objects at  $z_{phot} \leq 2.6$  and one at  $z_{phot} > 3.5$ . Sixty-three galaxies are classified as  $z_{phot} \sim 3$  LBGs according to equation 3.1. Among these, none are fit with ages greater than that of the  $z \sim 3$  universe. Twenty-four are younger than 30 Myr ( see right panel, Fig. 3.2). The best-fit parameters for these objects are listed in Appendix A in Table A.6.

### 3.3 $z \sim 2$

#### 3.3.1 Assuming Exponential Star Formation

From our  $z \sim 3$  model-fits, we learn the best-fit photometric redshift for any given object is relatively unaffected by the assumption of different star formation histories, or at least those tested here. To save computation time, we limit our refits of Sawicki's HDF sample to objects already fit with photometric redshifts ( $1.1 \leq z_{phot} \leq 2.9$ ) moderately close to the  $z \sim 2$  selection window ( $1.8 \leq z_{phot} \leq 2.6$ ). This reduces the size of the Sawicki et al. (2007) catalog from 284 to 171 objects.

#### The Positive $\tau$ Models

Again defining the star formation rate by equation 3.2, we refit the newly reduced Sawicki et al. (2007) sample for an e-folding of 700 Myr. SEDfit places 24 objects at  $z_{phot} < 1.8$  and 49 objects at  $z_{phot} > 2.6$ . In total, 99 galaxies are fit for  $1.8 \leq z_{phot} \leq 2.6$ . This star formation history produces a dramatic effect in the best-fit ages of these objects. The Sawicki group's initial modeling, which assumed constant star formation, generated a  $z_{phot} \sim 2$  sample with only 12 objects older than 3.22 Gyr, the age of the  $z \sim 2$  universe. However, under this new assumed SFR, 55 galaxies, or  $\sim 56\%$  of the sample, are best-fit by unphysical ages. For LBGs at  $z \sim 3$  in the HDF-S, the age distribution holds relatively constant for the  $\tau = 700$  Myr star formation history (see Fig. 3.2). Figure 3.3 shows this is not the case for  $z \sim 2$  galaxies in the HDF. For both  $z \sim 2$  and  $\sim 3$ , successively smaller values of  $\tau$  produce increasingly older populations. The best-fit parameters for these objects are listed in Appendix B in Table B.1.

For an e-folding of 500 Myr, SEDfit places 28 objects at  $z_{phot} < 1.8$  and 47 objects at  $z_{phot} > 2.6$ . In all, 96 objects are fit at  $z_{phot} \sim 2$ . Among these, 67 are fit with ages greater than that of the  $z \sim 2$  universe. Six are younger than 30 Myr. The best-fit parameters for these objects are listed in Appendix B in Table B.2.

For an e-folding of 350 Myr, SEDfit places 27 objects at  $z_{phot} < 1.8$  and 42 objects at  $z_{phot} >$

2.6. In total, 102 objects are fit at  $z_{phot} \sim 2$ . Among these, 77 are fit with ages greater than that of the  $z \sim 2$  universe. Seven are younger than 30 Myr. The best-fit parameters for these objects are listed in Appendix B in Table B.3.

For an e-folding of 250 Myr, SEDfit places 24 objects at  $z_{phot} < 1.8$  and 24 objects at  $z_{phot} > 2.6$ . In all, 64 objects are fit at  $z_{phot} \sim 2$ . Among these, 50 are fit with ages greater than that of the  $z \sim 2$  universe. Six are younger than 30 Myr. As with the  $z \sim 3$  model-fits for  $\tau = 250$  Myr, SEDfit determines a best-fit age of 20 Gyr for 53 objects and returns no stellar mass, SFR, flux normalization, or  $\chi^2$  for them. Again, we do not include these objects in the tallies presented here. The best-fit parameters for these objects are listed in Appendix B in Table B.4.

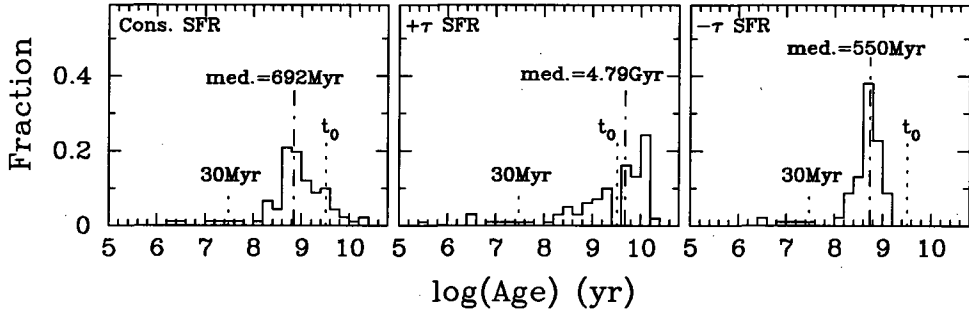


Figure 3.3: Number counts for best-fit ages output by SEDfit for  $z_{phot} \sim 2$  galaxies in the HDF assuming constant, exponentially increasing ( $\tau = 700$  Myr), and exponentially decreasing ( $\tau = -700$  Myr) star formation. The median best-fit age is given in each plot. The 3.22 Gyr age of the universe at  $z \sim 2$  is represented by  $t_0$ .

### The Negative $\tau$ Model

The same negative e-folding we assume for the  $z \sim 3$  fits,  $\tau = -700$  Myr, is assumed here. SEDfit places 21 objects at  $z_{phot} < 1.8$  and 58 objects at  $z_{phot} > 2.6$ . In total, 92 galaxies are fit at  $z_{phot} \sim 2$  according to equation 2.8. Among these, none are best-fit by unphysical ages. This is consistent with the age distribution we find for  $z \sim 3$  LBGs. Five galaxies are younger than 30 Myr. The best-fit parameters for these objects are listed in Appendix B in Table B.5.

Figure 3.4 shows best-fit model spectra and corresponding photometry for four objects from

Sawicki's HDF sample fit at  $z_{phot} \sim 2$ . The first column presents constant star formation, and its best-fit parameters come from Sawicki's upcoming  $z \sim 2$  paper. The second and third columns display exponentially increasing ( $\tau = 700$  Myr) and exponentially decreasing ( $\tau = -700$  Myr) star formation, respectively, and feature best-fit parameters determined by the refitting process described here.

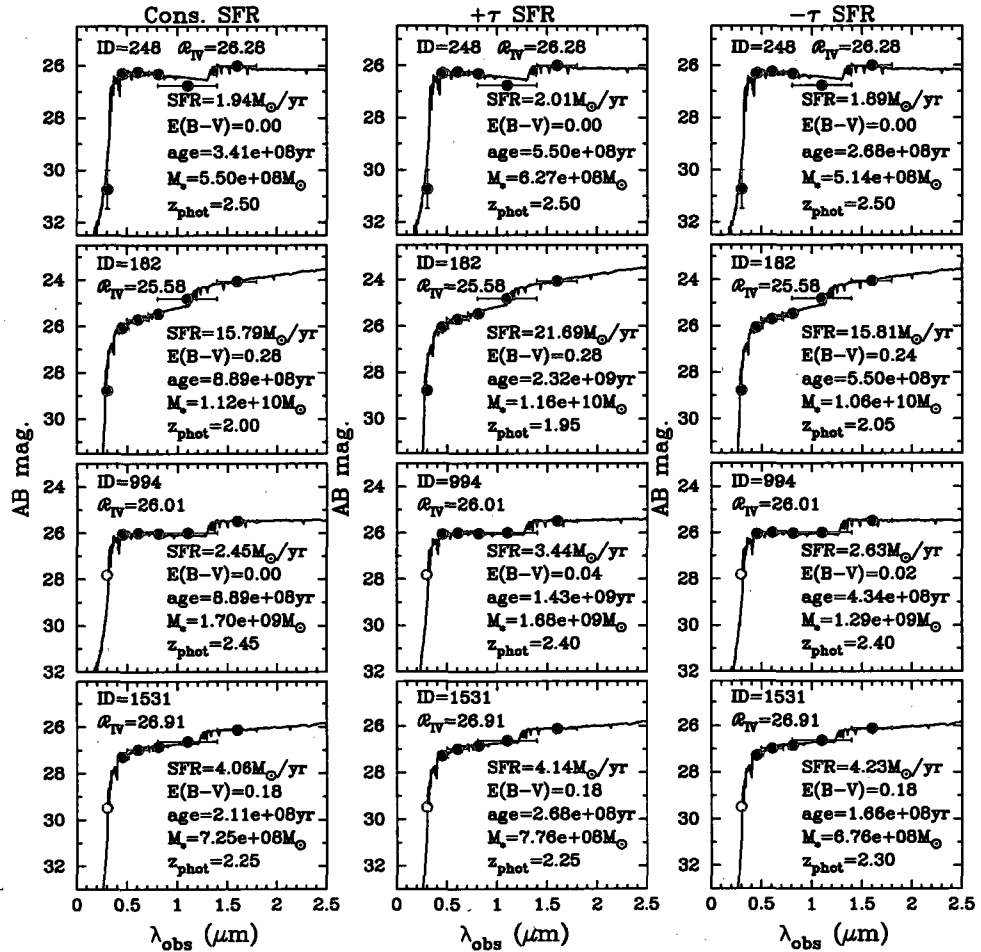


Figure 3.4: Example plots of best-fit model spectra determined by SEDfit assuming 3 different star formation histories. Left to right, the columns assume a constant SFR, an exponentially increasing ( $\tau = 700$  Myr) SFR, and an exponentially decreasing ( $\tau = -700$  Myr) SFR. The spectra are overlaid with the corresponding real-world photometry of  $z \sim 2$  galaxies from the HDF. Solid red circles indicate a detection, while open circles represent upper limits. The horizontal wavelength uncertainties are indicative of the FWHM of that filter's transmission curve. Uncertainties of the magnitudes themselves are mostly on the order of 0.01 or smaller. Best-fit parameters for each LBG are listed in the panels. Photometry courtesy Sawicki.

### 3.4 Age Considerations

In Chapter 4, we present, for inspection, data encompassing the entire range of model-fit ages but limit our calculations to objects whose ages are best fit between  $\sim 30$  Myr and the age of the universe at their particular redshift.

$$30\text{Myr} < \text{age} < t_0 \quad (3.3)$$

The reason for the latter cut is the unphysical nature of the best-fit ages caused by an incorrectly assumed SFH. We enact the young-end age cut because the star formation rates SEDfit calculates for galaxies dominated by young stellar populations are disproportionately high given their masses. This creates a secondary population of very young objects whose best-fit parameters clash with those of more mature galaxies. This population may be seen in the model-fit catalogs of Shapley et al. (2005) and Yabe et al. (2009), as well as our own  $z \sim 3$  HDF-S catalog (see Fig. 4.1).

Let us first assume these suspiciously high SFRs are real. This project investigates the evolution of galaxy parameters across cosmological timescales. To do so, we rely upon trends in the best-fit parameters output by SEDfit. At  $z \sim 5$ ,  $\sim 3$ , and  $\sim 2$ , it is unlikely these objects are legitimately young. More probably, these are older galaxies whose underlying, more representative stellar populations are being obscured by very young starbursts. So to include this offset population of extremely young objects in our analysis would bias our results against those objects that parameterize the majority of a galaxy's lifetime ( $\sim 30$  Myr  $\leq$  age  $\leq$   $t_0$ ). Put another way, we do not wish to obscure the trends of stable, sustained evolution in favor of the transient, rapid evolution of newly starbursting galaxies.

Let us now assume the alternative. The aberrantly high model-fit SFRs of young galaxies are an unphysical artifact of the fitting process itself. This interpretation is bolstered by the lack of a natural spread in the data; the relation between SFR and stellar mass is suspiciously tight among these objects. In either case, we restrict them from our analysis.

We stress that the existence of these outlying young and old populations is to be expected based on the results of previous SED-fitting studies. Our age restriction is relatively innocuous

to the analyses of constant star formation and the  $\pm 700$  Myr  $\tau$  models. The usable population is still large enough to reliably identify trends in the model-fit data. However, the subset of galaxies satisfying equation 3.3 becomes disadvantageously small for the 500 Myr  $\tau$  model-fits and statistically untenable for the 350 and 250 Myr e-folding fits. This aging effect is more pronounced in the Sawicki group's HDF catalog, but is also seen in our HDF-S sample. We are therefore forced to limit our analyses of exponentially increasing SFRs to the 700 and 500 Myr e-folding model-fits.

# Chapter 4

# Analysis

## 4.1 The Stellar Mass-Star Formation Rate Relation

### 4.1.1 For Constant Star Formation

We first consider the stellar mass-star formation rate relation as it applies to galaxies model-fit assuming constant star formation. Figure 4.1 presents the dependence of star formation rate on stellar mass. Excluding the age  $\geq t_0$  and age  $\leq \sim 30$  Myr outlying populations (see section 3.4), the remaining galaxies are fit with the following formula:

$$\log\left(\frac{\text{SFR}}{M_\odot/\text{yr}}\right) = 0.83\log\left(\frac{M_{\text{stars}}}{M_\odot}\right) - 7.14 + \delta_z, \quad (4.1)$$

where

$$\delta_{z\sim 2} = 0.00, \delta_{z\sim 3} = 0.20, \text{ and } \delta_{z\sim 5} = 1.01. \quad (4.2)$$

We use a standard matrix inversion technique to calculate a least squares/minimum  $\chi^2$  second-order polynomial fit to the combined  $z\sim 2$  data sets of Sawicki and Shapley et al. (2005). This calculation accounts for the first three terms of equation 4.1. We assume the  $z\sim 2$  slope for all data sets because, for higher redshifts, the data are not good enough to reliably constrain both the slope of the line and its normalization. This is not an ideal situation, but, until more data are acquired, it will have to suffice. Next, we calculate the median residual offset of each population from the  $z\sim 2$  line of best-fit (see Fig. 4.1, bottom right panel). The  $\delta$ -term then comes directly from each population's

median residual offset relative to the median  $z \sim 2$  residual offset:

$$\delta_z = \kappa_z - \kappa_{z \sim 2}. \quad (4.3)$$

The variable  $\kappa$  represents the median residual offset, and the subscript  $z$  indexes the  $z \sim 2$ , 3, and 5 galaxy populations. Hence,  $\delta_{z \sim 2}$  is always zero. We adopt this process to calculate linear relationships throughout our analysis.

The simple assumption we make in equation 4.1 and Figure 4.1 is that a single unifying slope describes the  $M_{stars}$ -SFR relation, regardless of redshift. As a population of galaxies evolves over cosmological time, here converting gas into stars at an assumed constant rate, that slope translates accordingly to higher and higher stellar masses, but its essential character remains unchanged. In the bottom right panel of Figure 4.1, the increased spread at  $z \sim 3$  and  $\sim 5$  argues that this assumption is not perfectly valid, but it does not appear to be altogether unreasonable, either. Again, given the relatively poor quality of the  $z \sim 3$  and  $\sim 5$  data, this analysis must suffice for now.

Having observed some progression in the model-fit data, our next task is to test the efficacy of the constant star formation assumption. Toward this end, we evolve a toy galaxy from  $z \sim 5$  to  $z \sim 2$  and compare the agreement between the toy's evolutionary track and the limits set by the model-fit data.

We quantify the data's spread by calculating the population root-mean-square (PRMS) deviation for each galaxy set. This measures each sample's average deviation from its  $\kappa_z$  according to

$$PRMS_z = \sqrt{\frac{\sum_{n=0}^N (x_{n,z} - \kappa_z)^2}{N}} \quad (4.4)$$

where

$$x_{n,z} = \log \left( \frac{SFR_{n,z}}{SFR_{best-fit\ line,z \sim 2}} \right) \quad (4.5)$$

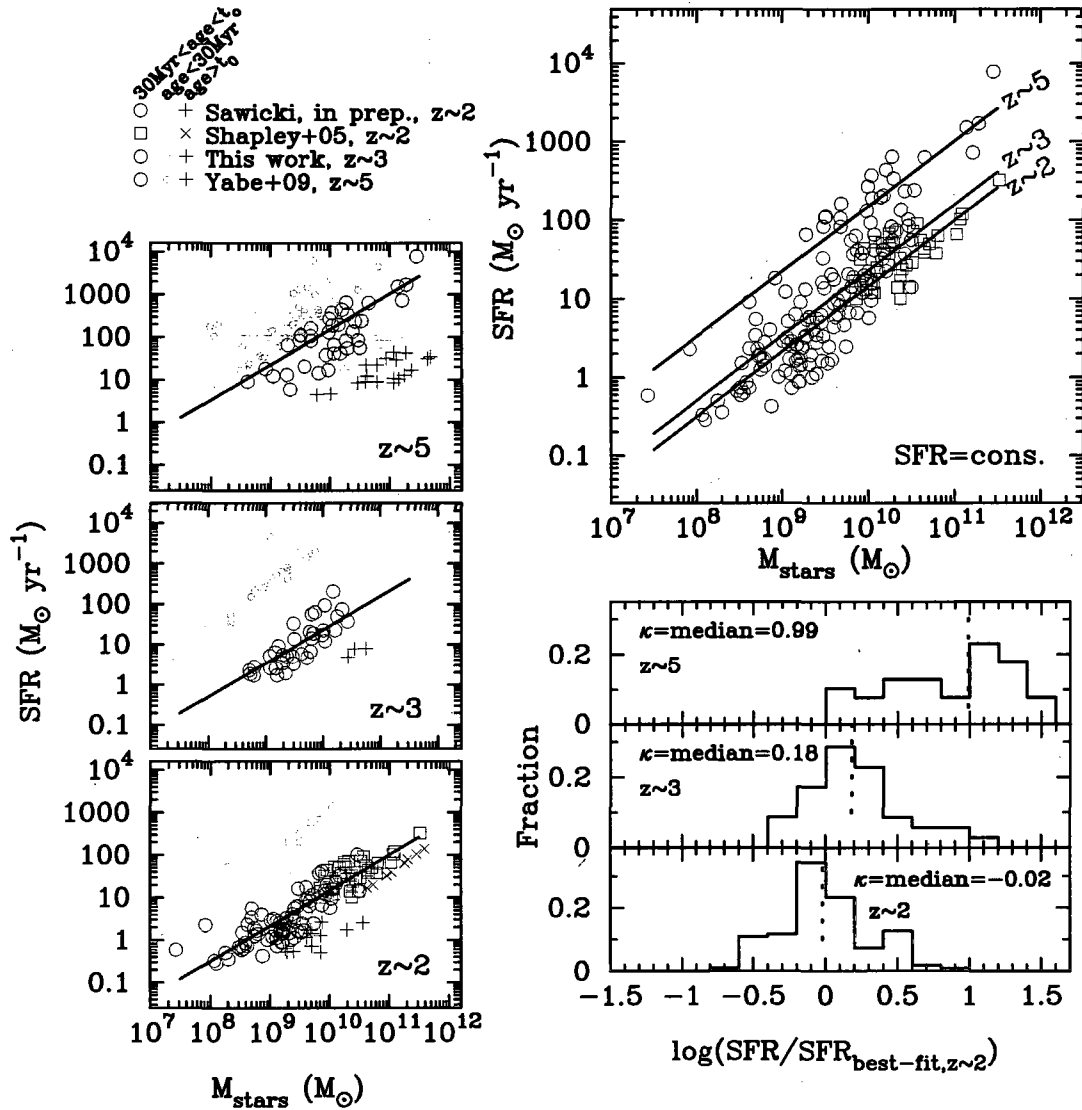


Figure 4.1: Stellar masses versus constant star formation rates. The three leftmost vertical panels display the complete data set(s) at each redshift. Uncertainties are plotted in light grey for all objects  $\sim 30 \text{ Myr} \leq \text{age} \leq t_0$ . The top right panel shows these intermediate aged objects and their corresponding lines of best-fit. The best-fit slope is calculated from the combined  $z \sim 2$  data sets of Sawicki et al. (2007) and Shapley et al. (2005). That slope is then assumed for the  $z \sim 3$  and  $z \sim 5$  populations. The bottom right panel displays the residual offsets for all data relative to the  $z \sim 2$  line of best-fit. We use these offsets to calculate the  $\delta$ -term for each redshift in Equation 4.1.

for the  $n^{\text{th}}$  element in a galaxy set  $z$  containing  $N$  elements. We broaden the best-fit line for each redshift group by  $\pm \text{PRMS}_z$ . This defines the region of acceptable agreement in the  $M_{\text{stars}}\text{-SFR}$  parameter-plane at each redshift. For galaxies fit assuming constant star formation, the PRMS

values are

$$\text{PRMS}_{z \sim 2} = 0.32, \text{ PRMS}_{z \sim 3} = 0.33, \text{ and } \text{PRMS}_{z \sim 5} = 0.41. \quad (4.6)$$

Note that some of the data spread's broadening (i.e., the magnitude of  $\text{PRMS}_z$ ) at  $z \sim 3$  and  $\sim 5$  is artificial and caused by our assumption of a fixed slope for all populations.

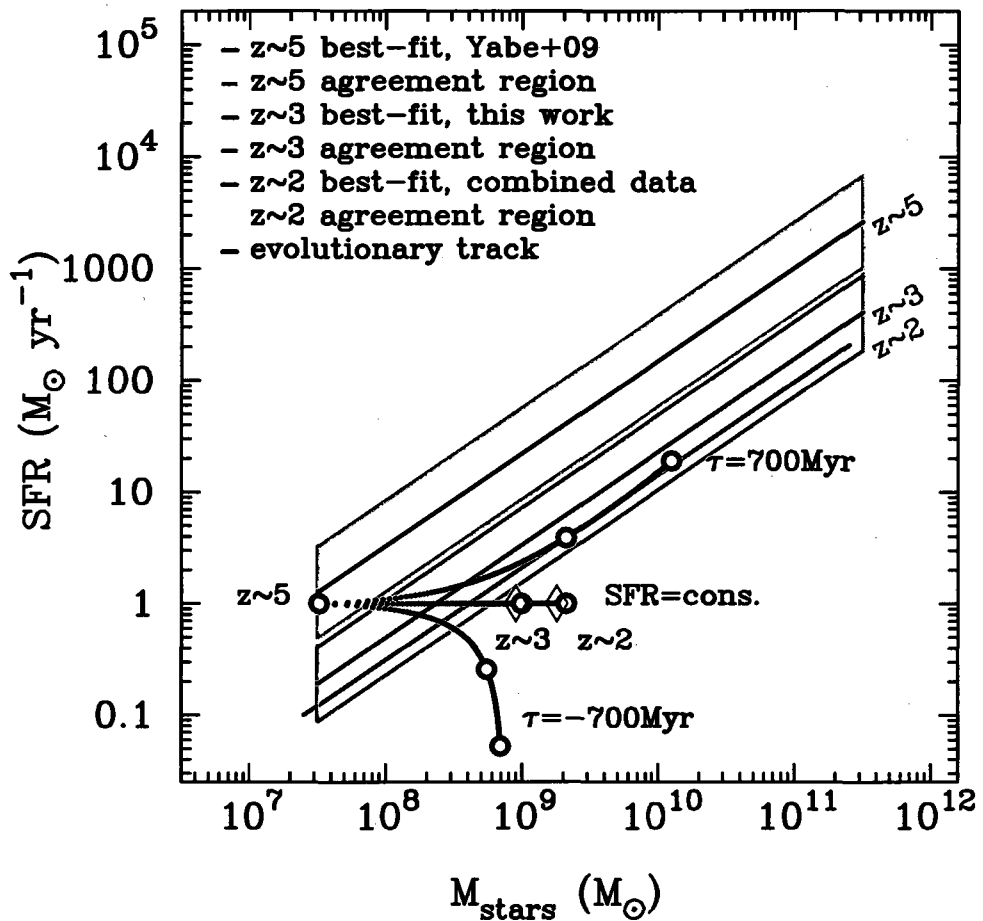


Figure 4.2: Stellar masses versus constant star formation rates. The black line is the evolutionary track of a toy galaxy evolved from  $z \sim 5$  to  $z \sim 2$ . The open circles mark the location of the toy without accounting for mass loss, while the diamonds correct for mass loss. The  $z \sim 5$ ,  $\sim 3$ , and  $\sim 2$  best-fit lines are displayed in green, blue, and red, respectively. The light green, light blue, and pink lines enclose each redshift group's region of acceptable agreement (see Eqs. 4.4 and 4.5). At  $z \sim 3$ , the toy galaxy is  $4.02 \times 10^8 M_\odot$ , or  $\sim 70\%$ , more massive than the upper limit acceptable mass. At  $z \sim 2$ , the toy is  $1.14 \times 10^9 M_\odot$ , or  $\sim 120\%$ , more massive than the acceptable upper limit.

Our toy galaxy begins its evolution at  $z \sim 5$  as a  $3.25 \times 10^7 M_\odot$  object transforming gas into

stars at a constant rate of  $1.0 \text{ M}_\odot \text{ yr}^{-1}$ . Note this evolutionary track is completely independent of galaxy age, meaning its epoch of formation is irrelevant to any subsequent evolution. Also note that the shape of this track, and all tracks explored in this work, are independent of initial stellar mass. The evolutionary track simply translates along the  $z \sim 5$  best-fit line according to its initial stellar mass and initial SFR. At  $z \sim 3$ , we find the toy evolved to  $9.77 \times 10^8 \text{ M}_\odot$ . To agree with the  $z \sim 3$  data spread, a galaxy with a  $1.0 \text{ M}_\odot \text{ yr}^{-1}$  SFR must not be more massive than  $5.75 \times 10^8 \text{ M}_\odot$ . The mass of the toy already overshoots the data by  $\sim 70\%$ . At  $z \sim 2$ , the toy has grown to  $2.09 \times 10^9 \text{ M}_\odot$ , which surpasses the upper limit acceptable mass by  $\sim 120\%$ . The open circles in Figure 4.2 mark this evolution, which does not account for stellar mass loss due to gas recycled back into the interstellar medium by stellar winds and supernovae. Using the Bruzual & Charlot (2003) model-construction files, we correct the stellar mass of the toy galaxy at  $z \sim 3$  and  $z \sim 2$  to account for this mass loss (shown as diamonds in Fig. 4.2). We calculate that, at  $z \sim 3$ , a galaxy retains  $\sim 91\%$  of the stellar mass it has created. At  $z \sim 2$ , this figure decreases to  $\sim 84\%$ . The mass loss correction trivially improves the agreement between the toy's evolutionary track and the model-fit data, with the masses still overshooting at both epochs. This result argues against the SFHs of high-redshift galaxies being best characterized by CSF.

#### 4.1.2 For Exponential Star Formation

$\tau = 700 \text{ Myr}$

We now turn our attention to the  $M_{stars}$ -SFR relation as derived from data model-fit assuming exponential star formation of the form  $\text{SFR}(t) \propto e^{t/\tau}$  (see Eq. 1.7). We first investigate  $\tau = 700 \text{ Myr}$ . Figure 4.3 shows a revised plot of the dependence of star formation rate on stellar mass. Again ignoring extremely old or young outliers (see section 3.4), we fit the remaining populations by

$$\log \left( \frac{\text{SFR}}{M_\odot/\text{yr}} \right) = 0.81 \log \left( \frac{M_{stars}}{M_\odot} \right) - 6.73 + \delta_z, \quad (4.7)$$

where

$$\delta_{z \sim 2} = 0.00 \text{ and } \delta_{z \sim 3} = 0.16. \quad (4.8)$$

Without the Shapley group's photometry to refit, we rely solely upon the Sawicki group's  $z \sim 2$  sample from the HDF to calculate the new best-fit line coefficients. The least-squares/minimum  $\chi^2$  polynomial fit here returns a slightly shallower slope and a reduced offset between the  $z \sim 2$  and  $z \sim 3$  populations. However, these shifts are minor despite the dramatic reduction in the sample's size. Recall the median value of the 700 Myr  $\tau$ -assuming best-fit ages is greater than the age of the universe at  $z \sim 2$  (see Fig. 3.3). The stubborn consistency of the best-fit slope is certainly noteworthy. The more massive galaxies in each redshift group have systematically higher SFRs. Most importantly, the data remain suggestive that our assumption of a fixed slope for all galaxy populations remains reasonable, if not ideal.

Once again, we test the efficacy of the underlying star formation assumption by evolving a toy galaxy from  $z \sim 5$  to  $z \sim 2$ . For this analysis, we must also regrettably proceed without any refit  $z \sim 5$  photometry from Yabe et al. (2009). We are nonetheless confident in retaining approximately the same  $z \sim 5$  starting point for the toy model's evolution (calculated assuming  $\delta_{z \sim 5} = 1.01$ ) given the enduring consistency of the  $M_{stars}$ -SFR relation. The best-fit lines for each redshift are broadened into regions of acceptable agreement by

$$\text{PRMS}_{z \sim 2} = 0.27 \text{ and } \text{PRMS}_{z \sim 3} = 0.28. \quad (4.9)$$

When assuming an exponential star formation history, we must consider the age of the galaxy at the epoch we begin to track its evolution because the galaxy's SFR is increasing exponentially right from its inception. To test the effects of this time dependency, we evolve toy galaxies with 1, 10, and 100 Myr ages at  $z \sim 5$ . These ages correspond to  $z \sim 5$  SFRs of 1.00, 1.02, and  $1.16 M_{\odot} \text{ yr}^{-1}$ , respectively. The effects in both  $\log(M_{stars}/M_{\odot})$  and  $\log(\text{SFR}/(M_{\odot}/\text{yr}))$  are found to be negligible, on the order of  $\sim 0.01$ . We assign the toy galaxy an age $_{z \sim 5}$  of 100 Myr. Irrefutably, this would be

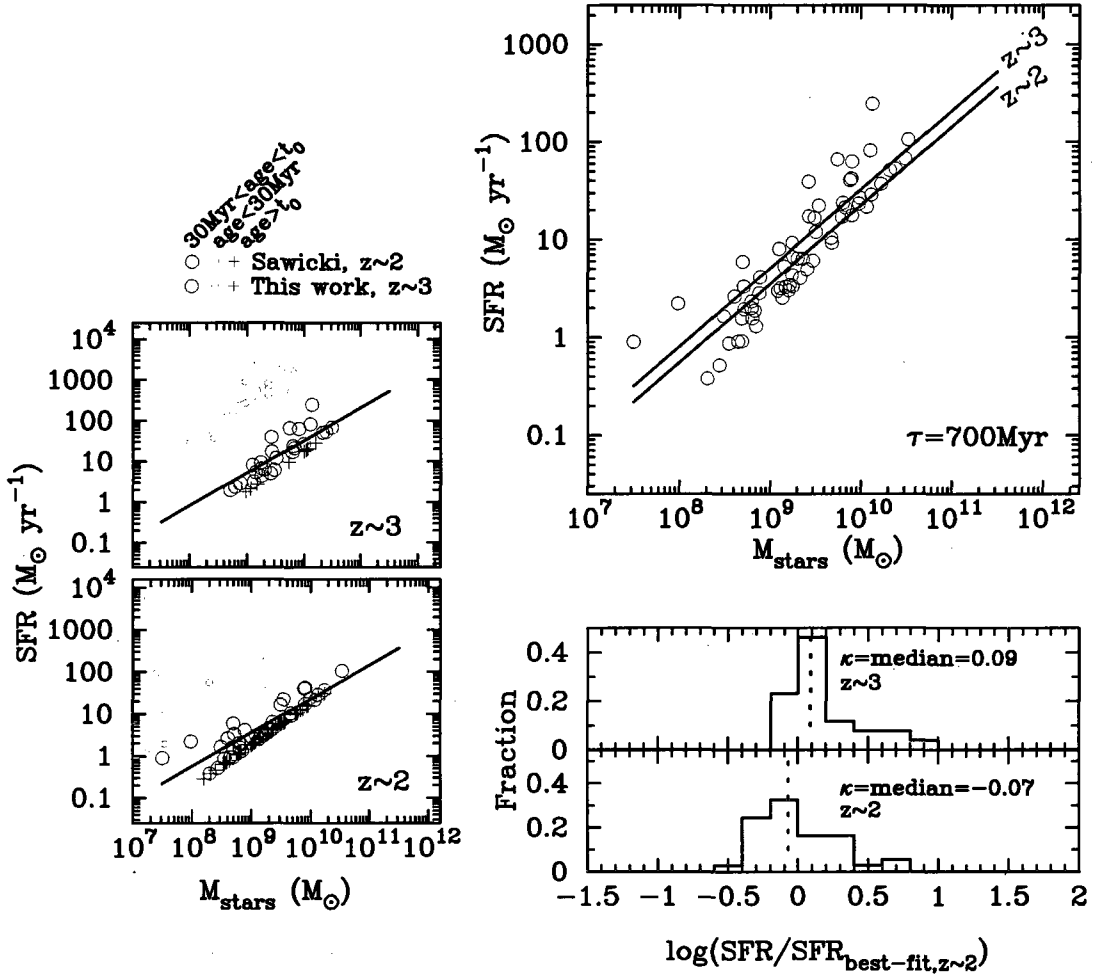


Figure 4.3: Stellar masses versus exponentially increasing star formation rates ( $\tau = 700$  Myr). The two leftmost vertical panels display the complete data set at each redshift. Uncertainties are plotted in light grey for all objects  $\sim 30$  Myr  $\leq$  age  $\leq t_0$ . The top right panel shows these intermediate aged objects and their corresponding lines of best-fit. The best-fit slope is calculated from the Sawicki et al. (2007)  $z \sim 2$  data set. That slope is then assumed for the  $z \sim 3$  population. The bottom right panel displays the residual offsets for all data relative to the  $z \sim 2$  line of best-fit. We use these offsets to calculate the  $\delta$ -term for each redshift in Equation 4.7.

a late forming galaxy because surveys have identified galaxy populations at  $z \geq 7$  (Bouwens et al. 2008, Labb   et al. 2010). However, the 100 Myr  $\text{age}_{z \sim 5}$  is consistent with the median age fit by Yabe et al. (2009), and we assume these objects are experiencing their inaugural starburst episodes. If the formation epoch of the toy is not completely consistent with observations, the toy itself is still useful in qualitatively assessing the star formation history.

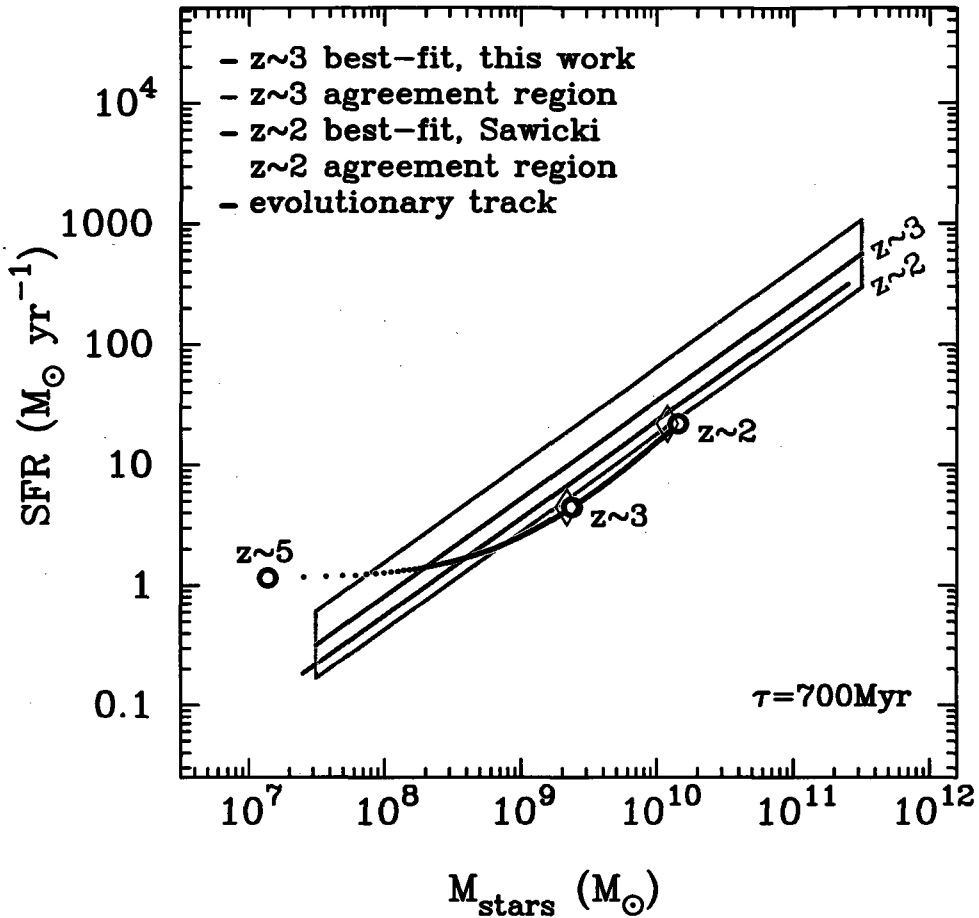


Figure 4.4: Stellar masses versus exponentially increasing star formation rates ( $\tau = 700$  Myr). The black line is the evolutionary track of a toy galaxy evolved from  $z \sim 5$  to  $z \sim 2$ . The open circles mark the evolution of toy with no correction for mass loss. The diamonds mark its evolution as adjusted for mass loss. The  $z \sim 2$  and  $\sim 3$  best-fit lines are shown in red and blue, respectively. The pink and light blue lines outline each redshift group's region of acceptable agreement. At  $z \sim 3$ , the toy galaxy is  $\sim 58\%$  more massive than the spread in observational data allows. By  $z \sim 2$ , the toy has evolved into a  $1.45 \times 10^{10} M_{\odot}$  object forming stars at  $21.88 M_{\odot} \text{ yr}^{-1}$ . These values lie within the  $z \sim 2$  region of acceptable agreement.

The toy begins its evolution at  $z \sim 5$  as a  $1.38 \times 10^7 M_{\odot}$  object converting gas into stars at a rate of  $1.16 M_{\odot} \text{ yr}^{-1}$ . At  $z \sim 3$ , the toy galaxy has evolved to  $2.34 \times 10^9 M_{\odot}$ , which overshoots the upper limit acceptable mass by  $8.60 \times 10^8 M_{\odot}$ , or  $\sim 58\%$ . Correcting for mass loss does not bring this evolution into agreement with the model-fit data. However, 1.11 Gyr later, the toy galaxy has evolved into a  $1.45 \times 10^{10} M_{\odot}$  object generating new stars at  $21.88 M_{\odot} \text{ yr}^{-1}$ . This position on the

$M_{stars}$ -SFR plain lies within the  $z \sim 2$  region of acceptable agreement (see Fig. 4.4).

$\tau = 500$  Myr

We next fit the  $M_{stars}$ -SFR relation as it applies to the 500 Myr e-folding model-fits:

$$\log\left(\frac{\text{SFR}}{M_\odot/\text{yr}}\right) = 0.86\log\left(\frac{M_{stars}}{M_\odot}\right) - 7.07 + \delta_z, \quad (4.10)$$

where

$$\delta_{z \sim 2} = 0.00 \text{ and } \delta_{z \sim 3} = 0.08. \quad (4.11)$$

Figure 4.5 shows the dependence of star formation rate on stellar mass for these galaxies. We note here the drastic reduction in sample size for the 500 Myr e-folding. This reduction is enforced by the age cut of equation 3.3 (see section 3.4). The  $z \sim 2$  sample consists of 23 galaxies (down from 37 for  $\tau = 700$  Myr), and the  $z \sim 3$  sample consists of 22.

To test the efficacy of 500 Myr e-folding SFR, we broaden the best-fit lines defined by equations 4.10 and 4.11 according to the PRMS deviations of the model-fit data:

$$\text{PRMS}_{z \sim 2} = 0.24 \text{ and } \text{PRMS}_{z \sim 3} = 0.25. \quad (4.12)$$

We now track the evolution of a toy galaxy from  $z \sim 5$  to  $z \sim 2$ . The toy begins at  $z \sim 5$  with a stellar mass of  $1.41 \times 10^7 M_\odot$  and an SFR of  $1.23 M_\odot \text{ yr}^{-1}$ . At  $z \sim 3$ , the toy evolves to a  $3.55 \times 10^7 M_\odot$  galaxy creating new stars at a rate of  $8.32 M_\odot \text{ yr}^{-1}$ . This mass overshoots the  $3.09 \times 10^9 M_\odot$  upper limit of the data's spread by  $\sim 15\%$ . Correcting for mass loss does not bring the toy galaxy and model-fit data values into agreement. By  $z \sim 2$ , the toy has become a  $3.80 \times 10^{10} M_\odot$  object with a  $75.86 M_\odot \text{ yr}^{-1}$  SFR, which resides inside the  $z \sim 2$  region of acceptable agreement. A mass loss correction is unnecessary here (see Fig. 4.6). For both the 700 Myr and 500 Myr e-foldings, the agreement between the toy galaxy's evolutionary track and the model-fit observations

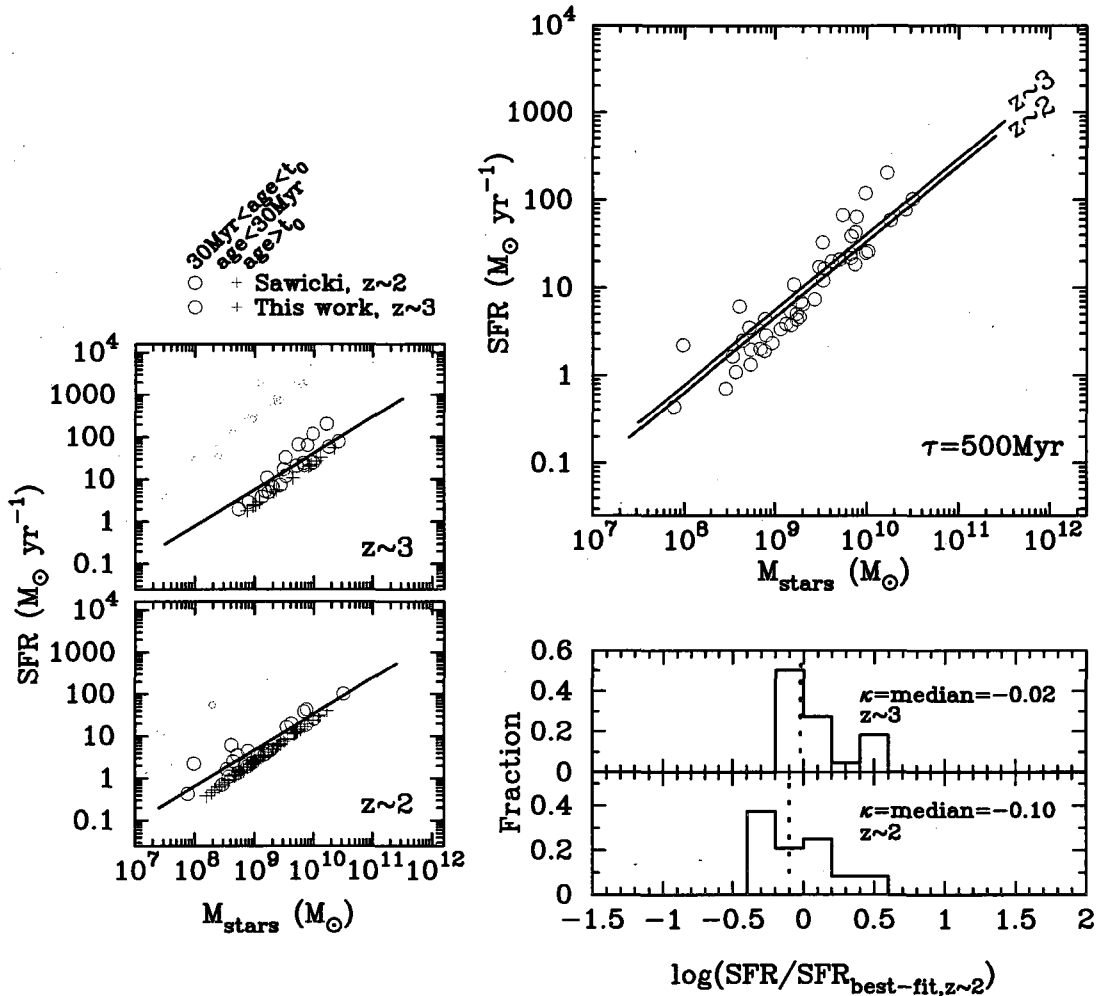


Figure 4.5: Stellar masses versus exponentially increasing star formation rates ( $\tau = 500$  Myr). The two leftmost vertical panels display the complete data set at each redshift. Uncertainties are not calculated for these model-fits but are assumed to be similar to the 700 Myr e-folding model. The top right panel shows these intermediate aged objects and their corresponding lines of best-fit. The best-fit slope is calculated from the Sawicki et al. (2007)  $z \sim 2$  data set. That slope is then assumed for the  $z \sim 3$  population. The bottom right panel displays the residual offsets for all data relative to the  $z \sim 2$  line of best-fit. We use these offsets to calculate the  $\delta$ -term for each redshift in Equation 4.10

are qualitatively very similar because of small adjustments in the  $M_{\text{stars}}$ -SFR relation between the two e-foldings. Even so, the  $\tau = 500$  Myr evolutionary track better agrees with its model-fit data than the 700 Myr track, though both exponential models show better agreement than the CSF model.

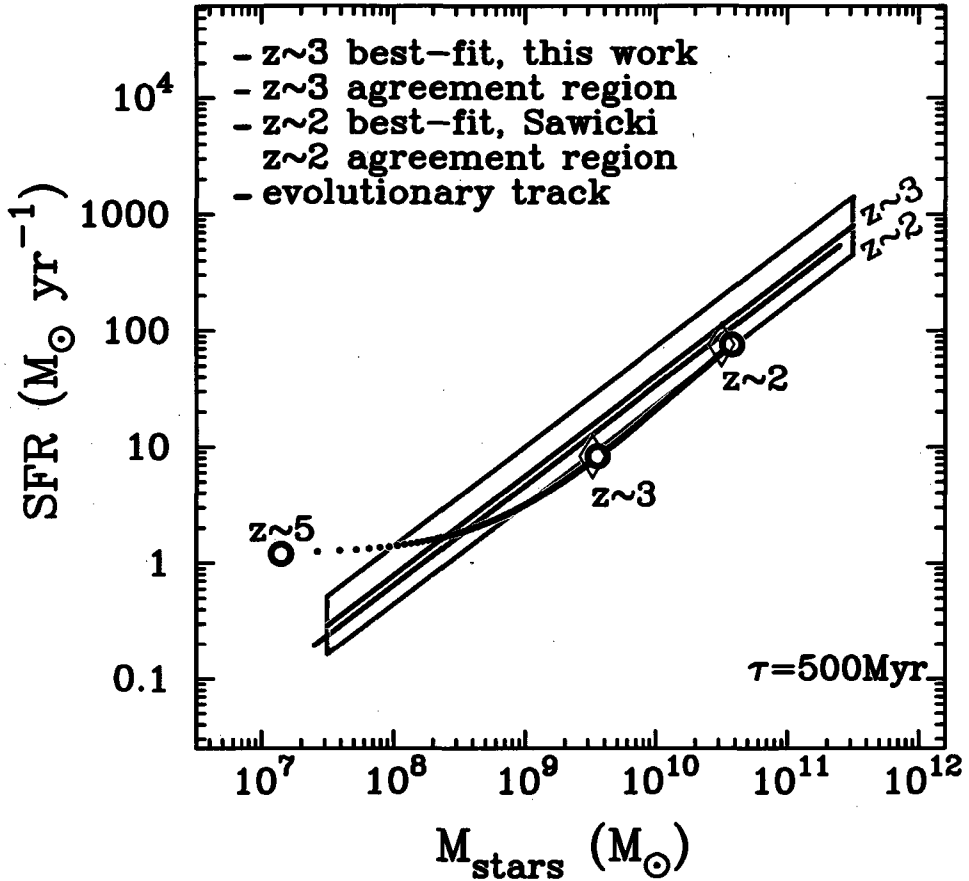


Figure 4.6: Stellar mass versus exponentially increasing star formation rates ( $\tau = 500$  Myr). The black line is the evolutionary track of a toy galaxy evolved from  $z \sim 5$  to  $z \sim 2$ . The open circles mark the evolution of toy with no correction for mass loss. The diamonds mark its evolution as adjusted for mass loss. The  $z \sim 2$  and  $\sim 3$  best-fit lines are shown in red and blue, respectively. The pink and light blue lines outline each redshift group's region of acceptable agreement. At  $z \sim 3$ , the mass of the toy overshoots the upper limit acceptable mass  $\sim 15\%$ . Correcting for mass loss does not bring the toy galaxy into agreement with the data. At  $z \sim 2$ , the toy's evolution is consistent with the data spread, and no correction for mass loss is necessary.

$\tau = 350, 250$  Myr

We once more reiterate that we model-fit the Sawicki group's  $z \sim 2$  HDF catalog and our  $z \sim 3$  HDF-S catalog for e-foldings of 350 and 250 Myr. However, the number of usable galaxies, given our age cut, is so low that we cannot identify meaningful trends in the data. Furthermore, the trend of successively smaller e-foldings producing older and older best-fit ages in the populations signals

that our assumed star formation histories are flawed. These galaxies would be better fit by SFHs that generate less stellar mass. The star formation histories of real galaxies are most likely much more complex than the simple exponential with which we fit them. Also, the ages model-fit to the observational data are indicative of the time elapsed since the onset of the current starburst, while we determine the e-foldings to which the data are fit from toy galaxy evolutionary tracks that assume a single starburst that lasts the toy's entire lifetime. Again, this is greatly simplified against reality and contributes to the unphysical model-fits to the data.

### The Negative $\tau$ Model

The final star formation assumption this work explores is the negative  $\tau$  model. This SFR is structurally identical to the positive  $\tau$  model, except the e-folding time is negative instead of positive. To appropriately contrast the two exponential regimes, we have adopted  $\tau = -700$  Myr. Figure 4.7 shows the dependence of star formation rate on stellar mass for galaxies fit with decreasing exponential SFRs.

As neither galaxy population contains any objects best-fit for ages  $\geq t_0$ , we need only restrict the extremely young outliers from our calculations (see section 3.4). Galaxies with ages  $\geq \sim 30$  Myr are fit by

$$\log\left(\frac{\text{SFR}}{M_\odot/\text{yr}}\right) = 0.80\log\left(\frac{M_{\text{stars}}}{M_\odot}\right) - 7.00 + \delta_z, \quad (4.13)$$

where

$$\delta_{z\sim 2} = 0.00 \text{ and } \delta_{z\sim 3} = 0.27. \quad (4.14)$$

Best-fit line coefficients are again calculated exclusively from the Sawicki et al. (2007)  $z\sim 2$  sample. Now fit for three markedly divergent star formation archetypes, the slope of the  $M_{\text{stars}}$ -SFR relation remains conspicuously robust. Indeed, the choice of underlying star formation history impacts the total  $M_{\text{stars}}$ -SFR relation very little, even as that assumption shifts and reshuffles parameters within the galaxy populations (see Figs. 3.1 and 3.4).

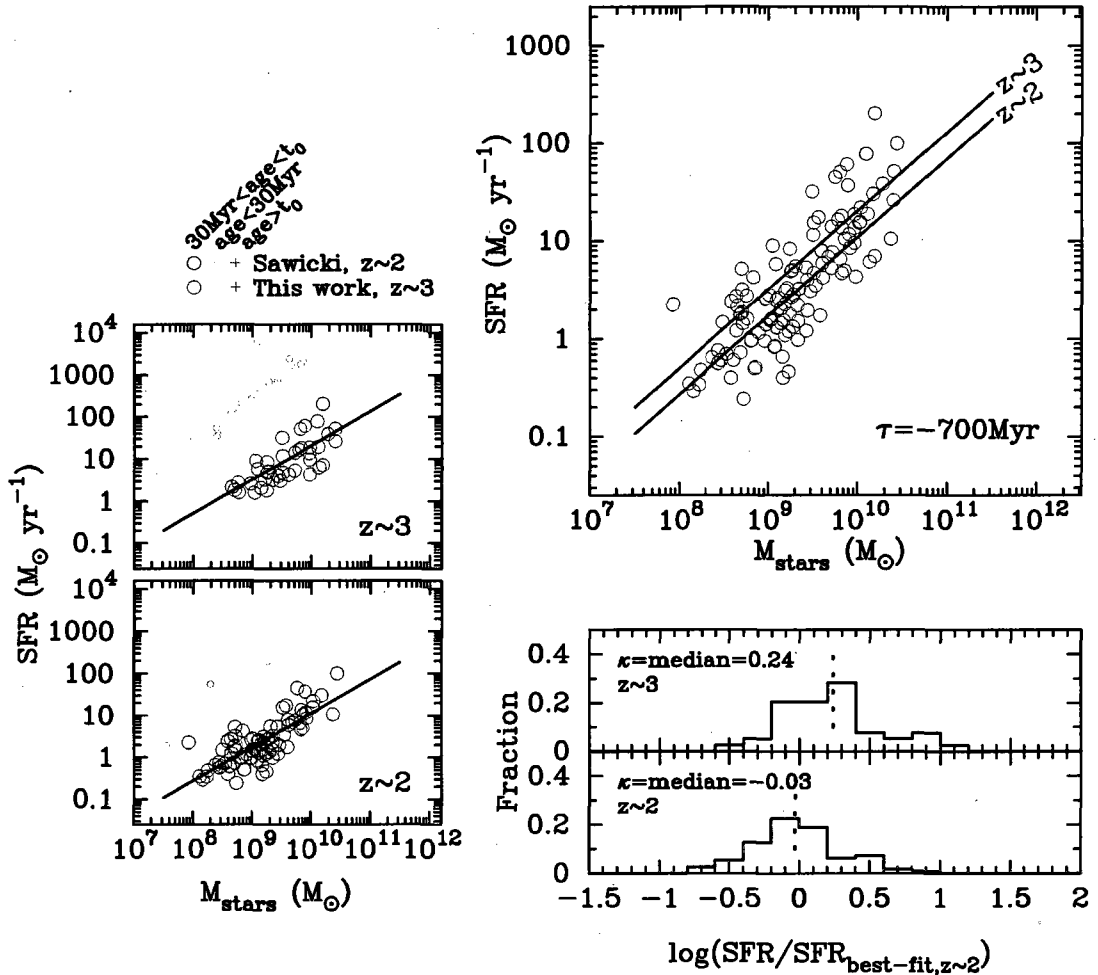


Figure 4.7: Stellar masses versus star formation rates, assuming exponential star formation ( $\tau = -700$  Myr). The two leftmost vertical panels display the complete data set at each redshift. Uncertainties are plotted in light grey for all objects  $\sim 30$  Myr  $\leq$  age  $\leq t_0$ . The top right panel shows these intermediate aged objects and their corresponding lines of best-fit. The best-fit slope is calculated from Sawicki's  $z \sim 2$  data set. That slope is then assumed for the  $z \sim 3$  population. The bottom right panel displays the residual offsets for both data sets relative to the  $z \sim 2$  line of best-fit. We use these offsets to calculate the  $\delta$ -term for each redshift in Equation 4.13.

We now test the capacity of the negative  $\tau$  model to describe an individual galaxy's evolution from  $z \sim 5$  to  $z \sim 2$ . Best-fit lines are broadened according to the appropriate PRMS deviations,

$$\text{PRMS}_{z \sim 2} = 0.34 \text{ and } \text{PRMS}_{z \sim 3} = 0.35. \quad (4.15)$$

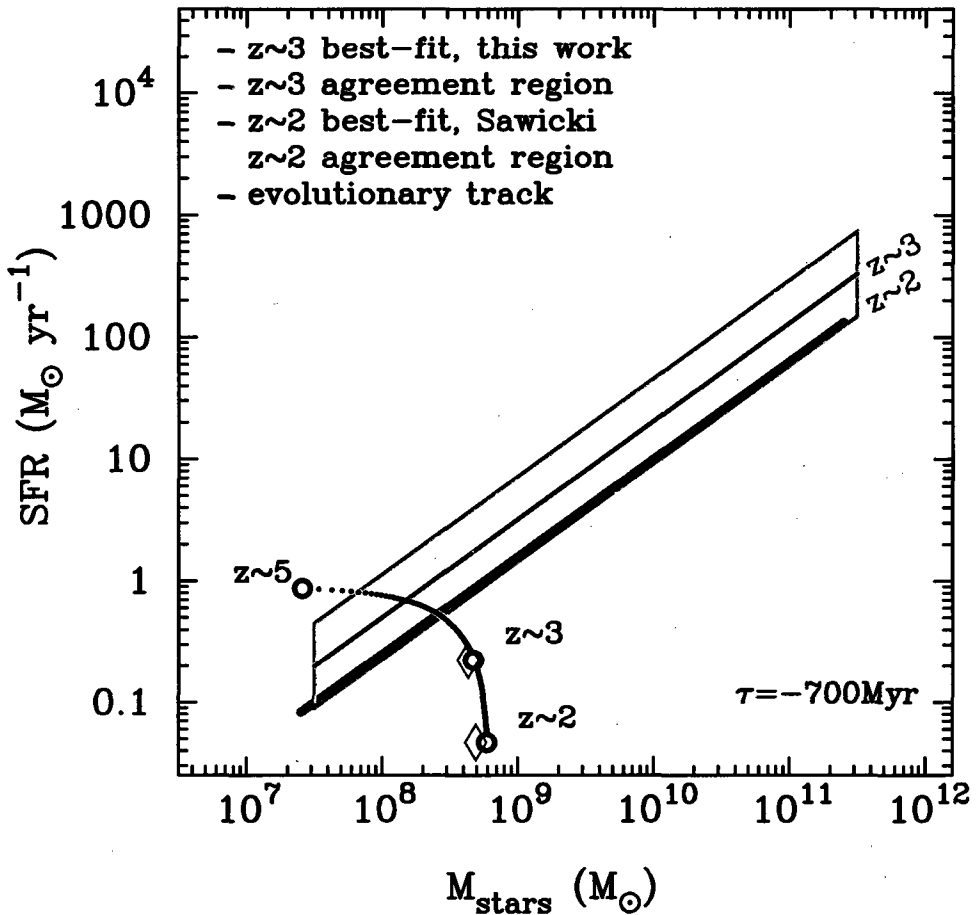


Figure 4.8: Stellar masses versus exponentially decreasing star formation rates ( $\tau = -700$  Myr). The black line is the evolutionary track of a toy galaxy evolved from  $z \sim 5$  to  $z \sim 2$ . The best-fit lines for the  $z \sim 2$  and  $\sim 3$  populations are displayed in red and blue, respectively. The pink and light blue lines enclose the region of acceptable agreement at each redshift. At  $z \sim 3$ , the stellar mass of the toy galaxy is  $\sim 250\%$  too large for its SFR. The agreement worsens at  $z \sim 2$  where its stellar mass ( $5.89 \times 10^8 M_\odot$ ) is  $\sim 1000\%$  larger than the acceptable upper limit.

With an assumed age $_{z \sim 5}$  of  $\sim 100$  Myr, the toy galaxy begins its evolution as a  $2.57 \times 10^7 M_\odot$  object creating new stars at a rate of  $0.99 M_\odot \text{ yr}^{-1}$ . At  $z \sim 3$ , the toy galaxy has evolved to  $4.67 \times 10^8 M_\odot$ , which overshoots the upper limit acceptable mass by  $3.32 \times 10^8 M_\odot$ , or  $\sim 250\%$ . At  $z \sim 2$ , the toy's  $5.89 \times 10^8 M_\odot$  stellar mass is  $\sim 1000\%$  too large for its  $0.05 M_\odot \text{ yr}^{-1}$  SFR. The assumption of exponentially decreasing star formation in high-redshift galaxies matches observations poorly, and so we limit further analysis to the more physically plausible mechanisms of constant and exponentially

increasing star formation.

## 4.2 Dust

### 4.2.1 For Constant Star Formation

It is well established that LBGs may contain significant quantities of dust, which attenuate their spectra. This extinction effect is particularly strong at UV wavelengths (Meurer et al. 1997; Sawicki & Yee 1998). Figures 3.1 and 3.4 display how dust attenuation steepens the rest-frame UV spectral slope for galaxies presented in this study. Specifically, objects fit for larger color excesses have steeper best-fit model spectral slopes at rest-frame UV wavelengths (e.g., object 182 versus object 994 in Fig. 3.4). Figure 4.9 shows the dependence of dust extinction on absolute rest-frame UV magnitude for galaxies model-fit assuming constant star formation.

We calculate absolute rest-frame UV magnitudes for a rest-frame wavelength of  $\sim 1700 \text{ \AA}$  according to the typical cosmological distance modulus (DM) and  $k$ -correction (K):

$$M_{1700} = m_{\lambda obs.} - DM - K. \quad (4.16)$$

Here, the  $k$ -correction provides the color difference between rest-frame  $\sim 1700 \text{ \AA}$  and the rest-frame  $R$ -filter. At  $z \sim 2$  and  $z \sim 3$ , we expect  $k$ -corrections to be modest because the “observed”  $R$ -band reasonably approximates rest-frame  $\sim 1700 \text{ \AA}$ . Since the quantity  $DM + K$  varies little across each particular redshift range, we opt to assume an estimated  $DM + K$  value for each redshift group rather than calculate a separate correction for each object based on its photometric redshift. For  $z \sim 2$ , we adopt Sawicki’s value of  $DM + K = 44.9$ . For  $z \sim 3$ , we estimate  $DM + K = 45.6$ .

We limit our analysis of dust extinction to rest-frame UV magnitudes  $-19 \geq M_{1700} \geq -21$ , where our  $z \sim 3$  sample significantly overlaps in luminosity with the  $z \sim 2$  samples of Sawicki et al. (2007) and Shapley et al. (2005). For the entire analyzed range, we calculate median color excesses of 0.15

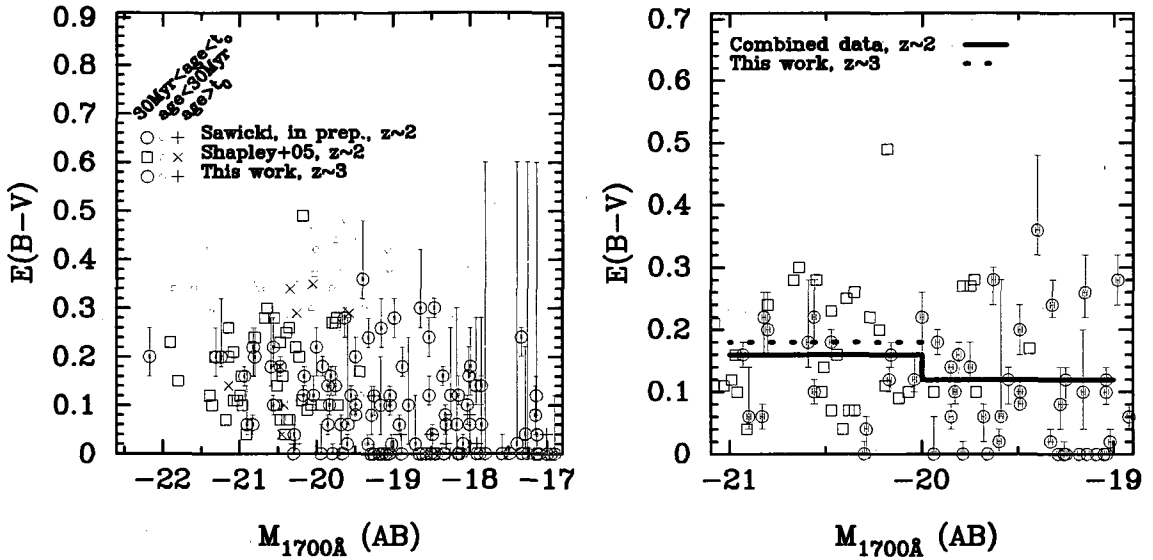


Figure 4.9: Color excess versus rest-frame UV magnitude for galaxies model-fit with constant star formation. The left panel shows all data regardless of magnitude or age. The right panel is limited to magnitudes where the samples at each redshift have significant overlap and presents only data for objects with ages greater than  $\sim 30$  Myr but less than the age of the universe. The red and dotted blue lines show median  $E(B - V)$  values for magnitude bins -19 to -20 and -20 to -21. Across the fainter bin, we find  $E(B - V)_{med.} = 0.12$  for both  $z \sim 2$  and  $z \sim 3$ . Across the brighter bin, we find  $E(B - V)_{med.} = 0.16$  for  $z \sim 2$  and  $E(B - V)_{med.} = 0.18$  for  $z \sim 3$ . Shapley et al. (2005) provide no uncertainties for their data here.

and 0.14 for  $z \sim 2$  and  $\sim 3$ , respectively. These medians agree to within the data's uncertainty ( $\pm 0.02$  median uncertainty). The  $z \sim 2$  and  $\sim 3$  median color excesses are transformed into median  $V$ -band extinctions of 0.61 and 0.57 by the formula

$$A(V) = R(V) \times E(B - V). \quad (4.17)$$

where, in accordance with the Calzetti et al. (2000) starburst extinction law,  $R(V) = 4.05$ .

To investigate how extinction varies with magnitude, we divide the data into two magnitude bins,  $-19 \geq M_{1700} > -20$  and  $-20 \geq M_{1700} \geq -21$ . The right panel of Figure 4.9 shows the binned median color excesses for each redshift group, while the median color excess and  $V$ -band extinction values for each bin are listed below in Table 4.1. For each bin, the  $z \sim 2$  and  $\sim 3$  values agree to

within uncertainty, and so we must conclude there is no detectable dust evolution between the two redshifts.

Rest-frame UV mag.	$z \sim 2$	$z \sim 2$	$z \sim 3$	$z \sim 3$
	$E(B - V)$	$A(V)$	$E(B - V)$	$A(V)$
$-19 \geq M_{1700} > -20$	$0.12 \pm 0.02$	$0.47 \pm 0.08$	$0.12 \pm 0.02$	$0.47 \pm 0.08$
$-20 \geq M_{1700} \geq -21$	$0.16 \pm 0.02$	$0.65 \pm 0.08$	$0.18 \pm 0.02$	$0.73 \pm 0.08$

Table 4.1: Median color excess and  $V$ -band extinction values for galaxies model-fit assuming constant star formation and binned according to rest-frame UV magnitude.

However, when the bins are considered in tandem, the  $z \sim 3$  color excesses display an unmistakable dependence on rest-frame UV magnitude, with the UV-brighter objects suffering higher extinction than the UV-faint. The  $z \sim 2$  color excess medians superficially display the same trend; however, to within the  $\pm 0.02$  median uncertainty, these values are indistinguishable. Adelberger & Steidel (2000) also identify this dependence.

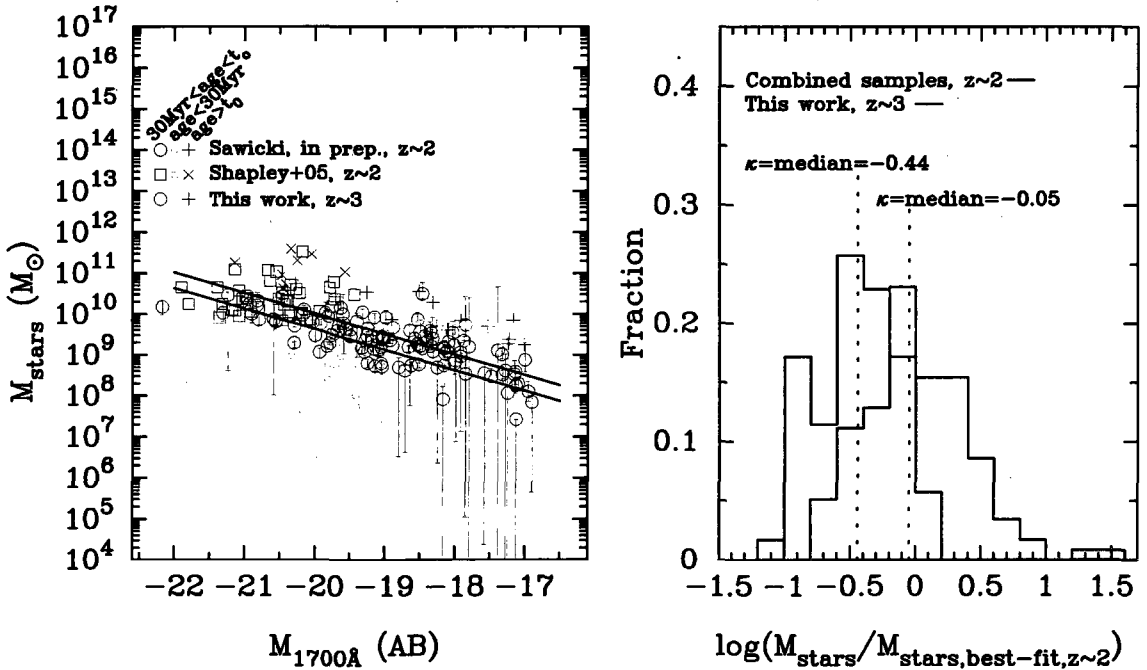


Figure 4.10: Stellar mass versus rest-frame UV magnitude for galaxies model-fit with constant star formation. The left panel shows all data regardless of age. The right panel presents the  $z \sim 2$  to  $z \sim 3$  population offset for those objects with ages greater than  $\sim 30$  Myr but less than the age of the universe.

The dependence of stellar mass on rest-frame UV magnitude may be seen in Figure 4.10. For a given stellar mass, objects at  $z \sim 3$  are UV-brighter than their  $z \sim 2$  counterparts. A possible explanation for this is that galaxies at  $z \sim 2$  are dustier than those at  $z \sim 3$ , but the color excess data do not bear this hypothesis out. We instead interpret this in the context of the  $M_{stars}$ -SFR relation (see section 4.2.1). According to those data, for a given stellar mass, a galaxy at  $z \sim 3$  will have a higher star formation rate than one at  $z \sim 2$ . This results in the stellar mass-UV magnitude relation observed here because the rest-frame UV magnitude of a galaxy is a reliable tracer of its star formation.

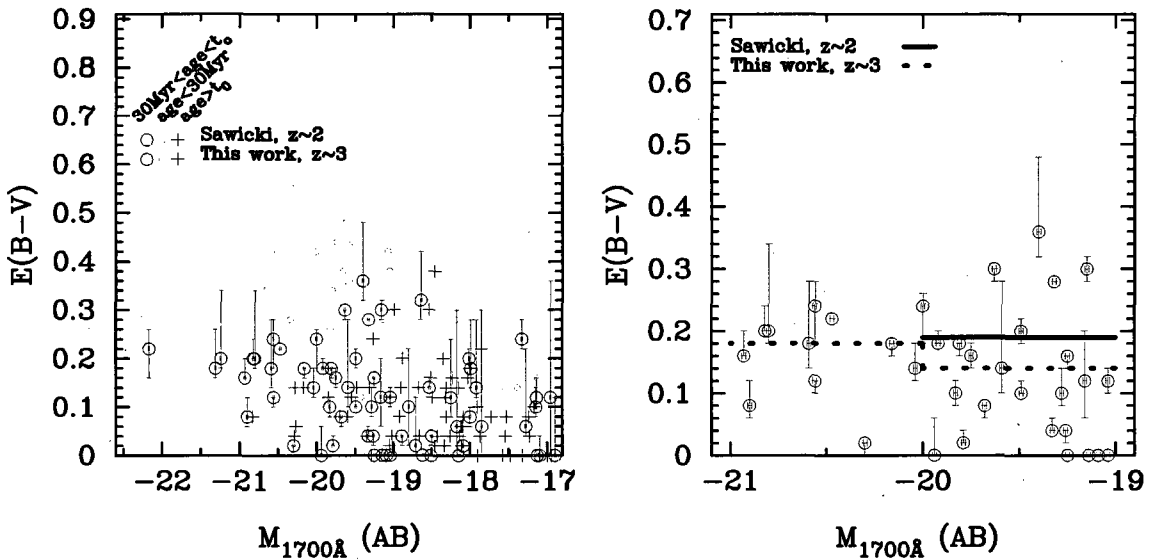


Figure 4.11: Color excess versus rest-frame UV magnitude for galaxies model-fit with exponential star formation ( $\tau = 700$  Myr). The left panel shows all data regardless of magnitude or age. The right panel is limited to magnitudes where the samples at each redshift display overlap and presents only data for objects with ages greater than  $\sim 30$  Myr but less than the age of the universe. The red and dotted blue lines show median color excesses for the data binned according to UV magnitude. Across the fainter bin, we find median color excesses of 0.19 and 0.14 for  $z \sim 2$  and  $z \sim 3$  galaxies, respectively. Across the brighter bin, objects at  $z \sim 3$  are found to have a median color excess of 0.18.

### 4.2.2 For Exponential Star Formation

#### The Positive $\tau$ Model ( $\tau = 700$ Myr)

We now apply the same analysis to galaxies fit for exponentially increasing star formation, where  $\tau = 700$  Myr. Figure 4.11 shows the dependence of dust extinction on rest-frame UV magnitude for these objects. Without model-fits for the UV-bright Shapley et al. (2005) catalog, our analysis of  $z \sim 2$  galaxies is limited to the fainter magnitude bin,  $-19 \geq M_{1700} > -20$ . Here we can conclusively say that  $z \sim 2$  galaxies are dustier than those at  $z \sim 3$ . Across the entire analyzed range, the  $z \sim 3$  color excess medians are once again suggestive that UV-brighter galaxies are more obscured by dust than the UV-faint, but the medians are indistinguishable given the  $\pm 0.02$  uncertainty. Table 4.2 lists the median color excesses,  $V$ -band extinctions, and uncertainties according to UV magnitude bin.

Rest-frame UV mag.	$z \sim 2$ $E(B - V)$	$z \sim 2$ $A(V)$	$z \sim 3$ $E(B - V)$	$z \sim 3$ $A(V)$
$-19 \geq M_{1700} > -20$	$0.19 \pm 0.02$	$0.77 \pm 0.08$	$0.14 \pm 0.02$	$0.57 \pm 0.08$
$-20 \geq M_{1700} \geq -21$	N/A	N/A	$0.18 \pm 0.02$	$0.73 \pm 0.08$

Table 4.2: Median color excess and  $V$ -band extinction values for galaxies model-fit assuming exponential star formation ( $\tau = 700$  Myr) and binned according to rest-frame UV magnitude.

The dependence of stellar mass on rest-frame UV magnitude for galaxies fit with exponentially increasing SFRs is shown in Figure 4.12. Once more, we see that, for a given stellar mass, galaxies at  $z \sim 3$  are UV-brighter than their  $z \sim 2$  counterparts. This effect may be, in part, a result of these  $z \sim 2$  galaxies being dustier than their  $z \sim 3$  analogs (see Fig. 4.11), but we must again note that rest-frame UV magnitude is a faithful indicator of star formation activity. Given the  $M_{stars}$ -SFR relation for these objects, we must conclude the primary driver for the observed stellar mass-UV magnitude dependence is the  $z \sim 3$  population's higher SFR for a given mass.

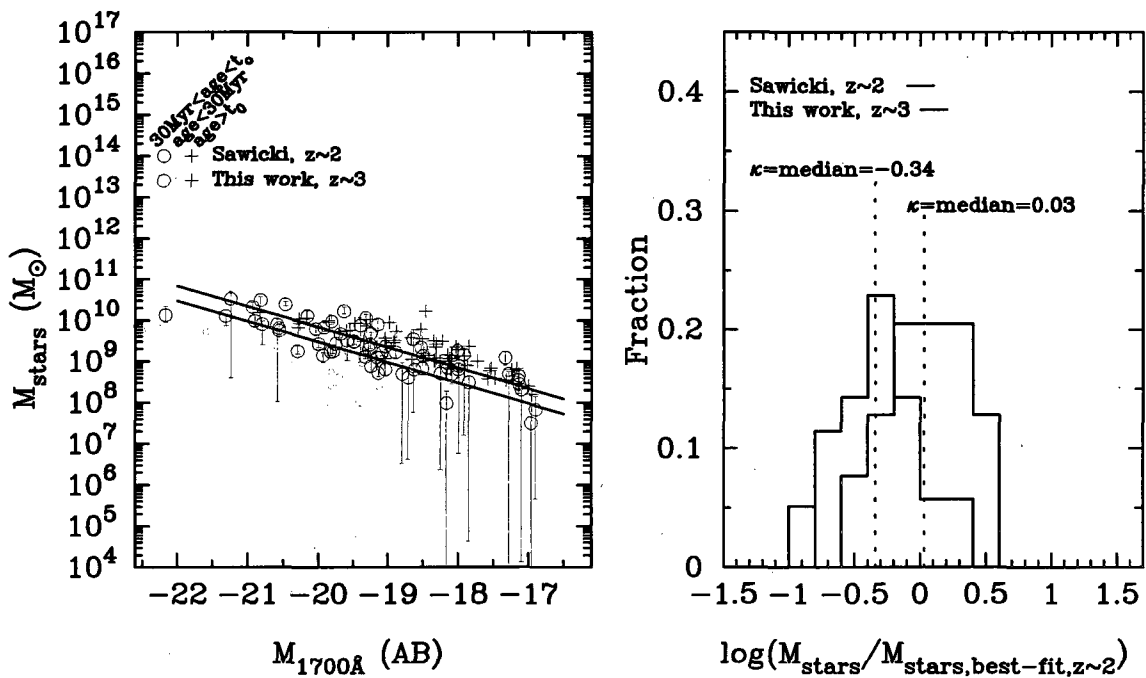


Figure 4.12: Stellar mass versus rest-frame UV magnitude for galaxies model-fit with exponential star formation ( $\tau = 700$  Myr). The left panel shows all data regardless of age. The right panel presents the  $z \sim 2$  to  $z \sim 3$  population offset for those objects with ages greater than  $\sim 30$  Myr but less than the age of the universe.

# Chapter 5

# Summary and Conclusions

This work uses publicly available image mosaics of the HDF-S to create a catalog of  $z \sim 3$  LBGs. Optical data ( $U_{300}$ ,  $B_{450}$ ,  $V_{606}$ ,  $I_{814}$ ) are provided by WFPC2/*HST*. ISAAC/VLT supply the NIR data ( $J_s$ ,  $H$ ,  $K_s$ ). We procure photometry using SExtractor on the image convolutions of Labb   et al. (2003) and define a sample of  $z \sim 3$  LBG candidates using the color-color selection criteria of Steidel et al. (1996). We model-fit this sample using the SEDfit software package and define the  $z \sim 3$  subsample with the photometric redshift cut  $2.6 < z_{phot} \leq 3.5$ . We repeat this process for three archetypal star formation histories: the constant SFR, the exponentially increasing SFR (for  $\tau = 700, 500, 350$ , and  $250$  Myr), and the exponentially decreasing SFR ( $\tau = -700$  Myr).

Throughout, we employ the  $z \sim 2$  sample of Sawicki et al. (2007). We use their catalog of model-fit parameters in our analyses of constant star formation, and, having been granted access to their photometry, we refit the Sawicki group's sample assuming exponentially increasing and decreasing SFRs. Where possible we also employ the  $z \sim 2$  sample of Shapley et al. (2005) and the  $z \sim 5$  sample of Yabe et al. (2009).

Using these data, we study the  $M_{stars}$ -SFR relation and dust content of high-redshift galaxies. We conclude:

1. The  $M_{stars}$ -SFR relation is qualitatively independent of the underlying star formation history.

We model-fit observational data with three dramatically divergent archetypal star formation histories and find only minor changes in the mathematical formulation of the relationship.

With a much steeper declining exponential than the  $-700$  Myr e-folding model we assume, one more akin to the single stellar population model discussed in section 1.1, this relationship would likely break down

2. The assumption of an exponentially increasing star formation history with a 500 Myr e-folding provides the best match between the model-fit observational data and the evolutionary track of a toy galaxy. For this SFR, the toy galaxy overshoots the upper limit data mass at  $z \sim 3$  by  $\sim 15\%$ , but the toy's evolution is consistent with the spread in model-fit observational data at  $z \sim 2$ . We identify the 500 Myr e-folding as an approximate upper limit constraint on the value of  $\tau$ . However, we are unable to constrain  $\tau$  at the low end because the e-foldings that might produce such a lower limit also produce an epidemic of unphysical ages in the model-fit catalogs. We attribute this trend to the overly simplistic star formation history we adopt in our model-fitting and analysis.
3. We identify no conspicuous dust evolution between  $z \sim 3$  and  $z \sim 2$ . For the  $z \sim 3$  constant star formation model-fits, we find that UV-brighter galaxies are more highly obscured by dust than the UV-faint. This trend is inconclusive for all other data.
4. For a given stellar mass, galaxies at  $z \sim 3$  are UV-brighter than their  $z \sim 2$  counterparts. We interpret this trend in the context of the  $M_{stars}$ -SFR relation, wherein, for a given stellar mass, objects at  $z \sim 3$  have higher SFRs than those at  $z \sim 2$ . Because rest-frame UV magnitude is a reliable tracer of star formation activity, we believe the observed  $M_{stars}$ -UV magnitude trend is driven by the SFR offset between  $z \sim 3$  and  $\sim 2$ .

We find, for redshifts  $5 \gtrsim z \gtrsim 2$ , galaxies likely build up their stellar masses in an exponentially increasing manner. This is contrary to previous assumptions about the star formation histories of high-redshift galaxies, which treated these objects as isolated from the intergalactic medium. Even so, the specific formulation of the exponentially increasing SFH we use to model-fit our galaxy samples produces unphysical ages in an alarming number of objects. In the future, a more nuanced SFR function should be explored. We propose a sawtooth-type function wherein the peaks increase exponentially with time but are separated by valleys of lower star formation activity. This would allow for periods of relative quiescence and almost certainly more closely resemble the SFHs of actual

galaxies. Future analysis would be greatly aided by the inclusion of a galaxy sample at  $z \sim 4$ , as well.

# Bibliography

- [1] Adelberger, K.L. & Steidel, C.C. 2000, ApJ, 544, 218
- [2] Bertin, E. & Arnouts, S. 1996, A&AS, 117, 393
- [3] Bouwens, R.J., Illingworth, G.D., Franx, M., & Ford, H. 2008, ApJ, 686, 230
- [4] Bruzual, G. & Charlot, S. 2003, MNRAS, 344, 1000
- [5] Calzetti, D., Armus, L., Bohlin, R.C., Kinney, A.L., Koornneef, J., & Storchi-Bergmann, T. 2000, ApJ, 533, 682
- [6] Capak, P., et al. 2004, AJ, 127, 180
- [7] Casertano, S., et al. 2000, AJ, 120, 2747
- [8] Dickinson, M., Giavalisco, M., & The GOODS Team 2003, in The Mass of Galaxies at Low and High Redshift, ed. R. Bender & A. Renzini (Berlin: Springer), 324
- [9] Fazio, G.G., et al. 2004, ApJ, 154, 10
- [10] Finkelstein, S.L., Papovich, C., Giavalisco, M., Reddy, N.A., Ferguson, H.C., Koekemoer, A.M., & Dickinson, M. 2010, ApJ, 719, 1250
- [11] Franx, M., Moorwood, A., Rix, H.-W., Kuijken, K., Röttgering, H., van der Werf, P., van Dokkum, P., Labb  , I., & Rudnick, G. 2000, The Messenger, 99, 20
- [12] Glazebrook, K. & Economou, F. 1997, The Perl Journal, 5, 5
- [13] Hopkins, A.M. & Beacom, J.F. 2006, ApJ, 651, 142

- [14] Ichikawa, T., Suzuki, R., Tokoku, C., Uchimoto, Y.K., Konishi, M., Yoshikawa, T., Yamada, T., Tanaka, I., Omata, K., & Nishimura, T. 2006, Proc. of SPIE, 6269, 38
- [15] Iwata, I., Ohta, K., Tamura, N., Akiyama, M., Aoki, K., Ando, M., Kiuchi, G., & Sawicki, M. 2007, MRAS, 376, 1557
- [16] Kajisawa, M., et al. 2009, ApJ, 702, 1393
- [17] Labb  , I., et al. 2002, The Messenger, 110, 38
- [18] Labb  , I., et al. 2003, AJ, 125, 1107
- [19] Labb  , I., et al. 2010, ApJL, 716, L103
- [20] Madau, P. 1995, ApJ, 441, 18
- [21] Meurer, G.R., Heckman, T.M., Lehnert, M.D., Leitherer, C., & Lowenthal, J. 1997, AJ, 114, 1
- [22] Mihos, J.C. & Hernquist, L. 1996, ApJ, 464, 641
- [23] Miyazaki, S., et al. 2002, PASJ, 54, 833
- [24] Papovich, C., Dickinson, M., & Ferguson, H.C. 2001, ApJ, 559, 620
- [25] Salpeter, E.E. 1955, ApJ, 121, 161
- [26] Sawicki, M. & Yee, H.K.C. 1998, AJ, 115, 1329
- [27] Sawicki, M., Iwata, I., Ohta, K., Thompson, D., Tamura, N., Akiyama, M., Aoki, K., Ando, M., & Kiuchi, G. 2007, in Astronomical Society of the Pacific Conference Series, “Deepest Astronomical Surveys,” eds. J. Afonso, H.C. Ferguson, B. Mobasher, & R. Norris, 433
- [28] Schechter, P. 1976, ApJ, 203, 297
- [29] Shapley, A.E., Steidel, C.C., Adelberger, K.L., Dickinson, M., Giavalisco, M., & Pettini, M. 2001, ApJ, 562, 95

- [30] Shapley, A.E., Erb, D.K., Pettini, M., Steidel, C.C., & Adelberger, K.L. 2004, ApJ, 612, 108
- [31] Shapley, A.E., Steidel, C.C., Erb, D.K., Reddy, N.A., Adelberger, K.L., Pettini, M., Barmby, P., & Huang, J. 2005, ApJ, 626, 698
- [32] Stark, D.P., Ellis, R.S., Bunker, A., Bundy, K., Targett, T., Benson, A., & Lacy, M. 2009, ApJ, 697, 1493
- [33] Steidel, C.C., Pettini, M., & Hamilton, D. 1995, AJ, 110, 2519
- [34] Steidel, C.C., Giavalisco, M., Dickinson, M., & Adelberger, K.L. 1996, AJ, 112, 352
- [35] Steidel, C.C., Adelberger, K.L., Giavalisco, M., Dickinson, M., & Pettini, M. 1999, ApJ, 519, 1
- [36] Williams, R.E., et al. 1996, AJ, 112, 1335
- [37] Wright, E.L. 2006, PASP, 118, 1711
- [38] Yabe, K., Ohta, K., Iwata, I., Sawicki, M., Tamura, N., Akiyama, M., & Aoki, K. 2009, ApJ, 693, 507

## Appendix A

## $z \sim 3$ Best-fit SEDfit Parameters

Table A.1: Best-fit parameters for this work's HDF-S catalog, constant SFR.

ID	$\mathcal{R}_{VJ}$	$z_{phot}$	$E(B - V)$	$\log(Age/\text{yr})$	$\log(M_*/M_\odot)$	$\log(\text{SFR}/(M_\odot/\text{yr}))$	$\chi^2$
3	26.37	1.50	$0.14^{+0.02}_{-0.02}$	$7.60^{+0.10}_{-0.10}$	$8.02^{+0.09}_{-0.08}$	$0.47^{+0.09}_{-0.03}$	75.62
147	23.02	3.05	$0.26^{+0.02}_{-0.02}$	$6.56^{+0.10}_{-0.10}$	$9.86^{+0.06}_{-0.06}$	$3.30^{+0.03}_{-0.03}$	77.34
156	25.25	1.95	$0.08^{+0.02}_{-0.02}$	$8.64^{+0.10}_{-0.10}$	$9.34^{+0.07}_{-0.07}$	$0.79^{+0.12}_{-0.12}$	32.41
172	25.24	1.50	$0.32^{+0.02}_{-0.02}$	$8.74^{+0.10}_{-0.10}$	$9.91^{+0.13}_{-0.13}$	$1.26^{+0.07}_{-0.07}$	15.03
177	25.51	2.30	$0.00^{+0.04}_{-0.04}$	$8.74^{+0.10}_{-0.10}$	$9.20^{+0.04}_{-0.04}$	$0.55^{+0.31}_{-0.31}$	4.43
201	26.40	1.50	$0.22^{+0.02}_{-0.02}$	$7.49^{+0.10}_{-0.10}$	$8.17^{+0.07}_{-0.07}$	$0.71^{+0.09}_{-0.06}$	27.58
356	24.38	1.55	$0.66^{+0.00}_{-0.00}$	$6.76^{+0.10}_{-0.10}$	$9.94^{+0.04}_{-0.04}$	$3.18^{+0.04}_{-0.04}$	74.53
401	26.00	1.70	$0.14^{+0.02}_{-0.02}$	$8.74^{+0.10}_{-0.10}$	$9.21^{+0.13}_{-0.13}$	$0.56^{+0.14}_{-0.14}$	10.79
428	25.90	3.05	$0.26^{+0.02}_{-0.02}$	$6.35^{+0.10}_{-0.10}$	$8.76^{+0.04}_{-0.04}$	$2.41^{+0.14}_{-0.14}$	106.15
430	26.08	2.55	$0.08^{+0.02}_{-0.02}$	$7.60^{+0.21}_{-0.21}$	$8.34^{+0.16}_{-0.16}$	$0.78^{+0.11}_{-0.12}$	133.62
447	25.71	1.50	$0.20^{+0.02}_{-0.02}$	$6.76^{+0.20}_{-0.20}$	$8.03^{+0.12}_{-0.12}$	$1.27^{+0.06}_{-0.06}$	51.09
462	25.99	1.50	$0.50^{+0.04}_{-0.04}$	$5.41^{+0.31}_{-0.31}$	$8.86^{+0.17}_{-0.17}$	$3.45^{+0.31}_{-0.31}$	64.16
472	26.15	1.50	$0.58^{+0.02}_{-0.02}$	$6.66^{+0.14}_{-0.14}$	$8.91^{+0.04}_{-0.04}$	$2.25^{+0.32}_{-0.32}$	115.82
475	26.29	1.50	$0.56^{+0.02}_{-0.02}$	$6.66^{+0.10}_{-0.10}$	$8.75^{+0.04}_{-0.04}$	$2.12^{+0.14}_{-0.14}$	110.33
481	25.90	1.50	$0.26^{+0.02}_{-0.02}$	$6.76^{+0.00}_{-0.00}$	$8.13^{+0.04}_{-0.04}$	$1.37^{+0.24}_{-0.24}$	101.14
650	26.27	2.75	$0.02^{+0.00}_{-0.00}$	$8.84^{+0.21}_{-0.21}$	$9.17^{+0.13}_{-0.13}$	$0.42^{+0.06}_{-0.06}$	97.70
715	24.29	2.90	$0.20^{+0.02}_{-0.02}$	$8.12^{+0.52}_{-0.52}$	$10.03^{+0.21}_{-0.21}$	$1.97^{+0.16}_{-0.16}$	19.51
720	26.20	1.80	$0.14^{+0.08}_{-0.08}$	$8.01^{+0.31}_{-0.31}$	$8.56^{+0.13}_{-0.13}$	$0.61^{+0.29}_{-0.29}$	15.53
726	24.92	1.85	$0.26^{+0.02}_{-0.02}$	$8.53^{+0.42}_{-0.42}$	$9.92^{+0.24}_{-0.24}$	$1.46^{+0.23}_{-0.23}$	8.94
779	25.39	2.00	$0.18^{+0.02}_{-0.02}$	$9.16^{+0.21}_{-0.21}$	$10.13^{+0.15}_{-0.15}$	$1.08^{+0.28}_{-0.28}$	2.75
797	26.15	2.35	$0.00^{+0.00}_{-0.00}$	$9.47^{+0.30}_{-0.30}$	$9.65^{+0.02}_{-0.02}$	$0.31^{+0.02}_{-0.02}$	22.85
818	26.08	1.50	$0.14^{+0.04}_{-0.04}$	$8.22^{+0.10}_{-0.10}$	$8.63^{+0.09}_{-0.09}$	$0.48^{+0.17}_{-0.17}$	140.53
824	25.75	2.45	$0.02^{+0.02}_{-0.02}$	$9.68^{+0.21}_{-0.21}$	$10.09^{+0.12}_{-0.12}$	$0.54^{+0.08}_{-0.08}$	5.82
876	26.10	2.00	$0.00^{+0.00}_{-0.00}$	$8.32^{+0.21}_{-0.21}$	$8.49^{+0.08}_{-0.08}$	$0.23^{+0.16}_{-0.16}$	19.89
878	24.94	2.95	$0.34^{+0.04}_{-0.04}$	$6.76^{+0.00}_{-0.00}$	$9.37^{+0.06}_{-0.06}$	$2.61^{+0.16}_{-0.16}$	56.32
901	25.05	1.50	$0.60^{+0.02}_{-0.02}$	$6.66^{+0.10}_{-0.10}$	$9.35^{+0.00}_{-0.00}$	$2.70^{+0.00}_{-0.00}$	192.91
1029	25.66	2.15	$0.10^{+0.02}_{-0.02}$	$8.66^{+0.00}_{-0.00}$	$9.52^{+0.21}_{-0.21}$	$0.77^{+0.10}_{-0.10}$	5.20
1089	25.09	1.50	$0.30^{+0.04}_{-0.04}$	$8.84^{+0.10}_{-0.10}$	$9.42^{+0.04}_{-0.04}$	$1.36^{+0.16}_{-0.16}$	15.77
1102	24.70	3.20	$0.06^{+0.02}_{-0.02}$	$8.74^{+0.52}_{-0.52}$	$10.00^{+0.22}_{-0.22}$	$1.35^{+0.26}_{-0.26}$	10.30
1159	26.32	1.50	$0.00^{+0.00}_{-0.00}$	$8.64^{+0.01}_{-0.01}$	$8.48^{+0.03}_{-0.03}$	$-0.07^{+0.28}_{-0.28}$	30.90
1191	25.61	2.45	$0.02^{+0.02}_{-0.02}$	$7.18^{+0.31}_{-0.31}$	$8.00^{+0.10}_{-0.10}$	$0.84^{+0.18}_{-0.18}$	14.20
1366	24.92	1.50	$0.32^{+0.04}_{-0.04}$	$8.84^{+0.31}_{-0.31}$	$9.52^{+0.21}_{-0.21}$	$0.77^{+0.10}_{-0.10}$	5.20
1441	25.66	1.50	$0.40^{+0.06}_{-0.06}$	$6.66^{+1.56}_{-1.56}$	$8.54^{+0.08}_{-0.08}$	$1.89^{+0.18}_{-0.18}$	9.37
1451	25.45	1.70	$0.16^{+0.02}_{-0.02}$	$8.12^{+0.42}_{-0.42}$	$9.42^{+0.14}_{-0.14}$	$1.03^{+0.19}_{-0.19}$	3.51
1467	24.30	2.55	$0.28^{+0.04}_{-0.04}$	$7.39^{+0.10}_{-0.10}$	$8.19^{+0.11}_{-0.11}$	$0.83^{+0.03}_{-0.03}$	91.69
1478	25.90	1.70	$0.08^{+0.02}_{-0.02}$	$8.84^{+0.10}_{-0.10}$	$10.13^{+0.05}_{-0.05}$	$3.25^{+0.12}_{-0.12}$	70.83
1482	24.27	1.85	$0.26^{+0.02}_{-0.02}$	$6.56^{+0.19}_{-0.19}$	$9.80^{+0.10}_{-0.10}$	$0.84^{+0.18}_{-0.18}$	18.58
1484	25.12	1.65	$0.36^{+0.02}_{-0.02}$	$8.84^{+0.10}_{-0.10}$	$9.72^{+0.03}_{-0.03}$	$1.37^{+0.18}_{-0.18}$	68.60
1498	23.49	1.85	$0.26^{+0.02}_{-0.02}$	$8.53^{+1.66}_{-1.66}$	$10.29^{+0.12}_{-0.12}$	$1.54^{+0.19}_{-0.19}$	15.38
1521	25.78	3.05	$0.26^{+0.02}_{-0.02}$	$6.56^{+0.21}_{-0.21}$	$10.47^{+0.61}_{-0.61}$	$2.02^{+0.22}_{-0.22}$	20.32
					$8.74^{+0.06}_{-0.06}$	$2.19^{+0.06}_{-0.06}$	234.24

Table A.1: Best-fit parameters for this work's HDF-S catalog, constant SFR.

ID	$\mathcal{R}_{VI}$	$z_{phot}$	$E(B - V)$	$\log(\text{Age}/\text{yr})$	$\log(M_*/M_\odot)$	$\log(\text{SFR}/(\text{M}_\odot/\text{yr}))$	$\chi^2$
1533	26.40	1.65	0.24 $^{+0.02}_{-0.02}$	8.95 $^{+0.10}_{-0.10}$	9.51 $^{+0.08}_{-0.09}$	0.66 $^{+0.00}_{-0.07}$	174.32
1565	25.54	1.85	0.30 $^{+0.02}_{-0.04}$	8.53 $^{+0.21}_{-0.21}$	9.79 $^{+0.19}_{-0.19}$	1.34 $^{+0.07}_{-0.18}$	4.40
1576	26.02	1.50	0.10 $^{+0.04}_{-0.02}$	7.80 $^{+0.10}_{-0.31}$	8.22 $^{+0.06}_{-0.32}$	0.47 $^{+0.11}_{-0.11}$	18.96
1598	25.26	2.85	0.28 $^{+0.02}_{-0.02}$	6.56 $^{+0.10}_{-0.09}$	8.98 $^{+0.06}_{-0.06}$	2.42 $^{+0.00}_{-0.21}$	139.67
1604	26.05	2.45	0.04 $^{+0.02}_{-0.02}$	8.43 $^{+0.09}_{-0.09}$	8.89 $^{+0.43}_{-0.43}$	0.54 $^{+0.21}_{-0.18}$	193.59
1634	25.04	2.85	0.22 $^{+0.02}_{-0.02}$	8.12 $^{+0.42}_{-0.21}$	9.15 $^{+0.15}_{-0.15}$	1.75 $^{+0.18}_{-0.18}$	1.61
1695	26.23	1.65	0.08 $^{+0.02}_{-0.02}$	8.84 $^{+0.60}_{-0.60}$	9.02 $^{+0.05}_{-0.05}$	0.27 $^{+0.26}_{-0.26}$	61.00
1817	26.17	1.50	0.56 $^{+0.04}_{-0.04}$	6.56 $^{+0.10}_{-0.10}$	8.82 $^{+0.14}_{-0.14}$	2.26 $^{+0.24}_{-0.24}$	82.71
1933	24.50	2.35	0.22 $^{+0.02}_{-0.02}$	8.43 $^{+0.10}_{-0.10}$	10.10 $^{+0.83}_{-0.83}$	1.75 $^{+0.19}_{-0.19}$	13.30
1973	25.69	1.70	0.08 $^{+0.00}_{-0.00}$	8.74 $^{+0.10}_{-0.10}$	9.14 $^{+0.05}_{-0.05}$	0.49 $^{+0.03}_{-0.03}$	54.97
1985	26.55	2.75	0.00 $^{+0.00}_{-0.00}$	8.64 $^{+0.10}_{-0.10}$	8.79 $^{+0.09}_{-0.09}$	0.24 $^{+0.02}_{-0.02}$	30.76
2005	26.06	1.50	0.14 $^{+0.02}_{-0.02}$	7.70 $^{+0.10}_{-0.10}$	8.25 $^{+0.09}_{-0.09}$	0.59 $^{+0.03}_{-0.03}$	92.91
2033	26.35	2.20	0.04 $^{+0.02}_{-0.02}$	9.05 $^{+0.10}_{-0.10}$	9.27 $^{+0.13}_{-0.13}$	0.32 $^{+0.16}_{-0.16}$	26.12
2042	26.06	2.20	0.00 $^{+0.00}_{-0.00}$	9.47 $^{+0.10}_{-0.10}$	9.63 $^{+0.11}_{-0.11}$	0.28 $^{+0.02}_{-0.02}$	31.07
2050	25.86	2.60	0.24 $^{+0.04}_{-0.04}$	7.18 $^{+0.21}_{-0.21}$	8.72 $^{+0.12}_{-0.12}$	1.56 $^{+0.18}_{-0.18}$	39.33
2192	26.46	2.70	0.00 $^{+0.00}_{-0.00}$	8.53 $^{+0.10}_{-0.10}$	8.72 $^{+0.18}_{-0.18}$	0.27 $^{+0.17}_{-0.17}$	36.51
2207	25.00	2.45	0.04 $^{+0.02}_{-0.02}$	8.74 $^{+0.10}_{-0.10}$	9.59 $^{+0.02}_{-0.02}$	0.94 $^{+0.08}_{-0.08}$	29.19
2306	25.77	2.75	0.10 $^{+0.02}_{-0.02}$	8.32 $^{+0.10}_{-0.10}$	9.21 $^{+0.06}_{-0.06}$	0.96 $^{+0.03}_{-0.03}$	64.76
2361	25.30	2.70	0.00 $^{+0.00}_{-0.00}$	8.64 $^{+0.21}_{-0.21}$	9.29 $^{+0.19}_{-0.19}$	0.74 $^{+0.03}_{-0.03}$	6.08
2387	25.71	2.55	0.06 $^{+0.02}_{-0.02}$	8.43 $^{+0.31}_{-0.31}$	8.11 $^{+0.15}_{-0.15}$	0.76 $^{+0.12}_{-0.12}$	17.76
2389	24.01	2.85	0.34 $^{+0.04}_{-0.04}$	6.56 $^{+0.52}_{-0.52}$	9.71 $^{+0.08}_{-0.08}$	3.16 $^{+0.62}_{-0.62}$	86.27
2560	26.08	1.50	0.26 $^{+0.04}_{-0.04}$	6.56 $^{+0.10}_{-0.10}$	9.59 $^{+0.02}_{-0.02}$	1.15 $^{+0.73}_{-0.73}$	6.07
2575	25.90	2.00	0.06 $^{+0.02}_{-0.02}$	6.97 $^{+0.25}_{-0.25}$	9.13 $^{+0.16}_{-0.16}$	0.48 $^{+0.16}_{-0.16}$	5.53
2597	26.56	2.95	0.00 $^{+0.00}_{-0.00}$	8.64 $^{+0.90}_{-0.90}$	8.72 $^{+0.12}_{-0.12}$	0.67 $^{+0.18}_{-0.18}$	204.98
2661	26.46	1.60	0.00 $^{+0.00}_{-0.00}$	8.43 $^{+0.30}_{-0.30}$	7.43 $^{+0.03}_{-0.03}$	0.67 $^{+0.12}_{-0.12}$	7.07
2728	24.56	1.70	0.16 $^{+0.04}_{-0.04}$	6.56 $^{+0.10}_{-0.10}$	8.57 $^{+0.08}_{-0.08}$	-0.08 $^{+0.01}_{-0.01}$	14.44
2799	26.59	2.45	0.00 $^{+0.02}_{-0.02}$	9.26 $^{+0.10}_{-0.10}$	9.71 $^{+0.08}_{-0.08}$	0.10 $^{+0.06}_{-0.06}$	134.19
2747	26.50	1.65	0.42 $^{+0.04}_{-0.04}$	6.66 $^{+0.10}_{-0.10}$	9.66 $^{+0.09}_{-0.09}$	1.21 $^{+0.19}_{-0.19}$	84.68
2763	25.91	1.70	0.06 $^{+0.04}_{-0.04}$	8.74 $^{+0.21}_{-0.21}$	8.41 $^{+0.04}_{-0.04}$	1.75 $^{+0.04}_{-0.04}$	49.53
2837	26.36	1.50	0.24 $^{+0.06}_{-0.06}$	8.22 $^{+0.42}_{-0.42}$	8.55 $^{+0.05}_{-0.05}$	0.40 $^{+0.27}_{-0.27}$	24.54
2784	25.79	1.50	0.00 $^{+0.00}_{-0.00}$	6.76 $^{+0.16}_{-0.16}$	7.43 $^{+0.03}_{-0.03}$	0.63 $^{+0.18}_{-0.18}$	11.48
2889	25.21	2.50	0.20 $^{+0.02}_{-0.02}$	6.97 $^{+0.10}_{-0.10}$	7.94 $^{+0.03}_{-0.03}$	0.98 $^{+0.39}_{-0.39}$	7.88
2913	23.43	2.75	0.20 $^{+0.04}_{-0.04}$	7.91 $^{+0.42}_{-0.42}$	8.05 $^{+0.15}_{-0.15}$	1.59 $^{+0.68}_{-0.68}$	8.96
2958	25.82	2.55	0.04 $^{+0.06}_{-0.06}$	9.05 $^{+0.31}_{-0.31}$	9.58 $^{+0.13}_{-0.13}$	2.75 $^{+0.33}_{-0.33}$	21.95
3043	23.09	2.60	0.24 $^{+0.06}_{-0.06}$	6.97 $^{+0.18}_{-0.18}$	9.71 $^{+0.05}_{-0.05}$	1.29 $^{+0.67}_{-0.67}$	355.14
2849	25.15	2.45	0.16 $^{+0.04}_{-0.04}$	8.74 $^{+0.21}_{-0.21}$	9.94 $^{+0.08}_{-0.08}$	0.10 $^{+0.00}_{-0.00}$	84.68
2889	25.21	2.50	0.20 $^{+0.02}_{-0.02}$	6.87 $^{+0.10}_{-0.10}$	9.44 $^{+0.18}_{-0.18}$	0.09 $^{+0.00}_{-0.00}$	24.54
2913	23.43	2.75	0.20 $^{+0.04}_{-0.04}$	7.91 $^{+0.42}_{-0.42}$	10.17 $^{+0.19}_{-0.19}$	2.32 $^{+0.17}_{-0.17}$	7.09
3166	25.59	1.90	0.18 $^{+0.04}_{-0.04}$	8.43 $^{+0.21}_{-0.21}$	9.33 $^{+0.06}_{-0.06}$	0.97 $^{+0.22}_{-0.22}$	42.16
3169	26.52	1.50	0.32 $^{+0.06}_{-0.06}$	6.87 $^{+0.36}_{-0.36}$	8.05 $^{+0.03}_{-0.03}$	1.19 $^{+0.12}_{-0.12}$	45.12
3217	26.59	2.05	0.10 $^{+0.02}_{-0.02}$	5.52 $^{+0.52}_{-0.52}$	9.44 $^{+0.18}_{-0.18}$	2.75 $^{+0.33}_{-0.33}$	8.96
3321	26.30	1.85	0.32 $^{+0.02}_{-0.02}$	8.53 $^{+0.10}_{-0.10}$	8.74 $^{+0.03}_{-0.03}$	3.22 $^{+0.38}_{-0.38}$	21.16
3330	26.18	1.50	0.16 $^{+0.04}_{-0.04}$	8.64 $^{+0.21}_{-0.21}$	10.28 $^{+0.19}_{-0.19}$	1.82 $^{+0.43}_{-0.43}$	10.98
3397	26.57	1.85	0.08 $^{+0.04}_{-0.04}$	8.53 $^{+0.21}_{-0.21}$	9.33 $^{+0.06}_{-0.06}$	0.97 $^{+0.22}_{-0.22}$	5.64
3407	25.96	1.50	0.28 $^{+0.06}_{-0.06}$	6.87 $^{+0.21}_{-0.21}$	8.05 $^{+0.03}_{-0.03}$	0.97 $^{+0.23}_{-0.23}$	135.08
3419	26.05	1.50	0.10 $^{+0.04}_{-0.04}$	7.18 $^{+0.02}_{-0.02}$	8.31 $^{+0.07}_{-0.07}$	0.34 $^{+0.12}_{-0.12}$	20.86
3554	26.47	1.70	0.00 $^{+0.00}_{-0.00}$	8.64 $^{+0.31}_{-0.31}$	8.49 $^{+0.14}_{-0.14}$	0.23 $^{+0.45}_{-0.45}$	20.40
3560	25.95	1.60	0.04 $^{+0.04}_{-0.04}$	8.95 $^{+0.31}_{-0.31}$	9.07 $^{+0.09}_{-0.09}$	0.22 $^{+0.25}_{-0.25}$	103.08
3625	26.28	1.50	0.56 $^{+0.06}_{-0.06}$	6.66 $^{+0.20}_{-0.20}$	8.81 $^{+0.07}_{-0.07}$	2.15 $^{+0.77}_{-0.77}$	109.51
3639	25.13	3.05	0.18 $^{+0.02}_{-0.02}$	8.95 $^{+0.10}_{-0.10}$	10.42 $^{+0.09}_{-0.09}$	1.15 $^{+0.21}_{-0.21}$	38.48
3666	25.93	1.85	0.04 $^{+0.02}_{-0.02}$	8.74 $^{+0.21}_{-0.21}$	9.23 $^{+0.17}_{-0.17}$	0.28 $^{+0.03}_{-0.03}$	20.36
3689	26.16	2.45	0.10 $^{+0.06}_{-0.06}$	8.32 $^{+0.62}_{-0.62}$	8.99 $^{+0.31}_{-0.31}$	0.34 $^{+0.16}_{-0.16}$	30.46
3782	25.43	1.85	0.08 $^{+0.02}_{-0.02}$	8.64 $^{+0.10}_{-0.10}$	9.23 $^{+0.10}_{-0.10}$	0.71 $^{+0.31}_{-0.31}$	199.21
3789	26.42	1.50	0.34 $^{+0.02}_{-0.02}$	6.76 $^{+0.20}_{-0.20}$	8.16 $^{+0.06}_{-0.06}$	1.40 $^{+0.16}_{-0.16}$	104.35
3795	25.94	3.40	0.00 $^{+0.00}_{-0.00}$	9.16 $^{+0.21}_{-0.21}$	9.72 $^{+0.03}_{-0.03}$	0.67 $^{+0.32}_{-0.32}$	199.21
3808	24.78	3.00	0.22 $^{+0.06}_{-0.06}$	8.53 $^{+0.21}_{-0.21}$	10.33 $^{+0.08}_{-0.08}$	1.87 $^{+0.30}_{-0.30}$	7.68
				8.53 $^{+0.42}_{-0.42}$	10.33 $^{+0.20}_{-0.20}$	1.87 $^{+0.14}_{-0.14}$	

Table A.1: Best-fit parameters for this work's HDF-S catalog, constant SFR.

ID	$\mathcal{R}_{VI}$	$z_{phot}$	$E(B - V)$	$\log(Age/\text{yr})$	$\log(M_*/\text{M}_\odot)$	$\log(\text{SFR}/(\text{M}_\odot/\text{yr}))$	$\chi^2$
59	25.81	2.95	0.16 $^{+0.10}_{-0.06}$	6.87 $^{+0.21}_{-0.25}$	8.39 $^{+0.03}_{-0.08}$	1.53 $^{+0.66}_{-0.34}$	13.48
69	25.82	1.65	0.32 $^{+0.06}_{-0.04}$	6.76 $^{+0.10}_{-0.10}$	8.39 $^{+0.08}_{-0.10}$	1.63 $^{+0.20}_{-0.19}$	112.31
73	26.47	1.50	0.14 $^{+0.04}_{-0.04}$	7.39 $^{+0.31}_{-1.04}$	7.84 $^{+0.04}_{-0.07}$	0.48 $^{+0.25}_{-0.25}$	8.04
100	25.97	2.25	0.40 $^{+0.04}_{-0.04}$	6.56 $^{+0.10}_{-0.10}$	8.85 $^{+0.07}_{-0.07}$	2.30 $^{+0.27}_{-0.24}$	106.11
190	25.76	1.50	0.20 $^{+0.04}_{-0.04}$	7.49 $^{+0.30}_{-0.30}$	8.38 $^{+0.09}_{-0.09}$	0.92 $^{+0.04}_{-0.04}$	60.81
203	25.80	2.10	0.14 $^{+0.04}_{-0.04}$	8.64 $^{+0.10}_{-0.10}$	9.38 $^{+0.11}_{-0.11}$	0.83 $^{+0.15}_{-0.15}$	67.25
207	25.26	1.50	0.58 $^{+0.20}_{-0.20}$	6.97 $^{+1.00}_{-1.00}$	9.37 $^{+0.05}_{-0.05}$	2.41 $^{+0.85}_{-0.85}$	55.35
242	25.91	2.05	0.38 $^{+0.02}_{-0.02}$	6.87 $^{+0.10}_{-0.10}$	8.78 $^{+0.03}_{-0.03}$	1.92 $^{+0.03}_{-0.03}$	112.03
288	25.09	2.45	0.40 $^{+0.02}_{-0.02}$	6.76 $^{+0.10}_{-0.10}$	9.35 $^{+0.07}_{-0.07}$	2.59 $^{+0.19}_{-0.19}$	2.60
296	25.59	3.70	0.08 $^{+0.02}_{-0.02}$	6.45 $^{+0.21}_{-0.21}$	8.33 $^{+0.07}_{-0.07}$	1.88 $^{+0.22}_{-0.22}$	119.13
310	26.06	2.45	0.00 $^{+0.00}_{-0.00}$	7.49 $^{+0.00}_{-0.00}$	7.92 $^{+0.08}_{-0.08}$	0.46 $^{+0.20}_{-0.20}$	303.02
313	25.64	1.85	0.06 $^{+0.00}_{-0.00}$	7.74 $^{+0.10}_{-0.10}$	9.18 $^{+0.10}_{-0.10}$	0.53 $^{+0.24}_{-0.24}$	145.74
328	25.49	2.45	0.04 $^{+0.02}_{-0.02}$	7.08 $^{+0.21}_{-0.21}$	8.02 $^{+0.06}_{-0.06}$	0.96 $^{+0.16}_{-0.16}$	180.90
339	24.91	2.30	0.16 $^{+0.02}_{-0.02}$	6.56 $^{+0.31}_{-0.31}$	8.49 $^{+0.15}_{-0.15}$	1.94 $^{+0.02}_{-0.02}$	65.50
448	25.60	2.80	0.22 $^{+0.02}_{-0.02}$	8.01 $^{+0.31}_{-0.31}$	9.47 $^{+0.14}_{-0.14}$	1.52 $^{+0.23}_{-0.23}$	3.35
464	25.68	2.95	0.18 $^{+0.02}_{-0.02}$	8.53 $^{+0.42}_{-0.42}$	9.77 $^{+0.17}_{-0.17}$	1.32 $^{+0.18}_{-0.18}$	69.59
470	25.97	2.75	0.36 $^{+0.02}_{-0.02}$	6.56 $^{+0.46}_{-0.46}$	8.96 $^{+0.05}_{-0.05}$	2.41 $^{+0.06}_{-0.06}$	24.31
480	26.11	2.65	0.10 $^{+0.02}_{-0.02}$	8.95 $^{+0.21}_{-0.21}$	9.62 $^{+0.13}_{-0.13}$	0.77 $^{+0.04}_{-0.04}$	56.31
520	26.31	2.40	0.36 $^{+0.02}_{-0.02}$	6.56 $^{+0.00}_{-0.00}$	8.64 $^{+0.02}_{-0.02}$	2.08 $^{+0.02}_{-0.02}$	131.14
533	25.69	2.30	0.38 $^{+0.02}_{-0.02}$	6.56 $^{+0.00}_{-0.00}$	8.60 $^{+0.02}_{-0.02}$	2.36 $^{+0.02}_{-0.02}$	137.72
542	26.10	1.50	0.42 $^{+0.02}_{-0.02}$	6.66 $^{+0.10}_{-0.10}$	8.91 $^{+0.02}_{-0.02}$	2.78 $^{+0.02}_{-0.02}$	132.30
544	26.46	1.50	0.40 $^{+0.02}_{-0.02}$	6.66 $^{+0.06}_{-0.06}$	8.25 $^{+0.13}_{-0.13}$	1.59 $^{+0.07}_{-0.07}$	136.30
570	26.25	2.35	0.32 $^{+0.02}_{-0.02}$	6.56 $^{+0.00}_{-0.00}$	8.51 $^{+0.32}_{-0.32}$	1.95 $^{+0.23}_{-0.23}$	170.18
572	25.78	1.50	0.42 $^{+0.02}_{-0.02}$	6.66 $^{+0.00}_{-0.00}$	8.60 $^{+0.02}_{-0.02}$	1.94 $^{+0.00}_{-0.00}$	165.20
579	25.66	1.65	0.46 $^{+0.02}_{-0.02}$	6.66 $^{+0.00}_{-0.00}$	8.85 $^{+0.00}_{-0.00}$	2.19 $^{+0.00}_{-0.00}$	198.13
590	26.47	1.50	0.06 $^{+0.00}_{-0.00}$	9.05 $^{+0.10}_{-0.10}$	8.44 $^{+0.00}_{-0.00}$	1.78 $^{+0.00}_{-0.00}$	338.40
639	25.98	2.80	0.48 $^{+0.04}_{-0.04}$	6.56 $^{+1.46}_{-1.46}$	9.41 $^{+0.12}_{-0.12}$	2.85 $^{+0.23}_{-0.23}$	6.40
649	26.58	2.45	0.26 $^{+0.02}_{-0.02}$	7.80 $^{+0.31}_{-0.31}$	8.91 $^{+0.12}_{-0.12}$	1.16 $^{+0.11}_{-0.11}$	63.39
665	25.50	2.90	0.46 $^{+0.04}_{-0.04}$	6.24 $^{+0.21}_{-0.21}$	9.61 $^{+0.18}_{-0.18}$	3.37 $^{+0.49}_{-0.49}$	12.78
673	25.59	2.90	0.42 $^{+0.04}_{-0.04}$	6.56 $^{+0.46}_{-0.46}$	9.37 $^{+0.13}_{-0.13}$	2.81 $^{+0.24}_{-0.24}$	9.35
692	25.18	1.50	0.18 $^{+0.02}_{-0.02}$	8.84 $^{+0.21}_{-0.21}$	9.64 $^{+0.11}_{-0.11}$	0.89 $^{+0.09}_{-0.09}$	14.62
721	25.32	3.20	0.02 $^{+0.02}_{-0.02}$	9.99 $^{+0.00}_{-0.00}$	10.74 $^{+0.02}_{-0.02}$	0.90 $^{+0.04}_{-0.04}$	87.94
746	26.07	2.85	0.44 $^{+0.02}_{-0.02}$	6.45 $^{+0.35}_{-0.35}$	9.27 $^{+0.11}_{-0.11}$	0.88 $^{+0.39}_{-0.39}$	144.37
848	25.57	2.30	0.20 $^{+0.02}_{-0.02}$	9.57 $^{+0.10}_{-0.10}$	9.65 $^{+0.03}_{-0.03}$	2.81 $^{+0.15}_{-0.15}$	19.30
871	25.43	3.05	0.12 $^{+0.02}_{-0.02}$	8.84 $^{+0.21}_{-0.21}$	9.74 $^{+0.13}_{-0.13}$	1.20 $^{+0.10}_{-0.10}$	4.99
972	26.43	2.45	0.30 $^{+0.02}_{-0.02}$	7.28 $^{+0.42}_{-0.42}$	8.74 $^{+0.13}_{-0.13}$	1.23 $^{+0.09}_{-0.09}$	3.74
1047	26.19	3.20	0.02 $^{+0.02}_{-0.02}$	6.87 $^{+0.93}_{-0.93}$	7.74 $^{+0.37}_{-0.37}$	1.48 $^{+0.43}_{-0.43}$	18.63
1106	26.05	2.60	0.48 $^{+0.02}_{-0.02}$	6.76 $^{+0.94}_{-0.94}$	7.74 $^{+0.54}_{-0.54}$	0.88 $^{+0.39}_{-0.39}$	19.30
1108	24.77	3.35	0.06 $^{+0.00}_{-0.00}$	9.55 $^{+0.10}_{-0.10}$	10.65 $^{+0.03}_{-0.03}$	1.20 $^{+0.10}_{-0.10}$	35.70
1124	26.47	2.35	0.32 $^{+0.02}_{-0.02}$	6.76 $^{+0.10}_{-0.10}$	9.47 $^{+0.12}_{-0.12}$	1.36 $^{+0.06}_{-0.06}$	0.57
1140	26.52	1.85	0.36 $^{+0.04}_{-0.04}$	6.66 $^{+0.10}_{-0.10}$	8.47 $^{+0.04}_{-0.04}$	1.71 $^{+0.21}_{-0.21}$	115.30
1225	26.56	3.25	0.00 $^{+0.00}_{-0.00}$	8.43 $^{+0.10}_{-0.10}$	9.74 $^{+0.22}_{-0.22}$	1.68 $^{+0.24}_{-0.24}$	127.50
1273	25.32	1.50	0.26 $^{+0.02}_{-0.02}$	7.49 $^{+0.26}_{-0.26}$	8.47 $^{+0.07}_{-0.07}$	2.51 $^{+0.14}_{-0.14}$	59.47
1403	26.34	3.50	0.00 $^{+0.00}_{-0.00}$	9.05 $^{+0.31}_{-0.31}$	10.21 $^{+0.13}_{-0.13}$	1.20 $^{+0.09}_{-0.09}$	466.73
1471	26.50	2.50	0.18 $^{+0.04}_{-0.04}$	8.64 $^{+0.10}_{-0.10}$	9.47 $^{+0.11}_{-0.11}$	1.71 $^{+0.21}_{-0.21}$	53.40
1527	26.37	2.60	0.08 $^{+0.00}_{-0.00}$	9.05 $^{+0.21}_{-0.21}$	9.40 $^{+0.07}_{-0.07}$	0.85 $^{+0.11}_{-0.11}$	37.40
1473	25.78	1.65	0.26 $^{+0.02}_{-0.02}$	8.84 $^{+0.10}_{-0.10}$	9.74 $^{+0.03}_{-0.03}$	0.99 $^{+0.10}_{-0.10}$	79.66
1501	25.94	3.05	0.38 $^{+0.02}_{-0.02}$	6.45 $^{+1.35}_{-1.35}$	9.17 $^{+0.11}_{-0.11}$	0.36 $^{+0.03}_{-0.03}$	39.02
1523	25.86	2.20	0.38 $^{+0.06}_{-0.06}$	6.56 $^{+0.29}_{-0.29}$	8.82 $^{+0.45}_{-0.45}$	2.72 $^{+1.74}_{-1.74}$	131.75
1572	25.99	1.50	0.56 $^{+0.16}_{-0.16}$	5.20 $^{+0.10}_{-0.10}$	9.06 $^{+0.32}_{-0.32}$	2.26 $^{+0.11}_{-0.11}$	49.91
1585	26.27	1.50	0.60 $^{+0.00}_{-0.00}$	5.93 $^{+0.56}_{-0.56}$	9.08 $^{+0.12}_{-0.12}$	0.57 $^{+0.43}_{-0.43}$	3.85 $^{+1.78}_{-1.78}$
1590	26.06	1.60	0.18 $^{+0.02}_{-0.02}$	8.84 $^{+0.21}_{-0.21}$	9.33 $^{+0.15}_{-0.15}$	1.69 $^{+0.26}_{-0.26}$	174.90
1593	25.52	1.50	0.40 $^{+0.00}_{-0.00}$	9.26 $^{+0.10}_{-0.10}$	10.50 $^{+0.00}_{-0.00}$	0.58 $^{+0.87}_{-0.87}$	33.63
1647	25.44	1.70	0.12 $^{+0.02}_{-0.02}$	8.74 $^{+0.20}_{-0.20}$	9.36 $^{+0.13}_{-0.13}$	0.71 $^{+0.10}_{-0.10}$	123.18
						0.71 $^{+0.12}_{-0.12}$	30.49

Table A.1: Best-fit parameters for this work's HDF-S catalog, constant SFR.

ID	$\mathcal{R}_{VI}$	$z_{phot}$	$E(B - V)$	$\log(\text{Age}/\text{yr})$	$\log(M_*/\text{M}_\odot)$	$\log(\text{SFR}/(\text{M}_\odot/\text{yr}))$	$\chi^2$
1676	25.94	1.70	0.112 $^{+0.022}_{-0.022}$	8.74 $^{+0.21}_{-0.21}$	9.16 $^{+0.16}_{-0.16}$	0.51 $^{+0.00}_{-0.00}$	8.75
1696	26.55	2.55	0.10 $^{+0.02}_{-0.02}$	8.74 $^{+0.31}_{-0.31}$	9.20 $^{+0.19}_{-0.19}$	0.55 $^{+0.10}_{-0.10}$	43.48
1699	26.53	2.80	0.42 $^{+0.02}_{-0.02}$	5.41 $^{+0.31}_{-0.31}$	9.07 $^{+0.22}_{-0.22}$	3.66 $^{+1.37}_{-1.37}$	98.81
1739	25.04	2.95	0.10 $^{+0.02}_{-0.02}$	8.64 $^{+0.21}_{-0.21}$	9.83 $^{+0.04}_{-0.04}$	1.28 $^{+0.06}_{-0.06}$	7.81
1863	25.24	1.50	0.30 $^{+0.02}_{-0.02}$	8.74 $^{+0.21}_{-0.21}$	9.85 $^{+0.03}_{-0.03}$	1.19 $^{+0.07}_{-0.07}$	25.86
1881	25.15	2.60	0.08 $^{+0.02}_{-0.02}$	9.05 $^{+0.10}_{-0.10}$	10.00 $^{+0.05}_{-0.05}$	1.05 $^{+0.06}_{-0.06}$	5.04
1908	26.01	3.35	0.06 $^{+0.02}_{-0.02}$	9.05 $^{+0.16}_{-0.16}$	9.78 $^{+0.24}_{-0.24}$	0.83 $^{+0.94}_{-0.94}$	
1915	26.55	2.80	0.00 $^{+0.02}_{-0.02}$	9.05 $^{+0.10}_{-0.10}$	9.19 $^{+0.09}_{-0.09}$	0.24 $^{+0.03}_{-0.03}$	60.85
1926	25.69	2.55	0.36 $^{+0.02}_{-0.02}$	8.43 $^{+0.21}_{-0.21}$	10.20 $^{+0.07}_{-0.07}$	1.85 $^{+0.10}_{-0.10}$	6.82
1954	26.00	2.40	0.04 $^{+0.02}_{-0.02}$	9.05 $^{+0.21}_{-0.21}$	9.45 $^{+0.11}_{-0.11}$	0.50 $^{+0.09}_{-0.09}$	9.13
1960	26.23	2.40	0.44 $^{+0.02}_{-0.02}$	6.56 $^{+1.46}_{-1.46}$	8.97 $^{+0.22}_{-0.22}$	2.42 $^{+0.69}_{-0.69}$	32.65
2021	26.47	2.50	0.42 $^{+0.02}_{-0.02}$	6.56 $^{+0.52}_{-0.52}$	8.82 $^{+0.24}_{-0.24}$	2.26 $^{+0.67}_{-0.67}$	209.02
2025	25.67	1.50	0.66 $^{+0.02}_{-0.02}$	6.56 $^{+0.00}_{-0.00}$	9.27 $^{+0.02}_{-0.02}$	2.71 $^{+0.02}_{-0.02}$	218.99
2030	25.66	3.15	0.00 $^{+0.02}_{-0.02}$	8.43 $^{+0.20}_{-0.20}$	9.07 $^{+0.16}_{-0.16}$	0.72 $^{+0.01}_{-0.01}$	2.24
2052	26.18	2.85	0.12 $^{+0.02}_{-0.02}$	6.56 $^{+1.46}_{-1.46}$	8.00 $^{+0.14}_{-0.14}$	1.44 $^{+0.24}_{-0.24}$	9.36
2071	25.56	2.95	0.12 $^{+0.02}_{-0.02}$	8.74 $^{+0.31}_{-0.31}$	9.80 $^{+0.17}_{-0.17}$	1.15 $^{+0.06}_{-0.06}$	
2188	26.09	2.55	0.32 $^{+0.02}_{-0.02}$	7.70 $^{+0.21}_{-0.21}$	9.23 $^{+0.11}_{-0.11}$	1.58 $^{+0.11}_{-0.11}$	151.19
2219	26.20	1.50	0.56 $^{+0.02}_{-0.02}$	7.60 $^{+0.21}_{-0.21}$	9.32 $^{+0.08}_{-0.08}$	1.76 $^{+0.12}_{-0.12}$	41.77
2257	26.39	1.80	0.24 $^{+0.02}_{-0.02}$	10.30 $^{+0.00}_{-0.00}$	10.90 $^{+0.04}_{-0.04}$	0.76 $^{+0.04}_{-0.04}$	20.07
2266	25.40	2.10	0.22 $^{+0.02}_{-0.02}$	9.57 $^{+0.21}_{-0.21}$	10.68 $^{+0.02}_{-0.02}$	1.23 $^{+0.10}_{-0.10}$	33.95
2300	25.78	2.45	0.48 $^{+0.02}_{-0.02}$	6.45 $^{+1.35}_{-1.35}$	9.33 $^{+0.12}_{-0.12}$	2.88 $^{+0.03}_{-0.03}$	164.83
2315	26.37	2.30	0.22 $^{+0.02}_{-0.02}$	6.45 $^{+0.10}_{-0.10}$	9.31 $^{+0.16}_{-0.16}$	0.95 $^{+0.10}_{-0.10}$	53.61
2329	26.11	2.70	0.08 $^{+0.02}_{-0.02}$	8.84 $^{+0.10}_{-0.10}$	9.45 $^{+0.04}_{-0.04}$	0.70 $^{+0.05}_{-0.05}$	38.09
2356	25.55	1.70	0.14 $^{+0.02}_{-0.02}$	8.74 $^{+0.21}_{-0.21}$	9.38 $^{+0.12}_{-0.12}$	0.73 $^{+0.19}_{-0.19}$	37.57
2427	26.22	3.05	0.30 $^{+0.02}_{-0.02}$	6.56 $^{+1.46}_{-1.46}$	8.74 $^{+0.15}_{-0.15}$	2.18 $^{+0.23}_{-0.23}$	14.38
2429	26.34	1.50	0.48 $^{+0.02}_{-0.02}$	6.45 $^{+0.10}_{-0.10}$	9.33 $^{+0.12}_{-0.12}$	2.80 $^{+0.03}_{-0.03}$	251.04
2529	26.08	1.50	0.58 $^{+0.02}_{-0.02}$	5.41 $^{+0.31}_{-0.31}$	9.07 $^{+0.00}_{-0.00}$	3.66 $^{+0.53}_{-0.53}$	119.19
2545	25.75	2.75	0.14 $^{+0.02}_{-0.02}$	9.05 $^{+0.10}_{-0.10}$	10.03 $^{+0.09}_{-0.09}$	1.08 $^{+0.04}_{-0.04}$	38.23
2553	26.47	2.65	0.28 $^{+0.06}_{-0.06}$	6.66 $^{+0.21}_{-0.21}$	8.39 $^{+0.12}_{-0.12}$	1.73 $^{+0.51}_{-0.51}$	56.67
2561	26.34	1.50	0.42 $^{+0.02}_{-0.02}$	7.39 $^{+0.21}_{-0.21}$	8.63 $^{+0.13}_{-0.13}$	1.34 $^{+0.12}_{-0.12}$	
2568	26.04	2.25	0.32 $^{+0.02}_{-0.02}$	6.97 $^{+0.21}_{-0.21}$	8.69 $^{+0.09}_{-0.09}$	1.73 $^{+0.39}_{-0.39}$	13.16
2652	26.12	1.60	0.00 $^{+0.02}_{-0.02}$	9.16 $^{+0.10}_{-0.10}$	9.33 $^{+0.09}_{-0.09}$	0.29 $^{+0.08}_{-0.08}$	47.28
2684	26.55	2.80	0.38 $^{+0.04}_{-0.04}$	6.45 $^{+0.95}_{-0.95}$	8.99 $^{+0.12}_{-0.12}$	1.66 $^{+0.00}_{-0.00}$	141.20
2759	25.90	3.50	0.00 $^{+0.06}_{-0.06}$	9.88 $^{+0.10}_{-0.10}$	10.43 $^{+0.10}_{-0.10}$	2.36 $^{+0.22}_{-0.22}$	113.07
2768	26.34	3.10	0.12 $^{+0.06}_{-0.06}$	9.78 $^{+0.42}_{-0.42}$	10.54 $^{+0.26}_{-0.26}$	1.73 $^{+0.51}_{-0.51}$	
2772	25.81	2.80	0.00 $^{+0.06}_{-0.06}$	8.84 $^{+0.10}_{-0.10}$	8.70 $^{+0.06}_{-0.06}$	0.89 $^{+0.14}_{-0.14}$	6.33
2751	26.42	2.70	0.32 $^{+0.04}_{-0.04}$	6.97 $^{+0.21}_{-0.21}$	8.69 $^{+0.09}_{-0.09}$	1.73 $^{+0.39}_{-0.39}$	49.14
2754	26.45	1.50	0.42 $^{+0.02}_{-0.02}$	9.16 $^{+0.10}_{-0.10}$	9.33 $^{+0.09}_{-0.09}$	0.29 $^{+0.08}_{-0.08}$	
2759	25.90	3.50	0.00 $^{+0.06}_{-0.06}$	6.66 $^{+0.52}_{-0.52}$	8.32 $^{+0.00}_{-0.00}$	1.66 $^{+0.00}_{-0.00}$	47.28
2854	25.54	1.50	0.42 $^{+0.02}_{-0.02}$	7.39 $^{+0.21}_{-0.21}$	8.70 $^{+0.06}_{-0.06}$	1.73 $^{+0.39}_{-0.39}$	
2946	25.85	3.00	0.14 $^{+0.06}_{-0.06}$	8.43 $^{+0.21}_{-0.21}$	9.49 $^{+0.10}_{-0.10}$	1.14 $^{+0.08}_{-0.08}$	20.67
2955	25.05	2.30	0.18 $^{+0.06}_{-0.06}$	8.95 $^{+0.31}_{-0.31}$	10.19 $^{+0.14}_{-0.14}$	1.34 $^{+0.03}_{-0.03}$	
3275	26.35	3.40	0.00 $^{+0.06}_{-0.06}$	8.43 $^{+0.10}_{-0.10}$	8.80 $^{+0.19}_{-0.19}$	0.45 $^{+0.02}_{-0.02}$	141.58
2989	26.49	2.20	0.46 $^{+0.10}_{-0.10}$	6.56 $^{+0.10}_{-0.10}$	8.84 $^{+0.05}_{-0.05}$	2.28 $^{+0.19}_{-0.19}$	291.29
3145	25.38	2.30	0.20 $^{+0.02}_{-0.02}$	8.12 $^{+1.04}_{-1.04}$	9.39 $^{+0.49}_{-0.49}$	1.33 $^{+0.10}_{-0.10}$	
3163	26.16	2.40	0.28 $^{+0.02}_{-0.02}$	8.53 $^{+0.21}_{-0.21}$	9.74 $^{+0.07}_{-0.07}$	1.29 $^{+0.14}_{-0.14}$	
3258	26.31	3.20	0.00 $^{+0.06}_{-0.06}$	8.74 $^{+0.10}_{-0.10}$	9.07 $^{+0.10}_{-0.10}$	0.42 $^{+0.03}_{-0.03}$	125.91
3411	25.86	2.85	0.44 $^{+0.04}_{-0.04}$	6.45 $^{+0.42}_{-0.42}$	9.36 $^{+0.11}_{-0.11}$	2.91 $^{+0.21}_{-0.21}$	68.06
3420	25.98	2.40	0.30 $^{+0.02}_{-0.02}$	6.76 $^{+0.10}_{-0.10}$	8.61 $^{+0.08}_{-0.08}$	1.85 $^{+0.02}_{-0.02}$	
3294	25.37	1.65	0.50 $^{+0.02}_{-0.02}$	8.64 $^{+0.42}_{-0.42}$	10.41 $^{+0.04}_{-0.04}$	1.86 $^{+0.02}_{-0.02}$	26.35
3349	26.55	1.50	0.16 $^{+0.04}_{-0.04}$	8.84 $^{+0.21}_{-0.21}$	9.17 $^{+0.12}_{-0.12}$	1.33 $^{+0.37}_{-0.37}$	
3399	26.48	1.50	0.56 $^{+0.04}_{-0.04}$	6.56 $^{+0.52}_{-0.52}$	8.79 $^{+0.14}_{-0.14}$	2.12 $^{+0.24}_{-0.24}$	194.47
3480	26.33	1.70	0.12 $^{+0.02}_{-0.02}$	8.74 $^{+0.10}_{-0.10}$	9.02 $^{+0.08}_{-0.08}$	0.42 $^{+0.03}_{-0.03}$	
3485	26.31	1.50	0.30 $^{+0.02}_{-0.02}$	6.87 $^{+0.10}_{-0.10}$	8.09 $^{+0.06}_{-0.06}$	1.23 $^{+0.75}_{-0.75}$	
3491	26.01	1.70	0.16 $^{+0.06}_{-0.06}$	6.78 $^{+0.62}_{-0.62}$	8.49 $^{+0.17}_{-0.17}$	0.74 $^{+0.37}_{-0.37}$	49.19
3503	25.49	2.20	0.20 $^{+0.06}_{-0.06}$	6.66 $^{+1.56}_{-1.56}$	8.38 $^{+0.12}_{-0.12}$	0.42 $^{+0.34}_{-0.34}$	
3511	25.57	2.40	0.20 $^{+0.06}_{-0.06}$	7.80 $^{+0.42}_{-0.42}$	9.09 $^{+0.23}_{-0.23}$	1.72 $^{+0.33}_{-0.33}$	
3542	25.31	1.60	0.68 $^{+0.04}_{-0.04}$	6.76 $^{+0.20}_{-0.20}$	9.68 $^{+0.18}_{-0.18}$	2.92 $^{+0.25}_{-0.25}$	82.01
3548	25.80	3.10	0.34 $^{+0.04}_{-0.04}$	6.56 $^{+0.92}_{-0.92}$	9.08 $^{+0.03}_{-0.03}$	2.53 $^{+0.00}_{-0.00}$	78.90

Table A.1: Best-fit parameters for this work's HDF-S catalog, constant SFR.

ID	$\mathcal{R}_{VI}$	$z_{phot}$	$E(B - V)$	$\log(\text{Age}/\text{yr})$	$\log(M_*/M_\odot)$	$\log(\text{SFR}/(M_\odot/\text{yr}))$	$\chi^2$
3563	24.80	2.95	$0.20^{+0.04}_{-0.06}$	$8.12^{+0.42}_{-0.31}$	$9.86^{+0.16}_{-0.14}$	$1.80^{+0.16}_{-0.24}$	24.48
3578	26.16	1.50	$0.62^{+0.08}_{-0.02}$	$6.56^{+0.10}_{-0.00}$	$8.94^{+0.00}_{-0.04}$	$2.38^{+0.28}_{-0.00}$	163.96
3635	24.67	3.05	$0.16^{+0.02}_{-0.02}$	$8.64^{+0.10}_{-0.21}$	$10.24^{+0.11}_{-0.11}$	$1.69^{+0.09}_{-0.06}$	2.88
3641	26.09	1.50	$0.26^{+0.00}_{-0.04}$	$8.95^{+0.21}_{-0.00}$	$9.59^{+0.03}_{-0.08}$	$0.74^{+0.00}_{-0.21}$	90.82
3646	25.77	2.80	$0.18^{+0.12}_{-0.06}$	$6.87^{+0.21}_{-1.14}$	$8.42^{+0.06}_{-0.43}$	$1.56^{+0.67}_{-0.32}$	28.74
3687	26.32	3.00	$0.08^{+0.04}_{-0.06}$	$8.74^{+0.42}_{-0.21}$	$9.35^{+0.24}_{-0.03}$	$0.70^{+0.12}_{-0.22}$	9.26
3767	26.58	2.20	$0.46^{+0.02}_{-0.00}$	$6.56^{+0.00}_{-0.00}$	$8.81^{+0.03}_{-0.05}$	$2.25^{+0.03}_{-0.05}$	103.03
3779	26.44	3.15	$0.10^{+0.06}_{-0.00}$	$8.43^{+0.33}_{-0.42}$	$9.15^{+0.25}_{-0.24}$	$0.80^{+0.20}_{-0.43}$	85.66
3797	26.34	1.50	$0.18^{+0.06}_{-0.04}$	$8.43^{+0.31}_{-0.42}$	$8.80^{+0.13}_{-0.54}$	$0.45^{+0.07}_{-0.35}$	13.71
3867	25.76	2.45	$0.18^{+0.02}_{-0.06}$	$8.22^{+0.62}_{-0.21}$	$9.31^{+0.32}_{-0.13}$	$1.16^{+0.12}_{-0.32}$	16.98
3897	26.05	1.60	$0.44^{+0.00}_{-0.04}$	$6.66^{+0.10}_{-0.00}$	$8.60^{+0.07}_{-0.07}$	$1.94^{+0.07}_{-0.17}$	75.37

Table A.2: Best-fit parameters for this work's HDF-S catalog, 700 Myr e-folding exponential SFR.

ID	$\mathcal{R}_{V,I}$	$z_{phot}$	$E(B - V)$	$\log(\text{Age}/\text{yr})$	$\log(M_*/\text{M}_\odot)$	$\log(\text{SFR}/\text{M}_\odot/\text{yr})$	$\chi^2$
3	26.37	1.50	0.14 $^{+0.00}_{-0.00}$	7.60 $^{+0.10}_{-0.10}$	8.02 $^{+0.07}_{-0.07}$	0.47 $^{+0.00}_{-0.00}$	75.67
147	23.02	3.05	0.26 $^{+0.02}_{-0.02}$	6.56 $^{+0.20}_{-0.20}$	9.86 $^{+0.00}_{-0.00}$	3.31 $^{+0.34}_{-0.34}$	76.55
156	25.25	1.90	0.10 $^{+0.02}_{-0.02}$	8.64 $^{+0.31}_{-0.31}$	9.29 $^{+0.13}_{-0.13}$	0.86 $^{+0.12}_{-0.12}$	34.78
172	25.24	1.50	0.34 $^{+0.02}_{-0.02}$	8.74 $^{+0.31}_{-0.31}$	9.86 $^{+0.14}_{-0.14}$	1.36 $^{+0.08}_{-0.08}$	15.05
177	25.51	2.25	0.00 $^{+0.00}_{-0.02}$	9.88 $^{+0.94}_{-0.42}$	9.30 $^{+0.04}_{-0.04}$	0.55 $^{+0.04}_{-0.04}$	3.96
201	26.40	1.50	0.22 $^{+0.02}_{-0.02}$	7.49 $^{+0.42}_{-0.42}$	8.17 $^{+0.07}_{-0.07}$	0.72 $^{+0.08}_{-0.08}$	27.57
356	24.38	1.60	0.66 $^{+0.00}_{-0.00}$	6.76 $^{+0.00}_{-0.00}$	9.98 $^{+0.03}_{-0.03}$	3.23 $^{+0.08}_{-0.08}$	74.97
401	26.00	1.70	0.16 $^{+0.02}_{-0.02}$	8.84 $^{+0.21}_{-0.21}$	9.21 $^{+0.13}_{-0.13}$	0.65 $^{+0.15}_{-0.15}$	12.56
428	25.90	3.05	0.24 $^{+0.02}_{-0.02}$	6.56 $^{+0.31}_{-0.31}$	8.64 $^{+0.06}_{-0.06}$	2.09 $^{+0.06}_{-0.06}$	106.14
430	26.08	2.55	0.08 $^{+0.02}_{-0.02}$	7.60 $^{+0.21}_{-0.21}$	8.33 $^{+0.09}_{-0.09}$	0.78 $^{+0.11}_{-0.11}$	133.71
447	25.71	1.50	0.20 $^{+0.04}_{-0.04}$	6.76 $^{+0.00}_{-0.00}$	8.03 $^{+0.10}_{-0.10}$	1.27 $^{+0.20}_{-0.20}$	51.03
462	25.99	1.50	0.50 $^{+0.04}_{-0.04}$	5.20 $^{+0.10}_{-0.10}$	8.86 $^{+0.08}_{-0.08}$	3.87 $^{+1.74}_{-1.74}$	63.98
472	26.15	1.50	0.58 $^{+0.02}_{-0.02}$	6.66 $^{+0.00}_{-0.00}$	8.91 $^{+0.07}_{-0.07}$	2.26 $^{+0.00}_{-0.00}$	115.53
475	26.29	1.50	0.56 $^{+0.02}_{-0.02}$	6.66 $^{+0.00}_{-0.00}$	8.78 $^{+0.02}_{-0.02}$	2.13 $^{+0.02}_{-0.02}$	111.25
481	25.90	1.50	0.26 $^{+0.04}_{-0.04}$	6.76 $^{+0.00}_{-0.00}$	8.13 $^{+0.14}_{-0.14}$	1.38 $^{+0.24}_{-0.24}$	100.93
650	26.27	2.70	0.04 $^{+0.00}_{-0.00}$	8.95 $^{+0.21}_{-0.21}$	9.11 $^{+0.05}_{-0.05}$	0.50 $^{+0.02}_{-0.02}$	101.11
715	24.29	2.95	0.18 $^{+0.02}_{-0.02}$	8.32 $^{+0.62}_{-0.62}$	10.10 $^{+0.24}_{-0.24}$	1.91 $^{+0.06}_{-0.06}$	19.54
720	26.20	1.70	0.12 $^{+0.02}_{-0.02}$	8.22 $^{+0.32}_{-0.32}$	8.58 $^{+0.03}_{-0.03}$	0.48 $^{+0.19}_{-0.19}$	15.64
726	24.92	1.85	0.26 $^{+0.02}_{-0.02}$	8.74 $^{+0.21}_{-0.21}$	9.97 $^{+0.22}_{-0.22}$	1.48 $^{+0.35}_{-0.35}$	9.75
779	25.39	1.55	0.24 $^{+0.02}_{-0.02}$	9.99 $^{+0.33}_{-0.33}$	9.80 $^{+0.07}_{-0.07}$	1.05 $^{+0.04}_{-0.04}$	12.11
797	26.15	2.30	0.08 $^{+0.00}_{-0.00}$	9.68 $^{+0.31}_{-0.31}$	9.36 $^{+0.25}_{-0.25}$	0.62 $^{+0.25}_{-0.25}$	93.02
818	26.08	1.50	0.14 $^{+0.04}_{-0.04}$	8.32 $^{+0.30}_{-0.30}$	8.67 $^{+0.09}_{-0.09}$	0.48 $^{+0.15}_{-0.15}$	139.99
824	25.75	2.45	0.12 $^{+0.02}_{-0.02}$	9.78 $^{+0.30}_{-0.30}$	9.70 $^{+0.09}_{-0.09}$	0.96 $^{+0.00}_{-0.00}$	59.26
876	26.10	1.90	0.00 $^{+0.00}_{-0.00}$	8.32 $^{+0.21}_{-0.21}$	8.41 $^{+0.10}_{-0.10}$	0.22 $^{+0.06}_{-0.06}$	19.96
878	24.94	2.95	0.34 $^{+0.02}_{-0.02}$	6.99 $^{+0.21}_{-0.21}$	9.37 $^{+0.17}_{-0.17}$	2.62 $^{+0.13}_{-0.13}$	56.69
1029	25.66	2.10	0.12 $^{+0.02}_{-0.02}$	9.05 $^{+0.32}_{-0.32}$	9.50 $^{+0.20}_{-0.20}$	0.85 $^{+0.07}_{-0.07}$	5.64
1089	25.09	1.50	0.32 $^{+0.14}_{-0.14}$	8.01 $^{+0.25}_{-0.25}$	9.38 $^{+0.09}_{-0.09}$	1.45 $^{+0.17}_{-0.17}$	15.58
1102	24.70	3.15	0.08 $^{+0.02}_{-0.02}$	8.84 $^{+0.42}_{-0.42}$	9.99 $^{+0.14}_{-0.14}$	1.43 $^{+0.06}_{-0.06}$	8.72
1159	26.32	1.50	0.00 $^{+0.00}_{-0.00}$	8.84 $^{+0.10}_{-0.10}$	8.51 $^{+0.06}_{-0.06}$	-0.05 $^{+0.00}_{-0.00}$	32.34
1191	25.61	2.45	0.02 $^{+0.02}_{-0.02}$	7.18 $^{+0.21}_{-0.21}$	8.00 $^{+0.09}_{-0.09}$	0.84 $^{+0.18}_{-0.18}$	14.25
1366	24.92	1.60	0.36 $^{+0.02}_{-0.02}$	9.05 $^{+0.31}_{-0.31}$	9.50 $^{+0.20}_{-0.20}$	0.85 $^{+0.07}_{-0.07}$	5.64
1441	25.66	1.50	0.40 $^{+0.02}_{-0.02}$	6.66 $^{+1.36}_{-1.36}$	8.54 $^{+0.16}_{-0.16}$	1.89 $^{+0.20}_{-0.20}$	9.41
1228	24.95	1.70	0.18 $^{+0.06}_{-0.06}$	9.05 $^{+0.30}_{-0.30}$	9.78 $^{+0.32}_{-0.32}$	1.13 $^{+0.18}_{-0.18}$	2.66
1451	25.45	1.60	0.30 $^{+0.02}_{-0.02}$	7.60 $^{+0.21}_{-0.21}$	8.93 $^{+0.16}_{-0.16}$	1.39 $^{+0.35}_{-0.35}$	91.71
1467	24.30	2.55	0.10 $^{+0.00}_{-0.00}$	7.28 $^{+0.00}_{-0.00}$	8.18 $^{+0.08}_{-0.08}$	0.93 $^{+0.12}_{-0.12}$	3.27
1478	25.90	1.70	0.44 $^{+0.02}_{-0.02}$	6.56 $^{+0.21}_{-0.21}$	9.81 $^{+0.14}_{-0.14}$	3.26 $^{+0.00}_{-0.00}$	70.05
1482	24.27	1.85	0.28 $^{+0.02}_{-0.02}$	7.80 $^{+0.62}_{-0.62}$	9.38 $^{+0.33}_{-0.33}$	1.62 $^{+0.08}_{-0.08}$	23.40
1484	25.12	1.65	0.38 $^{+0.02}_{-0.02}$	8.74 $^{+0.31}_{-0.31}$	10.23 $^{+0.12}_{-0.12}$	1.38 $^{+0.08}_{-0.08}$	9.98
1576	26.02	1.50	0.10 $^{+0.00}_{-0.00}$	8.95 $^{+0.21}_{-0.21}$	10.25 $^{+0.05}_{-0.05}$	1.64 $^{+0.04}_{-0.04}$	21.20
1498	23.49	1.85	0.28 $^{+0.02}_{-0.02}$	8.53 $^{+0.66}_{-0.66}$	10.46 $^{+0.37}_{-0.37}$	2.11 $^{+0.19}_{-0.19}$	22.03
1521	25.78	3.05	0.26 $^{+0.02}_{-0.02}$	6.56 $^{+0.21}_{-0.21}$	10.22 $^{+0.33}_{-0.33}$	1.48 $^{+0.20}_{-0.20}$	3.27
1533	26.40	1.65	0.28 $^{+0.02}_{-0.02}$	8.95 $^{+0.52}_{-0.52}$	9.44 $^{+0.12}_{-0.12}$	1.65 $^{+0.02}_{-0.02}$	23.40
1565	25.54	1.85	0.30 $^{+0.02}_{-0.02}$	8.74 $^{+0.31}_{-0.31}$	9.85 $^{+0.08}_{-0.08}$	1.35 $^{+0.19}_{-0.19}$	4.78
1695	26.23	1.65	0.12 $^{+0.04}_{-0.04}$	7.80 $^{+0.31}_{-0.31}$	8.21 $^{+0.10}_{-0.10}$	0.47 $^{+0.18}_{-0.18}$	19.30
1817	26.17	1.50	0.56 $^{+0.04}_{-0.04}$	6.56 $^{+0.30}_{-0.30}$	9.89 $^{+0.10}_{-0.10}$	2.11 $^{+0.09}_{-0.09}$	22.03
1933	24.50	2.30	0.18 $^{+0.02}_{-0.02}$	9.26 $^{+0.97}_{-0.97}$	10.29 $^{+0.07}_{-0.07}$	2.20 $^{+0.06}_{-0.06}$	233.41
1604	26.05	2.45	0.04 $^{+0.02}_{-0.02}$	8.64 $^{+0.21}_{-0.21}$	8.97 $^{+0.16}_{-0.16}$	0.83 $^{+0.33}_{-0.33}$	190.08
1634	25.04	2.80	0.24 $^{+0.02}_{-0.02}$	8.01 $^{+0.21}_{-0.21}$	9.74 $^{+0.13}_{-0.13}$	1.81 $^{+0.20}_{-0.20}$	9.98
1985	26.23	1.65	0.12 $^{+0.04}_{-0.04}$	8.95 $^{+0.42}_{-0.42}$	9.03 $^{+0.05}_{-0.05}$	1.35 $^{+0.19}_{-0.19}$	4.78
2005	26.06	1.50	0.14 $^{+0.00}_{-0.00}$	7.70 $^{+0.10}_{-0.10}$	8.24 $^{+0.01}_{-0.01}$	0.42 $^{+0.17}_{-0.17}$	72.57
2033	26.35	2.10	0.08 $^{+0.00}_{-0.00}$	10.30 $^{+1.14}_{-1.14}$	9.19 $^{+0.06}_{-0.06}$	2.43 $^{+0.00}_{-0.00}$	139.65
2042	26.06	2.05	0.08 $^{+0.14}_{-0.14}$	9.68 $^{+1.87}_{-0.87}$	9.29 $^{+0.13}_{-0.13}$	0.45 $^{+0.02}_{-0.02}$	33.30
2050	25.86	2.60	0.24 $^{+0.14}_{-0.14}$	7.18 $^{+0.62}_{-0.62}$	8.72 $^{+0.35}_{-0.35}$	0.55 $^{+0.05}_{-0.05}$	50.92

Table A.2: Best-fit parameters for this work's HDF-S catalog, 700 Myr e-folding exponential SFR.

ID	$\mathcal{R}_{VI}$	$z_{phot}$	$E(B - V)$	$\log(\text{Age}/\text{yr})$	$\log(M_*/M_\odot)$	$\log(\text{SFR}/(M_\odot/\text{yr}))$	$\chi^2$
2192	26.46	2.70	$0.00^{+0.00}_{-0.00}$	$8.64^{+1.10}_{-0.90}$	$8.72^{+0.08}_{-0.08}$	$0.29^{+0.02}_{-0.02}$	35.89
2207	25.00	2.45	$0.06^{+0.02}_{-0.00}$	$8.84^{+0.10}_{-0.21}$	$9.60^{+0.08}_{-0.11}$	$1.04^{+0.16}_{-0.02}$	32.85
2306	25.77	2.75	$0.10^{+0.02}_{-0.02}$	$8.43^{+0.21}_{-0.21}$	$9.24^{+0.10}_{-0.09}$	$0.97^{+0.09}_{-0.09}$	64.53
2361	25.30	2.65	$0.02^{+0.02}_{-0.00}$	$8.64^{+0.10}_{-0.31}$	$9.25^{+0.07}_{-0.13}$	$0.82^{+0.08}_{-0.04}$	6.36
2367	25.71	2.55	$0.06^{+0.00}_{-0.04}$	$8.53^{+0.42}_{-0.10}$	$9.13^{+0.18}_{-0.07}$	$0.78^{+0.06}_{-0.17}$	18.71
2389	24.01	2.85	$0.34^{+0.00}_{-0.08}$	$6.56^{+0.42}_{-0.00}$	$9.71^{+0.03}_{-0.19}$	$3.17^{+0.03}_{-0.62}$	86.47
2560	26.08	1.50	$0.26^{+0.16}_{-0.02}$	$6.97^{+0.00}_{-0.35}$	$8.11^{+0.01}_{-0.15}$	$1.15^{+0.55}_{-0.16}$	6.11
2575	25.90	1.95	$0.08^{+0.02}_{-0.02}$	$8.84^{+0.21}_{-0.21}$	$9.11^{+0.07}_{-0.11}$	$0.55^{+0.11}_{-0.12}$	6.31
2597	26.56	2.95	$0.00^{+0.00}_{-0.00}$	$6.87^{+1.77}_{-0.62}$	$7.47^{+0.07}_{-0.45}$	$0.62^{+0.22}_{-2.50}$	7.15
2661	26.46	1.60	$0.00^{+0.00}_{-0.00}$	$8.95^{+0.10}_{-0.00}$	$8.56^{+0.05}_{-0.04}$	$-0.05^{+0.00}_{-0.05}$	137.93
2728	24.56	1.70	$0.16^{+0.02}_{-0.02}$	$8.64^{+0.21}_{-0.21}$	$9.66^{+0.12}_{-0.08}$	$1.23^{+0.12}_{-0.14}$	14.23
2747	26.50	1.50	$0.44^{+0.02}_{-0.04}$	$6.66^{+0.10}_{-0.00}$	$8.37^{+0.00}_{-0.14}$	$1.72^{+0.00}_{-0.24}$	49.44
2763	25.91	1.70	$0.06^{+0.04}_{-0.06}$	$8.32^{+0.12}_{-0.31}$	$8.59^{+0.19}_{-0.06}$	$0.40^{+0.25}_{-0.11}$	204.82
2765	26.36	1.50	$0.24^{+0.02}_{-0.02}$	$6.97^{+1.46}_{-0.42}$	$7.94^{+0.01}_{-0.82}$	$0.98^{+0.54}_{-0.11}$	14.50
2784	25.79	1.50	$0.08^{+0.00}_{-0.00}$	$9.68^{+0.42}_{-0.62}$	$9.15^{+0.03}_{-0.03}$	$0.40^{+0.00}_{-0.03}$	106.70
2799	26.59	2.45	$0.08^{+0.06}_{-0.00}$	$9.36^{+0.21}_{-0.94}$	$9.15^{+0.60}_{-0.02}$	$0.43^{+0.61}_{-0.00}$	378.46
2817	26.04	2.05	$0.32^{+0.00}_{-0.06}$	$6.66^{+0.42}_{-0.00}$	$8.48^{+0.05}_{-0.28}$	$1.83^{+0.05}_{-0.70}$	24.53
2837	25.41	1.60	$0.30^{+0.04}_{-0.04}$	$6.97^{+1.10}_{-0.10}$	$8.55^{+0.06}_{-0.45}$	$1.60^{+0.08}_{-0.62}$	7.54
2849	25.15	2.45	$0.18^{+0.06}_{-0.02}$	$8.84^{+0.00}_{-0.21}$	$9.95^{+0.02}_{-0.02}$	$1.39^{+0.08}_{-0.38}$	24.10
2889	25.21	2.50	$0.20^{+0.06}_{-0.02}$	$6.87^{+0.10}_{-0.62}$	$8.65^{+0.05}_{-0.23}$	$1.79^{+0.38}_{-0.14}$	5.98
2913	23.43	2.70	$0.22^{+0.06}_{-0.04}$	$7.80^{+0.42}_{-0.52}$	$10.13^{+0.18}_{-0.21}$	$2.39^{+0.25}_{-0.21}$	7.06
2958	25.82	2.55	$0.08^{+0.00}_{-0.00}$	$10.20^{+1.14}_{-1.10}$	$9.55^{+0.09}_{-0.02}$	$0.81^{+0.04}_{-0.02}$	16.31
3043	23.09	2.75	$0.22^{+0.04}_{-0.16}$	$7.08^{+1.98}_{-0.42}$	$9.76^{+0.10}_{-0.40}$	$2.70^{+0.22}_{-2.64}$	8.92
3098	25.83	1.60	$0.40^{+0.14}_{-0.02}$	$5.72^{+0.12}_{-1.14}$	$8.74^{+0.53}_{-0.63}$	$3.07^{+0.72}_{-0.95}$	2.20
3127	24.50	1.85	$0.32^{+0.02}_{-0.02}$	$8.74^{+0.21}_{-0.21}$	$10.33^{+0.23}_{-0.08}$	$1.84^{+0.23}_{-0.11}$	6.38
3166	25.59	1.90	$0.20^{+0.04}_{-0.22}$	$8.43^{+1.56}_{-0.42}$	$9.33^{+0.59}_{-0.18}$	$1.06^{+0.28}_{-0.83}$	42.83
3169	26.52	1.50	$0.32^{+0.06}_{-0.06}$	$6.87^{+0.21}_{-0.21}$	$8.05^{+0.02}_{-0.17}$	$1.19^{+0.12}_{-0.35}$	45.19
3217	26.59	1.95	$0.10^{+0.00}_{-0.04}$	$9.16^{+0.62}_{-1.14}$	$9.00^{+0.28}_{-0.13}$	$0.32^{+0.03}_{-0.17}$	40.60
3321	26.30	2.55	$0.36^{+0.02}_{-0.04}$	$6.56^{+1.46}_{-0.00}$	$8.74^{+0.05}_{-0.22}$	$2.19^{+0.05}_{-0.07}$	10.95
3330	26.18	1.50	$0.16^{+0.02}_{-0.04}$	$8.84^{+0.31}_{-1.46}$	$9.00^{+0.44}_{-0.44}$	$0.44^{+0.49}_{-0.09}$	136.78
3397	26.57	1.85	$0.08^{+0.00}_{-0.04}$	$8.64^{+0.31}_{-0.10}$	$8.68^{+0.10}_{-0.11}$	$0.25^{+0.09}_{-0.18}$	22.18
3407	25.96	1.50	$0.26^{+0.00}_{-0.02}$	$7.39^{+0.21}_{-0.00}$	$8.38^{+0.07}_{-0.00}$	$1.03^{+0.00}_{-0.13}$	38.08
3419	26.05	1.50	$0.14^{+0.00}_{-0.02}$	$10.30^{+1.35}_{-0.00}$	$9.20^{+0.07}_{-0.03}$	$0.45^{+0.00}_{-0.09}$	6.44
3554	26.47	1.80	$0.02^{+0.02}_{-0.04}$	$8.64^{+0.31}_{-0.21}$	$8.50^{+0.14}_{-0.10}$	$0.08^{+0.14}_{-0.20}$	55.70
3560	25.95	1.60	$0.08^{+0.02}_{-0.02}$	$9.05^{+0.00}_{-0.25}$	$9.04^{+0.10}_{-0.07}$	$0.38^{+0.09}_{-0.07}$	28.53
3625	26.28	1.60	$0.56^{+0.00}_{-0.02}$	$6.66^{+0.00}_{-0.00}$	$8.88^{+0.02}_{-0.00}$	$2.23^{+0.00}_{-0.00}$	48.78
3639	25.13	3.00	$0.22^{+0.00}_{-0.00}$	$9.05^{+0.10}_{-1.25}$	$10.38^{+0.04}_{-0.07}$	$1.73^{+0.03}_{-0.00}$	27.77
3666	25.93	1.85	$0.06^{+0.00}_{-0.02}$	$8.74^{+0.21}_{-0.10}$	$8.94^{+0.09}_{-0.06}$	$0.44^{+0.09}_{-0.09}$	33.28
3689	26.16	2.45	$0.08^{+0.02}_{-0.06}$	$8.64^{+0.73}_{-0.42}$	$9.06^{+0.32}_{-0.18}$	$0.63^{+0.08}_{-0.28}$	102.72
3782	25.43	1.85	$0.10^{+0.02}_{-0.00}$	$8.74^{+0.10}_{-0.21}$	$9.26^{+0.07}_{-0.04}$	$0.77^{+0.07}_{-0.03}$	112.21
3789	26.42	1.50	$0.34^{+0.02}_{-0.02}$	$6.76^{+0.00}_{-0.00}$	$8.16^{+0.06}_{-0.06}$	$1.40^{+0.06}_{-0.06}$	104.31
3795	25.94	2.25	$0.26^{+0.24}_{-0.04}$	$7.39^{+0.31}_{-2.91}$	$8.73^{+0.33}_{-0.81}$	$1.38^{+0.60}_{-0.21}$	214.88
3808	24.78	3.05	$0.20^{+0.00}_{-0.04}$	$9.05^{+0.52}_{-1.25}$	$10.49^{+0.19}_{-0.09}$	$1.83^{+0.03}_{-0.14}$	5.92
59	25.81	2.95	$0.16^{+0.10}_{-0.06}$	$6.87^{+0.21}_{-1.14}$	$8.39^{+0.02}_{-0.44}$	$1.54^{+0.62}_{-0.34}$	13.55
69	25.82	1.50	$0.34^{+0.04}_{-0.02}$	$6.76^{+0.10}_{-0.10}$	$8.36^{+0.07}_{-0.12}$	$1.61^{+0.17}_{-0.22}$	112.30
73	26.47	1.50	$0.14^{+0.14}_{-0.04}$	$7.39^{+0.31}_{-0.46}$	$7.83^{+0.13}_{-0.07}$	$0.48^{+0.25}_{-0.26}$	8.12
100	25.97	2.25	$0.40^{+0.04}_{-0.00}$	$6.56^{+0.00}_{-0.09}$	$8.86^{+0.04}_{-0.13}$	$2.31^{+0.07}_{-0.24}$	105.58
190	25.76	1.50	$0.22^{+0.02}_{-0.02}$	$7.39^{+0.21}_{-0.10}$	$8.36^{+0.07}_{-0.13}$	$1.01^{+0.09}_{-0.13}$	60.62
203	25.80	2.10	$0.14^{+0.00}_{-0.02}$	$8.95^{+0.31}_{-0.00}$	$9.45^{+0.13}_{-0.00}$	$0.84^{+0.05}_{-0.07}$	70.68
207	25.26	1.70	$0.40^{+0.02}_{-0.18}$	$8.32^{+1.35}_{-0.10}$	$9.89^{+0.51}_{-0.13}$	$1.70^{+0.07}_{-0.76}$	54.22
242	25.91	2.05	$0.38^{+0.00}_{-0.02}$	$6.87^{+0.10}_{-0.00}$	$8.78^{+0.03}_{-0.07}$	$1.93^{+0.03}_{-0.17}$	111.81
288	25.09	2.45	$0.40^{+0.02}_{-0.04}$	$6.76^{+0.10}_{-0.21}$	$9.35^{+0.09}_{-0.37}$	$2.59^{+0.19}_{-0.17}$	2.77
296	25.59	3.65	$0.10^{+0.04}_{-0.00}$	$6.45^{+0.31}_{-0.10}$	$8.40^{+0.18}_{-0.03}$	$1.96^{+0.29}_{-0.35}$	119.00
310	26.06	2.45	$0.00^{+0.00}_{-0.00}$	$7.49^{+0.10}_{-0.00}$	$7.91^{+0.07}_{-0.00}$	$0.47^{+0.06}_{-0.02}$	303.12
313	25.64	1.85	$0.08^{+0.00}_{-0.02}$	$8.84^{+0.21}_{-0.10}$	$9.18^{+0.06}_{-0.05}$	$0.62^{+0.02}_{-0.10}$	153.68
328	25.49	2.45	$0.04^{+0.02}_{-0.02}$	$7.08^{+0.21}_{-0.21}$	$8.02^{+0.04}_{-0.08}$	$0.97^{+0.14}_{-0.16}$	180.93
339	24.91	2.35	$0.16^{+0.00}_{-0.00}$	$6.56^{+0.00}_{-0.00}$	$8.51^{+0.03}_{-0.03}$	$1.96^{+0.03}_{-0.03}$	65.62
448	25.60	2.75	$0.24^{+0.06}_{-0.02}$	$7.91^{+0.21}_{-0.52}$	$9.42^{+0.08}_{-0.21}$	$1.59^{+0.23}_{-0.11}$	3.85

Table A.2: Best-fit parameters for this work's HDF-S catalog, 700 Myr e-folding exponential SFR.

ID	$\mathcal{R}_{VI}$	$z_{phot}$	$E(B - V)$	$\log(\text{Age}/\text{yr})$	$\log(M_*/M_\odot)$	$\log(\text{SFR}/(M_\odot/\text{yr}))$	$\chi^2$
464	25.68	2.95	$0.18^{+0.00}_{-0.02}$	$8.74^{+0.21}_{-0.00}$	$9.82^{+0.08}_{-0.00}$	$1.33^{+0.02}_{-0.06}$	71.85
470	25.97	2.75	$0.36^{+0.02}_{-0.06}$	$6.56^{+1.46}_{-0.00}$	$8.96^{+0.03}_{-0.00}$	$2.42^{+0.03}_{-1.97}$	24.14
480	26.11	2.60	$0.14^{+0.02}_{-0.00}$	$8.95^{+0.10}_{-1.35}$	$9.54^{+0.07}_{-0.10}$	$0.93^{+0.10}_{-0.02}$	62.99
520	26.31	2.30	$0.38^{+0.02}_{-0.00}$	$6.56^{+0.00}_{-0.00}$	$8.66^{+0.03}_{-0.02}$	$2.12^{+0.03}_{-0.02}$	131.13
533	25.69	2.30	$0.38^{+0.00}_{-0.00}$	$6.56^{+0.00}_{-0.00}$	$8.92^{+0.02}_{-0.00}$	$2.37^{+0.02}_{-0.00}$	137.39
542	26.10	1.50	$0.42^{+0.02}_{-0.04}$	$6.66^{+0.00}_{-0.00}$	$8.44^{+0.00}_{-0.15}$	$1.79^{+0.00}_{-0.25}$	131.85
544	26.46	1.50	$0.40^{+0.00}_{-0.06}$	$6.66^{+0.56}_{-0.00}$	$8.25^{+0.00}_{-0.38}$	$1.60^{+0.00}_{-2.20}$	136.36
570	26.25	2.35	$0.32^{+0.04}_{-0.02}$	$6.56^{+0.00}_{-0.10}$	$8.51^{+0.14}_{-0.04}$	$1.96^{+0.25}_{-0.04}$	170.34
572	25.78	1.50	$0.42^{+0.00}_{-0.00}$	$6.66^{+0.00}_{-0.00}$	$8.60^{+0.00}_{-0.00}$	$1.93^{+0.00}_{-0.00}$	165.62
579	25.66	1.65	$0.46^{+0.00}_{-0.00}$	$6.66^{+0.00}_{-0.00}$	$8.85^{+0.00}_{-0.00}$	$2.20^{+0.00}_{-0.00}$	198.64
590	26.47	1.50	$0.12^{+0.02}_{-0.02}$	$9.05^{+0.21}_{-1.25}$	$8.85^{+0.04}_{-0.07}$	$0.20^{+0.06}_{-0.07}$	362.44
639	25.98	2.80	$0.48^{+0.04}_{-0.04}$	$6.56^{+1.46}_{-0.00}$	$9.41^{+0.13}_{-0.10}$	$2.86^{+0.23}_{-0.25}$	6.40
649	26.58	2.45	$0.28^{+0.04}_{-0.02}$	$7.70^{+0.21}_{-0.21}$	$8.89^{+0.10}_{-0.11}$	$1.25^{+0.19}_{-0.11}$	63.39
665	25.50	2.90	$0.46^{+0.04}_{-0.00}$	$6.35^{+0.21}_{-0.21}$	$9.60^{+0.17}_{-0.02}$	$3.27^{+0.38}_{-0.24}$	12.81
673	25.59	2.90	$0.42^{+0.04}_{-0.04}$	$6.56^{+1.46}_{-0.10}$	$9.37^{+0.13}_{-0.22}$	$2.82^{+0.23}_{-1.97}$	9.22
692	25.18	1.50	$0.20^{+0.00}_{-0.02}$	$9.88^{+0.94}_{-0.42}$	$9.72^{+0.07}_{-0.07}$	$0.97^{+0.00}_{-0.14}$	15.74
721	25.32	2.95	$0.14^{+0.00}_{-0.00}$	$10.20^{+0.31}_{-0.00}$	$10.04^{+0.00}_{-0.00}$	$1.29^{+0.06}_{-0.00}$	164.01
746	26.07	2.85	$0.44^{+0.02}_{-0.02}$	$6.45^{+1.35}_{-0.10}$	$9.27^{+0.11}_{-0.14}$	$2.83^{+0.21}_{-0.78}$	19.32
848	25.57	2.35	$0.32^{+0.00}_{-0.00}$	$10.09^{+0.21}_{-0.21}$	$10.44^{+0.06}_{-0.03}$	$1.69^{+0.06}_{-0.03}$	49.89
871	25.43	3.00	$0.14^{+0.00}_{-0.00}$	$9.99^{+0.83}_{-0.31}$	$10.06^{+0.06}_{-0.02}$	$1.31^{+0.00}_{-0.03}$	5.88
972	26.43	2.45	$0.30^{+0.08}_{-0.04}$	$7.28^{+0.42}_{-0.83}$	$8.74^{+0.13}_{-0.36}$	$1.49^{+0.42}_{-0.30}$	18.72
1047	26.19	3.20	$0.00^{+0.00}_{-0.06}$	$7.18^{+0.42}_{-0.73}$	$7.84^{+0.17}_{-0.51}$	$0.68^{+0.17}_{-0.39}$	144.38
1106	26.05	2.60	$0.48^{+0.02}_{-0.06}$	$6.76^{+0.21}_{-0.10}$	$9.27^{+0.04}_{-0.18}$	$2.52^{+0.14}_{-0.39}$	35.84
1108	24.77	3.30	$0.08^{+0.00}_{-0.00}$	$10.09^{+0.94}_{-0.21}$	$10.19^{+0.06}_{-0.02}$	$1.44^{+0.02}_{-0.02}$	3.51
1124	26.47	2.35	$0.32^{+0.04}_{-0.04}$	$6.76^{+0.00}_{-0.10}$	$8.47^{+0.05}_{-0.05}$	$1.72^{+0.11}_{-0.16}$	115.23
1140	26.52	1.85	$0.36^{+0.04}_{-0.02}$	$6.66^{+0.00}_{-0.10}$	$8.34^{+0.14}_{-0.03}$	$1.69^{+0.24}_{-0.03}$	127.74
1225	26.56	3.25	$0.00^{+0.00}_{-0.00}$	$8.64^{+0.21}_{-1.66}$	$8.80^{+0.15}_{-0.31}$	$0.37^{+0.02}_{-0.02}$	57.74
1273	25.92	1.50	$0.26^{+0.00}_{-0.00}$	$7.49^{+0.10}_{-0.00}$	$8.46^{+0.07}_{-0.00}$	$1.01^{+0.00}_{-0.03}$	467.35
1403	26.34	3.45	$0.04^{+0.02}_{-0.00}$	$9.26^{+0.31}_{-1.04}$	$9.41^{+0.10}_{-0.03}$	$0.70^{+0.08}_{-0.00}$	56.05
1471	26.50	2.55	$0.18^{+0.00}_{-0.02}$	$8.84^{+0.21}_{-0.21}$	$9.44^{+0.10}_{-0.07}$	$0.89^{+0.05}_{-0.08}$	38.49
1473	25.78	1.65	$0.30^{+0.00}_{-0.00}$	$8.95^{+0.10}_{-0.90}$	$9.75^{+0.04}_{-0.00}$	$1.14^{+0.00}_{-0.01}$	48.57
1501	25.94	3.05	$0.38^{+0.02}_{-0.02}$	$6.45^{+1.35}_{-0.21}$	$9.17^{+0.11}_{-0.61}$	$2.73^{+1.68}_{-1.78}$	131.74
1523	25.86	2.20	$0.38^{+0.04}_{-0.04}$	$6.56^{+0.31}_{-0.00}$	$8.82^{+0.11}_{-0.17}$	$2.27^{+0.11}_{-0.47}$	49.40
1527	26.37	2.55	$0.12^{+0.00}_{-0.02}$	$9.88^{+0.83}_{-0.42}$	$9.48^{+0.09}_{-0.04}$	$0.73^{+0.02}_{-0.07}$	87.36
1540	25.86	1.60	$0.42^{+0.04}_{-0.02}$	$7.18^{+0.10}_{-0.42}$	$8.85^{+0.07}_{-0.25}$	$1.69^{+0.18}_{-0.10}$	174.82
1543	25.04	1.70	$0.30^{+0.02}_{-0.02}$	$8.64^{+0.21}_{-0.21}$	$9.89^{+0.14}_{-0.09}$	$1.46^{+0.14}_{-0.18}$	14.91
1551	26.54	1.85	$0.34^{+0.02}_{-0.00}$	$8.95^{+0.10}_{-0.31}$	$9.69^{+0.18}_{-0.13}$	$1.08^{+0.20}_{-0.04}$	44.70
1572	25.99	1.50	$0.56^{+0.16}_{-0.16}$	$5.10^{+0.00}_{-0.00}$	$9.06^{+0.32}_{-0.32}$	$4.26^{+0.77}_{-0.08}$	54.98
1585	26.27	1.50	$0.60^{+0.00}_{-0.00}$	$5.20^{+0.10}_{-0.10}$	$9.08^{+0.05}_{-0.07}$	$4.09^{+1.29}_{-0.22}$	139.44
1590	26.06	1.70	$0.22^{+0.02}_{-0.00}$	$8.74^{+0.00}_{-0.31}$	$9.31^{+0.09}_{-0.08}$	$0.81^{+0.20}_{-0.08}$	35.97
1593	25.52	1.50	$0.48^{+0.00}_{-0.02}$	$10.20^{+1.14}_{-0.10}$	$10.40^{+0.03}_{-0.00}$	$1.66^{+0.00}_{-0.06}$	162.59
1647	25.44	1.70	$0.14^{+0.00}_{-0.02}$	$8.74^{+0.10}_{-0.00}$	$9.31^{+0.03}_{-0.00}$	$0.82^{+0.03}_{-0.06}$	32.39
1676	25.94	1.70	$0.14^{+0.02}_{-0.02}$	$8.74^{+0.21}_{-0.21}$	$9.11^{+0.08}_{-0.13}$	$0.62^{+0.10}_{-0.14}$	9.01
1696	26.55	2.50	$0.12^{+0.02}_{-0.02}$	$8.84^{+0.31}_{-0.46}$	$9.18^{+0.12}_{-0.15}$	$0.63^{+0.08}_{-0.03}$	42.84
1699	26.53	2.80	$0.42^{+0.04}_{-0.02}$	$5.72^{+0.62}_{-0.62}$	$9.07^{+0.22}_{-0.03}$	$3.40^{+0.10}_{-0.99}$	98.81
1739	25.04	2.95	$0.12^{+0.02}_{-0.00}$	$8.64^{+0.00}_{-0.31}$	$9.80^{+0.02}_{-0.12}$	$1.38^{+0.08}_{-0.00}$	8.69
1863	25.24	1.65	$0.32^{+0.02}_{-0.02}$	$8.74^{+0.21}_{-0.21}$	$9.90^{+0.11}_{-0.10}$	$1.41^{+0.18}_{-0.11}$	27.31
1881	25.15	2.60	$0.12^{+0.00}_{-0.00}$	$10.20^{+0.83}_{-0.10}$	$9.98^{+0.02}_{-0.02}$	$1.23^{+0.02}_{-0.02}$	11.59
1908	26.01	3.10	$0.14^{+0.04}_{-0.14}$	$8.64^{+1.25}_{-1.66}$	$9.50^{+0.48}_{-0.25}$	$1.08^{+0.14}_{-0.59}$	80.12
1915	26.55	2.75	$0.02^{+0.00}_{-0.02}$	$10.09^{+0.94}_{-0.21}$	$9.07^{+0.06}_{-0.06}$	$0.32^{+0.02}_{-0.06}$	63.04
1926	25.69	2.55	$0.38^{+0.04}_{-0.02}$	$8.43^{+0.21}_{-0.22}$	$10.21^{+0.11}_{-0.05}$	$1.93^{+0.06}_{-0.09}$	6.57
1954	26.00	2.40	$0.08^{+0.00}_{-0.00}$	$9.68^{+0.52}_{-0.62}$	$9.42^{+0.07}_{-0.04}$	$0.68^{+0.04}_{-0.04}$	14.18
1960	26.23	2.40	$0.44^{+0.10}_{-0.04}$	$6.56^{+1.46}_{-0.52}$	$8.97^{+0.24}_{-0.24}$	$2.43^{+0.69}_{-1.99}$	32.76
2021	26.47	2.45	$0.42^{+0.00}_{-0.02}$	$6.56^{+0.00}_{-0.00}$	$8.80^{+0.00}_{-0.05}$	$2.25^{+0.00}_{-0.05}$	209.10
2025	25.67	1.50	$0.66^{+0.04}_{-0.00}$	$6.56^{+0.00}_{-0.10}$	$9.27^{+0.14}_{-0.00}$	$2.72^{+0.24}_{-0.00}$	219.03
2030	25.66	3.15	$0.00^{+0.00}_{-0.06}$	$8.64^{+0.52}_{-0.10}$	$9.15^{+0.19}_{-0.06}$	$0.72^{+0.00}_{-0.23}$	1.72
2052	26.18	2.85	$0.12^{+0.04}_{-0.06}$	$6.56^{+1.46}_{-0.10}$	$8.00^{+0.13}_{-0.28}$	$1.45^{+0.23}_{-0.63}$	9.24
2071	25.56	2.90	$0.14^{+0.02}_{-0.04}$	$8.84^{+0.42}_{-0.42}$	$9.79^{+0.14}_{-0.10}$	$1.23^{+0.06}_{-0.14}$	4.39

Table A.2: Best-fit parameters for this work's HDF-S catalog, 700 Myr e-folding exponential SFR.

ID	$\mathcal{R}_{VI}$	$z_{phot}$	$E(B - V)$	$\log(\text{Age}/\text{yr})$	$\log(M_*/M_\odot)$	$\log(\text{SFR}/(M_\odot/\text{yr}))$	$\chi^2$
2188	26.09	2.55	$0.32^{+0.02}_{-0.02}$	$7.70^{+0.21}_{-0.21}$	$9.22^{+0.08}_{-0.11}$	$1.58^{+0.11}_{-0.11}$	151.48
2219	26.20	1.50	$0.56^{+0.02}_{-0.02}$	$7.60^{+0.21}_{-0.21}$	$9.32^{+0.08}_{-0.08}$	$1.77^{+0.12}_{-0.12}$	42.10
2257	26.39	1.80	$0.48^{+0.02}_{-0.02}$	$10.20^{+0.73}_{-0.73}$	$10.33^{+0.05}_{-0.05}$	$1.59^{+0.04}_{-0.04}$	144.87
2266	25.40	2.05	$0.32^{+0.02}_{-0.02}$	$10.20^{+0.73}_{-0.73}$	$10.35^{+0.04}_{-0.04}$	$1.61^{+0.03}_{-0.03}$	67.65
2300	25.78	2.50	$0.48^{+0.02}_{-0.02}$	$6.45^{+0.36}_{-0.36}$	$9.36^{+0.04}_{-0.04}$	$2.91^{+0.95}_{-0.95}$	164.60
2315	26.37	2.25	$0.24^{+0.02}_{-0.02}$	$8.32^{+0.21}_{-0.21}$	$9.22^{+0.13}_{-0.13}$	$1.03^{+0.16}_{-0.16}$	53.71
2329	26.11	2.65	$0.10^{+0.02}_{-0.02}$	$9.16^{+0.31}_{-0.31}$	$9.47^{+0.16}_{-0.16}$	$0.78^{+0.06}_{-0.06}$	41.86
2356	25.55	1.70	$0.18^{+0.02}_{-0.02}$	$8.64^{+0.10}_{-0.10}$	$9.33^{+0.09}_{-0.09}$	$0.90^{+0.16}_{-0.16}$	40.05
2427	26.22	3.00	$0.34^{+0.08}_{-0.08}$	$6.04^{+0.94}_{-0.94}$	$8.96^{+0.35}_{-0.35}$	$2.95^{+1.99}_{-1.99}$	14.33
2429	26.34	1.50	$0.48^{+0.02}_{-0.02}$	$5.52^{+0.42}_{-0.42}$	$8.63^{+0.03}_{-0.03}$	$3.21^{+0.24}_{-0.24}$	251.04
2529	26.08	1.50	$0.58^{+0.02}_{-0.02}$	$5.72^{+0.92}_{-0.92}$	$9.07^{+0.09}_{-0.09}$	$3.40^{+0.93}_{-0.93}$	119.19
2545	25.75	2.70	$0.18^{+0.02}_{-0.02}$	$9.88^{+0.52}_{-0.52}$	$9.99^{+0.02}_{-0.02}$	$1.24^{+0.08}_{-0.08}$	49.74
2553	26.47	2.65	$0.28^{+0.06}_{-0.06}$	$6.66^{+0.42}_{-0.42}$	$8.38^{+0.12}_{-0.12}$	$1.73^{+0.51}_{-0.51}$	56.47
2561	26.34	1.50	$0.42^{+0.02}_{-0.02}$	$7.39^{+0.52}_{-0.52}$	$8.69^{+0.02}_{-0.02}$	$1.34^{+0.12}_{-0.12}$	49.38
2568	26.04	2.25	$0.32^{+0.02}_{-0.02}$	$6.97^{+0.10}_{-0.10}$	$8.69^{+0.05}_{-0.05}$	$1.74^{+0.06}_{-0.06}$	13.20
2652	26.12	1.60	$0.04^{+0.00}_{-0.00}$	$9.68^{+0.21}_{-0.21}$	$8.96^{+0.05}_{-0.05}$	$0.21^{+0.06}_{-0.06}$	65.02
2684	26.55	2.85	$0.38^{+0.04}_{-0.04}$	$6.35^{+0.71}_{-0.71}$	$8.85^{+0.07}_{-0.07}$	$2.51^{+0.39}_{-0.39}$	113.19
2698	26.34	2.85	$0.24^{+0.06}_{-0.06}$	$10.30^{+1.24}_{-1.24}$	$10.02^{+0.05}_{-0.05}$	$1.27^{+0.52}_{-0.52}$	24.90
2722	25.81	2.80	$0.02^{+0.00}_{-0.00}$	$8.95^{+0.21}_{-0.21}$	$9.25^{+0.05}_{-0.05}$	$0.64^{+0.02}_{-0.02}$	274.78
2751	26.42	2.70	$0.00^{+0.00}_{-0.00}$	$10.20^{+0.83}_{-0.83}$	$9.07^{+0.03}_{-0.03}$	$0.32^{+0.01}_{-0.01}$	161.56
2784	26.45	1.50	$0.42^{+0.02}_{-0.02}$	$6.66^{+1.56}_{-1.56}$	$8.32^{+0.06}_{-0.06}$	$1.67^{+0.00}_{-0.00}$	141.32
2759	25.90	3.30	$0.08^{+0.06}_{-0.06}$	$10.30^{+0.04}_{-0.04}$	$9.73^{+0.05}_{-0.05}$	$0.98^{+0.04}_{-0.04}$	91.22
2854	25.54	1.55	$0.68^{+0.02}_{-0.02}$	$6.56^{+0.00}_{-0.00}$	$9.49^{+0.02}_{-0.02}$	$2.94^{+0.02}_{-0.02}$	31.16
2946	25.85	3.00	$0.16^{+0.02}_{-0.02}$	$8.32^{+0.10}_{-0.10}$	$9.43^{+0.04}_{-0.04}$	$1.24^{+0.06}_{-0.06}$	22.03
2955	25.05	2.30	$0.22^{+0.02}_{-0.02}$	$8.95^{+0.21}_{-0.21}$	$10.13^{+0.05}_{-0.05}$	$1.52^{+0.10}_{-0.10}$	3.32
2989	26.49	2.20	$0.46^{+0.02}_{-0.02}$	$6.56^{+0.35}_{-0.35}$	$8.84^{+0.05}_{-0.05}$	$2.29^{+0.05}_{-0.05}$	290.94
3145	25.38	2.30	$0.22^{+0.02}_{-0.02}$	$8.01^{+0.94}_{-0.94}$	$9.35^{+0.45}_{-0.45}$	$1.43^{+0.20}_{-0.20}$	11.30
3163	26.16	2.35	$0.16^{+0.02}_{-0.02}$	$8.74^{+0.21}_{-0.21}$	$9.77^{+0.09}_{-0.09}$	$1.28^{+0.10}_{-0.10}$	38.25
3258	26.31	3.20	$0.00^{+0.00}_{-0.00}$	$9.47^{+0.52}_{-0.52}$	$9.18^{+0.34}_{-0.34}$	$0.44^{+0.02}_{-0.02}$	122.41
3275	26.35	3.40	$0.00^{+0.00}_{-0.00}$	$8.64^{+0.21}_{-0.21}$	$8.88^{+0.15}_{-0.15}$	$0.45^{+0.02}_{-0.02}$	140.26
3294	25.37	1.65	$0.52^{+0.02}_{-0.02}$	$8.64^{+0.00}_{-0.00}$	$10.38^{+0.04}_{-0.04}$	$1.95^{+0.11}_{-0.11}$	29.64
3349	26.55	1.50	$0.16^{+0.02}_{-0.02}$	$8.84^{+0.52}_{-0.52}$	$9.24^{+0.02}_{-0.02}$	$0.50^{+0.02}_{-0.02}$	47.63
3389	26.48	1.50	$0.56^{+0.02}_{-0.02}$	$8.54^{+0.10}_{-0.10}$	$8.81^{+0.15}_{-0.15}$	$0.26^{+0.07}_{-0.07}$	179.94
3411	25.86	2.85	$0.44^{+0.02}_{-0.02}$	$6.56^{+1.46}_{-1.46}$	$9.02^{+0.03}_{-0.03}$	$1.28^{+0.10}_{-0.10}$	3.32
3420	25.98	2.45	$0.30^{+0.02}_{-0.02}$	$6.45^{+0.31}_{-0.31}$	$9.36^{+0.11}_{-0.11}$	$2.92^{+0.21}_{-0.21}$	68.30
3465	26.53	2.55	$0.08^{+0.02}_{-0.02}$	$6.76^{+0.10}_{-0.10}$	$8.63^{+0.04}_{-0.04}$	$1.88^{+0.04}_{-0.04}$	74.64
3480	26.33	1.70	$0.16^{+0.02}_{-0.02}$	$8.64^{+0.00}_{-0.00}$	$9.47^{+0.02}_{-0.02}$	$1.95^{+0.11}_{-0.11}$	29.64
3485	26.31	1.50	$0.30^{+0.18}_{-0.18}$	$8.74^{+0.10}_{-0.10}$	$9.24^{+0.02}_{-0.02}$	$0.50^{+0.02}_{-0.02}$	47.63
3491	26.01	1.70	$0.14^{+0.04}_{-0.04}$	$8.01^{+0.83}_{-0.83}$	$8.57^{+0.38}_{-0.38}$	$1.73^{+0.22}_{-0.22}$	179.94
3503	25.49	2.20	$0.20^{+0.02}_{-0.02}$	$6.66^{+0.16}_{-0.16}$	$8.38^{+0.13}_{-0.13}$	$1.73^{+0.33}_{-0.33}$	32.55
3511	25.57	2.45	$0.20^{+0.12}_{-0.12}$	$7.80^{+0.42}_{-0.42}$	$9.10^{+0.03}_{-0.03}$	$0.53^{+0.09}_{-0.09}$	128.32
3542	25.31	1.60	$0.16^{+0.02}_{-0.02}$	$6.56^{+0.00}_{-0.00}$	$8.68^{+0.03}_{-0.03}$	$2.13^{+0.19}_{-0.19}$	194.34
3548	25.80	3.10	$0.34^{+0.02}_{-0.02}$	$6.87^{+0.00}_{-0.00}$	$8.09^{+0.06}_{-0.06}$	$1.24^{+0.74}_{-0.74}$	10.19
3641	26.09	1.70	$0.14^{+0.04}_{-0.04}$	$8.01^{+0.10}_{-0.10}$	$8.57^{+0.34}_{-0.34}$	$0.65^{+0.27}_{-0.27}$	49.16
3646	25.77	2.80	$0.18^{+0.02}_{-0.02}$	$6.76^{+0.10}_{-0.10}$	$8.22^{+0.95}_{-0.95}$	$0.50^{+0.02}_{-0.02}$	47.63
3653	24.80	2.95	$0.20^{+0.02}_{-0.02}$	$6.10^{+0.98}_{-0.98}$	$8.74^{+0.44}_{-0.44}$	$9.30^{+0.17}_{-0.17}$	10.03
3687	26.32	3.00	$0.10^{+0.02}_{-0.02}$	$6.66^{+0.16}_{-0.16}$	$8.38^{+0.09}_{-0.09}$	$1.73^{+0.33}_{-0.33}$	32.55
3578	26.16	1.50	$0.62^{+0.02}_{-0.02}$	$6.56^{+0.10}_{-0.10}$	$8.94^{+0.08}_{-0.08}$	$0.26^{+0.07}_{-0.07}$	164.51
3635	24.67	3.05	$0.16^{+0.02}_{-0.02}$	$8.95^{+0.42}_{-0.42}$	$10.32^{+0.14}_{-0.14}$	$1.37^{+0.13}_{-0.13}$	4.28
3641	26.09	1.65	$0.32^{+0.04}_{-0.04}$	$8.84^{+0.00}_{-0.00}$	$9.68^{+0.04}_{-0.04}$	$2.93^{+0.24}_{-0.24}$	82.50
3646	25.77	2.80	$0.18^{+0.02}_{-0.02}$	$6.56^{+0.00}_{-0.00}$	$9.09^{+0.05}_{-0.05}$	$2.54^{+0.00}_{-0.00}$	78.66
3687	26.32	3.00	$0.10^{+0.02}_{-0.02}$	$6.10^{+0.98}_{-0.98}$	$8.74^{+0.44}_{-0.44}$	$9.30^{+0.17}_{-0.17}$	24.59
3767	26.58	2.25	$0.46^{+0.02}_{-0.02}$	$6.56^{+0.00}_{-0.00}$	$8.56^{+0.19}_{-0.19}$	$0.81^{+0.09}_{-0.09}$	9.58
3779	26.44	3.15	$0.12^{+0.06}_{-0.06}$	$8.32^{+0.62}_{-0.62}$	$9.83^{+0.03}_{-0.03}$	$2.29^{+0.03}_{-0.03}$	102.82
3797	26.34	1.50	$0.20^{+0.06}_{-0.06}$	$8.32^{+1.98}_{-1.98}$	$9.09^{+0.21}_{-0.21}$	$1.08^{+0.14}_{-0.14}$	105.53
3867	25.76	2.40	$0.20^{+0.04}_{-0.04}$	$8.12^{+0.73}_{-0.73}$	$8.74^{+0.68}_{-0.68}$	$0.90^{+0.24}_{-0.24}$	85.93
3897	26.05	1.60	$0.44^{+0.06}_{-0.06}$	$6.66^{+0.02}_{-0.02}$	$8.60^{+0.01}_{-0.01}$	$1.23^{+0.18}_{-0.18}$	13.30
						$1.95^{+0.01}_{-0.01}$	16.92
						$1.95^{+0.01}_{-0.01}$	75.93

Table A.3: Best-fit parameters for this work's HDF-S catalog, 500 Myr e-folding exponential SFR.

ID	$\mathcal{R}_{VI}$	$z_{phot}$	$E(B - V)$	$\log(\text{Age}/\text{yr})$	$\log(M_*/M_\odot)$	$\log(\text{SFR}/(M_\odot/\text{yr}))$	$\chi^2$
3	26.37	1.50	0.14	7.60	8.01	0.47	75.77
147	23.02	3.05	0.26	6.56	9.86	3.31	76.55
156	25.25	1.90	0.10	8.74	9.31	0.87	35.61
172	25.24	1.50	0.34	8.95	9.90	1.37	15.87
177	25.51	2.25	0.02	9.78	9.25	0.63	6.66
201	26.40	1.50	0.22	7.49	8.16	0.72	27.56
356	24.38	1.60	0.66	6.76	9.98	3.23	74.97
401	26.00	1.70	0.18	8.74	9.17	0.73	13.59
428	25.90	3.05	0.24	6.56	8.64	2.09	106.14
430	26.08	2.55	0.08	7.60	8.33	0.79	133.76
447	25.71	1.50	0.20	6.76	8.03	1.28	50.99
462	25.99	1.50	0.50	5.52	8.86	3.44	64.16
472	26.15	1.50	0.58	6.66	8.91	2.26	115.37
475	26.29	1.50	0.56	6.66	8.78	2.13	111.25
481	25.90	1.50	0.26	6.76	8.13	1.38	101.16
650	26.27	2.70	0.06	8.95	9.12	0.59	102.95
715	24.29	2.90	0.22	8.01	9.99	2.08	19.64
720	26.20	1.70	0.12	8.22	8.57	0.49	15.66
726	24.92	1.85	0.26	8.84	9.97	1.49	10.39
779	25.39	1.55	0.26	10.30	9.74	1.13	17.21
797	26.15	2.10	0.08	9.99	9.16	0.55	111.10
818	26.08	1.50	0.14	8.32	8.66	0.49	140.21
824	25.75	2.45	0.14	9.78	9.65	1.04	77.25
876	26.10	1.95	0.00	8.43	8.48	0.23	20.03
878	24.94	2.95	0.34	6.76	9.37	2.62	56.38
901	25.05	1.50	0.60	6.66	9.36	2.71	191.87
1029	25.66	2.10	0.14	8.95	9.46	0.93	6.00
1089	25.09	1.50	0.32	8.01	9.37	1.46	15.63
1102	24.70	3.15	0.08	9.78	10.04	1.43	8.23
1159	26.32	1.50	0.00	9.05	8.52	-0.04	33.69
1191	25.61	2.45	0.02	7.18	8.00	0.85	14.21
1195	25.49	2.30	0.24	6.66	8.54	1.89	9.42
1228	24.95	1.60	0.20	8.95	9.68	1.15	3.23
1239	26.58	1.50	0.30	7.28	8.18	0.93	91.61
1267	23.34	3.05	0.28	6.56	9.81	3.26	70.05
1366	24.92	1.60	0.38	8.95	10.23	1.70	29.93
1441	25.66	1.50	0.42	8.43	9.70	1.46	69.70
1451	25.45	1.70	0.28	7.80	9.07	1.34	5.24
1467	24.30	2.55	0.12	9.36	10.16	1.56	6.70
1478	25.90	1.70	0.44	7.80	9.38	1.65	23.36
1482	24.27	1.85	0.28	8.74	10.25	1.81	10.93
1484	25.12	1.65	0.40	8.95	10.25	1.72	24.09
1498	23.49	1.85	0.28	8.53	10.44	2.12	21.29
1521	25.78	3.05	0.26	6.56	8.74	2.20	233.41
1533	26.40	1.85	0.30	8.84	9.53	1.04	195.40
1565	25.54	1.85	0.32	8.64	9.81	1.43	5.40
1576	26.02	1.50	0.10	7.80	8.21	0.48	19.37
1598	25.26	2.85	0.28	6.56	8.98	2.43	139.65
1604	26.05	2.45	0.04	8.64	8.93	0.55	195.06
1634	25.04	2.80	0.24	8.01	9.74	1.83	1.66
1695	26.23	1.65	0.12	9.99	9.04	0.43	77.63
1817	26.17	1.50	0.56	6.56	8.82	2.28	82.51
1933	24.50	2.30	0.20	9.05	10.22	1.66	9.77
1973	25.69	1.85	0.12	8.74	9.18	0.74	61.32
1985	26.55	2.75	0.00	10.30	8.87	0.26	28.11
2005	26.06	1.50	0.14	7.70	8.24	0.61	93.66
2033	26.35	2.10	0.10	9.78	9.14	0.53	37.63
2042	26.06	1.50	0.22	7.80	8.56	0.83	52.09

Table A.3: Best-fit parameters for this work's HDF-S catalog, 500 Myr e-folding exponential SFR.

ID	$\mathcal{R}_{VI}$	$z_{phot}$	$E(B - V)$	$\log(\text{Age/yr})$	$\log(M_*/M_\odot)$	$\log(\text{SFR}/(M_\odot/\text{yr}))$	$\chi^2$
2192	26.46	2.70	0.00	8.74	8.73	0.29	35.85
2207	25.00	2.45	0.06	9.99	9.66	1.04	34.93
2306	25.77	2.70	0.12	8.32	9.20	1.04	65.36
2361	25.30	2.70	0.02	8.74	9.28	0.84	6.56
2367	25.71	2.50	0.08	8.43	9.09	0.84	18.32
2389	24.01	2.85	0.34	6.56	9.71	3.17	86.47
2560	26.08	1.50	0.26	6.97	8.11	1.15	6.11
2575	25.90	1.95	0.08	9.05	9.12	0.56	6.88
2597	26.56	2.95	0.00	6.87	7.47	0.62	7.15
2661	26.46	1.70	0.00	10.09	8.61	0.00	141.66
2728	24.56	1.70	0.16	8.74	9.68	1.24	14.95
2747	26.50	1.70	0.42	6.66	8.44	1.79	49.43
2763	25.91	1.70	0.06	8.32	8.58	0.41	205.07
2765	26.36	1.50	0.24	6.97	7.94	0.98	14.44
2784	25.79	1.50	0.10	9.68	9.09	0.48	115.54
2799	26.59	1.50	0.06	10.09	8.56	-0.05	382.14
2817	26.04	1.95	0.36	6.56	8.57	2.03	24.50
2837	25.41	1.60	0.30	6.97	8.55	1.60	7.50
2849	25.15	2.45	0.18	9.05	9.96	1.40	25.89
2889	25.21	2.50	0.20	6.87	8.65	1.79	6.01
2913	23.43	2.75	0.20	8.01	10.22	2.31	7.03
2958	25.82	2.50	0.10	9.26	9.47	0.87	21.66
3043	23.09	2.60	0.24	6.97	9.71	2.76	8.91
3098	25.83	1.60	0.40	5.83	8.74	2.95	2.20
3127	24.50	1.85	0.34	8.64	10.30	1.92	7.51
3166	25.59	1.90	0.18	8.64	9.37	0.99	43.71
3169	26.52	1.50	0.32	6.87	8.05	1.19	45.16
3217	26.59	1.95	0.12	9.16	8.98	0.40	40.13
3321	26.30	2.55	0.36	6.56	8.74	2.19	10.95
3330	26.18	1.50	0.16	10.30	9.05	0.44	137.98
3397	26.57	1.85	0.10	8.53	8.65	0.33	22.42
3407	25.96	1.50	0.26	7.39	8.38	1.03	37.87
3419	26.05	1.50	0.18	9.05	9.15	0.59	8.50
3554	26.47	1.80	0.04	8.53	8.47	0.16	56.32
3560	25.95	1.60	0.10	8.95	8.99	0.46	32.34
3625	26.28	1.60	0.56	6.66	8.88	2.23	48.69
3639	25.13	3.00	0.22	10.30	10.35	1.74	31.31
3666	25.93	1.85	0.08	8.64	8.90	0.52	34.35
3689	26.16	2.45	0.10	8.53	9.03	0.72	102.63
3782	25.43	1.85	0.10	8.84	9.27	0.78	113.78
3789	26.42	1.50	0.34	6.76	8.16	1.40	104.19
3795	25.94	2.25	0.26	7.39	8.73	1.38	214.91
3808	24.78	3.00	0.22	8.95	10.42	1.89	6.02
8	25.68	1.50	0.64	6.56	9.18	2.64	230.06
59	25.81	2.95	0.16	6.87	8.39	1.54	13.63
69	25.82	1.50	0.34	6.76	8.36	1.61	112.37
73	26.47	1.50	0.14	7.39	7.83	0.49	8.05
100	25.97	2.25	0.40	6.56	8.86	2.31	105.58
190	25.76	1.50	0.22	7.39	8.36	1.01	60.77
203	25.80	2.05	0.16	8.84	9.38	0.90	71.83
207	25.26	1.75	0.40	8.32	9.90	1.74	55.12
242	25.91	2.05	0.38	6.87	8.78	1.93	111.89
288	25.09	2.45	0.40	6.76	9.35	2.59	2.77
296	25.59	3.65	0.10	6.45	8.40	1.96	119.03
310	26.06	2.45	0.00	7.49	7.91	0.47	302.70
313	25.64	1.85	0.10	8.74	9.14	0.70	156.88
328	25.49	2.45	0.04	7.08	8.02	0.97	181.18
339	24.91	2.35	0.16	6.56	8.51	1.96	65.62
448	25.60	2.80	0.22	8.12	9.52	1.52	3.72

Table A.3: Best-fit parameters for this work's HDF-S catalog, 500 Myr e-folding exponential SFR.

ID	$\mathcal{R}_{VI}$	$z_{phot}$	$E(B - V)$	$\log(\text{Age/yr})$	$\log(M_*/M_\odot)$	$\log(\text{SFR}/(M_\odot/\text{yr}))$	$\chi^2$
464	25.68	2.95	0.18	8.84	9.83	1.34	73.20
470	25.97	2.75	0.36	6.56	8.96	2.42	24.14
480	26.11	2.60	0.14	9.88	9.55	0.94	65.32
520	26.31	2.30	0.38	6.56	8.66	2.12	131.13
533	25.69	2.30	0.38	6.56	8.92	2.37	137.39
542	26.10	1.50	0.42	6.66	8.44	1.79	131.76
544	26.46	1.50	0.40	6.66	8.25	1.60	136.58
570	26.25	2.40	0.32	6.56	8.53	1.98	170.79
572	25.78	1.50	0.42	6.66	8.60	1.95	165.54
579	25.66	1.65	0.46	6.66	8.85	2.20	198.26
590	26.47	1.50	0.14	9.05	8.83	0.27	369.47
639	25.98	2.80	0.48	6.56	9.41	2.86	6.40
649	26.58	2.45	0.28	7.70	8.89	1.25	63.38
665	25.50	2.90	0.46	6.35	9.60	3.27	12.82
673	25.59	2.90	0.42	6.56	9.37	2.82	9.22
692	25.18	1.50	0.22	9.78	9.66	1.05	18.06
721	25.32	2.90	0.16	10.30	9.96	1.35	181.94
746	26.07	2.85	0.44	6.45	9.27	2.83	19.21
848	25.57	2.35	0.34	10.09	10.38	1.77	65.31
871	25.43	3.00	0.16	9.26	9.99	1.40	8.56
972	26.43	2.45	0.30	7.28	8.74	1.49	18.71
1047	26.19	3.20	0.02	6.87	7.74	0.88	144.28
1106	26.05	2.60	0.48	6.76	9.27	2.52	35.78
1108	24.77	3.25	0.10	9.57	10.12	1.51	7.85
1124	26.47	2.35	0.32	6.76	8.47	1.72	115.09
1140	26.52	1.85	0.36	6.66	8.34	1.69	127.74
1225	26.56	3.25	0.00	9.36	8.97	0.37	56.11
1273	25.92	1.50	0.26	7.49	8.46	1.02	467.34
1403	26.34	3.45	0.04	10.30	9.32	0.70	57.17
1471	26.50	2.50	0.20	8.74	9.39	0.95	39.00
1473	25.78	1.65	0.30	10.09	9.77	1.15	53.16
1501	25.94	3.55	0.10	8.74	9.59	1.15	131.28
1523	25.86	2.20	0.38	6.56	8.82	2.28	49.40
1527	26.37	2.55	0.14	10.20	9.42	0.81	91.38
1540	25.86	1.50	0.44	7.08	8.77	1.72	174.64
1543	25.04	1.70	0.30	8.74	9.90	1.47	15.90
1551	26.54	1.85	0.34	9.78	9.71	1.09	48.50
1572	25.99	1.50	0.56	5.41	9.06	3.77	55.07
1585	26.27	1.50	0.60	5.62	9.08	3.53	139.44
1590	26.06	1.70	0.22	8.95	9.35	0.82	37.89
1593	25.52	1.50	0.50	10.20	10.34	1.73	174.71
1647	25.44	1.70	0.16	8.64	9.28	0.90	33.84
1676	25.94	1.70	0.14	8.95	9.15	0.62	9.94
1696	26.55	2.50	0.12	9.26	9.23	0.63	42.63
1699	26.53	2.80	0.42	5.83	9.07	3.29	98.81
1739	25.04	2.95	0.12	8.74	9.82	1.38	8.85
1863	25.24	1.70	0.34	8.64	9.90	1.52	29.21
1881	25.15	2.60	0.14	10.20	9.92	1.31	19.48
1908	26.01	3.10	0.14	8.74	9.52	1.08	79.37
1915	26.55	2.70	0.04	10.30	9.00	0.39	66.10
1926	25.69	2.55	0.36	8.64	10.24	1.86	6.27
1954	26.00	2.40	0.10	10.30	9.37	0.76	19.12
1960	26.23	2.40	0.44	6.56	8.97	2.43	32.84
2021	26.47	2.45	0.42	6.56	8.80	2.25	209.10
2025	25.67	1.50	0.66	6.56	9.27	2.72	219.03
2030	25.66	3.15	0.00	8.74	9.17	0.73	1.99
2052	26.18	2.85	0.12	6.56	8.00	1.46	9.24

Table A.3: Best-fit parameters for this work's HDF-S catalog, 500 Myr e-folding exponential SFR.

ID	$\mathcal{R}_{VI}$	$z_{phot}$	$E(B - V)$	$\log(\text{Age}/\text{yr})$	$\log(M_*/M_\odot)$	$\log(\text{SFR}/(M_\odot/\text{yr}))$	$\chi^2$
2071	25.56	2.90	0.16	8.64	9.70	1.32	4.36
2188	26.09	2.55	0.32	7.70	9.22	1.59	151.81
2219	26.20	1.50	0.56	7.60	9.32	1.78	42.23
2257	26.39	1.55	0.50	10.20	10.08	1.47	161.08
2266	25.40	2.05	0.34	10.09	10.30	1.69	79.46
2300	25.78	2.50	0.48	6.45	9.36	2.91	164.68
2315	26.37	2.25	0.24	8.32	9.20	1.04	53.73
2329	26.11	2.65	0.12	9.05	9.43	0.87	43.53
2356	25.55	1.70	0.18	8.74	9.34	0.90	41.11
2427	26.22	3.00	0.34	5.10	8.96	4.17	14.43
2429	26.34	1.50	0.48	5.62	8.63	3.08	251.04
2529	26.08	1.50	0.58	5.31	9.07	3.92	119.19
2545	25.75	2.65	0.20	9.99	9.92	1.30	58.55
2553	26.47	2.65	0.28	6.66	8.39	1.73	56.58
2561	26.34	1.50	0.42	7.39	8.69	1.34	49.66
2568	26.04	2.15	0.32	7.08	8.70	1.64	13.25
2652	26.12	1.60	0.06	9.78	8.90	0.29	72.80
2684	26.55	2.85	0.38	6.35	8.85	2.51	113.19
2698	26.34	2.80	0.26	10.20	9.94	1.33	29.84
2722	25.81	2.75	0.04	8.95	9.23	0.70	277.33
2751	26.42	2.70	0.02	10.30	9.01	0.40	176.45
2754	26.45	1.50	0.42	6.66	8.32	1.67	141.11
2759	25.90	3.20	0.10	9.88	9.64	1.03	106.70
2854	25.54	1.55	0.68	6.56	9.49	2.94	31.16
2946	25.85	3.00	0.16	8.43	9.48	1.24	21.54
2955	25.05	2.30	0.22	9.88	10.14	1.53	5.41
2989	26.49	2.20	0.46	6.56	8.84	2.29	290.94
3145	25.38	2.30	0.22	8.01	9.34	1.43	10.99
3163	26.16	2.35	0.30	8.64	9.74	1.36	38.56
3258	26.31	3.25	0.00	9.68	9.07	0.46	124.60
3275	26.35	3.40	0.00	8.74	8.90	0.46	139.83
3294	25.37	1.65	0.52	8.74	10.40	1.96	31.24
3349	26.55	1.50	0.16	10.30	8.87	0.26	179.92
3399	26.48	1.50	0.54	6.66	8.59	1.94	194.18
3411	25.86	2.85	0.44	6.45	9.36	2.92	68.15
3420	25.98	2.40	0.30	6.76	8.61	1.85	74.53
3465	26.53	2.50	0.10	9.88	9.18	0.57	48.83
3480	26.33	1.70	0.16	8.84	9.02	0.54	130.47
3485	26.31	1.50	0.30	6.87	8.09	1.24	10.09
3491	26.01	1.80	0.18	7.70	8.52	0.88	49.32
3503	25.49	2.20	0.20	6.66	8.38	1.73	32.55
3511	25.57	2.45	0.20	7.80	9.10	1.37	9.95
3542	25.31	1.60	0.68	6.76	9.68	2.93	82.50
3548	25.80	3.10	0.34	6.56	9.09	2.54	78.66
3563	24.80	2.95	0.20	8.22	9.89	1.81	24.31
3578	26.16	1.50	0.62	6.56	8.94	2.40	164.51
3635	24.67	3.00	0.18	8.84	10.26	1.77	5.62
3641	26.09	1.65	0.34	8.84	9.64	1.15	111.52
3646	25.77	2.80	0.18	6.87	8.41	1.56	28.76
3687	26.32	3.00	0.10	8.84	9.30	0.81	9.84
3767	26.58	2.25	0.46	6.56	8.83	2.29	102.82
3779	26.44	3.20	0.08	9.47	9.36	0.75	86.14
3797	26.34	1.50	0.18	8.53	8.79	0.48	13.45
3867	25.76	2.45	0.20	8.12	9.26	1.26	16.97
3897	26.05	1.60	0.44	6.66	8.60	1.95	75.87

Table A.4: Best-fit parameters for this work's HDF-S catalog, 350 Myr e-folding exponential SFR.

ID	$\mathcal{R}_{VI}$	$z_{phot}$	$E(B - V)$	$\log(\text{Age}/\text{yr})$	$\log(M_*/M_\odot)$	$\log(\text{SFR}/(M_\odot/\text{yr}))$	$\chi^2$
3	26.37	1.50	0.14	7.60	8.01	0.48	75.79
147	23.02	3.05	0.26	6.56	9.86	3.32	76.72
156	25.25	1.90	0.12	8.74	9.31	0.95	37.51
172	25.24	1.50	0.36	8.84	9.85	1.45	17.04
177	25.51	2.25	0.04	10.09	9.19	0.72	11.43
201	26.40	1.50	0.22	7.49	8.16	0.72	27.40
356	24.38	1.60	0.66	6.76	9.98	3.23	75.05
401	26.00	1.70	0.18	10.30	9.21	0.74	14.73
428	25.90	3.05	0.24	6.56	8.64	2.09	105.80
430	26.08	2.55	0.08	7.60	8.32	0.79	133.84
447	25.71	1.50	0.20	6.76	8.03	1.28	50.79
462	25.99	1.50	0.50	5.20	8.86	3.87	64.16
472	26.15	1.50	0.58	6.66	8.91	2.26	115.70
475	26.29	1.60	0.56	6.66	8.86	2.21	111.16
481	25.90	1.50	0.26	6.76	8.13	1.38	100.94
650	26.27	2.70	0.06	9.78	9.07	0.60	104.93
715	24.29	2.90	0.20	8.22	10.05	1.99	19.69
720	26.20	1.70	0.14	8.12	8.55	0.57	15.37
726	24.92	1.85	0.28	8.74	9.93	1.57	11.65
779	25.39	1.55	0.28	9.99	9.68	1.21	23.79
797	26.15	2.05	0.10	9.68	9.08	0.60	127.32
818	26.08	1.50	0.12	8.64	8.74	0.42	140.63
824	25.75	2.45	0.16	10.09	9.59	1.12	97.89
876	26.10	1.95	0.00	8.43	8.44	0.24	20.10
878	24.94	2.95	0.34	6.76	9.37	2.62	56.49
901	25.05	1.50	0.60	6.66	9.36	2.71	192.16
1029	25.66	2.05	0.16	8.84	9.39	0.99	7.66
1089	25.09	1.50	0.30	8.22	9.43	1.38	15.72
1102	24.70	3.15	0.10	9.36	9.98	1.53	8.77
1159	26.32	1.50	0.02	9.99	8.51	0.03	37.58
1191	25.61	2.45	0.02	7.18	8.00	0.85	14.14
1195	25.49	2.30	0.24	6.66	8.54	1.89	9.42
1228	24.95	1.60	0.22	8.84	9.63	1.24	5.34
1239	26.58	1.50	0.28	7.49	8.25	0.81	91.79
1267	23.34	3.05	0.28	6.56	9.81	3.26	70.04
1366	24.92	1.65	0.40	8.95	10.24	1.82	35.65
1441	25.66	1.50	0.40	8.74	9.76	1.40	70.45
1451	25.45	1.60	0.28	7.80	9.01	1.29	5.03
1467	24.30	2.55	0.14	9.36	10.10	1.65	13.44
1478	25.90	1.70	0.44	7.80	9.37	1.66	23.38
1482	24.27	1.85	0.30	8.64	10.21	1.90	13.17
1484	25.12	1.65	0.42	8.84	10.20	1.80	29.52
1498	23.49	1.85	0.30	8.43	10.41	2.21	22.48
1521	25.78	3.05	0.26	6.56	8.74	2.20	233.39
1533	26.40	1.85	0.30	10.20	9.52	1.05	203.13
1565	25.54	1.85	0.32	8.84	9.84	1.44	6.42
1576	26.02	1.50	0.10	7.80	8.20	0.48	19.64
1598	25.26	2.85	0.28	6.56	8.98	2.43	139.65
1604	26.05	2.45	0.06	8.53	8.90	0.64	195.58
1634	25.04	2.85	0.22	8.22	9.82	1.76	1.59
1695	26.23	1.65	0.14	10.20	8.98	0.51	83.47
1817	26.17	1.50	0.56	6.56	8.82	2.28	82.62
1933	24.50	2.30	0.22	9.36	10.20	1.74	9.74
1973	25.69	1.85	0.14	8.64	9.14	0.82	63.26
1985	26.55	2.75	0.00	10.09	8.74	0.27	31.57
2005	26.06	1.50	0.14	7.70	8.24	0.61	93.84
2033	26.35	1.50	0.10	9.99	8.72	0.25	42.80
2042	26.06	1.50	0.22	7.80	8.55	0.84	52.36
2050	25.86	2.60	0.24	7.18	8.72	1.57	39.36

Table A.4: Best-fit parameters for this work's HDF-S catalog, 350 Myr e-folding exponential SFR.

ID	$\mathcal{R}_{VI}$	$z_{phot}$	$E(B - V)$	$\log(\text{Age/yr})$	$\log(M_*/M_\odot)$	$\log(\text{SFR}/(M_\odot/\text{yr}))$	$\chi^2$
2192	26.46	2.70	0.00	9.57	8.77	0.30	36.21
2207	25.00	2.45	0.08	9.88	9.60	1.13	37.74
2306	25.77	2.75	0.10	8.64	9.29	0.98	65.94
2361	25.30	2.70	0.02	9.47	9.31	0.85	7.15
2367	25.71	2.55	0.08	8.43	9.07	0.87	18.88
2389	24.01	2.85	0.34	6.56	9.71	3.17	86.57
2560	26.08	1.50	0.26	6.97	8.11	1.15	6.13
2575	25.90	1.90	0.10	8.95	9.04	0.62	7.89
2597	26.56	2.95	0.00	6.87	7.47	0.62	7.16
2661	26.46	1.70	0.02	10.20	8.55	0.08	147.67
2728	24.56	1.70	0.18	8.64	9.64	1.32	15.65
2747	26.50	1.50	0.44	6.66	8.37	1.72	49.44
2763	25.91	1.70	0.06	8.43	8.61	0.41	205.53
2765	26.36	1.50	0.24	6.97	7.94	0.98	14.48
2784	25.79	1.50	0.14	9.78	9.08	0.61	123.81
2799	26.59	1.50	0.08	9.16	8.49	0.04	383.45
2817	26.04	1.95	0.36	6.56	8.57	2.03	24.61
2837	25.41	1.60	0.30	6.97	8.55	1.60	7.35
2849	25.15	2.45	0.20	8.95	9.91	1.49	27.27
2889	25.21	2.50	0.20	6.87	8.65	1.79	6.06
2913	23.43	2.75	0.20	8.01	10.21	2.32	6.66
2958	25.82	2.50	0.12	9.26	9.41	0.96	29.72
3043	23.09	2.75	0.22	7.08	9.76	2.70	8.84
3098	25.83	1.60	0.40	5.20	8.74	3.75	2.20
3127	24.50	1.85	0.34	8.74	10.29	1.93	8.68
3166	25.59	1.90	0.20	8.53	9.34	1.07	44.29
3169	26.52	1.50	0.32	6.87	8.05	1.19	45.19
3217	26.59	1.95	0.14	9.36	8.94	0.48	40.78
3321	26.30	2.55	0.36	6.56	8.74	2.20	10.93
3330	26.18	1.50	0.18	10.30	9.00	0.52	138.72
3397	26.57	1.85	0.10	8.64	8.65	0.34	23.00
3407	25.96	1.50	0.26	7.39	8.38	1.03	37.95
3419	26.05	1.50	0.20	8.95	9.10	0.67	11.06
3554	26.47	1.85	0.04	8.64	8.50	0.19	56.94
3560	25.95	1.70	0.12	9.05	9.03	0.59	37.95
3625	26.28	1.60	0.56	6.66	8.88	2.23	48.63
3639	25.13	2.95	0.24	9.99	10.27	1.80	37.21
3666	25.93	1.85	0.08	8.84	8.93	0.53	36.33
3689	26.16	2.45	0.10	8.64	9.04	0.73	102.37
3782	25.43	1.85	0.12	8.74	9.22	0.86	115.75
3789	26.42	1.50	0.34	6.76	8.16	1.40	104.30
3795	25.94	2.25	0.26	7.39	8.73	1.39	214.60
3808	24.78	2.95	0.24	9.36	10.41	1.95	7.17
8	25.68	1.50	0.64	6.56	9.18	2.64	230.12
59	25.81	2.95	0.16	6.87	8.39	1.54	13.67
69	25.82	1.50	0.34	6.76	8.36	1.61	112.39
73	26.47	1.50	0.14	7.39	7.83	0.49	8.05
100	25.97	2.40	0.38	6.56	8.86	2.31	105.76
190	25.76	1.50	0.22	7.39	8.36	1.01	60.40
203	25.80	2.05	0.16	9.57	9.38	0.91	74.26
207	25.26	1.70	0.40	8.43	9.90	1.70	55.16
242	25.91	2.05	0.38	6.87	8.78	1.93	111.89
288	25.09	2.45	0.40	6.76	9.35	2.60	2.80
296	25.59	3.65	0.08	6.56	8.29	1.75	119.07
310	26.06	2.45	0.00	7.49	7.91	0.47	302.75
313	25.64	1.85	0.10	10.30	9.18	0.71	161.56
328	25.49	2.45	0.04	7.08	8.02	0.97	180.93
339	24.91	2.35	0.16	6.56	8.51	1.96	65.74
448	25.60	2.80	0.22	8.12	9.50	1.53	3.31

Table A.4: Best-fit parameters for this work's HDF-S catalog, 350 Myr e-folding exponential SFR.

ID	$\mathcal{R}_{VI}$	$z_{phot}$	$E(B - V)$	$\log(\text{Age}/\text{yr})$	$\log(M_*/M_\odot)$	$\log(\text{SFR}/(M_\odot/\text{yr}))$	$\chi^2$
464	25.68	2.90	0.20	8.74	9.77	1.40	74.65
470	25.97	2.75	0.36	6.56	8.96	2.42	23.94
480	26.11	2.60	0.16	10.30	9.49	1.02	70.97
520	26.31	2.30	0.38	6.56	8.66	2.12	130.99
533	25.69	2.30	0.38	6.56	8.92	2.37	137.20
542	26.10	1.50	0.42	6.66	8.44	1.79	131.76
544	26.46	1.50	0.40	6.66	8.25	1.60	136.06
570	26.25	2.35	0.32	6.56	8.51	1.96	170.21
572	25.78	1.50	0.42	6.66	8.60	1.95	165.54
579	25.66	1.65	0.46	6.66	8.85	2.20	198.64
590	26.47	1.50	0.44	6.76	8.41	1.66	374.41
639	25.98	2.80	0.48	6.56	9.41	2.86	6.40
649	26.58	2.45	0.28	7.70	8.88	1.26	63.16
665	25.50	2.90	0.46	6.35	9.60	3.27	12.82
673	25.59	2.90	0.42	6.56	9.37	2.82	9.23
692	25.18	1.50	0.24	10.30	9.60	1.13	22.44
721	25.32	2.80	0.18	9.68	9.86	1.39	200.31
746	26.07	2.80	0.46	6.14	9.35	3.23	19.28
848	25.57	2.35	0.36	9.99	10.32	1.85	82.09
871	25.43	2.95	0.18	10.09	9.93	1.46	12.01
972	26.43	2.45	0.30	7.28	8.74	1.49	18.67
1047	26.19	3.20	0.00	7.28	7.91	0.66	144.45
1106	26.05	2.60	0.48	6.76	9.27	2.52	35.79
1108	24.77	3.20	0.12	9.26	10.04	1.58	15.48
1124	26.47	2.35	0.32	6.76	8.47	1.72	115.27
1140	26.52	1.85	0.36	6.66	8.34	1.69	127.74
1225	26.56	3.25	0.00	9.36	8.84	0.38	55.93
1273	25.92	1.50	0.26	7.49	8.46	1.02	467.21
1403	26.34	3.40	0.06	9.36	9.24	0.78	60.62
1471	26.50	2.50	0.20	9.47	9.42	0.96	39.55
1473	25.78	1.65	0.32	9.88	9.71	1.23	58.70
1501	25.94	3.55	0.10	9.36	9.61	1.16	130.90
1523	25.86	2.20	0.38	6.56	8.82	2.28	49.59
1527	26.37	2.50	0.16	9.57	9.35	0.88	97.10
1540	25.86	1.70	0.40	7.39	8.98	1.64	174.93
1543	25.04	1.70	0.30	8.95	9.91	1.48	16.90
1551	26.54	1.85	0.36	9.78	9.65	1.17	52.38
1572	25.99	1.50	0.56	5.93	9.06	3.16	54.98
1585	26.27	1.50	0.60	5.41	9.08	3.79	139.44
1590	26.06	1.70	0.24	8.84	9.30	0.90	40.53
1593	25.52	1.50	0.52	10.30	10.28	1.81	190.75
1647	25.44	1.70	0.16	8.84	9.30	0.91	35.85
1676	25.94	1.70	0.16	8.95	9.12	0.70	10.85
1696	26.55	2.50	0.14	9.26	9.18	0.72	42.87
1699	26.53	2.80	0.42	5.20	9.07	4.09	98.81
1739	25.04	2.95	0.12	9.78	9.86	1.39	9.93
1863	25.24	1.70	0.34	8.84	9.93	1.53	31.24
1881	25.15	2.55	0.16	10.30	9.85	1.37	31.16
1908	26.01	3.10	0.14	9.57	9.56	1.09	78.91
1915	26.55	2.70	0.04	10.30	8.87	0.40	70.67
1926	25.69	2.55	0.36	9.36	10.32	1.87	5.85
1954	26.00	2.40	0.12	9.68	9.31	0.84	26.55
1960	26.23	2.40	0.46	6.45	9.08	2.64	32.88
2021	26.47	2.50	0.42	6.56	8.82	2.27	209.02
2025	25.67	1.50	0.66	6.56	9.27	2.73	218.28
2030	25.66	3.15	0.02	8.53	9.09	0.82	2.17
2052	26.18	2.85	0.12	6.56	8.00	1.46	9.20
2071	25.56	2.90	0.16	8.95	9.75	1.33	4.51

Table A.4: Best-fit parameters for this work's HDF-S catalog, 350 Myr e-folding exponential SFR.

ID	$\mathcal{R}_{VI}$	$z_{phot}$	$E(B - V)$	$\log(\text{Age}/\text{yr})$	$\log(M_*/M_\odot)$	$\log(\text{SFR}/(M_\odot/\text{yr}))$	$\chi^2$
2188	26.09	2.55	0.32	7.70	9.22	1.59	152.01
2219	26.20	1.50	0.56	7.60	9.31	1.78	42.28
2257	26.39	1.55	0.52	9.78	10.02	1.55	176.48
2266	25.40	1.50	0.38	9.36	9.90	1.45	91.42
2300	25.78	2.50	0.48	6.45	9.36	2.91	164.60
2315	26.37	2.25	0.24	8.43	9.24	1.04	54.14
2329	26.11	2.65	0.14	9.16	9.41	0.95	48.55
2356	25.55	1.70	0.18	10.30	9.38	0.91	43.31
2427	26.22	3.00	0.34	6.04	8.96	2.95	14.37
2429	26.34	1.50	0.48	5.41	8.63	3.34	251.04
2529	26.08	1.50	0.58	5.41	9.07	3.78	119.19
2545	25.75	2.65	0.22	9.88	9.86	1.39	71.38
2553	26.47	2.65	0.22	7.08	8.33	1.28	56.55
2561	26.34	1.50	0.42	7.49	8.75	1.31	49.72
2568	26.04	2.15	0.32	7.08	8.70	1.65	13.18
2652	26.12	1.60	0.08	10.20	8.84	0.37	82.53
2684	26.55	2.85	0.38	6.35	8.85	2.51	113.19
2698	26.34	2.80	0.28	9.36	9.88	1.42	34.14
2722	25.81	2.80	0.04	9.99	9.20	0.73	282.84
2751	26.42	2.70	0.02	10.20	8.89	0.41	193.14
2754	26.45	1.50	0.42	6.66	8.32	1.67	141.11
2759	25.90	3.15	0.12	9.88	9.56	1.09	121.12
2854	25.54	1.55	0.68	6.56	9.49	2.95	30.98
2946	25.85	3.00	0.16	8.53	9.50	1.24	22.07
2955	25.05	2.30	0.24	9.57	10.08	1.61	8.50
2989	26.49	2.85	0.38	6.56	8.87	2.32	291.14
3145	25.38	2.30	0.22	8.01	9.33	1.44	10.88
3163	26.16	2.35	0.30	8.84	9.76	1.37	38.65
3258	26.31	3.25	0.00	9.57	8.94	0.47	128.77
3275	26.35	3.40	0.00	10.30	8.93	0.46	139.33
3294	25.37	1.65	0.54	8.64	10.36	2.04	33.93
3349	26.55	1.50	0.18	9.68	8.81	0.34	180.18
3399	26.48	1.50	0.54	6.66	8.59	1.94	194.57
3411	25.86	2.85	0.44	6.45	9.36	2.92	68.30
3420	25.98	2.45	0.30	6.76	8.63	1.88	74.73
3465	26.53	2.50	0.12	9.26	9.11	0.65	51.12
3480	26.33	1.85	0.18	8.74	9.06	0.70	133.72
3485	26.31	1.50	0.30	6.87	8.09	1.24	10.18
3491	26.01	1.80	0.16	7.91	8.59	0.78	49.27
3503	25.49	2.20	0.20	6.66	8.38	1.73	32.55
3511	25.57	2.45	0.20	7.80	9.09	1.38	9.96
3542	25.31	1.60	0.68	6.76	9.68	2.93	82.49
3548	25.80	3.10	0.34	6.56	9.09	2.54	78.65
3563	24.80	2.95	0.20	8.22	9.87	1.82	24.53
3578	26.16	1.50	0.62	6.56	8.94	2.40	164.29
3635	24.67	3.05	0.18	10.30	10.28	1.80	6.48
3641	26.09	1.70	0.34	9.57	9.66	1.19	116.68
3646	25.77	2.80	0.18	6.87	8.41	1.56	28.66
3687	26.32	2.95	0.12	8.84	9.28	0.88	10.14
3767	26.58	2.25	0.46	6.56	8.83	2.29	102.63
3779	26.44	3.15	0.10	9.47	9.28	0.82	85.75
3797	26.34	1.50	0.20	8.43	8.76	0.56	13.37
3867	25.76	2.45	0.20	8.12	9.25	1.27	16.94
3897	26.05	1.60	0.44	6.66	8.60	1.95	75.87

Table A.5: Best-fit parameters for this work's HDF-S catalog, 250 Myr e-folding exponential SFR.

ID	$\mathcal{R}_{VI}$	$z_{phot}$	$E(B - V)$	$\log(\text{Age}/\text{yr})$	$\log(M_*/M_\odot)$	$\log(\text{SFR}/(M_\odot/\text{yr}))$	$\chi^2$
3	26.37	1.50	0.16	7.39	7.93	0.59	77.72
147	23.02	2.80	0.94	10.30	nan	nan	nan
156	25.25	1.90	0.12	9.99	9.30	0.95	38.45
172	25.24	1.60	0.38	8.84	9.90	1.61	19.19
177	25.51	3.20	0.94	10.30	nan	nan	nan
201	26.40	1.50	0.22	7.49	8.16	0.73	27.51
356	24.38	1.90	0.76	10.30	nan	nan	nan
401	26.00	2.70	0.42	10.30	nan	nan	nan
428	25.90	3.05	0.24	6.56	8.64	2.09	105.80
430	26.08	2.60	0.08	7.60	8.34	0.81	134.05
447	25.71	1.50	0.20	6.76	8.03	1.28	50.88
462	25.99	1.50	0.50	6.04	8.85	2.84	64.11
472	26.15	1.50	0.58	6.66	8.91	2.26	115.11
475	26.29	1.50	0.56	6.66	8.78	2.13	111.06
481	25.90	1.50	0.26	6.76	8.13	1.38	100.85
650	26.27	2.60	0.08	10.20	9.00	0.65	111.25
715	24.29	2.95	0.20	8.22	10.04	2.02	19.38
720	26.20	1.70	0.14	8.12	8.53	0.58	15.64
726	24.92	2.80	0.78	10.30	nan	nan	nan
779	25.39	1.55	0.30	10.09	9.64	1.29	29.71
797	26.15	1.50	0.10	10.20	8.70	0.35	133.00
818	26.08	1.50	0.14	8.53	8.70	0.50	140.50
824	25.75	2.50	0.16	9.57	9.50	1.16	117.71
876	26.10	1.90	0.00	8.53	8.43	0.24	20.48
878	24.94	2.95	0.34	6.76	9.37	2.62	56.46
901	25.05	2.20	0.56	10.30	nan	nan	nan
1029	25.66	2.00	0.16	9.99	9.33	0.98	10.65
1089	25.09	1.50	0.26	10.09	9.57	1.23	15.78
1102	24.70	2.70	0.58	10.30	nan	nan	nan
1159	26.32	1.60	0.04	10.20	8.51	0.16	42.26
1191	25.61	2.20	0.02	7.18	7.92	0.78	18.88
1195	25.49	2.30	0.24	6.66	8.54	1.90	9.42
1228	24.95	1.60	0.24	8.84	9.61	1.31	8.95
1239	26.58	1.50	0.28	7.49	8.25	0.82	91.53
1267	23.34	3.00	0.82	10.30	nan	nan	nan
1366	24.92	1.90	0.42	8.74	10.34	2.08	50.37
1441	25.66	1.85	0.38	10.30	nan	nan	nan
1451	25.45	1.75	0.28	7.80	9.09	1.39	6.07
1467	24.30	2.55	0.16	9.36	10.05	1.73	22.63
1478	25.90	1.70	0.42	8.01	9.44	1.57	23.52
1482	24.27	1.80	0.30	10.09	10.21	1.87	16.10
1484	25.12	2.10	0.58	10.30	nan	nan	nan
1498	23.49	1.85	0.28	9.99	10.48	2.13	24.72
1521	25.78	2.85	0.88	10.30	nan	nan	nan
1533	26.40	2.20	0.06	10.30	nan	nan	nan
1565	25.54	1.85	0.34	8.74	9.80	1.53	8.37
1576	26.02	1.50	0.10	7.91	8.26	0.47	19.63
1598	25.26	2.90	0.28	6.56	9.00	2.45	142.04
1604	26.05	2.85	0.70	10.30	nan	nan	nan
1634	25.04	2.85	0.98	10.30	nan	nan	nan
1695	26.23	1.70	0.16	9.78	8.97	0.62	90.51
1817	26.17	1.50	0.56	6.56	8.82	2.28	82.62
1933	24.50	2.35	0.24	8.84	10.15	1.86	11.69
1973	25.69	1.85	0.14	9.68	9.17	0.82	66.22
1985	26.55	2.80	0.00	9.68	8.64	0.29	36.03
2005	26.06	3.05	0.34	10.30	nan	nan	nan
2033	26.35	1.50	0.12	10.20	8.67	0.32	45.06
2042	26.06	1.50	0.22	7.80	8.55	0.84	52.50

Table A.5: Best-fit parameters for this work's HDF-S catalog, 250 Myr e-folding exponential SFR.

ID	$\mathcal{R}_{VI}$	$z_{phot}$	$E(B - V)$	$\log(\text{Age}/\text{yr})$	$\log(M_*/M_\odot)$	$\log(\text{SFR}/(M_\odot/\text{yr}))$	$\chi^2$
2050	25.86	2.60	0.24	7.18	8.72	1.57	39.17
2192	26.46	2.70	0.00	9.68	8.66	0.31	37.94
2207	25.00	2.40	0.10	9.36	9.52	1.20	44.87
2306	25.77	2.65	0.12	8.53	9.23	1.03	66.43
2361	25.30	2.65	0.04	8.95	9.23	0.93	8.83
2367	25.71	2.50	0.08	8.64	9.10	0.86	19.11
2389	24.01	2.75	0.38	6.24	9.87	3.64	92.34
2560	26.08	1.50	0.26	6.97	8.11	1.16	6.17
2575	25.90	1.90	0.12	8.95	9.01	0.70	10.23
2597	26.56	2.85	0.08	5.10	7.79	2.99	7.89
2661	26.46	1.70	0.04	9.99	8.50	0.16	154.50
2728	24.56	1.70	0.18	9.88	9.67	1.32	16.70
2747	26.50	3.00	0.24	10.30	nan	nan	nan
2763	25.91	1.70	0.08	8.22	8.53	0.51	206.09
2765	26.36	1.50	0.24	6.97	7.93	0.99	14.53
2784	25.79	1.50	0.16	10.09	9.03	0.68	132.23
2799	26.59	1.50	0.10	9.26	8.44	0.12	384.33
2817	26.04	2.10	0.32	6.66	8.50	1.85	24.68
2837	25.41	1.60	0.30	6.97	8.55	1.60	7.41
2849	25.15	2.45	0.22	8.84	9.86	1.57	31.50
2889	25.21	2.50	0.20	6.87	8.65	1.79	6.04
2913	23.43	2.95	0.74	10.30	nan	nan	nan
2958	25.82	2.50	0.12	10.20	9.32	0.97	36.44
3043	23.09	2.75	0.02	10.30	nan	nan	nan
3098	25.83	1.60	0.40	5.20	8.74	3.75	2.20
3127	24.50	2.25	0.96	10.30	nan	nan	nan
3166	25.59	2.00	0.20	8.74	9.41	1.14	47.38
3169	26.52	1.80	0.28	6.97	8.14	1.19	45.73
3217	26.59	1.75	0.14	10.20	8.74	0.39	42.45
3321	26.30	2.55	0.36	6.56	8.74	2.20	10.88
3330	26.18	1.80	0.20	9.68	9.12	0.78	142.22
3397	26.57	1.85	0.10	9.57	8.69	0.34	23.89
3407	25.96	3.40	0.10	10.30	nan	nan	nan
3419	26.05	1.90	0.22	9.88	9.32	0.97	22.67
3554	26.47	2.05	0.06	8.64	8.59	0.35	63.39
3560	25.95	3.45	0.02	10.30	nan	nan	nan
3625	26.28	1.60	0.56	6.66	8.88	2.23	48.62
3639	25.13	2.60	0.30	8.95	10.16	1.85	94.42
3666	25.93	1.85	0.10	8.84	8.91	0.61	38.89
3689	26.16	2.45	0.10	10.20	9.07	0.73	102.34
3782	25.43	1.85	0.12	9.68	9.21	0.87	117.77
3789	26.42	2.10	0.30	6.76	8.35	1.60	123.41
3795	25.94	2.25	0.26	7.39	8.73	1.39	214.75
3808	24.78	2.95	0.26	8.74	10.32	2.05	8.11
8	25.68	1.50	0.64	6.56	9.18	2.64	230.07
59	25.81	2.95	0.16	6.87	8.39	1.54	13.72
69	25.82	1.50	0.34	6.76	8.36	1.61	112.44
73	26.47	1.50	0.14	7.39	7.83	0.49	8.13
100	25.97	2.25	0.40	6.56	8.86	2.31	105.67
190	25.76	2.85	0.12	10.30	nan	nan	nan
203	25.80	2.05	0.18	9.57	9.33	0.99	76.87
207	25.26	2.05	0.94	10.30	nan	nan	nan
242	25.91	2.05	0.38	6.87	8.78	1.93	111.79
288	25.09	2.45	0.40	6.76	9.35	2.60	2.89
296	25.59	2.85	0.44	10.30	nan	nan	nan
310	26.06	2.45	0.00	7.49	7.91	0.47	303.63
313	25.64	1.85	0.12	9.99	9.14	0.79	165.59
328	25.49	2.45	0.04	7.08	8.02	0.97	180.90
339	24.91	2.35	0.16	6.56	8.51	1.97	65.65
448	25.60	2.90	0.18	8.95	9.71	1.40	7.72

Table A.5: Best-fit parameters for this work's HDF-S catalog, 250 Myr e-folding exponential SFR.

ID	$\mathcal{R}_{VI}$	$z_{phot}$	$E(B - V)$	$\log(\text{Age}/\text{yr})$	$\log(M_*/M_\odot)$	$\log(\text{SFR}/(M_\odot/\text{yr}))$	$\chi^2$
464	25.68	3.15	0.60	10.30	nan	nan	nan
470	25.97	2.75	0.38	6.24	9.09	2.87	24.77
480	26.11	2.75	0.24	10.30	nan	nan	nan
520	26.31	2.30	0.38	6.56	8.66	2.12	130.99
533	25.69	2.30	0.38	6.56	8.92	2.37	137.20
542	26.10	3.10	0.84	10.30	nan	nan	nan
544	26.46	1.50	0.40	6.66	8.25	1.60	136.38
570	26.25	2.35	0.32	6.56	8.51	1.96	170.21
572	25.78	1.50	0.42	6.66	8.60	1.95	165.92
579	25.66	1.65	0.46	6.66	8.85	2.20	198.35
590	26.47	2.95	0.06	10.30	nan	nan	nan
639	25.98	3.05	0.92	10.30	nan	nan	nan
649	26.58	2.45	0.28	7.70	8.88	1.26	63.44
665	25.50	2.90	0.46	6.35	9.60	3.27	12.81
673	25.59	2.90	0.42	6.56	9.37	2.82	9.35
692	25.18	2.45	0.72	10.30	nan	nan	nan
721	25.32	2.90	0.26	10.30	nan	nan	nan
746	26.07	2.85	0.44	6.45	9.27	2.83	19.21
848	25.57	2.30	0.82	10.30	nan	nan	nan
871	25.43	2.95	0.20	8.74	9.82	1.56	21.30
972	26.43	2.40	0.32	7.18	8.71	1.57	19.12
1047	26.19	3.05	0.58	10.30	nan	nan	nan
1106	26.05	2.75	0.62	10.30	nan	nan	nan
1108	24.77	3.15	0.14	9.36	9.97	1.65	21.56
1124	26.47	2.35	0.32	6.76	8.47	1.72	115.17
1140	26.52	1.85	0.36	6.66	8.34	1.69	127.84
1225	26.56	3.30	0.00	9.26	8.73	0.41	57.05
1273	25.92	1.50	0.26	7.49	8.46	1.02	467.03
1403	26.34	3.40	0.06	9.88	9.13	0.79	63.85
1471	26.50	2.80	0.76	10.30	nan	nan	nan
1473	25.78	2.00	0.20	10.30	nan	nan	nan
1501	25.94	2.60	0.94	10.30	nan	nan	nan
1523	25.86	2.20	0.38	6.56	8.82	2.28	49.52
1527	26.37	2.50	0.16	9.57	9.24	0.89	103.95
1540	25.86	1.50	0.44	7.08	8.77	1.72	174.47
1543	25.04	1.70	0.32	8.84	9.86	1.57	18.06
1551	26.54	1.85	0.38	9.68	9.60	1.25	57.80
1572	25.99	1.70	0.54	5.93	9.14	3.24	55.68
1585	26.27	1.50	0.60	5.10	9.08	4.28	139.47
1590	26.06	1.70	0.24	10.20	9.26	0.91	44.52
1593	25.52	1.60	0.54	10.20	10.32	1.98	205.76
1647	25.44	1.70	0.18	8.84	9.28	0.99	38.53
1676	25.94	1.70	0.18	8.84	9.08	0.79	12.99
1696	26.55	2.95	0.78	10.30	nan	nan	nan
1699	26.53	2.80	0.42	5.20	9.07	4.09	98.81
1739	25.04	2.90	0.14	9.68	9.80	1.45	11.05
1863	25.24	1.70	0.36	8.74	9.88	1.61	34.20
1881	25.15	3.10	0.70	10.30	nan	nan	nan
1908	26.01	3.10	0.10	10.30	nan	nan	nan
1915	26.55	2.70	0.06	9.57	8.84	0.49	74.11
1926	25.69	2.35	0.20	10.30	nan	nan	nan
1954	26.00	2.40	0.14	10.20	9.27	0.92	35.66
1960	26.23	2.40	0.44	6.56	8.97	2.43	32.92
2021	26.47	3.10	0.20	10.30	nan	nan	nan
2025	25.67	1.55	0.66	6.56	9.31	2.76	223.55
2030	25.66	3.15	0.02	9.36	9.15	0.83	1.71
2052	26.18	2.85	0.12	6.56	8.00	1.46	9.20
2071	25.56	2.85	0.18	8.95	9.70	1.40	5.83

Table A.5: Best-fit parameters for this work's HDF-S catalog, 250 Myr e-folding exponential SFR.

ID	$\mathcal{R}_{VI}$	$z_{phot}$	$E(B - V)$	$\log(\text{Age}/\text{yr})$	$\log(M_*/M_\odot)$	$\log(\text{SFR}/(M_\odot/\text{yr}))$	$\chi^2$
2188	26.09	2.55	0.32	7.80	9.28	1.58	152.53
2219	26.20	2.05	0.78	10.30	nan	nan	nan
2257	26.39	1.55	0.54	9.88	9.97	1.62	190.39
2266	25.40	1.50	0.40	9.36	9.85	1.53	91.69
2300	25.78	2.50	0.48	6.45	9.36	2.92	164.60
2315	26.37	2.25	0.24	8.53	9.25	1.05	54.38
2329	26.11	2.65	0.14	9.78	9.31	0.97	52.60
2356	25.55	1.65	0.20	9.47	9.30	0.96	45.96
2427	26.22	3.00	0.34	6.04	8.96	2.95	14.39
2429	26.34	3.05	0.08	10.30	nan	nan	nan
2529	26.08	1.50	0.58	5.83	9.07	3.28	119.19
2545	25.75	2.70	0.22	9.57	9.77	1.43	82.33
2553	26.47	2.70	0.98	10.30	nan	nan	nan
2561	26.34	1.50	0.42	7.49	8.75	1.32	49.45
2568	26.04	2.15	0.32	7.08	8.70	1.65	13.10
2652	26.12	1.60	0.10	9.68	8.79	0.44	91.79
2684	26.55	2.85	0.38	6.35	8.85	2.51	113.19
2698	26.34	2.75	0.30	9.26	9.81	1.49	38.38
2722	25.81	2.80	0.88	10.30	nan	nan	nan
2751	26.42	2.65	0.04	9.78	8.83	0.48	207.89
2754	26.45	1.50	0.42	6.66	8.32	1.67	141.39
2759	25.90	3.15	0.12	9.99	9.45	1.10	135.58
2854	25.54	1.55	0.68	6.56	9.49	2.95	31.11
2946	25.85	3.00	0.16	8.64	9.49	1.25	22.39
2955	25.05	2.30	0.26	10.20	10.04	1.69	12.73
2989	26.49	2.85	0.38	6.56	8.87	2.32	291.33
3145	25.38	2.10	0.32	7.08	8.94	1.89	13.15
3163	26.16	2.25	0.08	10.30	nan	nan	nan
3258	26.31	3.10	0.04	9.68	8.93	0.58	142.20
3275	26.35	3.40	0.00	9.88	8.82	0.47	140.55
3294	25.37	1.60	0.54	9.16	10.33	2.01	38.74
3349	26.55	1.50	0.20	10.20	8.76	0.42	181.14
3399	26.48	1.50	0.54	6.66	8.59	1.95	194.52
3411	25.86	2.85	0.44	6.45	9.36	2.92	68.15
3420	25.98	2.65	0.58	10.30	nan	nan	nan
3465	26.53	2.50	0.12	9.88	9.01	0.66	52.91
3480	26.33	1.85	0.18	9.57	9.05	0.70	136.69
3485	26.31	2.90	0.96	10.30	nan	nan	nan
3491	26.01	1.50	0.14	8.12	8.49	0.54	49.75
3503	25.49	2.20	0.20	6.66	8.38	1.73	32.56
3511	25.57	2.45	0.20	7.80	9.09	1.38	10.22
3542	25.31	1.95	0.10	10.30	nan	nan	nan
3548	25.80	3.10	0.34	6.56	9.09	2.54	78.48
3563	24.80	2.80	0.74	10.30	nan	nan	nan
3578	26.16	1.55	0.62	6.56	8.98	2.44	165.75
3635	24.67	3.00	0.20	9.68	10.21	1.86	7.38
3641	26.09	2.20	0.12	10.30	nan	nan	nan
3646	25.77	2.80	0.18	6.87	8.41	1.56	28.70
3687	26.32	2.95	0.12	10.09	9.23	0.88	11.06
3767	26.58	2.60	0.84	10.30	nan	nan	nan
3779	26.44	3.15	0.12	8.95	9.22	0.92	85.48
3797	26.34	1.60	0.18	10.20	8.90	0.55	14.34
3867	25.76	2.40	0.20	8.22	9.27	1.25	17.00
3897	26.05	1.60	0.44	6.66	8.60	1.96	75.91

Table A.6: Best-fit parameters for this work's HDF-S catalog,  $-700$  Myr e-folding exponential SFR.

ID	$\mathcal{R}_{VI}$	$z_{phot}$	$E(B-V)$	$\log(\text{Age}/\text{yr})$	$\log(M_*/M_\odot)$	$\log(\text{SFR}/(M_\odot/\text{yr}))$	$\chi^2$
3	26.37	1.50	$0.14^{+0.02}_{-0.02}$	$7.49^{+0.00}_{-0.00}$	$7.95^{+0.00}_{-0.00}$	$0.49^{+0.00}_{-0.00}$	75.46
147	23.02	3.05	$0.26^{+0.00}_{-0.00}$	$6.56^{+0.31}_{-0.31}$	$9.86^{+0.08}_{-0.08}$	$3.31^{+0.00}_{-0.45}$	76.55
156	25.25	2.00	$0.08^{+0.02}_{-0.02}$	$8.33^{+0.10}_{-0.10}$	$9.35^{+0.08}_{-0.08}$	$0.79^{+0.11}_{-0.11}$	30.91
172	25.24	1.50	$0.30^{+0.00}_{-0.00}$	$8.64^{+0.21}_{-0.21}$	$9.87^{+0.08}_{-0.08}$	$1.18^{+0.00}_{-0.00}$	13.34
177	25.51	2.35	$0.00^{+0.02}_{-0.02}$	$8.64^{+0.00}_{-0.00}$	$9.23^{+0.02}_{-0.02}$	$0.54^{+0.02}_{-0.02}$	5.50
201	26.40	1.50	$0.22^{+0.02}_{-0.02}$	$7.39^{+0.00}_{-0.00}$	$8.10^{+0.02}_{-0.02}$	$0.74^{+0.02}_{-0.02}$	27.50
356	24.38	1.60	$0.66^{+0.00}_{-0.00}$	$6.76^{+0.21}_{-0.21}$	$9.98^{+0.08}_{-0.08}$	$3.22^{+0.03}_{-0.03}$	74.60
401	26.00	1.70	$0.16^{+0.02}_{-0.02}$	$8.53^{+0.10}_{-0.10}$	$9.17^{+0.12}_{-0.12}$	$0.61^{+0.30}_{-0.30}$	10.31
428	25.90	3.05	$0.24^{+0.02}_{-0.02}$	$6.56^{+0.31}_{-0.31}$	$8.64^{+0.06}_{-0.06}$	$2.09^{+0.06}_{-0.06}$	106.07
430	26.08	2.55	$0.08^{+0.02}_{-0.02}$	$7.60^{+0.21}_{-0.21}$	$8.34^{+0.10}_{-0.10}$	$0.77^{+0.12}_{-0.12}$	133.53
447	25.71	1.50	$0.20^{+0.04}_{-0.04}$	$6.76^{+0.20}_{-0.20}$	$8.03^{+0.12}_{-0.12}$	$1.27^{+0.20}_{-0.20}$	51.09
462	25.99	1.50	$0.50^{+0.04}_{-0.04}$	$5.93^{+0.10}_{-0.10}$	$8.86^{+0.09}_{-0.09}$	$2.96^{+0.09}_{-0.09}$	64.16
472	26.15	1.50	$0.58^{+0.04}_{-0.04}$	$6.66^{+0.21}_{-0.21}$	$8.91^{+0.07}_{-0.07}$	$2.26^{+0.07}_{-0.07}$	115.29
475	26.29	1.50	$0.56^{+0.04}_{-0.04}$	$6.66^{+0.10}_{-0.10}$	$8.78^{+0.06}_{-0.06}$	$2.13^{+0.06}_{-0.06}$	110.94
481	25.90	1.50	$0.26^{+0.02}_{-0.02}$	$6.76^{+0.00}_{-0.00}$	$8.13^{+0.06}_{-0.06}$	$1.37^{+0.06}_{-0.06}$	100.92
650	26.27	2.75	$0.00^{+0.00}_{-0.00}$	$8.74^{+0.10}_{-0.10}$	$9.14^{+0.07}_{-0.07}$	$0.32^{+0.06}_{-0.06}$	94.77
715	24.29	2.95	$0.18^{+0.04}_{-0.04}$	$8.74^{+0.09}_{-0.09}$	$10.10^{+0.27}_{-0.27}$	$1.89^{+0.07}_{-0.07}$	19.73
720	26.20	1.80	$0.14^{+0.08}_{-0.08}$	$8.01^{+0.31}_{-0.31}$	$8.58^{+0.26}_{-0.26}$	$0.59^{+0.40}_{-0.40}$	15.30
726	24.92	1.85	$0.24^{+0.04}_{-0.04}$	$8.53^{+0.30}_{-0.30}$	$9.93^{+0.13}_{-0.13}$	$1.37^{+0.24}_{-0.24}$	8.01
779	25.39	2.05	$0.14^{+0.00}_{-0.00}$	$8.95^{+0.10}_{-0.10}$	$10.08^{+0.05}_{-0.05}$	$0.93^{+0.16}_{-0.16}$	6.79
797	26.15	2.40	$0.00^{+0.00}_{-0.00}$	$8.95^{+0.00}_{-0.00}$	$9.44^{+0.08}_{-0.08}$	$0.30^{+0.02}_{-0.02}$	35.62
818	26.08	1.50	$0.12^{+0.04}_{-0.04}$	$8.32^{+0.42}_{-0.42}$	$8.70^{+0.17}_{-0.17}$	$0.38^{+0.16}_{-0.16}$	139.64
824	25.75	2.50	$0.00^{+0.00}_{-0.00}$	$9.05^{+0.20}_{-0.20}$	$9.80^{+0.15}_{-0.15}$	$0.46^{+0.26}_{-0.26}$	3.98
876	26.10	1.95	$0.00^{+0.00}_{-0.00}$	$8.22^{+0.00}_{-0.00}$	$8.42^{+0.02}_{-0.02}$	$0.21^{+0.02}_{-0.02}$	19.85
878	24.94	2.95	$0.34^{+0.02}_{-0.02}$	$6.76^{+0.00}_{-0.00}$	$9.37^{+0.13}_{-0.13}$	$2.61^{+0.12}_{-0.12}$	56.19
901	25.05	1.50	$0.60^{+0.00}_{-0.00}$	$6.66^{+0.00}_{-0.00}$	$9.36^{+0.00}_{-0.00}$	$-0.04^{+0.05}_{-0.05}$	30.68
1029	25.66	2.15	$0.10^{+0.04}_{-0.04}$	$8.64^{+0.21}_{-0.21}$	$9.45^{+0.13}_{-0.13}$	$0.76^{+0.11}_{-0.11}$	4.69
1089	25.09	1.50	$0.32^{+0.04}_{-0.04}$	$7.91^{+0.10}_{-0.10}$	$9.33^{+0.08}_{-0.08}$	$1.45^{+0.12}_{-0.12}$	16.03
1102	24.70	3.25	$0.04^{+0.02}_{-0.02}$	$8.64^{+0.32}_{-0.32}$	$9.96^{+0.24}_{-0.24}$	$1.27^{+0.08}_{-0.08}$	11.52
1159	26.32	1.60	$0.00^{+0.00}_{-0.00}$	$8.53^{+0.00}_{-0.00}$	$8.52^{+0.07}_{-0.07}$	$-0.04^{+0.05}_{-0.05}$	30.68
1191	25.61	2.45	$0.02^{+0.02}_{-0.02}$	$7.18^{+0.21}_{-0.21}$	$8.00^{+0.10}_{-0.10}$	$0.84^{+0.15}_{-0.15}$	14.22
1195	25.49	2.30	$0.24^{+0.04}_{-0.04}$	$6.66^{+0.15}_{-0.15}$	$8.54^{+0.16}_{-0.16}$	$1.89^{+0.21}_{-0.21}$	9.39
1228	24.95	1.50	$0.16^{+0.02}_{-0.02}$	$8.64^{+0.10}_{-0.10}$	$9.58^{+0.32}_{-0.32}$	$0.90^{+0.09}_{-0.09}$	0.86
1239	26.58	1.50	$0.28^{+0.02}_{-0.02}$	$7.39^{+0.10}_{-0.10}$	$8.19^{+0.23}_{-0.23}$	$0.83^{+0.12}_{-0.12}$	91.48
1267	23.34	3.05	$0.28^{+0.02}_{-0.02}$	$6.56^{+0.31}_{-0.31}$	$9.81^{+0.15}_{-0.15}$	$2.70^{+0.00}_{-0.00}$	192.34
1366	24.92	1.50	$0.10^{+0.04}_{-0.04}$	$8.64^{+0.21}_{-0.21}$	$9.45^{+0.10}_{-0.10}$	$0.76^{+0.12}_{-0.12}$	4.69
1441	25.66	1.50	$0.38^{+0.04}_{-0.04}$	$8.43^{+0.21}_{-0.21}$	$9.56^{+0.13}_{-0.13}$	$1.77^{+0.24}_{-0.24}$	8.00
1451	25.45	1.70	$0.30^{+0.06}_{-0.06}$	$7.60^{+0.42}_{-0.42}$	$9.00^{+0.28}_{-0.28}$	$1.44^{+0.16}_{-0.16}$	5.51
1467	24.30	2.55	$0.06^{+0.00}_{-0.00}$	$8.74^{+0.10}_{-0.10}$	$10.11^{+0.17}_{-0.17}$	$1.28^{+0.15}_{-0.15}$	9.07
1478	25.90	1.70	$0.42^{+0.04}_{-0.04}$	$7.91^{+0.31}_{-0.31}$	$9.43^{+0.17}_{-0.17}$	$1.55^{+0.12}_{-0.12}$	23.12
1482	24.27	1.85	$0.28^{+0.06}_{-0.06}$	$8.43^{+0.21}_{-0.21}$	$10.21^{+0.16}_{-0.16}$	$1.77^{+0.24}_{-0.24}$	11.69
1484	25.12	1.65	$0.34^{+0.04}_{-0.04}$	$8.74^{+0.20}_{-0.20}$	$10.27^{+0.04}_{-0.04}$	$1.28^{+0.16}_{-0.16}$	68.99
1498	23.49	1.85	$0.26^{+0.04}_{-0.04}$	$8.43^{+0.21}_{-0.21}$	$10.44^{+0.19}_{-0.19}$	$1.44^{+0.16}_{-0.16}$	9.67
1521	25.78	3.05	$0.26^{+0.04}_{-0.04}$	$6.56^{+0.21}_{-0.21}$	$9.88^{+0.09}_{-0.09}$	$1.20^{+0.29}_{-0.29}$	17.60
1533	26.40	1.65	$0.20^{+0.02}_{-0.02}$	$8.84^{+0.00}_{-0.00}$	$8.74^{+0.06}_{-0.06}$	$2.19^{+0.06}_{-0.06}$	233.41
1634	25.04	2.80	$0.22^{+0.04}_{-0.04}$	$8.53^{+0.21}_{-0.21}$	$9.48^{+0.12}_{-0.12}$	$0.50^{+0.00}_{-0.00}$	151.16
1695	26.23	1.65	$0.04^{+0.06}_{-0.06}$	$8.53^{+0.21}_{-0.21}$	$9.84^{+0.15}_{-0.15}$	$1.28^{+0.24}_{-0.24}$	3.91
1756	26.02	1.50	$0.10^{+0.02}_{-0.02}$	$7.80^{+0.21}_{-0.21}$	$8.23^{+0.08}_{-0.08}$	$0.46^{+0.08}_{-0.08}$	18.89
1817	26.17	1.50	$0.56^{+0.02}_{-0.02}$	$6.56^{+0.10}_{-0.10}$	$8.82^{+0.03}_{-0.03}$	$2.43^{+0.00}_{-0.00}$	139.84
1933	24.50	1.50	$0.34^{+0.02}_{-0.02}$	$7.49^{+0.10}_{-0.10}$	$9.29^{+0.08}_{-0.08}$	$1.82^{+0.34}_{-0.34}$	14.08
1973	25.69	1.65	$0.04^{+0.02}_{-0.02}$	$8.74^{+0.21}_{-0.21}$	$9.99^{+0.14}_{-0.14}$	$0.43^{+0.08}_{-0.08}$	192.96
1985	26.55	2.70	$0.00^{+0.00}_{-0.00}$	$8.53^{+0.10}_{-0.10}$	$9.13^{+0.08}_{-0.08}$	$0.30^{+0.03}_{-0.03}$	51.45
2005	26.06	1.50	$0.14^{+0.02}_{-0.02}$	$7.70^{+0.21}_{-0.21}$	$8.77^{+0.11}_{-0.11}$	$0.21^{+0.03}_{-0.03}$	32.63
2033	26.35	2.20	$0.02^{+0.02}_{-0.02}$	$8.84^{+0.00}_{-0.00}$	$9.19^{+0.09}_{-0.09}$	$0.59^{+0.00}_{-0.00}$	92.37
2042	26.06	2.25	$0.00^{+0.00}_{-0.00}$	$8.42^{+0.02}_{-0.02}$	$9.42^{+0.04}_{-0.04}$	$0.27^{+0.04}_{-0.04}$	23.83
2050	25.86	2.60	$0.24^{+0.04}_{-0.04}$	$7.18^{+0.16}_{-0.16}$	$8.72^{+0.03}_{-0.03}$	$1.56^{+0.16}_{-0.16}$	45.68

 $2.60^{+0.14}_{-0.14}$ 

39.36

Table A.6: Best-fit parameters for this work's HDF-S catalog,  $-700$  Myr e-folding exponential SFR.

ID	$\mathcal{R}_{VJ}$	$z_{\text{phot}}$	$E(B - V)$	$\log(\text{Age}/\text{yr})$	$\log(M_*/M_\odot)$	$\log(\text{SFR}/(M_\odot/\text{yr}))$	$\chi^2$
21192	26.46	2.70	0.00 $^{+0.00}_{-0.00}$	8.43 $^{+0.10}_{-0.10}$	8.70 $^{+0.12}_{-0.02}$	0.26 $^{+0.03}_{-0.02}$	37.01
22207	25.00	2.45	0.00 $^{+0.00}_{-0.04}$	8.74 $^{+0.10}_{-0.10}$	9.60 $^{+0.02}_{-0.02}$	0.77 $^{+0.02}_{-0.02}$	29.11
2306	25.77	2.70	0.10 $^{+0.02}_{-0.04}$	8.32 $^{+0.10}_{-0.10}$	9.24 $^{+0.06}_{-0.06}$	0.92 $^{+0.15}_{-0.16}$	63.78
2361	25.30	2.65	0.00 $^{+0.02}_{-0.02}$	8.53 $^{+0.10}_{-0.10}$	9.26 $^{+0.08}_{-0.08}$	0.70 $^{+0.02}_{-0.02}$	6.43
2367	25.71	2.55	0.06 $^{+0.02}_{-0.02}$	8.32 $^{+0.21}_{-0.21}$	9.07 $^{+0.11}_{-0.10}$	0.76 $^{+0.12}_{-0.17}$	17.81
2389	24.01	2.85	0.34 $^{+0.04}_{-0.04}$	6.56 $^{+0.10}_{-0.10}$	9.71 $^{+0.10}_{-0.09}$	3.17 $^{+0.00}_{-0.17}$	86.48
2560	26.08	1.50	0.26 $^{+0.02}_{-0.02}$	6.97 $^{+0.10}_{-0.10}$	8.11 $^{+0.11}_{-0.11}$	1.15 $^{+0.35}_{-0.35}$	6.02
2575	25.90	2.05	0.08 $^{+0.02}_{-0.02}$	8.53 $^{+0.10}_{-0.10}$	9.11 $^{+0.13}_{-0.13}$	0.55 $^{+0.03}_{-0.03}$	6.52
2597	26.56	2.95	0.00 $^{+0.02}_{-0.12}$	6.76 $^{+0.16}_{-0.73}$	7.43 $^{+0.03}_{-0.03}$	0.67 $^{+0.26}_{-0.26}$	7.12
2661	26.46	1.60	0.00 $^{+0.00}_{-0.02}$	8.53 $^{+0.00}_{-0.00}$	8.47 $^{+0.02}_{-0.02}$	-0.09 $^{+0.03}_{-0.09}$	132.17
2728	24.56	1.70	0.16 $^{+0.02}_{-0.02}$	8.43 $^{+0.10}_{-0.10}$	9.63 $^{+0.09}_{-0.09}$	1.20 $^{+0.20}_{-0.20}$	11.77
2747	26.50	1.70	0.42 $^{+0.02}_{-0.02}$	6.66 $^{+0.10}_{-0.10}$	8.44 $^{+0.07}_{-0.07}$	1.78 $^{+0.07}_{-0.07}$	49.41
2763	25.91	1.70	0.04 $^{+0.04}_{-0.04}$	8.32 $^{+0.42}_{-0.42}$	8.62 $^{+0.17}_{-0.17}$	0.30 $^{+0.26}_{-0.26}$	204.26
2765	26.36	1.50	0.24 $^{+0.06}_{-0.06}$	6.97 $^{+0.20}_{-0.20}$	7.94 $^{+0.08}_{-0.08}$	0.98 $^{+0.34}_{-0.34}$	14.32
2784	25.79	2.05	0.00 $^{+0.02}_{-0.02}$	8.95 $^{+0.00}_{-0.00}$	9.46 $^{+0.73}_{-0.73}$	0.32 $^{+0.02}_{-0.02}$	91.01
2799	26.59	2.50	0.00 $^{+0.00}_{-0.00}$	8.95 $^{+0.00}_{-0.00}$	9.23 $^{+0.02}_{-0.02}$	0.08 $^{+0.02}_{-0.02}$	371.86
2817	26.04	1.95	0.36 $^{+0.04}_{-0.04}$	6.56 $^{+0.31}_{-0.31}$	8.57 $^{+0.15}_{-0.15}$	2.02 $^{+0.25}_{-0.25}$	24.58
2837	25.41	1.60	0.30 $^{+0.02}_{-0.02}$	6.97 $^{+0.10}_{-0.10}$	8.55 $^{+0.06}_{-0.06}$	1.59 $^{+0.17}_{-0.17}$	7.77
2849	25.15	2.45	0.14 $^{+0.06}_{-0.06}$	8.64 $^{+0.10}_{-0.10}$	9.89 $^{+0.15}_{-0.15}$	1.20 $^{+0.09}_{-0.09}$	22.39
2889	25.21	2.50	0.20 $^{+0.06}_{-0.06}$	6.87 $^{+0.08}_{-0.08}$	8.65 $^{+0.08}_{-0.08}$	1.79 $^{+0.34}_{-0.34}$	6.01
2913	23.43	2.75	0.20 $^{+0.00}_{-0.00}$	7.91 $^{+0.52}_{-0.52}$	10.18 $^{+0.23}_{-0.23}$	2.31 $^{+0.20}_{-0.20}$	6.50
2958	25.82	2.60	0.02 $^{+0.02}_{-0.02}$	8.84 $^{+0.31}_{-0.31}$	9.52 $^{+0.14}_{-0.14}$	2.02 $^{+0.50}_{-0.50}$	42.05
3043	23.09	2.60	0.24 $^{+0.06}_{-0.06}$	6.97 $^{+0.87}_{-0.87}$	9.71 $^{+0.03}_{-0.03}$	0.54 $^{+0.24}_{-0.24}$	7.74
3098	25.83	1.60	0.40 $^{+0.14}_{-0.14}$	5.52 $^{+0.42}_{-0.42}$	8.74 $^{+0.53}_{-0.53}$	2.75 $^{+0.25}_{-0.25}$	9.00
3127	24.50	1.85	0.30 $^{+0.02}_{-0.02}$	8.53 $^{+0.35}_{-0.35}$	9.09 $^{+0.08}_{-0.08}$	3.31 $^{+0.97}_{-0.97}$	2.20
3166	25.59	1.90	0.18 $^{+0.02}_{-0.02}$	8.43 $^{+0.16}_{-0.16}$	9.29 $^{+0.16}_{-0.16}$	1.73 $^{+0.20}_{-0.20}$	4.59
3169	26.52	1.50	0.32 $^{+0.06}_{-0.06}$	6.87 $^{+0.21}_{-0.21}$	8.05 $^{+0.07}_{-0.07}$	1.19 $^{+0.34}_{-0.34}$	45.24
3217	26.59	1.95	0.10 $^{+0.04}_{-0.04}$	8.53 $^{+0.42}_{-0.42}$	8.84 $^{+0.35}_{-0.35}$	0.28 $^{+0.12}_{-0.12}$	38.49
3321	26.30	2.55	0.36 $^{+0.02}_{-0.02}$	6.56 $^{+0.00}_{-0.00}$	8.74 $^{+0.05}_{-0.05}$	2.19 $^{+0.07}_{-0.07}$	10.85
3330	26.18	1.50	0.16 $^{+0.06}_{-0.06}$	8.53 $^{+0.10}_{-0.10}$	8.96 $^{+0.04}_{-0.04}$	0.40 $^{+0.22}_{-0.22}$	53.17
3397	26.57	1.85	0.08 $^{+0.04}_{-0.04}$	8.43 $^{+0.20}_{-0.20}$	8.65 $^{+0.09}_{-0.09}$	0.94 $^{+0.35}_{-0.35}$	42.05
3407	25.96	1.50	0.28 $^{+0.04}_{-0.04}$	7.18 $^{+0.20}_{-0.20}$	8.31 $^{+0.09}_{-0.09}$	1.15 $^{+0.22}_{-0.22}$	19.94
3419	26.05	1.50	0.14 $^{+0.06}_{-0.06}$	7.06 $^{+0.30}_{-0.30}$	8.09 $^{+0.26}_{-0.26}$	0.40 $^{+0.12}_{-0.12}$	8.02
3554	26.47	1.80	0.02 $^{+0.02}_{-0.02}$	8.43 $^{+0.10}_{-0.10}$	8.48 $^{+0.13}_{-0.13}$	0.04 $^{+0.22}_{-0.22}$	133.86
3560	25.95	1.50	0.00 $^{+0.00}_{-0.00}$	8.84 $^{+0.10}_{-0.10}$	9.89 $^{+0.08}_{-0.08}$	-0.00 $^{+0.12}_{-0.12}$	13.58
3625	26.28	1.60	0.56 $^{+0.00}_{-0.00}$	6.66 $^{+0.00}_{-0.00}$	8.88 $^{+0.07}_{-0.07}$	2.23 $^{+0.07}_{-0.07}$	48.78
3639	25.13	3.10	0.14 $^{+0.08}_{-0.08}$	8.84 $^{+0.21}_{-0.21}$	10.40 $^{+0.10}_{-0.10}$	1.42 $^{+0.00}_{-0.00}$	17.53
3666	25.93	1.70	0.02 $^{+0.02}_{-0.02}$	8.64 $^{+0.10}_{-0.10}$	8.87 $^{+0.05}_{-0.05}$	0.19 $^{+0.19}_{-0.19}$	27.53
3689	26.16	2.45	0.08 $^{+0.02}_{-0.02}$	8.43 $^{+0.73}_{-0.73}$	9.04 $^{+0.38}_{-0.38}$	0.40 $^{+0.22}_{-0.22}$	13.58
3782	25.43	1.85	0.06 $^{+0.02}_{-0.02}$	8.64 $^{+0.10}_{-0.10}$	9.27 $^{+0.12}_{-0.12}$	0.22 $^{+0.33}_{-0.33}$	38.49
3789	26.42	1.50	0.34 $^{+0.02}_{-0.02}$	6.76 $^{+0.00}_{-0.00}$	8.16 $^{+0.06}_{-0.06}$	1.15 $^{+0.22}_{-0.22}$	42.03
3795	25.94	3.45	0.00 $^{+0.00}_{-0.00}$	8.74 $^{+1.46}_{-1.46}$	9.50 $^{+0.84}_{-0.84}$	0.40 $^{+0.19}_{-0.19}$	8.02
3808	24.78	3.05	0.18 $^{+0.02}_{-0.02}$	8.64 $^{+0.62}_{-0.62}$	10.40 $^{+0.23}_{-0.23}$	0.67 $^{+0.03}_{-0.03}$	212.10
59	25.81	2.95	0.16 $^{+0.02}_{-0.02}$	6.87 $^{+0.21}_{-0.21}$	8.39 $^{+0.08}_{-0.08}$	1.71 $^{+0.73}_{-0.73}$	8.13
69	25.82	1.50	0.34 $^{+0.02}_{-0.02}$	6.76 $^{+0.10}_{-0.10}$	8.36 $^{+0.09}_{-0.09}$	1.53 $^{+0.34}_{-0.34}$	13.55
73	26.47	1.50	0.14 $^{+0.04}_{-0.04}$	7.39 $^{+0.31}_{-0.31}$	7.84 $^{+0.12}_{-0.12}$	1.60 $^{+0.37}_{-0.37}$	11.23
242	25.91	2.05	0.40 $^{+0.04}_{-0.04}$	6.56 $^{+0.10}_{-0.10}$	8.87 $^{+0.09}_{-0.09}$	0.47 $^{+0.27}_{-0.27}$	8.09
288	25.09	2.45	0.40 $^{+0.02}_{-0.02}$	6.76 $^{+0.10}_{-0.10}$	8.83 $^{+0.09}_{-0.09}$	0.19 $^{+0.11}_{-0.11}$	27.53
296	25.59	3.65	0.10 $^{+0.04}_{-0.04}$	7.49 $^{+0.00}_{-0.00}$	8.38 $^{+0.09}_{-0.09}$	1.71 $^{+0.36}_{-0.36}$	60.70
310	26.06	2.45	0.00 $^{+0.00}_{-0.00}$	8.64 $^{+0.10}_{-0.10}$	9.41 $^{+0.07}_{-0.07}$	0.58 $^{+0.18}_{-0.18}$	106.32
313	25.64	1.65	0.02 $^{+0.00}_{-0.00}$	8.32 $^{+0.10}_{-0.10}$	9.91 $^{+0.08}_{-0.08}$	1.40 $^{+0.06}_{-0.06}$	104.12
328	25.49	2.45	0.04 $^{+0.02}_{-0.02}$	7.49 $^{+0.00}_{-0.00}$	7.92 $^{+0.06}_{-0.06}$	0.67 $^{+0.03}_{-0.03}$	212.10
339	24.91	2.30	0.16 $^{+0.02}_{-0.02}$	6.56 $^{+0.00}_{-0.00}$	9.10 $^{+0.00}_{-0.00}$	0.27 $^{+0.04}_{-0.04}$	136.67
448	25.60	2.80	0.22 $^{+0.02}_{-0.02}$	8.01 $^{+0.42}_{-0.42}$	9.49 $^{+0.21}_{-0.21}$	1.51 $^{+0.25}_{-0.25}$	3.39

Table A.6: Best-fit parameters for this work's HDF-S catalog,  $-700$  Myr e-folding exponential SFR.

ID	$R_{V,I}$	$z_{phot}$	$E(B-V)$	$\log(Age/\text{yr})$	$\log(M_*/\text{M}_\odot)$	$\log(\text{SFR}/(\text{M}_\odot/\text{yr}))$	$\chi^2$
464	25.68	2.95	$0.16^{+0.02}_{-0.02}$	$8.53^{+0.10}_{-0.06}$	$9.78^{+0.04}_{-0.05}$	$1.22^{+0.06}_{-0.05}$	67.49
470	25.97	2.75	$0.36^{+0.02}_{-0.02}$	$6.56^{+0.14}_{-0.10}$	$8.96^{+0.05}_{-0.05}$	$2.41^{+0.05}_{-0.05}$	24.14
480	26.11	2.75	$0.06^{+0.02}_{-0.02}$	$8.84^{+0.10}_{-0.06}$	$9.61^{+0.10}_{-0.10}$	$0.63^{+0.94}_{-0.04}$	52.41
520	26.31	2.30	$0.38^{+0.02}_{-0.02}$	$6.56^{+0.06}_{-0.06}$	$8.66^{+0.03}_{-0.03}$	$2.11^{+0.12}_{-0.03}$	131.13
533	25.69	2.30	$0.38^{+0.02}_{-0.02}$	$6.56^{+0.06}_{-0.06}$	$8.92^{+0.06}_{-0.06}$	$2.37^{+0.05}_{-0.05}$	137.39
542	26.10	1.50	$0.42^{+0.02}_{-0.02}$	$6.66^{+0.10}_{-0.06}$	$8.44^{+0.05}_{-0.05}$	$1.78^{+0.05}_{-0.05}$	131.79
544	26.46	1.50	$0.40^{+0.04}_{-0.04}$	$6.66^{+0.15}_{-0.06}$	$8.25^{+0.06}_{-0.06}$	$1.60^{+0.06}_{-0.06}$	136.67
570	26.25	2.35	$0.32^{+0.02}_{-0.02}$	$6.56^{+0.06}_{-0.06}$	$8.51^{+0.14}_{-0.14}$	$1.96^{+0.25}_{-0.02}$	170.25
572	25.78	1.50	$0.42^{+0.02}_{-0.02}$	$6.66^{+0.10}_{-0.06}$	$8.60^{+0.06}_{-0.06}$	$1.94^{+0.06}_{-0.06}$	165.40
579	25.66	1.65	$0.46^{+0.02}_{-0.02}$	$6.66^{+0.06}_{-0.06}$	$8.85^{+0.06}_{-0.06}$	$2.20^{+0.06}_{-0.06}$	198.01
590	26.47	1.50	$0.00^{+0.00}_{-0.00}$	$8.95^{+0.08}_{-0.08}$	$8.88^{+0.08}_{-0.08}$	$-0.27^{+0.06}_{-0.06}$	306.33
639	25.98	2.80	$0.48^{+0.04}_{-0.04}$	$6.56^{+0.16}_{-0.10}$	$9.41^{+0.13}_{-0.13}$	$2.86^{+0.23}_{-0.23}$	6.47
649	26.58	2.45	$0.26^{+0.02}_{-0.02}$	$7.80^{+0.31}_{-0.31}$	$8.92^{+0.12}_{-0.12}$	$1.15^{+0.11}_{-0.11}$	63.20
665	25.50	2.90	$0.46^{+0.04}_{-0.04}$	$6.24^{+0.10}_{-0.10}$	$9.61^{+0.18}_{-0.18}$	$3.38^{+0.50}_{-0.50}$	12.88
673	25.59	2.90	$0.42^{+0.04}_{-0.04}$	$6.56^{+0.14}_{-0.14}$	$9.37^{+0.13}_{-0.13}$	$2.82^{+0.12}_{-0.12}$	9.38
692	25.18	1.50	$0.20^{+0.06}_{-0.06}$	$8.64^{+0.10}_{-0.10}$	$9.61^{+0.22}_{-0.22}$	$0.92^{+0.92}_{-0.07}$	12.10
721	25.32	3.15	$0.02^{+0.02}_{-0.02}$	$9.05^{+0.21}_{-0.21}$	$10.18^{+0.07}_{-0.07}$	$0.85^{+0.08}_{-0.08}$	88.87
746	26.07	2.85	$0.44^{+0.02}_{-0.02}$	$6.45^{+0.19}_{-0.19}$	$9.27^{+0.14}_{-0.14}$	$2.82^{+0.21}_{-0.21}$	19.21
848	25.57	2.35	$0.18^{+0.02}_{-0.02}$	$9.05^{+0.10}_{-0.10}$	$10.45^{+0.03}_{-0.03}$	$1.11^{+0.03}_{-0.03}$	14.63
871	25.43	3.05	$0.10^{+0.02}_{-0.02}$	$8.74^{+0.10}_{-0.10}$	$9.96^{+0.05}_{-0.05}$	$1.13^{+0.09}_{-0.09}$	2.39
972	26.43	2.45	$0.30^{+0.08}_{-0.08}$	$7.28^{+0.42}_{-0.42}$	$8.74^{+0.13}_{-0.13}$	$1.48^{+0.42}_{-0.30}$	18.60
1047	26.19	3.20	$0.02^{+0.04}_{-0.04}$	$6.87^{+0.73}_{-0.73}$	$7.74^{+0.32}_{-0.32}$	$0.88^{+0.36}_{-0.36}$	144.41
1106	26.05	2.60	$0.48^{+0.02}_{-0.02}$	$6.76^{+0.94}_{-0.94}$	$9.27^{+0.55}_{-0.55}$	$2.52^{+0.14}_{-0.14}$	35.88
1108	24.77	3.40	$0.04^{+0.06}_{-0.06}$	$8.74^{+0.10}_{-0.10}$	$10.11^{+0.03}_{-0.03}$	$1.28^{+0.02}_{-0.02}$	3.06
1124	26.47	2.35	$0.32^{+0.02}_{-0.02}$	$6.76^{+0.10}_{-0.10}$	$8.47^{+0.11}_{-0.11}$	$1.72^{+0.21}_{-0.21}$	115.06
1140	26.52	1.85	$0.36^{+0.04}_{-0.04}$	$6.66^{+0.10}_{-0.10}$	$8.34^{+0.14}_{-0.14}$	$1.68^{+0.24}_{-0.24}$	127.63
1225	26.56	3.20	$0.00^{+0.00}_{-0.00}$	$8.32^{+0.21}_{-0.21}$	$8.65^{+0.19}_{-0.19}$	$0.34^{+0.01}_{-0.01}$	60.48
1273	25.92	1.50	$0.26^{+0.00}_{-0.00}$	$7.49^{+0.10}_{-0.10}$	$9.17^{+0.13}_{-0.13}$	$2.73^{+0.78}_{-0.78}$	132.06
1403	26.34	3.50	$0.00^{+0.02}_{-0.02}$	$8.74^{+0.10}_{-0.10}$	$9.96^{+0.05}_{-0.05}$	$1.28^{+0.02}_{-0.02}$	3.06
1471	26.50	2.55	$0.16^{+0.04}_{-0.04}$	$6.66^{+0.10}_{-0.10}$	$9.45^{+0.05}_{-0.05}$	$0.51^{+0.03}_{-0.03}$	53.61
1473	25.78	1.65	$0.22^{+0.04}_{-0.04}$	$8.84^{+0.10}_{-0.10}$	$9.79^{+0.11}_{-0.11}$	$0.76^{+0.03}_{-0.03}$	37.83
1501	25.94	3.05	$0.38^{+0.32}_{-0.32}$	$6.45^{+1.35}_{-1.35}$	$9.86^{+0.34}_{-0.34}$	$0.81^{+0.25}_{-0.25}$	28.36
1523	25.86	2.20	$0.38^{+0.02}_{-0.02}$	$6.56^{+0.31}_{-0.31}$	$9.17^{+0.47}_{-0.47}$	$2.73^{+1.78}_{-1.78}$	13.45
1527	26.37	2.65	$0.06^{+0.02}_{-0.02}$	$8.84^{+0.00}_{-0.00}$	$8.82^{+0.11}_{-0.11}$	$2.27^{+0.11}_{-0.11}$	49.40
1540	25.86	1.50	$0.44^{+0.08}_{-0.08}$	$7.08^{+0.10}_{-0.10}$	$8.77^{+0.08}_{-0.08}$	$0.49^{+0.48}_{-0.02}$	74.38
1543	25.04	1.70	$0.30^{+0.06}_{-0.06}$	$8.43^{+0.10}_{-0.10}$	$9.86^{+0.37}_{-0.37}$	$1.71^{+0.29}_{-0.29}$	174.52
1551	26.54	1.65	$0.26^{+0.02}_{-0.02}$	$8.84^{+0.10}_{-0.10}$	$9.59^{+0.09}_{-0.09}$	$1.42^{+0.36}_{-0.36}$	3.06
1572	25.99	1.50	$0.56^{+0.12}_{-0.12}$	$5.52^{+0.42}_{-0.42}$	$8.02^{+0.16}_{-0.16}$	$0.61^{+0.08}_{-0.08}$	54.98
1590	26.06	1.50	$0.12^{+0.00}_{-0.00}$	$8.84^{+0.25}_{-0.25}$	$9.26^{+0.07}_{-0.07}$	$0.28^{+0.00}_{-0.00}$	28.94
1647	25.44	1.70	$0.10^{+0.02}_{-0.02}$	$8.64^{+0.10}_{-0.10}$	$9.32^{+0.11}_{-0.11}$	$0.63^{+0.20}_{-0.20}$	27.41
1676	25.94	1.70	$0.10^{+0.02}_{-0.02}$	$8.64^{+0.10}_{-0.10}$	$9.12^{+0.11}_{-0.11}$	$0.43^{+0.08}_{-0.08}$	7.66
1696	26.55	2.55	$0.10^{+0.04}_{-0.04}$	$8.53^{+0.01}_{-0.01}$	$9.10^{+0.08}_{-0.08}$	$0.54^{+0.39}_{-0.39}$	45.13
1699	26.53	2.80	$0.42^{+0.04}_{-0.04}$	$5.41^{+0.21}_{-0.21}$	$9.07^{+0.24}_{-0.24}$	$3.78^{+0.48}_{-0.48}$	98.81
1739	25.04	2.95	$0.10^{+0.02}_{-0.02}$	$8.53^{+0.10}_{-0.10}$	$9.82^{+0.08}_{-0.08}$	$1.26^{+0.15}_{-0.15}$	8.01
1764	25.24	1.50	$0.28^{+0.02}_{-0.02}$	$8.64^{+0.10}_{-0.10}$	$9.80^{+0.04}_{-0.04}$	$1.11^{+0.07}_{-0.07}$	20.27
1863	25.69	2.60	$0.36^{+0.04}_{-0.04}$	$8.32^{+0.21}_{-0.21}$	$10.19^{+0.01}_{-0.01}$	$1.87^{+0.07}_{-0.07}$	8.33
1881	25.15	2.60	$0.06^{+0.04}_{-0.04}$	$8.84^{+0.10}_{-0.10}$	$9.93^{+0.06}_{-0.06}$	$0.95^{+0.12}_{-0.12}$	6.49
1908	26.01	3.35	$0.04^{+0.02}_{-0.02}$	$8.84^{+1.46}_{-1.46}$	$9.70^{+0.68}_{-0.68}$	$0.72^{+0.02}_{-0.02}$	78.76
1915	26.55	2.75	$0.00^{+0.00}_{-0.00}$	$8.74^{+0.10}_{-0.10}$	$9.03^{+0.13}_{-0.13}$	$0.20^{+0.04}_{-0.04}$	64.26
1926	25.69	2.60	$0.36^{+0.04}_{-0.04}$	$8.32^{+0.21}_{-0.21}$	$10.19^{+0.01}_{-0.01}$	$1.87^{+0.07}_{-0.07}$	8.33
1954	26.00	2.45	$0.02^{+0.02}_{-0.02}$	$8.84^{+0.10}_{-0.10}$	$9.40^{+0.10}_{-0.10}$	$0.42^{+0.15}_{-0.15}$	8.42
1960	26.23	2.40	$0.44^{+0.12}_{-0.12}$	$6.56^{+1.46}_{-1.46}$	$8.97^{+0.24}_{-0.24}$	$2.42^{+0.75}_{-0.75}$	32.76
2021	26.47	2.45	$0.42^{+0.00}_{-0.00}$	$6.56^{+0.62}_{-0.62}$	$8.80^{+0.00}_{-0.00}$	$2.25^{+0.00}_{-0.00}$	208.82
2030	25.66	3.10	$0.02^{+0.02}_{-0.02}$	$8.32^{+0.31}_{-0.31}$	$9.08^{+0.16}_{-0.16}$	$0.76^{+0.07}_{-0.07}$	2.51
2052	26.18	2.85	$0.12^{+0.04}_{-0.04}$	$6.56^{+1.46}_{-1.46}$	$8.00^{+0.13}_{-0.13}$	$1.45^{+0.23}_{-0.23}$	9.24
2071	25.56	2.95	$0.12^{+0.04}_{-0.04}$	$8.53^{+0.10}_{-0.10}$	$9.70^{+0.28}_{-0.28}$	$1.15^{+0.15}_{-0.15}$	3.66

Table A.6: Best-fit parameters for this work's HDF-S catalog,  $-700$  Myr e-folding exponential SFR.

ID	$\mathcal{R}_{VJ}$	$z_{phot}$	$E(B - V)$	$\log(\text{Age}/\text{yr})$	$\log(M_*/M_\odot)$	$\log(\text{SFR}/(M_\odot/\text{yr}))$	$\chi^2$
2188	26.09	2.55	$0.32^{+0.02}_{-0.02}$	$7.70^{+0.21}_{-0.10}$	$9.24^{+0.11}_{-0.12}$	$1.57^{+0.11}_{-0.11}$	151.60
2219	26.20	1.50	$0.56^{+0.02}_{-0.02}$	$7.60^{+0.10}_{-0.10}$	$9.33^{+0.07}_{-0.07}$	$1.76^{+0.08}_{-0.08}$	41.52
2257	26.39	2.00	$0.12^{+0.00}_{-0.00}$	$9.36^{+0.10}_{-0.10}$	$10.52^{+0.02}_{-0.02}$	$0.39^{+0.00}_{-0.03}$	27.95
2266	25.40	2.15	$0.18^{+0.08}_{-0.08}$	$9.05^{+0.00}_{-0.00}$	$10.43^{+0.03}_{-0.03}$	$1.09^{+0.11}_{-0.11}$	52.77
2300	25.78	2.50	$0.48^{+0.02}_{-0.02}$	$6.45^{+1.35}_{-1.35}$	$9.36^{+0.14}_{-0.14}$	$2.91^{+0.25}_{-0.19}$	164.68
2315	26.37	2.30	$0.22^{+0.04}_{-0.04}$	$8.32^{+0.31}_{-0.31}$	$9.27^{+0.19}_{-0.19}$	$0.95^{+0.17}_{-0.17}$	52.11
2329	26.11	2.70	$0.06^{+0.02}_{-0.02}$	$8.74^{+0.10}_{-0.10}$	$9.43^{+0.07}_{-0.07}$	$0.60^{+0.09}_{-0.09}$	36.01
2356	25.55	1.50	$0.10^{+0.02}_{-0.02}$	$8.74^{+0.31}_{-0.31}$	$9.27^{+0.08}_{-0.08}$	$0.45^{+0.10}_{-0.10}$	36.16
2427	26.22	3.00	$0.34^{+0.10}_{-0.08}$	$6.14^{+1.04}_{-0.90}$	$8.94^{+0.14}_{-0.14}$	$2.82^{+0.50}_{-0.50}$	14.39
2429	26.34	1.50	$0.48^{+0.02}_{-0.02}$	$5.10^{+0.62}_{-0.62}$	$8.63^{+0.08}_{-0.08}$	$1.40^{+0.12}_{-0.12}$	251.04
2529	26.08	1.50	$0.58^{+0.00}_{-0.00}$	$5.93^{+0.84}_{-0.84}$	$9.07^{+0.09}_{-0.09}$	$3.17^{+1.00}_{-1.00}$	119.19
2545	25.75	2.75	$0.12^{+0.00}_{-0.00}$	$8.84^{+0.00}_{-0.00}$	$9.96^{+0.04}_{-0.04}$	$0.98^{+0.04}_{-0.04}$	29.50
2553	26.47	2.65	$0.28^{+0.06}_{-0.06}$	$6.66^{+0.52}_{-0.52}$	$8.38^{+0.12}_{-0.12}$	$1.73^{+0.50}_{-0.50}$	56.57
2561	26.34	1.50	$0.42^{+0.02}_{-0.02}$	$7.39^{+0.56}_{-0.56}$	$8.70^{+0.12}_{-0.12}$	$1.33^{+0.12}_{-0.12}$	48.83
2568	26.04	2.25	$0.32^{+0.08}_{-0.04}$	$6.97^{+0.10}_{-0.10}$	$8.69^{+0.09}_{-0.09}$	$1.73^{+0.09}_{-0.09}$	13.19
2652	26.12	1.60	$0.00^{+0.00}_{-0.00}$	$8.84^{+0.10}_{-0.10}$	$8.98^{+0.09}_{-0.09}$	$-0.00^{+0.13}_{-0.13}$	47.15
2684	26.55	2.80	$0.38^{+0.04}_{-0.04}$	$6.45^{+0.96}_{-0.96}$	$8.81^{+0.12}_{-0.12}$	$2.36^{+0.24}_{-0.24}$	113.04
2698	26.34	3.10	$0.10^{+0.04}_{-0.04}$	$9.05^{+0.00}_{-0.00}$	$10.33^{+0.00}_{-0.00}$	$0.79^{+0.14}_{-0.14}$	10.23
2722	25.81	2.80	$0.00^{+0.00}_{-0.00}$	$9.05^{+0.10}_{-0.10}$	$10.31^{+0.00}_{-0.00}$	$0.52^{+0.02}_{-0.02}$	261.77
2751	26.42	2.70	$0.00^{+0.00}_{-0.00}$	$8.84^{+0.10}_{-0.10}$	$9.24^{+0.00}_{-0.00}$	$0.26^{+0.00}_{-0.00}$	143.55
2754	26.45	1.50	$0.42^{+0.02}_{-0.02}$	$6.66^{+1.56}_{-1.56}$	$8.32^{+0.00}_{-0.00}$	$1.67^{+0.00}_{-0.00}$	141.08
2759	25.90	3.45	$0.00^{+0.00}_{-0.00}$	$9.05^{+0.00}_{-0.00}$	$9.97^{+0.00}_{-0.00}$	$0.63^{+0.00}_{-0.00}$	28.66
2854	25.54	1.55	$0.68^{+0.00}_{-0.00}$	$6.56^{+0.00}_{-0.00}$	$9.49^{+0.02}_{-0.02}$	$2.94^{+0.04}_{-0.04}$	31.17
2846	25.85	3.05	$0.12^{+0.02}_{-0.02}$	$8.64^{+0.10}_{-0.10}$	$9.21^{+0.10}_{-0.10}$	$0.52^{+0.03}_{-0.03}$	261.77
2955	25.05	2.35	$0.20^{+0.02}_{-0.02}$	$8.64^{+0.10}_{-0.10}$	$10.11^{+0.05}_{-0.05}$	$1.42^{+0.15}_{-0.15}$	2.09
2989	26.49	2.20	$0.46^{+0.10}_{-0.10}$	$6.56^{+0.10}_{-0.10}$	$8.84^{+0.05}_{-0.05}$	$2.29^{+0.05}_{-0.05}$	290.94
3145	25.38	2.30	$0.22^{+0.02}_{-0.02}$	$7.91^{+0.83}_{-0.83}$	$9.31^{+0.14}_{-0.14}$	$1.43^{+0.28}_{-0.28}$	11.58
3163	26.16	2.40	$0.26^{+0.02}_{-0.02}$	$8.53^{+0.21}_{-0.21}$	$9.75^{+0.08}_{-0.08}$	$1.19^{+0.11}_{-0.11}$	38.11
3258	26.31	3.20	$0.00^{+0.00}_{-0.00}$	$8.53^{+0.00}_{-0.00}$	$8.97^{+0.02}_{-0.02}$	$0.41^{+0.03}_{-0.03}$	128.98
3275	26.35	3.40	$0.00^{+0.00}_{-0.00}$	$8.32^{+0.10}_{-0.10}$	$8.76^{+0.10}_{-0.10}$	$0.44^{+0.03}_{-0.03}$	142.36
3294	25.37	1.65	$0.50^{+0.06}_{-0.06}$	$8.53^{+0.10}_{-0.10}$	$10.39^{+0.08}_{-0.08}$	$1.83^{+0.22}_{-0.22}$	24.48
3349	26.55	1.50	$0.18^{+0.08}_{-0.08}$	$8.43^{+0.21}_{-0.21}$	$8.73^{+0.05}_{-0.05}$	$0.32^{+0.10}_{-0.10}$	51.04
3399	26.48	1.50	$0.54^{+0.02}_{-0.02}$	$6.66^{+0.00}_{-0.00}$	$9.06^{+0.12}_{-0.12}$	$1.19^{+0.09}_{-0.09}$	19.96
3411	25.86	2.85	$0.44^{+0.02}_{-0.02}$	$6.45^{+0.01}_{-0.01}$	$9.36^{+0.09}_{-0.09}$	$1.94^{+0.09}_{-0.09}$	194.23
3420	25.98	2.40	$0.30^{+0.02}_{-0.02}$	$6.76^{+0.10}_{-0.10}$	$8.61^{+0.07}_{-0.07}$	$2.91^{+0.21}_{-0.21}$	68.15
3465	26.53	2.60	$0.04^{+0.04}_{-0.04}$	$8.74^{+0.20}_{-0.20}$	$9.15^{+0.12}_{-0.12}$	$1.85^{+0.32}_{-0.32}$	74.53
3480	26.33	1.65	$0.10^{+0.04}_{-0.04}$	$8.43^{+0.10}_{-0.10}$	$9.15^{+0.10}_{-0.10}$	$0.32^{+0.10}_{-0.10}$	51.04
3399	26.48	1.50	$0.54^{+0.02}_{-0.02}$	$6.66^{+0.00}_{-0.00}$	$9.75^{+0.08}_{-0.08}$	$1.19^{+0.11}_{-0.11}$	38.11
3411	25.86	2.85	$0.44^{+0.02}_{-0.02}$	$6.45^{+0.01}_{-0.01}$	$9.36^{+0.09}_{-0.09}$	$1.94^{+0.09}_{-0.09}$	194.23
3420	25.98	2.40	$0.30^{+0.02}_{-0.02}$	$6.76^{+0.10}_{-0.10}$	$8.61^{+0.07}_{-0.07}$	$2.91^{+0.21}_{-0.21}$	68.15
3465	26.53	2.60	$0.04^{+0.04}_{-0.04}$	$8.74^{+0.20}_{-0.20}$	$9.15^{+0.12}_{-0.12}$	$1.85^{+0.32}_{-0.32}$	74.53
3503	25.49	2.20	$0.20^{+0.02}_{-0.02}$	$6.66^{+0.12}_{-0.12}$	$8.38^{+0.12}_{-0.12}$	$1.73^{+0.25}_{-0.25}$	32.67
3511	25.57	2.40	$0.20^{+0.02}_{-0.02}$	$7.80^{+0.21}_{-0.21}$	$9.10^{+0.09}_{-0.09}$	$0.29^{+0.10}_{-0.10}$	178.23
3542	25.31	1.65	$0.32^{+0.04}_{-0.04}$	$8.74^{+0.10}_{-0.10}$	$9.59^{+0.10}_{-0.10}$	$0.23^{+0.14}_{-0.14}$	115.32
3548	25.80	3.10	$0.34^{+0.02}_{-0.02}$	$6.87^{+0.10}_{-0.10}$	$8.09^{+0.07}_{-0.07}$	$1.23^{+0.83}_{-0.83}$	10.06
3491	26.01	1.80	$0.16^{+0.06}_{-0.06}$	$7.80^{+0.62}_{-0.62}$	$8.55^{+0.63}_{-0.63}$	$0.78^{+0.43}_{-0.43}$	48.79
3563	24.80	2.95	$0.20^{+0.04}_{-0.04}$	$8.12^{+0.25}_{-0.25}$	$8.98^{+0.48}_{-0.48}$	$1.79^{+0.25}_{-0.25}$	24.12
3687	26.32	3.00	$0.08^{+0.06}_{-0.06}$	$6.66^{+0.12}_{-0.12}$	$8.38^{+0.12}_{-0.12}$	$1.73^{+0.33}_{-0.33}$	32.67
3578	26.16	1.50	$0.62^{+0.02}_{-0.02}$	$6.56^{+0.02}_{-0.02}$	$8.94^{+0.07}_{-0.07}$	$2.39^{+0.05}_{-0.05}$	164.60
3635	24.67	3.05	$0.14^{+0.04}_{-0.04}$	$8.64^{+0.02}_{-0.02}$	$10.28^{+0.10}_{-0.10}$	$1.53^{+0.14}_{-0.14}$	3.52
3641	26.09	1.50	$0.20^{+0.04}_{-0.04}$	$8.95^{+0.00}_{-0.00}$	$9.63^{+0.00}_{-0.00}$	$0.49^{+0.06}_{-0.06}$	68.31
3646	25.77	2.80	$0.18^{+0.04}_{-0.04}$	$6.56^{+0.00}_{-0.00}$	$9.09^{+0.05}_{-0.05}$	$2.54^{+0.00}_{-0.00}$	78.65
3563	24.80	2.95	$0.20^{+0.04}_{-0.04}$	$8.12^{+0.25}_{-0.25}$	$8.41^{+0.08}_{-0.08}$	$1.78^{+0.17}_{-0.17}$	48.79
3687	26.32	3.00	$0.08^{+0.06}_{-0.06}$	$8.53^{+0.31}_{-0.31}$	$9.25^{+0.13}_{-0.13}$	$1.79^{+0.75}_{-0.75}$	24.12
3767	26.58	2.25	$0.46^{+0.02}_{-0.02}$	$6.56^{+0.00}_{-0.00}$	$8.94^{+0.10}_{-0.10}$	$0.69^{+0.22}_{-0.22}$	8.70
3779	26.44	3.10	$0.14^{+0.08}_{-0.08}$	$8.12^{+0.21}_{-0.21}$	$9.05^{+0.03}_{-0.03}$	$2.28^{+0.05}_{-0.05}$	102.63
3797	26.34	1.50	$0.18^{+0.04}_{-0.04}$	$8.32^{+0.21}_{-0.21}$	$8.76^{+0.21}_{-0.21}$	$0.95^{+0.32}_{-0.32}$	85.77
3867	25.76	2.45	$0.20^{+0.06}_{-0.06}$	$8.01^{+0.42}_{-0.42}$	$9.23^{+0.55}_{-0.55}$	$0.44^{+0.16}_{-0.16}$	12.80
3897	26.05	1.60	$0.44^{+0.04}_{-0.04}$	$6.66^{+0.10}_{-0.10}$	$8.60^{+0.07}_{-0.07}$	$1.95^{+0.33}_{-0.33}$	17.00
						$75.83^{+0.18}_{-0.18}$	75.83

## Appendix B

# $z \sim 2$ Best-fit SEDfit Parameters

Table B.1: Best-fit parameters for Sawicki et al. (2007) HDF catalog, 700 Myr e-folding exponential SFR.

ID	$\mathcal{R}_{VI}$	$z_{phot}$	$E(B - V)$	$\log(\text{Age}/\text{yr})$	$\log(M_*/M_\odot)$	$\log(\text{SFR}/(M_\odot/\text{yr}))$	$\chi^2$
3	24.08	3.10	$0.26^{+0.16}_{-0.10}$	$6.76^{+1.66}_{-1.98}$	$9.46^{+0.05}_{-0.82}$	$2.70^{+0.92}_{-2.36}$	28.45
12	25.14	2.95	$0.14^{+0.02}_{-0.08}$	$8.53^{+0.73}_{-1.77}$	$9.78^{+0.31}_{-0.32}$	$1.43^{+0.09}_{-0.33}$	0.93
60	26.55	2.10	$0.20^{+0.00}_{-0.02}$	$10.20^{+1.14}_{-0.10}$	$9.49^{+0.03}_{-0.09}$	$0.75^{+0.00}_{-0.09}$	21.26
88	26.28	3.20	$0.00^{+0.00}_{-0.00}$	$9.26^{+0.62}_{-1.04}$	$9.18^{+0.28}_{-0.03}$	$0.47^{+0.00}_{-0.02}$	27.52
96	26.99	2.45	$0.10^{+0.00}_{-0.00}$	$9.78^{+0.62}_{-0.62}$	$9.13^{+0.06}_{-0.02}$	$0.38^{+0.04}_{-0.02}$	31.31
97	27.58	2.50	$0.00^{+0.00}_{-0.00}$	$10.09^{+0.23}_{-0.10}$	$8.54^{+0.02}_{-0.00}$	$-0.21^{+0.00}_{-0.00}$	30.99
182	25.58	1.95	$0.28^{+0.00}_{-0.00}$	$9.36^{+0.42}_{-0.94}$	$10.06^{+0.14}_{-0.09}$	$1.34^{+0.06}_{-0.09}$	1.00
196	26.32	2.80	$0.18^{+0.10}_{-0.08}$	$8.01^{+0.94}_{-2.29}$	$9.01^{+0.42}_{-0.55}$	$1.09^{+0.35}_{-0.45}$	0.28
210	27.51	1.90	$0.14^{+0.14}_{-0.20}$	$7.28^{+0.62}_{-1.56}$	$7.54^{+3.03}_{-0.59}$	$0.29^{+3.36}_{-0.53}$	0.07
215	27.05	2.10	$0.22^{+0.00}_{-0.00}$	$9.99^{+0.73}_{-0.31}$	$9.37^{+0.03}_{-0.05}$	$0.62^{+0.00}_{-0.05}$	28.74
242	26.71	2.55	$0.28^{+0.10}_{-0.30}$	$6.56^{+1.46}_{-0.62}$	$8.29^{+0.97}_{-0.28}$	$1.75^{+2.17}_{-0.03}$	0.91
248	26.28	2.50	$0.00^{+0.00}_{-0.00}$	$8.74^{+0.10}_{-0.10}$	$8.80^{+0.08}_{-0.08}$	$0.30^{+0.00}_{-0.03}$	32.84
284	26.80	2.85	$0.00^{+0.00}_{-0.04}$	$8.74^{+0.62}_{-1.56}$	$8.65^{+0.33}_{-0.27}$	$0.16^{+0.04}_{-0.15}$	122.68
317	25.96	2.70	$0.02^{+0.00}_{-0.00}$	$10.30^{+1.35}_{-0.00}$	$9.30^{+0.15}_{-0.02}$	$0.55^{+0.03}_{-0.02}$	27.94
323	26.73	2.20	$0.06^{+0.06}_{-0.24}$	$7.70^{+0.94}_{-0.52}$	$7.99^{+17.93}_{-0.28}$	$0.35^{+17.14}_{-0.57}$	0.71
325	26.11	3.05	$0.08^{+0.00}_{-0.02}$	$10.20^{+1.46}_{-0.10}$	$9.56^{+0.19}_{-0.05}$	$0.82^{+0.02}_{-0.06}$	14.88
336	27.28	2.40	$0.14^{+0.04}_{-0.02}$	$6.56^{+0.10}_{-0.10}$	$7.51^{+0.12}_{-0.03}$	$0.96^{+0.22}_{-0.23}$	62.87
338	26.99	2.50	$0.00^{+0.00}_{-0.02}$	$10.09^{+0.52}_{-0.21}$	$8.78^{+0.00}_{-0.08}$	$0.03^{+0.00}_{-0.08}$	30.89
364	27.90	2.40	$0.00^{+0.00}_{-0.08}$	$10.09^{+2.20}_{-0.21}$	$8.40^{+18.99}_{-0.03}$	$-0.34^{+0.03}_{-17.73}$	79.64
390	27.14	2.80	$0.04^{+0.00}_{-0.02}$	$9.88^{+1.25}_{-0.42}$	$8.94^{+0.27}_{-0.06}$	$0.19^{+0.02}_{-0.07}$	1.98
411	27.56	1.45	$0.10^{+0.04}_{-0.16}$	$8.43^{+1.56}_{-0.42}$	$7.99^{+0.58}_{-0.20}$	$-0.28^{+0.17}_{-0.87}$	69.46
425	26.37	1.85	$0.30^{+0.00}_{-0.02}$	$10.30^{+1.04}_{-0.00}$	$9.78^{+0.07}_{-0.12}$	$1.03^{+0.07}_{-0.12}$	9.29
442	24.00	2.90	$0.16^{+0.02}_{-0.02}$	$8.95^{+0.31}_{-1.35}$	$10.53^{+0.13}_{-0.14}$	$1.93^{+0.05}_{-0.06}$	5.23
452	26.68	2.70	$0.14^{+0.02}_{-0.02}$	$9.05^{+0.42}_{-0.25}$	$9.37^{+1.18}_{-0.11}$	$0.72^{+0.06}_{-0.06}$	1.51
454	26.26	2.80	$0.12^{+0.02}_{-0.04}$	$8.74^{+0.62}_{-1.56}$	$9.33^{+0.25}_{-0.31}$	$0.84^{+0.08}_{-0.16}$	3.28
463	26.62	2.80	$0.00^{+0.00}_{-0.02}$	$9.99^{+1.14}_{-0.31}$	$8.97^{+0.13}_{-0.06}$	$0.22^{+0.02}_{-0.06}$	53.59
470	26.23	2.50	$0.14^{+0.00}_{-0.00}$	$10.20^{+1.04}_{-0.10}$	$9.58^{+0.06}_{-0.04}$	$0.83^{+0.00}_{-0.04}$	7.04
478	24.22	2.90	$0.26^{+0.02}_{-0.02}$	$8.84^{+0.31}_{-1.46}$	$10.77^{+0.15}_{-0.17}$	$2.22^{+0.05}_{-0.08}$	4.56
510	26.47	2.50	$0.04^{+0.00}_{-0.00}$	$9.88^{+0.31}_{-0.42}$	$9.15^{+0.04}_{-0.00}$	$0.40^{+0.04}_{-0.00}$	52.50
552	26.43	1.50	$0.18^{+0.18}_{-0.10}$	$7.39^{+0.42}_{-0.41}$	$7.98^{+0.51}_{-0.83}$	$0.63^{+3.32}_{-0.02}$	0.81
578	26.59	2.10	$0.08^{+0.04}_{-0.02}$	$9.99^{+6.94}_{-0.31}$	$9.08^{+0.06}_{-0.07}$	$0.34^{+0.04}_{-0.07}$	6.08
592	25.94	2.70	$0.08^{+0.00}_{-0.00}$	$9.99^{+0.83}_{-0.31}$	$9.52^{+0.06}_{-0.00}$	$0.77^{+0.02}_{-0.00}$	61.22
604	27.35	2.50	$0.04^{+0.00}_{-0.02}$	$10.20^{+1.35}_{-0.10}$	$8.77^{+0.16}_{-0.07}$	$0.03^{+0.05}_{-0.08}$	2.58
610	25.50	1.90	$0.36^{+0.04}_{-0.12}$	$8.43^{+0.94}_{-0.42}$	$9.88^{+0.90}_{-0.19}$	$1.61^{+0.29}_{-0.23}$	4.16
621	27.60	1.55	$0.18^{+0.10}_{-0.26}$	$6.76^{+1.66}_{-0.83}$	$7.21^{+17.47}_{-0.49}$	$0.45^{+17.57}_{-2.44}$	0.67
653	26.26	2.20	$0.32^{+0.04}_{-0.10}$	$8.32^{+0.83}_{-0.42}$	$9.54^{+1.78}_{-0.24}$	$1.35^{+1.11}_{-0.7}$	2.99
668	25.35	2.20	$0.12^{+0.00}_{-0.02}$	$10.20^{+1.35}_{-0.10}$	$9.76^{+0.14}_{-0.05}$	$1.01^{+0.05}_{-0.09}$	1.10
673	26.33	1.60	$0.08^{+0.00}_{-0.00}$	$9.99^{+0.73}_{-0.31}$	$8.99^{+0.05}_{-0.03}$	$0.24^{+0.03}_{-0.03}$	35.86
709	27.66	2.45	$0.08^{+0.02}_{-0.00}$	$9.88^{+0.73}_{-0.42}$	$8.79^{+0.06}_{-0.02}$	$0.04^{+0.05}_{-0.02}$	36.61
712	27.95	1.85	$0.00^{+0.00}_{-0.00}$	$9.88^{+0.83}_{-0.42}$	$8.20^{+0.20}_{-0.08}$	$-0.55^{+0.11}_{-0.08}$	13.57
751	26.75	1.60	$0.04^{+0.00}_{-0.02}$	$9.78^{+0.62}_{-0.52}$	$8.69^{+0.06}_{-0.23}$	$-0.05^{+0.06}_{-0.23}$	17.99
762	25.92	1.85	$0.30^{+0.00}_{-0.02}$	$9.88^{+1.04}_{-0.42}$	$9.95^{+0.12}_{-0.12}$	$1.20^{+0.10}_{-0.16}$	2.69
766	27.48	1.55	$0.30^{+0.30}_{-0.10}$	$6.66^{+1.56}_{-3.64}$	$7.60^{+3.01}_{-0.44}$	$0.95^{+3.71}_{-2.29}$	2.55
789	26.76	2.50	$0.04^{+0.02}_{-0.00}$	$9.99^{+0.73}_{-0.31}$	$9.01^{+0.07}_{-0.00}$	$0.26^{+0.07}_{-0.00}$	30.22

Table B.1: Best-fit parameters for Sawicki et al. (2007) HDF catalog, 700 Myr e-folding exponential SFR.

ID	$\mathcal{R}_{VI}$	$z_{phot}$	$E(B - V)$	$\log(Age/\text{yr})$	$\log(M_*/M_\odot)$	$\log(\text{SFR}/(M_\odot/\text{yr}))$	$\chi^2$
790	25.23	1.40	0.58 $^{+0.00}_{-0.00}$	9.47 $^{+0.94}_{-0.83}$	10.69 $^{+0.12}_{-0.38}$	1.95 $^{+0.11}_{-0.04}$	4.72
797	25.27	2.65	0.08 $^{+0.00}_{-0.00}$	9.36 $^{+0.52}_{-0.94}$	9.77 $^{+0.17}_{-0.03}$	1.04 $^{+0.02}_{-0.02}$	6.93
801	27.91	1.45	0.00 $^{+0.00}_{-0.00}$	9.16 $^{+0.31}_{-1.14}$	7.98 $^{+0.13}_{-0.11}$	-0.71 $^{+0.03}_{-0.06}$	24.05
879	27.58	2.50	0.00 $^{+0.00}_{-0.00}$	10.09 $^{+0.21}_{-0.20}$	8.54 $^{+0.04}_{-0.04}$	-0.21 $^{+0.05}_{-0.06}$	17.72
880	27.40	2.60	0.00 $^{+0.00}_{-0.00}$	7.18 $^{+0.42}_{-0.42}$	7.22 $^{+0.18}_{-0.18}$	0.07 $^{+0.10}_{-0.07}$	73.64
891	27.94	1.30	0.02 $^{+0.00}_{-0.00}$	10.09 $^{+0.21}_{-0.21}$	8.00 $^{+0.26}_{-0.06}$	-0.75 $^{+0.26}_{-0.00}$	47.76
892	26.81	2.50	0.08 $^{+0.00}_{-0.00}$	10.20 $^{+0.64}_{-0.50}$	9.14 $^{+0.00}_{-0.00}$	-0.39 $^{+0.00}_{-0.00}$	17.07
893	26.59	2.40	0.14 $^{+0.00}_{-0.00}$	9.88 $^{+0.52}_{-0.42}$	9.42 $^{+0.07}_{-0.07}$	0.67 $^{+0.07}_{-0.00}$	50.62
896	26.64	2.20	0.04 $^{+0.00}_{-0.00}$	9.88 $^{+0.62}_{-0.62}$	8.99 $^{+0.03}_{-0.03}$	0.25 $^{+0.00}_{-0.00}$	115.15
921	26.75	1.95	0.14 $^{+0.00}_{-0.00}$	9.78 $^{+0.94}_{-0.94}$	9.16 $^{+0.07}_{-0.07}$	0.41 $^{+0.10}_{-0.07}$	10.88
933	25.77	2.95	0.34 $^{+0.00}_{-0.00}$	6.56 $^{+0.52}_{-0.52}$	9.02 $^{+0.42}_{-0.42}$	2.47 $^{+0.16}_{-0.16}$	14.13
954	27.75	2.10	0.10 $^{+0.00}_{-0.00}$	9.85 $^{+0.63}_{-0.63}$	8.55 $^{+0.24}_{-0.34}$	-0.06 $^{+0.13}_{-0.03}$	0.41
994	26.01	2.40	0.04 $^{+0.00}_{-0.00}$	9.16 $^{+0.31}_{-0.31}$	9.22 $^{+0.14}_{-0.14}$	0.54 $^{+0.10}_{-0.07}$	1.42
1006	27.62	2.40	0.06 $^{+0.00}_{-0.00}$	9.36 $^{+2.18}_{-0.94}$	8.69 $^{+1.94}_{-0.94}$	-0.04 $^{+0.78}_{-0.04}$	5.10
1007	27.81	2.70	0.10 $^{+0.00}_{-0.00}$	7.80 $^{+0.70}_{-0.70}$	7.92 $^{+1.19}_{-1.19}$	0.18 $^{+1.88}_{-1.00}$	11.49
1026	26.13	1.40	0.58 $^{+0.04}_{-0.04}$	9.58 $^{+0.50}_{-0.50}$	8.66 $^{+0.21}_{-0.21}$	1.62 $^{+0.21}_{-0.06}$	62.05
1048	26.33	2.80	0.14 $^{+0.00}_{-0.00}$	9.88 $^{+0.54}_{-0.54}$	9.63 $^{+0.18}_{-0.18}$	0.88 $^{+0.05}_{-0.05}$	14.52
1062	27.26	2.95	0.22 $^{+0.00}_{-0.00}$	6.76 $^{+1.66}_{-1.66}$	7.99 $^{+0.20}_{-0.20}$	1.24 $^{+0.94}_{-0.94}$	25.05
1073	25.75	2.85	0.02 $^{+0.00}_{-0.00}$	8.43 $^{+0.62}_{-0.62}$	8.08 $^{+0.60}_{-0.60}$	0.16 $^{+0.32}_{-0.09}$	4.14
1074	26.02	2.65	0.00 $^{+0.00}_{-0.00}$	8.32 $^{+0.42}_{-0.42}$	8.44 $^{+0.60}_{-0.60}$	-0.28 $^{+0.02}_{-0.02}$	32.89
1083	26.87	2.35	0.16 $^{+0.00}_{-0.00}$	9.78 $^{+0.10}_{-0.10}$	8.66 $^{+0.30}_{-0.30}$	0.47 $^{+0.24}_{-0.07}$	0.31
1095	27.66	2.75	0.00 $^{+0.00}_{-0.00}$	9.26 $^{+0.52}_{-0.52}$	8.52 $^{+0.23}_{-0.23}$	0.35 $^{+0.02}_{-0.02}$	13.03
1099	27.62	2.70	0.08 $^{+0.00}_{-0.00}$	8.01 $^{+2.95}_{-0.95}$	8.08 $^{+0.60}_{-0.60}$	-0.19 $^{+0.03}_{-0.03}$	39.86
1110	27.77	2.50	0.00 $^{+0.00}_{-0.00}$	9.36 $^{+0.62}_{-0.62}$	9.19 $^{+0.93}_{-0.93}$	0.16 $^{+0.32}_{-0.09}$	9.36
1112	27.37	2.40	0.10 $^{+0.00}_{-0.00}$	9.82 $^{+0.50}_{-0.50}$	8.32 $^{+0.07}_{-0.07}$	0.45 $^{+0.24}_{-0.07}$	74.36
1129	26.02	2.15	0.20 $^{+0.00}_{-0.00}$	9.99 $^{+1.25}_{-1.25}$	9.35 $^{+0.17}_{-0.17}$	0.61 $^{+0.07}_{-0.07}$	1.25
1131	26.50	2.75	0.00 $^{+0.00}_{-0.00}$	9.26 $^{+0.52}_{-0.52}$	8.52 $^{+0.23}_{-0.23}$	0.26 $^{+0.02}_{-0.02}$	46.11
1158	26.41	2.70	0.04 $^{+0.00}_{-0.00}$	9.78 $^{+0.42}_{-0.42}$	9.19 $^{+0.93}_{-0.93}$	0.45 $^{+0.09}_{-0.09}$	7.83
1190	27.37	2.20	0.08 $^{+0.00}_{-0.00}$	9.68 $^{+0.52}_{-0.52}$	8.32 $^{+0.07}_{-0.07}$	0.28 $^{+0.02}_{-0.02}$	67.14
1191	26.91	1.35	0.34 $^{+0.00}_{-0.00}$	10.09 $^{+0.94}_{-0.94}$	8.83 $^{+0.11}_{-0.11}$	0.08 $^{+0.09}_{-0.09}$	113.73
1226	27.67	2.40	0.04 $^{+0.00}_{-0.00}$	9.00 $^{+0.31}_{-0.31}$	9.34 $^{+0.06}_{-0.06}$	0.59 $^{+0.05}_{-0.05}$	43.36
1236	26.47	1.45	0.40 $^{+0.00}_{-0.00}$	6.76 $^{+0.10}_{-0.10}$	8.25 $^{+0.11}_{-0.11}$	-0.11 $^{+0.07}_{-0.07}$	63.76
1241	26.09	2.65	0.16 $^{+0.00}_{-0.00}$	9.99 $^{+0.94}_{-0.94}$	9.73 $^{+0.15}_{-0.15}$	1.50 $^{+0.22}_{-0.22}$	74.36
1264	26.44	2.50	0.02 $^{+0.00}_{-0.00}$	9.78 $^{+0.31}_{-0.31}$	8.83 $^{+0.06}_{-0.06}$	0.08 $^{+0.07}_{-0.07}$	67.14
1290	27.42	2.50	0.00 $^{+0.00}_{-0.00}$	9.78 $^{+0.83}_{-0.83}$	8.59 $^{+0.13}_{-0.13}$	0.59 $^{+0.05}_{-0.05}$	52.56
1294	26.39	2.50	0.00 $^{+0.00}_{-0.00}$	8.84 $^{+0.52}_{-0.52}$	8.83 $^{+0.07}_{-0.07}$	-0.15 $^{+0.03}_{-0.03}$	94.42
1295	26.12	1.60	0.30 $^{+0.00}_{-0.00}$	10.09 $^{+0.94}_{-0.94}$	9.73 $^{+0.17}_{-0.17}$	1.50 $^{+0.22}_{-0.22}$	74.36
1296	26.90	2.05	0.08 $^{+0.00}_{-0.00}$	9.99 $^{+0.31}_{-0.31}$	8.81 $^{+0.20}_{-0.20}$	1.01 $^{+0.25}_{-0.25}$	67.14
1328	26.75	2.50	0.00 $^{+0.00}_{-0.00}$	9.36 $^{+0.35}_{-0.35}$	9.07 $^{+0.04}_{-0.04}$	0.32 $^{+0.04}_{-0.04}$	118.15
1352	25.32	2.60	0.36 $^{+0.00}_{-0.00}$	9.78 $^{+0.83}_{-0.83}$	8.85 $^{+0.06}_{-0.06}$	0.12 $^{+0.00}_{-0.00}$	143.55
1362	27.45	2.75	0.12 $^{+0.00}_{-0.00}$	9.57 $^{+4.47}_{-0.12}$	9.25 $^{+0.24}_{-0.24}$	2.30 $^{+0.37}_{-0.37}$	13.96
1437	26.91	2.75	0.04 $^{+0.00}_{-0.00}$	9.16 $^{+0.73}_{-0.73}$	9.10 $^{+0.24}_{-0.24}$	0.35 $^{+0.37}_{-0.37}$	81.47
1474	25.86	2.25	0.12 $^{+0.00}_{-0.00}$	8.95 $^{+0.35}_{-0.35}$	8.95 $^{+0.04}_{-0.04}$	0.20 $^{+0.21}_{-0.21}$	0.87
1499	27.51	1.60	0.40 $^{+0.00}_{-0.00}$	9.68 $^{+0.94}_{-0.94}$	9.78 $^{+0.19}_{-0.19}$	0.82 $^{+0.09}_{-0.09}$	0.36
1501	27.77	2.05	0.16 $^{+0.00}_{-0.00}$	5.31 $^{+0.58}_{-0.58}$	8.08 $^{+0.21}_{-0.21}$	2.94 $^{+0.12}_{-0.12}$	143.55
1503	26.68	1.15	0.20 $^{+0.00}_{-0.00}$	5.52 $^{+0.42}_{-0.42}$	7.39 $^{+4.42}_{-0.24}$	1.96 $^{+0.54}_{-0.54}$	59.29
1516	26.10	2.45	0.10 $^{+0.00}_{-0.00}$	9.16 $^{+0.62}_{-0.62}$	8.78 $^{+0.13}_{-0.13}$	0.10 $^{+0.82}_{-0.82}$	29.20
1519	26.00	2.05	0.14 $^{+0.00}_{-0.00}$	9.68 $^{+0.94}_{-0.94}$	8.01 $^{+0.54}_{-0.54}$	0.26 $^{+0.04}_{-0.04}$	19.05
1525	26.79	2.10	0.02 $^{+0.00}_{-0.00}$	5.31 $^{+0.21}_{-0.21}$	9.52 $^{+0.60}_{-0.60}$	0.77 $^{+0.05}_{-0.05}$	27.49
1528	27.17	2.50	0.08 $^{+0.00}_{-0.00}$	9.68 $^{+0.42}_{-0.42}$	8.81 $^{+0.08}_{-0.08}$	0.07 $^{+0.04}_{-0.04}$	21.43
1531	26.91	2.25	0.18 $^{+0.00}_{-0.00}$	8.43 $^{+1.04}_{-1.04}$	8.89 $^{+2.13}_{-2.13}$	0.62 $^{+0.30}_{-0.30}$	0.24
1535	25.30	2.50	0.08 $^{+0.00}_{-0.00}$	10.20 $^{+0.62}_{-0.62}$	9.75 $^{+0.34}_{-0.34}$	1.00 $^{+0.02}_{-0.02}$	16.69
1539	26.87	1.55	0.16 $^{+0.00}_{-0.00}$	9.88 $^{+0.73}_{-0.73}$	8.43 $^{+0.52}_{-0.52}$	0.23 $^{+0.03}_{-0.03}$	43.23
1556	26.67	2.50	0.16 $^{+0.00}_{-0.00}$	9.68 $^{+0.52}_{-0.52}$	9.48 $^{+0.06}_{-0.06}$	0.74 $^{+0.28}_{-0.28}$	52.96
1561	26.78	2.50	0.06 $^{+0.00}_{-0.00}$	10.20 $^{+0.94}_{-0.94}$	9.06 $^{+0.07}_{-0.07}$	0.31 $^{+0.07}_{-0.07}$	109.70
1592	27.10	2.80	0.08 $^{+0.00}_{-0.00}$	10.20 $^{+0.46}_{-0.46}$	9.09 $^{+0.05}_{-0.05}$	0.35 $^{+0.06}_{-0.06}$	18.95

Table B.1: Best-fit parameters for Sawicki et al. (2007) HDF catalog, 700 Myr e-folding exponential SFR.

ID	$\mathcal{R}_{VI}$	$z_{phot}$	$E(B - V)$	$\log(\text{Age}/\text{yr})$	$\log(M_*/M_\odot)$	$\log(\text{SFR}/(M_\odot/\text{yr}))$	$\chi^2$
1606	26.80	2.50	$0.06^{+0.00}_{-0.00}$	$10.20^{+1.04}_{-0.10}$	$9.08^{+0.06}_{-0.00}$	$0.33^{+0.02}_{-0.00}$	56.62
1610	26.39	2.35	$0.16^{+0.02}_{-0.00}$	$9.68^{+0.42}_{-0.62}$	$9.55^{+0.10}_{-0.02}$	$0.80^{+0.09}_{-0.02}$	44.53
1611	26.41	1.85	$0.12^{+0.02}_{-0.02}$	$9.68^{+0.22}_{-0.22}$	$9.20^{+0.13}_{-0.13}$	$0.45^{+0.13}_{-0.13}$	23.80
1621	24.88	1.25	$0.12^{+0.02}_{-0.04}$	$9.05^{+0.25}_{-0.21}$	$9.34^{+0.09}_{-0.11}$	$0.68^{+0.10}_{-0.21}$	5.20
1654	25.27	2.05	$0.30^{+0.02}_{-0.00}$	$9.05^{+0.21}_{-0.25}$	$10.22^{+0.06}_{-0.06}$	$1.57^{+0.07}_{-0.06}$	8.43
1662	26.19	2.45	$0.02^{+0.02}_{-0.10}$	$8.32^{+1.14}_{-0.31}$	$8.61^{+1.99}_{-0.18}$	$0.42^{+1.38}_{-0.16}$	0.66
1700	27.17	1.40	$0.00^{+0.00}_{-0.02}$	$10.30^{+1.14}_{-0.00}$	$8.30^{+0.06}_{-0.09}$	$-0.45^{+0.03}_{-0.09}$	12.79
1709	26.40	2.50	$0.04^{+0.02}_{-0.00}$	$9.36^{+0.42}_{-0.94}$	$9.14^{+0.12}_{-0.02}$	$0.41^{+0.07}_{-0.00}$	7.56
1734	27.50	2.70	$0.02^{+0.00}_{-0.06}$	$9.99^{+0.83}_{-0.31}$	$8.69^{+0.06}_{-0.09}$	$-0.06^{+0.03}_{-0.09}$	174.95
1747	27.05	2.45	$0.06^{+0.06}_{-0.24}$	$8.43^{+1.06}_{-1.87}$	$8.49^{+1.99}_{-0.42}$	$0.22^{+1.78}_{-0.36}$	0.45
1777	25.01	2.65	$0.14^{+0.00}_{-0.00}$	$10.30^{+1.35}_{-0.00}$	$10.11^{+0.15}_{-0.02}$	$1.37^{+0.04}_{-0.02}$	7.44
1903	26.74	2.65	$0.46^{+0.26}_{-0.22}$	$6.14^{+1.04}_{-3.12}$	$9.04^{+2.16}_{-0.07}$	$2.92^{+4.11}_{-1.40}$	0.31
2006	26.89	1.90	$0.20^{+0.02}_{-0.02}$	$9.36^{+0.62}_{-0.94}$	$9.26^{+0.20}_{-0.17}$	$0.53^{+0.17}_{-0.16}$	21.63
2060	27.76	2.85	$0.12^{+0.06}_{-0.10}$	$8.43^{+1.35}_{-1.87}$	$8.54^{+0.66}_{-0.56}$	$0.27^{+0.23}_{-0.56}$	3.80
2066	27.12	2.65	$0.06^{+0.02}_{-0.00}$	$10.30^{+1.25}_{-0.00}$	$8.97^{+0.11}_{-0.02}$	$0.23^{+0.08}_{-0.02}$	59.29
2073	27.80	2.05	$0.00^{+0.00}_{-0.00}$	$10.20^{+0.30}_{-0.10}$	$8.32^{+0.64}_{-0.00}$	$-0.42^{+0.03}_{-0.00}$	14.09
2079	26.98	2.45	$0.14^{+0.02}_{-0.02}$	$9.05^{+1.66}_{-1.25}$	$9.17^{+1.97}_{-0.11}$	$0.52^{+0.78}_{-0.08}$	8.25
2095	26.55	2.65	$0.02^{+0.00}_{-0.02}$	$10.20^{+1.56}_{-0.10}$	$9.05^{+0.25}_{-0.03}$	$0.30^{+0.02}_{-0.10}$	13.89
2106	25.88	2.55	$0.04^{+0.00}_{-0.02}$	$10.09^{+1.14}_{-0.21}$	$9.38^{+0.08}_{-0.04}$	$0.63^{+0.02}_{-0.06}$	4.52
2111	26.57	2.40	$0.02^{+0.02}_{-0.00}$	$10.09^{+0.83}_{-0.21}$	$9.02^{+0.07}_{-0.03}$	$0.27^{+0.07}_{-0.03}$	141.35
2169	27.89	2.70	$0.10^{+0.10}_{-0.22}$	$6.76^{+1.66}_{-0.87}$	$7.21^{+1.13}_{-0.56}$	$0.45^{+1.13}_{-0.41}$	31.35
2171	25.55	2.50	$0.04^{+0.00}_{-0.00}$	$9.78^{+0.73}_{-0.52}$	$9.48^{+0.09}_{-0.03}$	$0.74^{+0.04}_{-0.04}$	20.45
2188	27.32	2.20	$0.00^{+0.00}_{-0.00}$	$9.78^{+0.52}_{-0.52}$	$8.58^{+0.69}_{-0.06}$	$-0.17^{+0.06}_{-0.06}$	37.00
2206	26.56	2.50	$0.02^{+0.00}_{-0.00}$	$9.88^{+0.10}_{-0.42}$	$9.03^{+0.00}_{-0.00}$	$0.28^{+0.00}_{-0.00}$	78.10
2208	26.58	2.45	$0.12^{+0.00}_{-0.00}$	$10.20^{+1.25}_{-0.10}$	$9.35^{+0.11}_{-0.02}$	$0.61^{+0.04}_{-0.03}$	5.23
2221	27.94	1.85	$0.12^{+0.12}_{-0.24}$	$7.60^{+2.50}_{-1.56}$	$7.50^{+17.98}_{-0.67}$	$-0.04^{+17.39}_{-2.90}$	0.10
2228	25.75	1.80	$0.30^{+0.02}_{-0.02}$	$9.05^{+0.31}_{-0.25}$	$9.90^{+0.19}_{-0.15}$	$1.25^{+0.27}_{-0.07}$	10.73
2255	27.25	1.40	$0.16^{+0.02}_{-0.02}$	$9.88^{+0.62}_{-0.42}$	$8.75^{+0.09}_{-0.16}$	$0.00^{+0.00}_{-0.00}$	95.88
2260	26.10	2.75	$0.22^{+0.02}_{-0.00}$	$9.05^{+0.21}_{-1.25}$	$9.90^{+0.09}_{-0.09}$	$1.25^{+0.05}_{-0.03}$	13.48
2282	24.63	2.50	$0.06^{+0.00}_{-0.00}$	$10.20^{+1.14}_{-0.10}$	$9.93^{+0.09}_{-0.02}$	$1.19^{+0.00}_{-0.02}$	4.01
2300	26.66	2.65	$0.16^{+0.02}_{-0.00}$	$9.05^{+0.21}_{-1.25}$	$9.44^{+0.11}_{-0.11}$	$0.79^{+0.03}_{-0.04}$	1.29
2306	25.42	2.60	$0.14^{+0.00}_{-0.02}$	$9.78^{+0.94}_{-0.52}$	$9.93^{+0.16}_{-0.04}$	$1.19^{+0.04}_{-0.04}$	1.24
2342	27.85	1.60	$0.12^{+0.02}_{-0.02}$	$9.88^{+0.73}_{-0.42}$	$8.50^{+0.27}_{-0.17}$	$-0.25^{+0.26}_{-0.17}$	31.77
2366	26.44	2.20	$0.38^{+0.00}_{-0.02}$	$9.99^{+0.83}_{-0.31}$	$10.23^{+0.00}_{-0.06}$	$1.48^{+0.10}_{-0.06}$	27.13
2404	27.76	2.00	$0.12^{+0.02}_{-0.04}$	$9.16^{+0.32}_{-1.14}$	$8.65^{+0.36}_{-0.12}$	$-0.04^{+0.19}_{-0.15}$	5.84
2409	26.90	2.05	$0.18^{+0.02}_{-0.00}$	$10.20^{+0.94}_{-0.10}$	$9.28^{+0.07}_{-0.02}$	$0.54^{+0.06}_{-0.02}$	14.55
2490	27.03	2.40	$0.04^{+0.02}_{-0.00}$	$10.09^{+0.52}_{-0.21}$	$8.90^{+0.07}_{-0.00}$	$0.15^{+0.07}_{-0.00}$	106.20
2501	25.98	2.45	$0.08^{+0.00}_{-0.02}$	$10.09^{+1.14}_{-0.21}$	$9.46^{+0.09}_{-0.02}$	$0.71^{+0.06}_{-0.05}$	3.00
2560	26.37	2.05	$0.14^{+0.00}_{-0.02}$	$9.36^{+0.62}_{-0.94}$	$9.34^{+0.21}_{-0.09}$	$0.61^{+0.13}_{-0.10}$	0.31
2616	25.58	2.75	$0.20^{+0.02}_{-0.02}$	$8.84^{+0.31}_{-0.46}$	$9.95^{+0.14}_{-0.16}$	$1.40^{+0.05}_{-0.06}$	1.04
2625	26.65	2.25	$0.12^{+0.04}_{-0.12}$	$8.32^{+1.14}_{-0.31}$	$8.71^{+2.34}_{-0.19}$	$0.52^{+0.71}_{-0.32}$	0.51
2702	25.73	2.65	$0.10^{+0.02}_{-0.00}$	$9.36^{+0.52}_{-0.94}$	$9.66^{+0.18}_{-0.05}$	$0.93^{+0.05}_{-0.04}$	5.45
2710	25.05	2.40	$0.12^{+0.02}_{-0.00}$	$10.20^{+1.14}_{-0.10}$	$9.96^{+0.09}_{-0.02}$	$1.21^{+0.09}_{-0.02}$	14.76
2808	27.75	2.70	$0.28^{+0.14}_{-0.26}$	$6.66^{+1.56}_{-1.35}$	$7.92^{+1.47}_{-0.45}$	$1.27^{+1.58}_{-2.24}$	5.79
2832	26.69	2.70	$0.10^{+0.00}_{-0.00}$	$9.78^{+0.42}_{-0.52}$	$9.30^{+0.02}_{-0.00}$	$0.53^{+0.02}_{-0.00}$	66.72
2835	27.68	2.75	$0.08^{+0.02}_{-0.02}$	$9.88^{+1.14}_{-0.42}$	$8.86^{+0.25}_{-0.08}$	$0.11^{+0.08}_{-0.08}$	11.95
2848	27.80	2.05	$0.00^{+0.00}_{-0.04}$	$9.36^{+0.68}_{-0.94}$	$8.31^{+0.06}_{-0.07}$	$-0.42^{+0.22}_{-0.06}$	17.22
2849	25.59	2.60	$0.14^{+0.00}_{-0.00}$	$10.30^{+1.14}_{-0.00}$	$9.86^{+0.04}_{-0.04}$	$1.12^{+0.04}_{-0.04}$	14.87
2853	25.22	2.50	$0.08^{+0.02}_{-0.00}$	$9.05^{+0.21}_{-1.25}$	$9.67^{+0.09}_{-0.11}$	$1.02^{+0.04}_{-0.04}$	0.72
2876	25.81	2.40	$0.00^{+0.00}_{-0.00}$	$9.36^{+0.31}_{-0.94}$	$9.21^{+0.07}_{-0.03}$	$0.48^{+0.02}_{-0.02}$	12.03
2894	27.17	2.75	$0.04^{+0.02}_{-0.00}$	$9.36^{+2.18}_{-0.94}$	$8.91^{+2.78}_{-0.04}$	$0.18^{+1.71}_{-0.11}$	5.85
2967	26.80	1.55	$0.18^{+0.00}_{-0.02}$	$9.68^{+0.73}_{-0.62}$	$9.05^{+0.07}_{-0.06}$	$0.30^{+0.03}_{-0.07}$	16.88
3025	26.97	2.90	$0.04^{+0.02}_{-0.04}$	$9.26^{+0.83}_{-1.04}$	$9.00^{+0.31}_{-0.05}$	$0.28^{+0.06}_{-0.06}$	5.70
3036	27.56	2.70	$0.02^{+0.02}_{-0.00}$	$9.99^{+1.14}_{-0.31}$	$8.67^{+0.02}_{-0.02}$	$-0.08^{+0.08}_{-0.02}$	8.64

Table B.1: Best-fit parameters for Sawicki et al. (2007) HDF catalog, 700 Myr e-folding exponential SFR.

ID	$\mathcal{R}_{VI}$	$z_{phot}$	$E(B - V)$	$\log(\text{Age}/\text{yr})$	$\log(M_*/M_\odot)$	$\log(\text{SFR}/(M_\odot/\text{yr}))$	$\chi^2$
3042	27.21	1.25	$0.24^{+0.22}_{-0.04}$	$6.87^{+0.10}_{-1.77}$	$7.39^{+0.17}_{-0.44}$	$0.54^{+1.16}_{-0.24}$	10.71
3048	24.74	2.20	$0.18^{+0.02}_{-0.00}$	$9.05^{+0.21}_{-1.25}$	$10.11^{+0.09}_{-0.13}$	$1.46^{+0.07}_{-0.07}$	1.44
3083	25.65	2.05	$0.16^{+0.02}_{-0.00}$	$9.26^{+0.21}_{-1.04}$	$9.68^{+0.11}_{-0.03}$	$0.97^{+0.14}_{-0.03}$	5.08
3087	26.46	2.80	$0.06^{+0.06}_{-0.06}$	$8.32^{+0.82}_{-1.98}$	$8.74^{+0.30}_{-0.45}$	$0.55^{+0.20}_{-0.28}$	1.32
3111	24.61	2.35	$0.04^{+0.04}_{-0.02}$	$10.20^{+1.35}_{-0.21}$	$9.83^{+0.13}_{-0.07}$	$1.08^{+0.06}_{-0.11}$	2.68
3115	25.41	2.10	$0.20^{+0.02}_{-0.02}$	$8.43^{+0.21}_{-0.31}$	$9.49^{+0.11}_{-0.13}$	$1.22^{+0.16}_{-0.09}$	13.07
3134	25.09	2.35	$0.18^{+0.02}_{-0.00}$	$8.95^{+0.10}_{-1.35}$	$9.98^{+0.07}_{-0.15}$	$1.37^{+0.09}_{-0.04}$	8.36
3176	25.86	2.20	$0.12^{+0.02}_{-0.02}$	$8.84^{+0.21}_{-1.46}$	$9.36^{+0.05}_{-0.23}$	$0.81^{+0.10}_{-0.14}$	5.89
3189	26.24	2.00	$0.04^{+0.00}_{-0.02}$	$9.78^{+0.62}_{-0.52}$	$9.05^{+0.10}_{-0.06}$	$0.30^{+0.06}_{-0.06}$	38.80
3201	27.16	1.55	$0.32^{+0.10}_{-0.06}$	$7.60^{+0.52}_{-0.53}$	$8.27^{+2.26}_{-0.61}$	$0.73^{+2.31}_{-0.33}$	3.86
3222	27.89	0.00	$0.02^{+0.02}_{-0.03}$	$7.49^{+0.31}_{-1.25}$	$-10.55^{+0.09}_{-1.25}$	$-18.00^{+1.20}_{-1.23}$	3.33
3250	27.14	2.70	$0.02^{+0.02}_{-0.06}$	$8.32^{+0.62}_{-0.42}$	$8.29^{+0.24}_{-0.24}$	$0.10^{+0.11}_{-0.27}$	0.73
3255	26.74	2.75	$0.12^{+0.00}_{-0.00}$	$9.88^{+0.42}_{-0.42}$	$9.34^{+0.13}_{-0.02}$	$0.60^{+0.02}_{-0.02}$	75.41
3256	26.90	2.05	$0.36^{+0.36}_{-0.26}$	$6.56^{+1.46}_{-3.74}$	$8.29^{+18.00}_{-0.29}$	$1.74^{+18.31}_{-2.04}$	0.21
3263	27.57	2.10	$0.24^{+0.02}_{-0.04}$	$8.95^{+0.42}_{-1.35}$	$9.09^{+0.19}_{-0.16}$	$0.48^{+0.10}_{-0.12}$	11.91
3264	23.66	2.35	$0.20^{+0.02}_{-0.14}$	$8.74^{+1.35}_{-1.56}$	$10.52^{+1.92}_{-0.18}$	$2.03^{+0.87}_{-0.16}$	7.89
3269	26.81	2.60	$0.02^{+0.02}_{-0.04}$	$8.74^{+0.42}_{-1.00}$	$8.69^{+0.24}_{-0.23}$	$0.20^{+0.08}_{-0.13}$	0.21
3373	24.31	2.15	$0.18^{+0.04}_{-0.10}$	$8.43^{+1.04}_{-0.42}$	$9.90^{+1.88}_{-0.14}$	$1.63^{+1.11}_{-0.17}$	2.35

Table B.2: Best-fit parameters for Sawicki et al. (2007) HDF catalog, 500 Myr e-folding exponential SFR.

ID	$\mathcal{R}_{VI}$	$z_{phot}$	$E(B - V)$	$\log(\text{Age}/\text{yr})$	$\log(M_*/M_\odot)$	$\log(\text{SFR}/(M_\odot/\text{yr}))$	$\chi^2$
3	24.08	2.90	0.38	6.24	9.85	3.62	39.80
12	25.14	2.90	0.16	8.43	9.73	1.49	0.63
60	26.55	2.10	0.22	9.68	9.44	0.83	24.38
88	26.28	2.90	0.26	5.83	8.57	2.78	64.82
96	26.99	2.40	0.12	9.99	9.06	0.45	38.73
97	27.58	2.50	0.00	9.99	8.41	-0.20	34.44
182	25.58	1.95	0.30	9.36	10.02	1.42	3.67
196	26.32	2.85	0.16	8.22	9.10	1.02	0.15
210	27.51	1.95	0.14	7.28	7.56	0.31	0.07
215	27.05	2.10	0.24	10.20	9.31	0.70	36.55
242	26.71	2.55	0.28	6.56	8.29	1.75	0.88
248	26.28	2.50	0.00	8.95	8.84	0.31	32.09
284	26.80	2.90	0.00	8.84	8.67	0.18	122.56
317	25.96	2.65	0.02	9.78	9.16	0.54	31.20
323	26.73	2.20	0.06	7.70	7.98	0.35	0.64
325	26.11	2.90	0.12	8.74	9.35	0.91	22.35
336	27.28	2.40	0.14	6.56	7.51	0.96	62.87
338	26.99	2.50	0.02	9.57	8.73	0.12	35.30
364	27.90	2.40	0.00	9.88	8.28	-0.34	83.85
390	27.14	2.75	0.06	9.36	8.86	0.26	2.34
411	27.56	1.50	0.10	8.43	8.00	-0.24	69.49
425	26.37	1.85	0.32	10.09	9.72	1.11	14.81
442	24.00	2.90	0.16	9.68	10.54	1.93	6.20
452	26.68	2.75	0.14	9.57	9.36	0.75	2.60
454	26.26	2.80	0.12	8.95	9.37	0.85	3.41
463	26.62	2.75	0.02	10.30	8.90	0.29	54.88
470	26.23	2.50	0.16	9.78	9.52	0.91	10.68
478	24.22	2.90	0.26	10.30	10.83	2.22	4.80
510	26.47	2.40	0.06	9.99	9.06	0.45	64.12
552	26.43	1.50	0.18	7.39	7.98	0.63	0.78
578	26.59	2.05	0.10	9.68	9.00	0.39	8.50
592	25.94	2.70	0.08	9.68	9.40	0.79	68.04
604	27.35	2.40	0.06	9.99	8.69	0.07	3.93
610	25.50	1.85	0.36	8.43	9.83	1.59	4.36
621	27.60	1.55	0.18	6.76	7.21	0.45	0.67
653	26.26	2.25	0.30	8.53	9.62	1.30	3.31
668	25.35	2.20	0.14	10.20	9.70	1.09	2.49
673	26.33	1.55	0.10	9.57	8.90	0.29	45.00
709	27.66	2.45	0.08	10.30	8.66	0.05	42.37
712	27.95	1.60	0.00	9.36	7.96	-0.64	14.79
751	26.75	1.55	0.06	9.68	8.61	-0.01	22.76
762	25.92	1.85	0.32	10.09	9.89	1.28	4.70
766	27.48	1.55	0.30	6.66	7.60	0.95	2.51
789	26.76	2.50	0.04	9.78	8.88	0.27	35.16
790	25.23	1.60	0.60	9.36	10.83	2.23	4.46
797	25.27	2.65	0.08	9.68	9.66	1.05	9.26
801	27.91	1.45	0.00	9.36	7.91	-0.69	24.21
879	27.58	2.50	0.00	9.78	8.41	-0.20	19.45
880	27.40	2.60	0.00	7.18	7.22	0.07	73.68
891	27.94	1.30	0.04	9.68	7.93	-0.68	54.55
892	26.81	2.50	0.08	9.68	9.01	0.40	23.62
893	26.59	2.40	0.14	10.09	9.29	0.68	61.70
896	26.64	2.20	0.06	9.68	8.93	0.32	130.66
921	26.75	1.95	0.16	10.09	9.10	0.49	11.83
933	25.77	2.90	0.38	6.24	9.20	2.97	14.75
954	27.75	2.10	0.10	9.78	8.56	-0.05	0.50
994	26.01	2.35	0.04	9.68	9.14	0.53	3.49

Table B.2: Best-fit parameters for Sawicki et al. (2007) HDF catalog, 500 Myr e-folding exponential SFR.

ID	$\mathcal{R}_{VI}$	$z_{phot}$	$E(B - V)$	$\log(\text{Age}/\text{yr})$	$\log(M_*/M_\odot)$	$\log(\text{SFR}/(M_\odot/\text{yr}))$	$\chi^2$
1006	27.62	2.40	0.06	9.68	8.58	-0.03	6.10
1007	27.81	2.70	0.10	7.80	7.91	0.18	11.46
1026	26.13	1.40	0.60	9.68	10.31	1.70	69.43
1048	26.33	2.80	0.14	9.78	9.50	0.89	16.51
1062	27.26	2.90	0.24	6.66	8.02	1.37	25.66
1073	25.75	2.85	0.02	8.43	8.94	0.70	4.26
1074	26.02	2.65	0.00	8.32	8.64	0.48	0.26
1083	26.87	2.20	0.18	10.09	9.23	0.62	19.61
1095	27.66	2.75	0.00	9.88	8.43	-0.18	40.58
1099	27.62	2.70	0.08	8.01	8.07	0.16	9.32
1106	27.77	2.50	0.00	9.99	8.33	-0.28	33.09
1112	27.73	2.40	0.10	9.99	8.70	0.09	120.86
1129	26.02	2.15	0.22	9.99	9.68	1.07	2.32
1131	26.50	2.75	0.00	9.88	8.88	0.27	48.88
1158	26.41	2.65	0.06	10.30	9.12	0.51	82.23
1190	27.37	2.20	0.10	9.88	8.77	0.16	74.64
1191	26.91	1.35	0.36	10.20	9.28	0.67	49.88
1226	27.67	2.20	0.06	9.68	8.51	-0.10	70.70
1236	26.47	1.45	0.40	6.76	8.25	1.50	7.83
1241	26.09	2.60	0.18	9.78	9.68	1.07	9.57
1264	26.44	2.50	0.04	9.78	9.01	0.40	60.33
1290	27.42	2.50	0.00	9.47	8.46	-0.15	95.55
1294	26.39	2.50	0.00	9.36	8.88	0.28	18.29
1295	26.12	1.60	0.32	10.20	9.67	1.06	20.00
1296	26.90	2.05	0.08	9.68	8.82	0.21	0.86
1328	26.75	2.50	0.00	9.36	8.73	0.13	119.29
1352	25.32	2.60	0.36	6.97	9.25	2.30	13.88
1362	27.45	1.75	0.28	7.80	8.28	0.56	113.30
1437	26.91	2.70	0.06	8.74	8.77	0.33	19.23
1474	25.86	2.20	0.14	9.78	9.49	0.88	0.64
1499	27.51	1.35	0.42	5.41	7.98	2.69	143.09
1501	27.77	1.55	0.22	5.93	7.39	1.49	59.30
1503	26.68	1.25	0.22	9.99	8.87	0.26	31.53
1516	26.10	2.25	0.12	7.91	8.61	0.79	0.27
1519	26.00	2.05	0.14	9.88	9.40	0.78	36.47
1525	26.79	2.10	0.04	9.68	8.76	0.15	26.58
1528	27.17	2.50	0.08	9.78	8.87	0.26	46.41
1531	26.91	2.30	0.18	8.43	8.89	0.65	0.38
1535	25.30	2.50	0.10	9.88	9.69	1.08	26.33
1539	26.87	1.55	0.16	8.43	8.48	0.24	43.23
1556	26.67	2.50	0.18	10.20	9.43	0.82	66.73
1561	26.78	2.50	0.06	9.68	8.93	0.32	117.89
1592	27.10	2.75	0.10	9.68	9.02	0.41	19.87
1606	26.80	2.50	0.08	9.78	9.02	0.41	66.08
1610	26.39	2.20	0.16	9.99	9.36	0.75	55.92
1611	26.41	1.85	0.14	10.09	9.14	0.53	31.75
1621	24.88	1.30	0.14	9.05	9.36	0.80	6.24
1654	25.27	2.10	0.30	10.20	10.22	1.61	9.73
1662	26.19	2.40	0.02	8.43	8.65	0.40	0.72
1700	27.17	1.40	0.02	10.20	8.24	-0.38	15.95
1709	26.40	2.50	0.04	9.78	9.03	0.42	9.56
1734	27.50	2.70	0.02	9.99	8.56	-0.05	182.30
1747	27.05	2.45	0.06	8.53	8.54	0.22	0.34
1777	25.01	2.65	0.14	10.20	9.99	1.38	12.35
1903	26.74	2.65	0.46	6.14	9.04	2.92	0.32
2006	26.89	1.85	0.22	9.26	9.17	0.58	23.57
2060	27.76	2.90	0.10	8.74	8.65	0.21	3.69
2066	27.12	2.65	0.06	10.30	8.85	0.23	64.37
2073	27.80	2.05	0.00	9.78	8.20	-0.42	15.96
2079	26.98	2.45	0.14	10.09	9.14	0.53	8.89
2095	26.55	2.60	0.04	9.26	8.97	0.37	14.57

Table B.2: Best-fit parameters for Sawicki et al. (2007) HDF catalog, 500 Myr e-folding exponential SFR.

ID	$\mathcal{R}_{VI}$	$z_{phot}$	$E(B - V)$	$\log(\text{Age}/\text{yr})$	$\log(M_*/M_\odot)$	$\log(\text{SFR}/(M_\odot/\text{yr}))$	$\chi^2$
2106	25.88	2.50	0.06	9.99	9.31	0.70	5.88
2111	26.57	2.40	0.04	9.99	8.96	0.35	159.61
2169	27.89	2.70	0.10	6.76	7.21	0.46	31.43
2171	25.55	2.50	0.04	10.20	9.36	0.75	27.32
2188	27.32	2.20	0.00	10.09	8.45	-0.16	42.85
2206	26.56	2.50	0.04	10.20	8.97	0.36	91.41
2208	26.58	2.40	0.14	9.26	9.26	0.67	9.44
2221	27.94	1.70	0.14	7.39	7.35	0.01	0.09
2228	25.75	1.70	0.30	10.30	9.81	1.20	12.38
2255	27.25	1.40	0.18	10.30	8.69	0.08	106.91
2260	26.10	2.75	0.22	9.68	9.87	1.26	14.75
2282	24.63	2.50	0.08	9.47	9.87	1.27	8.23
2300	26.66	2.70	0.16	10.20	9.43	0.81	2.36
2306	25.42	2.50	0.16	9.78	9.84	1.23	3.70
2342	27.85	1.35	0.12	10.20	8.21	-0.40	36.25
2366	26.44	2.10	0.40	9.68	10.11	1.50	35.53
2404	27.76	2.00	0.14	8.95	8.57	0.04	6.32
2409	26.90	2.05	0.18	9.88	9.16	0.55	20.36
2490	27.03	2.40	0.04	9.99	8.78	0.17	121.66
2501	25.98	2.40	0.10	9.99	9.38	0.77	5.48
2560	26.37	1.95	0.16	9.26	9.24	0.64	1.68
2616	25.58	2.75	0.20	10.30	10.01	1.40	1.21
2625	26.65	2.30	0.12	8.32	8.72	0.55	0.40
2702	25.73	2.65	0.10	10.30	9.56	0.95	8.36
2710	25.05	2.40	0.12	9.99	9.84	1.22	21.88
2808	27.75	2.70	0.28	6.66	7.92	1.27	5.86
2832	26.69	2.65	0.12	10.30	9.23	0.62	75.51
2835	27.68	2.75	0.08	9.78	8.73	0.12	13.38
2848	27.80	2.05	0.00	10.20	8.20	-0.41	18.33
2849	25.59	2.50	0.16	9.78	9.77	1.16	20.95
2853	25.22	2.55	0.08	10.30	9.66	1.05	2.12
2876	25.81	2.40	0.00	10.09	9.10	0.49	15.30
2894	27.17	2.75	0.04	9.68	8.79	0.18	6.88
2967	26.80	1.55	0.20	9.88	8.99	0.38	19.56
3025	26.97	2.90	0.04	10.30	8.90	0.29	6.83
3036	27.56	2.70	0.02	9.99	8.54	-0.07	10.57
3042	27.21	1.25	0.24	6.87	7.39	0.54	10.66
3048	24.74	2.20	0.18	10.09	10.08	1.47	3.72
3083	25.65	1.95	0.16	10.09	9.55	0.94	8.79
3087	26.46	2.80	0.06	8.32	8.72	0.56	1.47
3111	24.61	2.35	0.06	9.78	9.77	1.16	3.93
3115	25.41	2.10	0.20	8.53	9.54	1.22	13.08
3134	25.09	2.35	0.18	9.78	9.99	1.38	9.11
3176	25.86	2.20	0.12	9.68	9.42	0.81	5.64
3189	26.24	2.00	0.06	9.78	8.99	0.38	44.95
3201	27.16	1.55	0.32	7.60	8.27	0.73	3.85
3250	27.14	2.70	0.02	8.32	8.28	0.11	0.68
3255	26.74	2.75	0.14	9.68	9.29	0.68	80.23
3256	26.90	2.05	0.36	6.56	8.29	1.74	0.21
3263	27.57	2.05	0.26	8.95	9.06	0.53	12.16
3264	23.66	2.30	0.20	8.84	10.50	2.01	7.56
3269	26.81	2.65	0.02	8.95	8.75	0.22	0.20
3373	24.31	2.15	0.18	8.43	9.88	1.64	2.74

Table B.3: Best-fit parameters for Sawicki et al. (2007) HDF catalog, 350 Myr e-folding exponential SFR.

ID	$\mathcal{R}_{VI}$	$z_{phot}$	$E(B - V)$	$\log(\text{Age}/\text{yr})$	$\log(M_*/M_\odot)$	$\log(\text{SFR}/(M_\odot/\text{yr}))$	$\chi^2$
3	24.08	2.90	0.38	6.24	9.85	3.62	39.80
12	25.14	2.90	0.16	8.53	9.76	1.50	0.79
60	26.55	2.10	0.24	9.78	9.38	0.91	29.63
88	26.28	2.90	0.26	5.31	8.57	3.42	64.82
96	26.99	2.40	0.14	10.20	9.00	0.53	48.42
97	27.58	2.50	0.02	9.88	8.36	-0.11	40.09
182	25.58	1.95	0.32	9.26	9.96	1.50	8.01
196	26.32	2.85	0.16	8.22	9.08	1.02	0.16
210	27.51	1.95	0.14	7.28	7.56	0.31	0.07
215	27.05	2.10	0.26	10.09	9.25	0.78	46.15
242	26.71	2.55	0.28	6.56	8.29	1.75	0.91
248	26.28	2.50	0.00	10.09	8.79	0.32	33.03
284	26.80	2.90	0.00	9.05	8.63	0.19	122.50
317	25.96	2.65	0.04	10.30	9.10	0.63	34.92
323	26.73	2.20	0.06	7.70	7.98	0.35	0.60
325	26.11	2.90	0.12	9.78	9.39	0.92	22.77
336	27.28	2.60	0.06	6.97	7.38	0.42	65.36
338	26.99	2.40	0.04	10.09	8.64	0.17	41.07
364	27.90	2.40	0.00	10.09	8.14	-0.33	88.58
390	27.14	2.75	0.06	9.99	8.74	0.27	3.99
411	27.56	1.50	0.10	8.53	8.03	-0.23	69.72
425	26.37	1.85	0.34	9.57	9.66	1.19	21.88
442	24.00	2.90	0.18	9.26	10.48	2.02	7.09
452	26.68	2.65	0.16	9.88	9.27	0.79	3.51
454	26.26	2.75	0.14	8.74	9.28	0.91	3.56
463	26.62	2.75	0.04	9.26	8.84	0.38	59.15
470	26.23	2.50	0.18	9.26	9.46	1.00	17.35
478	24.22	2.90	0.28	9.26	10.77	2.31	6.01
510	26.47	2.40	0.08	10.09	9.00	0.53	78.43
552	26.43	1.50	0.18	7.39	7.98	0.63	0.80
578	26.59	2.05	0.12	10.30	8.95	0.47	12.58
592	25.94	2.65	0.10	9.57	9.32	0.85	78.04
604	27.35	2.35	0.08	10.20	8.61	0.14	6.21
610	25.50	1.85	0.36	8.53	9.86	1.60	4.05
621	27.60	1.55	0.18	6.76	7.21	0.45	0.67
653	26.26	2.20	0.32	8.43	9.56	1.36	2.92
668	25.35	2.10	0.16	9.88	9.60	1.13	6.44
673	26.33	1.55	0.12	10.30	8.84	0.36	54.80
709	27.66	2.40	0.10	9.88	8.59	0.12	48.29
712	27.95	1.55	0.00	9.78	7.82	-0.65	17.15
751	26.75	1.55	0.08	10.30	8.54	0.07	28.21
762	25.92	1.85	0.34	9.57	9.83	1.36	8.14
766	27.48	1.55	0.30	6.66	7.60	0.96	2.51
789	26.76	2.50	0.06	9.57	8.83	0.36	42.48
790	25.23	1.60	0.62	10.09	10.78	2.31	4.91
797	25.27	2.60	0.10	10.20	9.59	1.12	13.37
801	27.91	1.40	0.00	9.57	7.76	-0.71	26.16
879	27.58	2.45	0.02	10.09	8.34	-0.13	21.67
880	27.40	2.60	0.00	7.28	7.29	0.05	73.71
891	27.94	1.30	0.06	9.68	7.87	-0.60	61.79
892	26.81	2.50	0.10	9.68	8.96	0.49	29.84
893	26.59	2.35	0.16	10.09	9.21	0.74	74.96
896	26.64	2.20	0.08	9.99	8.88	0.40	148.48
921	26.75	1.95	0.18	9.78	9.04	0.57	14.28
933	25.77	2.90	0.38	6.24	9.20	2.97	14.75
954	27.75	2.05	0.12	10.30	8.48	0.01	0.83
994	26.01	2.35	0.06	9.88	9.08	0.61	6.56

Table B.3: Best-fit parameters for Sawicki et al. (2007) HDF catalog, 350 Myr e-folding exponential SFR.

ID	$\mathcal{R}_{VI}$	$z_{phot}$	$E(B - V)$	$\log(\text{Age}/\text{yr})$	$\log(M_*/M_\odot)$	$\log(\text{SFR}/(M_\odot/\text{yr}))$	$\chi^2$
1006	27.62	2.20	0.08	9.68	8.45	-0.02	7.02
1007	27.81	2.70	0.10	7.80	7.90	0.19	11.48
1026	26.13	1.40	0.62	9.78	10.25	1.78	77.76
1048	26.33	2.75	0.16	9.68	9.43	0.96	18.79
1062	27.26	2.90	0.24	6.66	8.02	1.37	25.66
1073	25.75	2.80	0.04	8.32	8.90	0.77	4.03
1074	26.02	2.65	0.00	8.43	8.68	0.48	0.31
1083	26.87	2.20	0.18	9.99	9.11	0.64	26.37
1095	27.66	2.70	0.02	9.57	8.36	-0.11	42.36
1099	27.62	2.70	0.08	8.01	8.06	0.17	9.34
1106	27.77	2.50	0.00	10.09	8.20	-0.27	34.45
1112	27.73	2.40	0.12	9.57	8.64	0.17	128.80
1129	26.02	2.10	0.24	9.88	9.60	1.13	4.81
1131	26.50	2.70	0.02	10.20	8.82	0.34	51.93
1158	26.41	2.60	0.08	10.20	9.05	0.58	93.58
1190	27.37	2.20	0.10	9.78	8.65	0.17	82.93
1191	26.91	1.35	0.38	9.78	9.22	0.74	58.01
1226	27.67	2.20	0.08	9.68	8.45	-0.02	77.99
1236	26.47	1.45	0.40	6.76	8.25	1.50	7.80
1241	26.09	2.50	0.20	10.20	9.58	1.11	14.09
1264	26.44	2.50	0.04	9.88	8.88	0.41	69.39
1290	27.42	2.50	0.00	9.88	8.33	-0.14	97.52
1294	26.39	2.50	0.00	9.88	8.77	0.29	21.50
1295	26.12	1.60	0.34	10.09	9.61	1.14	27.84
1296	26.90	1.95	0.10	9.68	8.71	0.24	2.00
1328	26.75	2.50	0.00	10.09	8.61	0.14	123.19
1352	25.32	2.60	0.36	6.97	9.25	2.30	13.88
1362	27.45	2.65	0.16	9.16	8.94	0.49	86.42
1437	26.91	2.70	0.06	9.78	8.81	0.33	19.34
1474	25.86	2.20	0.16	10.20	9.43	0.96	2.85
1499	27.51	2.20	0.12	9.26	8.63	0.17	91.59
1501	27.77	1.55	0.22	5.62	7.39	1.84	59.27
1503	26.68	1.25	0.24	10.09	8.81	0.34	34.73
1516	26.10	2.30	0.12	7.91	8.62	0.81	0.23
1519	26.00	2.05	0.16	9.57	9.34	0.86	47.50
1525	26.79	2.10	0.04	10.09	8.63	0.16	32.63
1528	27.17	2.40	0.10	10.09	8.78	0.31	53.86
1531	26.91	2.30	0.18	8.53	8.91	0.65	0.31
1535	25.30	2.50	0.10	9.68	9.57	1.10	37.29
1539	26.87	1.55	0.18	8.32	8.45	0.32	43.27
1556	26.67	2.50	0.18	10.30	9.31	0.83	81.10
1561	26.78	2.50	0.08	9.57	8.88	0.41	128.73
1592	27.10	2.70	0.12	9.26	8.94	0.48	23.11
1606	26.80	2.50	0.08	10.20	8.90	0.42	76.95
1610	26.39	2.20	0.18	9.78	9.30	0.83	66.92
1611	26.41	1.60	0.16	10.20	8.95	0.47	40.73
1621	24.88	1.30	0.16	9.16	9.33	0.88	7.66
1654	25.27	2.05	0.32	9.88	10.14	1.66	12.93
1662	26.19	2.45	0.02	8.43	8.63	0.43	0.66
1700	27.17	1.35	0.04	10.20	8.14	-0.33	20.06
1709	26.40	2.50	0.06	9.57	8.97	0.50	13.48
1734	27.50	2.70	0.04	10.20	8.51	0.04	189.66
1747	27.05	2.45	0.06	8.64	8.55	0.23	0.32
1777	25.01	2.60	0.16	9.78	9.92	1.44	17.43
1903	26.74	2.65	0.46	6.14	9.04	2.92	0.31
2006	26.89	1.85	0.24	9.26	9.12	0.66	26.44
2060	27.76	2.90	0.10	9.26	8.67	0.22	3.62
2066	27.12	2.60	0.08	10.20	8.77	0.30	69.80
2073	27.80	1.95	0.00	9.99	8.03	-0.44	18.83
2079	26.98	2.40	0.16	10.09	9.06	0.59	9.54

Table B.3: Best-fit parameters for Sawicki et al. (2007) HDF catalog, 350 Myr e-folding exponential SFR.

ID	$\mathcal{R}_{VI}$	$z_{phot}$	$E(B - V)$	$\log(\text{Age}/\text{yr})$	$\log(M_*/M_\odot)$	$\log(\text{SFR}/(M_\odot/\text{yr}))$	$\chi^2$
2095	26.55	2.65	0.04	10.30	8.87	0.40	16.07
2106	25.88	2.50	0.08	10.20	9.25	0.78	11.04
2111	26.57	2.40	0.04	10.09	8.83	0.36	177.62
2169	27.89	2.70	0.10	6.76	7.21	0.46	31.42
2171	25.55	2.50	0.06	9.57	9.30	0.83	34.68
2188	27.32	2.10	0.02	9.68	8.36	-0.11	49.64
2206	26.56	2.50	0.04	9.88	8.84	0.37	104.71
2208	26.58	2.45	0.14	10.30	9.17	0.70	14.82
2221	27.94	1.80	0.14	7.39	7.40	0.05	0.09
2228	25.75	1.60	0.32	9.57	9.68	1.21	14.96
2255	27.25	1.35	0.20	9.68	8.59	0.12	118.37
2260	26.10	2.75	0.24	9.57	9.81	1.34	17.39
2282	24.63	2.50	0.08	10.20	9.75	1.28	14.71
2300	26.66	2.60	0.18	10.20	9.33	0.86	4.13
2306	25.42	2.50	0.18	9.26	9.77	1.32	6.64
2342	27.85	1.35	0.14	10.20	8.15	-0.32	40.27
2366	26.44	2.10	0.42	9.88	10.05	1.58	44.86
2404	27.76	2.00	0.14	9.78	8.52	0.05	7.74
2409	26.90	2.05	0.20	9.57	9.10	0.63	27.37
2490	27.03	2.35	0.06	9.88	8.70	0.23	139.30
2501	25.98	2.40	0.12	9.57	9.33	0.85	10.84
2560	26.37	1.95	0.18	9.26	9.18	0.73	4.43
2616	25.58	2.70	0.22	9.99	9.94	1.46	2.59
2625	26.65	2.25	0.12	8.43	8.73	0.53	0.68
2702	25.73	2.60	0.12	9.57	9.48	1.01	11.73
2710	25.05	2.35	0.14	9.68	9.76	1.29	30.31
2808	27.75	2.70	0.28	6.66	7.92	1.27	5.86
2832	26.69	2.65	0.12	10.09	9.10	0.63	85.34
2835	27.68	2.75	0.10	9.57	8.68	0.21	14.92
2848	27.80	2.05	0.00	9.99	8.07	-0.40	21.00
2849	25.59	2.50	0.18	9.78	9.71	1.24	29.41
2853	25.22	2.50	0.10	9.68	9.59	1.11	3.66
2876	25.81	2.40	0.02	10.30	9.05	0.58	22.70
2894	27.17	2.25	0.10	8.64	8.57	0.25	7.23
2967	26.80	1.55	0.22	9.57	8.93	0.46	23.95
3025	26.97	2.85	0.06	10.30	8.83	0.36	7.45
3036	27.56	2.65	0.04	9.88	8.47	0.00	12.90
3042	27.21	1.25	0.24	6.87	7.39	0.54	10.59
3048	24.74	2.20	0.20	10.30	10.03	1.55	6.37
3083	25.65	1.95	0.18	9.78	9.49	1.02	13.79
3087	26.46	2.80	0.06	8.43	8.76	0.56	1.38
3111	24.61	2.35	0.08	10.30	9.72	1.25	8.23
3115	25.41	2.10	0.20	8.64	9.55	1.23	13.04
3134	25.09	2.30	0.20	10.30	9.91	1.44	13.06
3176	25.86	2.20	0.14	10.20	9.37	0.89	6.64
3189	26.24	1.65	0.06	10.20	8.71	0.24	52.84
3201	27.16	1.55	0.32	7.60	8.27	0.73	3.94
3250	27.14	2.70	0.02	8.43	8.31	0.11	0.72
3255	26.74	2.75	0.14	9.57	9.16	0.69	84.70
3256	26.90	2.05	0.36	6.56	8.29	1.74	0.23
3263	27.57	2.05	0.26	10.09	9.01	0.54	13.19
3264	23.66	2.35	0.22	8.74	10.48	2.12	7.74
3269	26.81	2.65	0.02	9.99	8.70	0.23	0.67
3373	24.31	2.15	0.18	8.53	9.90	1.64	2.42

Table B.4: Best-fit parameters for Sawicki et al. (2007) HDF catalog, 250 Myr e-folding exponential SFR.

ID	$\mathcal{R}_{VI}$	$z_{phot}$	$E(B - V)$	$\log(\text{Age}/\text{yr})$	$\log(M_*/M_\odot)$	$\log(\text{SFR}/(M_\odot/\text{yr}))$	$\chi^2$
3	24.08	2.90	0.38	5.62	9.89	4.34	41.06
12	25.14	2.35	0.36	6.76	9.11	2.36	21.35
60	26.55	2.10	0.26	9.88	9.33	0.99	36.12
88	26.28	2.85	0.26	6.14	8.52	2.40	70.19
96	26.99	2.40	0.14	10.20	8.89	0.54	56.10
97	27.58	2.50	0.02	10.09	8.25	-0.10	44.44
182	25.58	1.60	0.06	10.30	nan	nan	nan
196	26.32	2.35	0.78	10.30	nan	nan	nan
210	27.51	1.95	0.14	7.28	7.55	0.31	0.07
215	27.05	2.25	0.30	10.30	nan	nan	nan
242	26.71	2.55	0.28	6.56	8.29	1.75	0.91
248	26.28	2.65	0.06	10.30	nan	nan	nan
284	26.80	2.90	0.00	10.20	8.54	0.20	123.16
317	25.96	2.65	0.04	9.68	8.99	0.64	40.56
323	26.73	2.15	0.08	7.49	7.88	0.45	0.69
325	26.11	2.50	0.62	10.30	nan	nan	nan
336	27.28	1.10	0.30	5.93	7.53	1.63	67.56
338	26.99	2.40	0.04	10.20	8.53	0.18	46.39
364	27.90	1.10	0.00	9.36	7.42	-0.90	92.58
390	27.14	2.40	0.04	10.30	nan	nan	nan
411	27.56	2.50	0.70	10.30	nan	nan	nan
425	26.37	1.75	0.36	9.78	9.55	1.20	29.82
442	24.00	2.85	0.20	8.95	10.39	2.09	8.78
452	26.68	2.25	0.22	10.30	nan	nan	nan
454	26.26	2.30	0.50	10.30	nan	nan	nan
463	26.62	2.75	0.04	9.57	8.73	0.39	61.67
470	26.23	2.15	0.34	10.30	nan	nan	nan
478	24.22	2.35	0.94	10.30	nan	nan	nan
510	26.47	2.40	0.08	9.57	8.89	0.54	90.29
552	26.43	2.60	0.60	10.30	nan	nan	nan
578	26.59	2.35	0.78	10.30	nan	nan	nan
592	25.94	2.65	0.10	9.88	9.21	0.86	88.50
604	27.35	2.20	0.10	9.78	8.52	0.17	9.03
610	25.50	1.55	0.82	10.30	nan	nan	nan
621	27.60	1.55	0.18	6.76	7.21	0.46	0.67
653	26.26	2.15	0.98	10.30	nan	nan	nan
668	25.35	2.10	0.18	10.09	9.55	1.21	11.24
673	26.33	1.55	0.14	9.68	8.79	0.44	64.82
709	27.66	2.40	0.12	9.57	8.55	0.20	54.93
712	27.95	1.55	0.02	9.88	7.77	-0.57	21.05
751	26.75	1.55	0.10	10.20	8.50	0.15	33.43
762	25.92	2.10	0.36	9.57	9.94	1.59	19.10
766	27.48	2.30	0.78	10.30	nan	nan	nan
789	26.76	2.35	0.40	10.30	nan	nan	nan
790	25.23	1.50	0.64	9.68	10.64	2.29	6.47
797	25.27	2.50	0.12	9.88	9.51	1.16	17.91
801	27.91	2.15	0.24	10.30	nan	nan	nan
879	27.58	2.45	0.02	10.09	8.22	-0.12	23.50
880	27.40	2.60	0.00	7.28	7.29	0.05	73.77
891	27.94	1.30	0.08	9.68	7.82	-0.53	68.48
892	26.81	2.45	0.12	10.20	8.90	0.55	37.81
893	26.59	2.45	0.08	10.30	nan	nan	nan
896	26.64	2.55	0.14	10.30	nan	nan	nan
921	26.75	1.85	0.20	9.57	8.94	0.60	17.36
933	25.77	2.15	0.84	10.30	nan	nan	nan
954	27.75	1.95	0.14	9.68	8.39	0.04	1.92
994	26.01	2.20	0.08	9.68	8.99	0.64	10.98

Table B.4: Best-fit parameters for Sawicki et al. (2007) HDF catalog, 250 Myr e-folding exponential SFR.

ID	$\mathcal{R}_{VI}$	$z_{phot}$	$E(B - V)$	$\log(\text{Age}/\text{yr})$	$\log(M_*/M_\odot)$	$\log(\text{SFR}/(M_\odot/\text{yr}))$	$\chi^2$
1006	27.62	1.15	0.20	7.60	7.45	-0.07	8.67
1007	27.81	2.65	0.14	7.18	7.60	0.45	11.55
1026	26.13	1.40	0.64	9.99	10.20	1.86	85.72
1048	26.33	2.70	0.18	10.20	9.37	1.02	22.98
1062	27.26	2.60	0.66	10.30	nan	nan	nan
1073	25.75	2.80	0.04	8.43	8.92	0.78	3.97
1074	26.02	2.70	0.00	8.53	8.70	0.50	0.29
1083	26.87	2.30	0.80	10.30	nan	nan	nan
1095	27.66	2.70	0.02	9.68	8.24	-0.10	43.50
1099	27.62	2.80	0.04	9.78	8.36	0.01	9.77
1106	27.77	2.50	0.00	10.20	8.09	-0.26	36.46
1112	27.73	2.30	0.12	10.09	8.49	0.14	136.96
1129	26.02	2.05	0.26	10.20	9.53	1.18	8.79
1131	26.50	2.15	0.38	10.30	nan	nan	nan
1158	26.41	2.60	0.08	10.09	8.94	0.59	103.49
1190	27.37	2.10	0.12	10.20	8.56	0.21	90.09
1191	26.91	1.35	0.42	9.57	9.22	0.87	65.02
1226	27.67	2.35	0.72	10.30	nan	nan	nan
1236	26.47	1.45	0.40	6.76	8.25	1.50	7.90
1241	26.09	2.50	0.22	9.26	9.52	1.20	18.80
1264	26.44	2.35	0.56	10.30	nan	nan	nan
1290	27.42	2.50	0.00	9.57	8.22	-0.13	100.18
1294	26.39	2.45	0.02	10.09	8.71	0.36	29.11
1295	26.12	1.55	0.36	10.20	9.52	1.18	34.97
1296	26.90	1.95	0.12	9.68	8.67	0.32	4.24
1328	26.75	2.35	0.10	10.30	nan	nan	nan
1352	25.32	2.60	0.36	6.97	9.25	2.30	13.80
1362	27.45	2.70	0.16	9.16	8.84	0.52	90.03
1437	26.91	2.65	0.08	9.26	8.74	0.41	20.49
1474	25.86	2.20	0.18	9.88	9.39	1.04	7.05
1499	27.51	1.60	0.40	5.72	8.08	2.41	143.55
1501	27.77	2.40	0.12	5.41	7.35	2.06	60.20
1503	26.68	1.25	0.26	9.88	8.76	0.41	38.21
1516	26.10	2.30	0.12	7.91	8.61	0.82	0.24
1519	26.00	2.05	0.18	9.99	9.29	0.94	58.38
1525	26.79	2.05	0.06	9.68	8.57	0.22	37.53
1528	27.17	2.40	0.38	10.30	nan	nan	nan
1531	26.91	2.30	0.18	8.84	8.95	0.66	0.33
1535	25.30	2.40	0.12	9.57	9.48	1.14	47.29
1539	26.87	2.10	0.16	10.30	nan	nan	nan
1556	26.67	2.50	0.20	9.57	9.26	0.91	95.75
1561	26.78	2.50	0.08	10.20	8.76	0.42	137.75
1592	27.10	2.70	0.12	9.88	8.84	0.49	25.15
1606	26.80	2.50	0.90	10.30	nan	nan	nan
1610	26.39	2.20	0.20	10.09	9.26	0.91	78.36
1611	26.41	2.50	0.14	10.30	nan	nan	nan
1621	24.88	1.30	0.18	9.88	9.29	0.95	9.71
1654	25.27	1.85	0.34	9.78	9.97	1.62	21.87
1662	26.19	2.45	0.02	8.64	8.67	0.44	0.75
1700	27.17	1.35	0.06	10.09	8.09	-0.25	23.98
1709	26.40	2.35	0.62	10.30	nan	nan	nan
1734	27.50	2.70	0.04	10.20	8.39	0.04	196.39
1747	27.05	2.45	0.06	10.20	8.58	0.23	0.33
1777	25.01	2.40	0.18	10.30	nan	nan	nan
1903	26.74	2.75	0.42	6.56	8.87	2.32	0.46
2006	26.89	1.80	0.26	9.36	9.04	0.72	30.15
2060	27.76	2.85	0.12	9.05	8.60	0.29	3.68
2066	27.12	2.50	0.10	9.68	8.70	0.35	74.83
2073	27.80	2.35	0.46	10.30	nan	nan	nan
2079	26.98	2.45	0.82	10.30	nan	nan	nan

Table B.4: Best-fit parameters for Sawicki et al. (2007) HDF catalog, 250 Myr e-folding exponential SFR.

ID	$\mathcal{R}_{VI}$	$z_{phot}$	$E(B - V)$	$\log(\text{Age}/\text{yr})$	$\log(M_*/M_\odot)$	$\log(\text{SFR}/(M_\odot/\text{yr}))$	$\chi^2$
2095	26.55	2.55	0.06	9.99	8.80	0.45	17.20
2106	25.88	2.50	0.08	10.09	9.14	0.79	18.82
2111	26.57	2.40	0.06	10.09	8.79	0.44	195.34
2169	27.89	2.40	0.48	10.30	nan	nan	nan
2171	25.55	2.50	0.08	10.09	9.26	0.91	44.61
2188	27.32	2.25	0.34	10.30	nan	nan	nan
2206	26.56	2.40	0.70	10.30	nan	nan	nan
2208	26.58	2.50	0.52	10.30	nan	nan	nan
2221	27.94	1.90	0.12	7.60	7.51	-0.01	0.10
2228	25.75	1.60	0.34	9.99	9.64	1.29	17.48
2255	27.25	1.35	0.22	9.57	8.54	0.19	127.74
2260	26.10	2.70	0.26	9.57	9.75	1.40	22.89
2282	24.63	2.50	0.10	10.20	9.71	1.36	20.16
2300	26.66	2.55	0.20	10.09	9.27	0.92	7.26
2306	25.42	2.30	0.24	10.30	nan	nan	nan
2342	27.85	1.35	0.16	9.99	8.10	-0.25	44.03
2366	26.44	2.05	0.44	10.09	9.97	1.62	54.47
2404	27.76	1.65	0.16	10.09	8.30	-0.04	8.46
2409	26.90	1.95	0.22	9.68	9.01	0.66	34.14
2490	27.03	2.20	0.06	9.57	8.54	0.19	155.16
2501	25.98	2.40	0.12	9.57	9.22	0.87	17.65
2560	26.37	2.45	0.16	10.30	nan	nan	nan
2616	25.58	2.70	0.24	9.36	9.88	1.56	5.31
2625	26.65	2.25	0.14	8.22	8.65	0.63	0.56
2702	25.73	2.50	0.14	9.99	9.40	1.05	16.01
2710	25.05	2.30	0.16	10.20	9.69	1.35	40.78
2808	27.75	2.70	0.28	6.66	7.92	1.27	5.79
2832	26.69	2.65	0.14	10.20	9.06	0.71	94.92
2835	27.68	2.45	0.88	10.30	nan	nan	nan
2848	27.80	2.35	0.74	10.30	nan	nan	nan
2849	25.59	2.50	0.18	9.78	9.60	1.25	36.90
2853	25.22	2.50	0.12	9.88	9.54	1.20	8.16
2876	25.81	2.20	0.04	9.99	8.94	0.59	31.07
2894	27.17	2.25	0.10	9.88	8.60	0.25	7.29
2967	26.80	1.55	0.24	9.78	8.88	0.53	28.53
3025	26.97	2.85	0.08	9.68	8.79	0.45	9.57
3036	27.56	2.35	0.88	10.30	nan	nan	nan
3042	27.21	1.25	0.26	6.76	7.43	0.68	12.05
3048	24.74	2.25	0.22	9.68	10.01	1.66	12.62

Table B.5: Best-fit parameters for Sawicki et al. (2007) HDF catalog,  $-700$  Myr e-folding exponential SFR.

ID	$\mathcal{R}_{VI}$	$z_{phot}$	$E(B - V)$	$\log(\text{Age}/\text{yr})$	$\log(M_*/M_\odot)$	$\log(\text{SFR}/(M_\odot/\text{yr}))$	$\chi^2$
3	24.08	2.90	$0.38^{+0.00}_{-0.00}$	$6.24^{+0.21}_{-0.10}$	$9.85^{+0.01}_{-0.03}$	$3.62^{+0.12}_{-0.25}$	39.80
12	25.14	2.90	$0.16^{+0.02}_{-0.06}$	$8.22^{+0.42}_{-0.21}$	$9.67^{+0.19}_{-0.13}$	$1.47^{+0.10}_{-0.24}$	0.65
60	26.55	2.25	$0.14^{+0.02}_{-0.04}$	$8.84^{+0.10}_{-0.10}$	$9.52^{+0.09}_{-0.08}$	$0.54^{+0.08}_{-0.15}$	14.71
88	26.28	2.90	$0.26^{+0.16}_{-0.00}$	$5.52^{+0.42}_{-2.50}$	$8.57^{+0.39}_{-0.18}$	$3.14^{+2.38}_{-0.63}$	64.82
96	26.99	2.60	$0.00^{+0.00}_{-0.00}$	$9.05^{+0.00}_{-0.00}$	$9.33^{+0.04}_{-0.04}$	$-0.01^{+0.04}_{-0.04}$	5.86
97	27.58	2.50	$0.00^{+0.00}_{-0.00}$	$8.64^{+0.00}_{-0.00}$	$8.44^{+0.00}_{-0.00}$	$-0.25^{+0.00}_{-0.00}$	35.36
182	25.58	2.05	$0.24^{+0.04}_{-0.02}$	$8.74^{+0.10}_{-0.10}$	$10.03^{+0.15}_{-0.06}$	$1.20^{+0.20}_{-0.14}$	0.74
196	26.32	2.85	$0.16^{+0.06}_{-0.08}$	$8.12^{+0.83}_{-0.42}$	$9.09^{+0.41}_{-0.21}$	$1.00^{+0.26}_{-0.42}$	0.37
210	27.51	1.90	$0.14^{+0.14}_{-0.18}$	$7.28^{+2.18}_{-0.94}$	$7.54^{+0.39}_{-0.58}$	$0.28^{+0.42}_{-2.71}$	0.04
215	27.05	2.30	$0.12^{+0.08}_{-0.02}$	$8.95^{+0.00}_{-0.31}$	$9.44^{+0.05}_{-0.57}$	$0.29^{+0.11}_{-0.11}$	11.04
242	26.71	2.55	$0.28^{+0.10}_{-0.06}$	$6.56^{+1.46}_{-0.42}$	$8.29^{+0.21}_{-0.26}$	$1.74^{+0.59}_{-2.01}$	0.91
248	26.28	2.50	$0.00^{+0.00}_{-0.00}$	$8.43^{+0.10}_{-0.00}$	$8.71^{+0.10}_{-0.03}$	$0.28^{+0.00}_{-0.03}$	35.85
284	26.80	2.80	$0.00^{+0.04}_{-0.00}$	$8.43^{+0.22}_{-0.10}$	$8.55^{+0.26}_{-0.19}$	$0.12^{+0.03}_{-0.19}$	122.92
317	25.96	2.70	$0.00^{+0.00}_{-0.00}$	$8.64^{+0.00}_{-0.10}$	$9.12^{+0.03}_{-0.13}$	$0.44^{+0.03}_{-0.02}$	25.75
323	26.73	2.20	$0.06^{+0.06}_{-0.10}$	$7.60^{+0.83}_{-0.52}$	$7.92^{+0.65}_{-0.32}$	$0.36^{+0.29}_{-0.57}$	0.61
325	26.11	2.90	$0.10^{+0.00}_{-0.02}$	$8.53^{+0.21}_{-0.00}$	$9.35^{+0.14}_{-0.00}$	$0.79^{+0.00}_{-0.10}$	21.96
336	27.28	1.10	$0.30^{+0.30}_{-0.68}$	$5.72^{+0.62}_{-4.58}$	$7.53^{+inf}_{-1.20}$	$1.86^{+inf}_{-0.27}$	67.54
338	26.99	2.50	$0.00^{+0.00}_{-0.00}$	$8.74^{+0.00}_{-0.10}$	$8.82^{+0.03}_{-0.06}$	$-0.01^{+0.03}_{-0.00}$	27.87
364	27.90	2.40	$0.00^{+0.00}_{-0.00}$	$8.84^{+0.10}_{-0.00}$	$8.58^{+0.16}_{-0.08}$	$-0.40^{+0.02}_{-0.03}$	78.14
390	27.14	2.85	$0.00^{+0.00}_{-0.06}$	$8.74^{+0.21}_{-0.10}$	$8.84^{+0.21}_{-0.14}$	$0.01^{+0.20}_{-0.20}$	1.41
411	27.56	1.45	$0.08^{+0.08}_{-0.18}$	$8.32^{+1.46}_{-0.31}$	$7.95^{+0.24}_{-0.23}$	$-0.37^{+0.24}_{-0.96}$	69.63
425	26.37	1.95	$0.24^{+0.04}_{-0.00}$	$8.84^{+0.00}_{-0.10}$	$9.80^{+0.06}_{-0.14}$	$0.82^{+0.21}_{-0.09}$	1.69
442	24.00	2.90	$0.14^{+0.00}_{-0.02}$	$8.64^{+0.21}_{-0.00}$	$10.49^{+0.15}_{-0.00}$	$1.81^{+0.00}_{-0.10}$	6.19
452	26.68	2.80	$0.10^{+0.06}_{-0.04}$	$8.74^{+0.21}_{-0.21}$	$9.39^{+0.20}_{-0.19}$	$0.56^{+0.20}_{-0.33}$	1.01
454	26.26	2.80	$0.10^{+0.06}_{-0.06}$	$8.53^{+0.42}_{-0.42}$	$9.29^{+0.25}_{-0.21}$	$0.73^{+0.21}_{-0.28}$	3.56
463	26.62	2.75	$0.00^{+0.00}_{-0.00}$	$8.64^{+0.10}_{-0.00}$	$8.85^{+0.02}_{-0.02}$	$0.16^{+0.00}_{-0.02}$	51.49
470	26.23	2.70	$0.08^{+0.04}_{-0.02}$	$8.84^{+0.10}_{-0.21}$	$9.61^{+0.13}_{-0.25}$	$0.63^{+0.13}_{-0.08}$	0.63
478	24.22	2.90	$0.26^{+0.02}_{-0.02}$	$8.43^{+0.10}_{-0.21}$	$10.63^{+0.06}_{-0.15}$	$2.19^{+0.10}_{-0.06}$	5.31
510	26.47	2.50	$0.00^{+0.00}_{-0.00}$	$8.84^{+0.00}_{-0.00}$	$9.17^{+0.00}_{-0.00}$	$0.19^{+0.00}_{-0.00}$	24.43
552	26.43	1.50	$0.18^{+0.08}_{-0.06}$	$7.39^{+0.42}_{-0.62}$	$7.98^{+0.25}_{-0.48}$	$0.62^{+0.37}_{-0.33}$	0.83
578	26.59	2.25	$0.02^{+0.02}_{-0.04}$	$8.84^{+0.10}_{-0.10}$	$9.10^{+0.13}_{-0.09}$	$0.12^{+0.08}_{-0.03}$	3.38
592	25.94	2.80	$0.00^{+0.00}_{-0.00}$	$8.95^{+0.00}_{-0.00}$	$9.59^{+0.02}_{-0.00}$	$0.44^{+0.00}_{-0.00}$	40.61
604	27.35	2.60	$0.00^{+0.00}_{-0.04}$	$8.74^{+0.10}_{-0.10}$	$8.69^{+0.09}_{-0.18}$	$-0.14^{+0.03}_{-0.11}$	0.97
610	25.50	1.85	$0.38^{+0.06}_{-0.10}$	$8.12^{+0.73}_{-0.31}$	$9.75^{+0.77}_{-0.24}$	$1.65^{+0.36}_{-0.17}$	5.64
621	27.60	1.55	$0.18^{+0.08}_{-0.12}$	$6.76^{+1.66}_{-0.42}$	$7.21^{+0.16}_{-0.47}$	$0.45^{+0.35}_{-2.42}$	0.69
653	26.26	2.20	$0.30^{+0.04}_{-0.06}$	$8.32^{+0.42}_{-0.21}$	$9.56^{+0.22}_{-0.16}$	$1.24^{+0.17}_{-0.28}$	3.14
668	25.35	2.25	$0.08^{+0.02}_{-0.04}$	$8.74^{+0.10}_{-0.10}$	$9.67^{+0.10}_{-0.07}$	$0.84^{+0.08}_{-0.07}$	1.62
673	26.33	2.00	$0.00^{+0.00}_{-0.00}$	$8.95^{+0.00}_{-0.00}$	$9.23^{+0.04}_{-0.00}$	$0.08^{+0.04}_{-0.00}$	8.80
709	27.66	2.50	$0.00^{+0.00}_{-0.00}$	$8.95^{+0.00}_{-0.00}$	$8.85^{+0.00}_{-0.02}$	$-0.30^{+0.00}_{-0.02}$	20.74
712	27.95	2.00	$0.00^{+0.00}_{-0.00}$	$8.64^{+0.21}_{-0.00}$	$8.16^{+0.42}_{-0.02}$	$-0.53^{+0.18}_{-0.03}$	18.25
751	26.75	2.05	$0.00^{+0.00}_{-0.00}$	$8.95^{+0.10}_{-0.00}$	$9.08^{+0.18}_{-0.02}$	$-0.07^{+0.02}_{-0.02}$	5.88
762	25.92	1.95	$0.26^{+0.02}_{-0.04}$	$8.74^{+0.10}_{-0.10}$	$9.90^{+0.09}_{-0.13}$	$1.07^{+0.11}_{-0.20}$	3.15
766	27.48	1.55	$0.30^{+0.10}_{-0.08}$	$6.66^{+1.56}_{-0.52}$	$7.60^{+0.22}_{-0.42}$	$0.95^{+0.51}_{-2.27}$	2.50
789	26.76	2.50	$0.00^{+0.00}_{-0.00}$	$8.74^{+0.06}_{-0.00}$	$8.89^{+0.00}_{-0.05}$	$0.07^{+0.00}_{-0.05}$	22.62
790	25.23	1.60	$0.62^{+0.08}_{-0.02}$	$8.43^{+0.10}_{-0.31}$	$10.70^{+0.20}_{-0.28}$	$2.26^{+0.28}_{-0.22}$	6.11
797	25.27	2.70	$0.04^{+0.04}_{-0.02}$	$8.74^{+0.10}_{-0.21}$	$9.69^{+0.09}_{-0.23}$	$0.86^{+0.13}_{-0.08}$	3.82
801	27.91	1.45	$0.00^{+0.00}_{-0.00}$	$8.53^{+0.00}_{-0.10}$	$7.82^{+0.03}_{-0.17}$	$-0.74^{+0.03}_{-0.05}$	25.78
879	27.58	2.50	$0.00^{+0.00}_{-0.00}$	$8.64^{+0.10}_{-0.00}$	$8.44^{+0.16}_{-0.00}$	$-0.25^{+0.03}_{-0.01}$	19.78
880	27.40	2.60	$0.00^{+0.00}_{-0.02}$	$7.18^{+0.42}_{-0.31}$	$7.23^{+0.19}_{-0.20}$	$0.07^{+0.10}_{-0.26}$	73.49
891	27.94	1.35	$0.00^{+0.00}_{-0.00}$	$8.74^{+0.00}_{-0.00}$	$7.98^{+0.00}_{-0.00}$	$-0.85^{+0.00}_{-0.03}$	47.42
892	26.81	2.65	$0.00^{+0.00}_{-0.04}$	$8.95^{+0.11}_{-0.00}$	$9.23^{+0.20}_{-0.03}$	$0.08^{+0.05}_{-0.12}$	8.13
893	26.59	2.65	$0.00^{+0.00}_{-0.02}$	$9.16^{+0.10}_{-0.00}$	$9.72^{+0.18}_{-0.02}$	$0.17^{+0.02}_{-0.05}$	2.98
896	26.64	2.50	$0.00^{+0.00}_{-0.00}$	$8.95^{+0.00}_{-0.00}$	$9.28^{+0.02}_{-0.00}$	$0.13^{+0.02}_{-0.00}$	65.71
921	26.75	2.15	$0.10^{+0.02}_{-0.06}$	$8.74^{+0.21}_{-0.10}$	$9.14^{+0.25}_{-0.09}$	$0.31^{+0.14}_{-0.20}$	12.39
933	25.77	2.90	$0.38^{+0.00}_{-0.00}$	$6.24^{+1.14}_{-0.10}$	$9.20^{+0.01}_{-0.04}$	$2.97^{+0.12}_{-1.47}$	14.75
954	27.75	2.05	$0.10^{+0.08}_{-0.04}$	$8.53^{+0.31}_{-0.31}$	$8.44^{+0.31}_{-0.25}$	$-0.12^{+0.21}_{-0.19}$	0.79
994	26.01	2.40	$0.02^{+0.02}_{-0.02}$	$8.64^{+0.10}_{-0.10}$	$9.11^{+0.06}_{-0.11}$	$0.42^{+0.12}_{-0.08}$	0.89

Table B.5: Best-fit parameters for Sawicki et al. (2007) HDF catalog, -700 Myr e-folding exponential SFR.

ID	$\mathcal{R}_{VI}$	$z_{phot}$	$E(B - V)$	$\log(\text{Age}/\text{yr})$	$\log(M_*/M_\odot)$	$\log(\text{SFR}/(M_\odot/\text{yr}))$	$\chi^2$
1006	27.62	2.45	$0.02^{+0.02}_{-0.18}$	$8.74^{+1.25}_{-0.10}$	$8.61^{+1.25}_{-0.12}$	$-0.22^{+0.13}_{-0.21}$	5.29
1007	27.81	2.70	$0.10^{+0.10}_{-0.18}$	$7.80^{+2.70}_{-0.83}$	$7.94^{+0.55}_{-0.50}$	$0.16^{+0.43}_{-0.43}$	11.48
1026	26.13	1.50	$0.18^{+0.02}_{-0.02}$	$9.36^{+0.00}_{-0.10}$	$10.44^{+0.10}_{-0.05}$	$0.30^{+0.05}_{-0.05}$	14.58
1048	26.33	2.90	$0.06^{+0.00}_{-0.00}$	$8.95^{+0.10}_{-0.00}$	$9.70^{+0.16}_{-0.16}$	$0.56^{+0.00}_{-0.09}$	7.57
1062	27.26	2.90	$0.24^{+0.04}_{-0.08}$	$6.66^{+1.56}_{-0.42}$	$8.02^{+0.05}_{-0.39}$	$1.37^{+0.39}_{-2.24}$	25.71
1073	25.75	2.80	$0.04^{+0.04}_{-0.04}$	$8.12^{+0.31}_{-0.31}$	$8.85^{+0.17}_{-0.19}$	$0.75^{+0.19}_{-0.18}$	4.42
1074	26.02	2.60	$0.00^{+0.00}_{-0.06}$	$8.22^{+0.42}_{-0.00}$	$8.64^{+0.27}_{-0.04}$	$0.43^{+0.05}_{-0.26}$	0.41
1083	26.87	2.40	$0.10^{+0.06}_{-0.00}$	$8.84^{+0.00}_{-0.21}$	$9.33^{+0.05}_{-0.20}$	$0.35^{+0.16}_{-0.04}$	4.22
1095	27.66	2.70	$0.00^{+0.00}_{-0.06}$	$8.53^{+0.10}_{-0.10}$	$8.32^{+0.13}_{-0.12}$	$-0.24^{+0.11}_{-0.02}$	40.67
1099	27.62	2.70	$0.06^{+0.06}_{-0.12}$	$8.12^{+1.35}_{-0.52}$	$8.14^{+0.66}_{-0.36}$	$0.04^{+0.25}_{-0.76}$	9.36
1106	27.77	2.50	$0.00^{+0.00}_{-0.00}$	$8.53^{+0.21}_{-0.00}$	$8.24^{+0.24}_{-0.00}$	$-0.32^{+0.03}_{-0.02}$	36.62
1112	27.73	2.50	$0.00^{+0.00}_{-0.00}$	$9.16^{+0.00}_{-0.00}$	$9.23^{+0.00}_{-0.00}$	$-0.33^{+0.00}_{-0.00}$	64.61
1129	26.02	2.20	$0.18^{+0.02}_{-0.04}$	$8.64^{+0.10}_{-0.10}$	$9.59^{+0.10}_{-0.12}$	$0.90^{+0.13}_{-0.11}$	1.82
1131	26.50	2.70	$0.00^{+0.00}_{-0.00}$	$8.53^{+0.00}_{-0.00}$	$8.78^{+0.02}_{-0.02}$	$0.22^{+0.02}_{-0.02}$	47.62
1158	26.41	2.70	$0.00^{+0.00}_{-0.00}$	$8.84^{+0.00}_{-0.00}$	$9.22^{+0.00}_{-0.00}$	$0.24^{+0.00}_{-0.00}$	49.46
1190	27.37	2.50	$0.00^{+0.00}_{-0.00}$	$9.05^{+0.10}_{-0.00}$	$9.16^{+0.20}_{-0.00}$	$-0.18^{+0.02}_{-0.02}$	36.46
1191	26.91	1.35	$0.12^{+0.08}_{-0.06}$	$9.16^{+0.10}_{-0.10}$	$9.34^{+0.05}_{-0.04}$	$-0.22^{+0.31}_{-0.21}$	12.92
1226	27.67	2.50	$0.00^{+0.00}_{-0.00}$	$8.95^{+0.00}_{-0.00}$	$8.86^{+0.05}_{-0.00}$	$-0.29^{+0.05}_{-0.00}$	40.02
1236	26.47	1.45	$0.40^{+0.02}_{-0.04}$	$6.76^{+0.10}_{-0.10}$	$8.25^{+0.11}_{-0.15}$	$1.49^{+0.22}_{-0.25}$	7.74
1241	26.09	2.70	$0.12^{+0.06}_{-0.02}$	$8.74^{+0.10}_{-0.31}$	$9.66^{+0.10}_{-0.34}$	$0.83^{+0.17}_{-0.11}$	4.44
1264	26.44	2.50	$0.00^{+0.00}_{-0.00}$	$8.74^{+0.00}_{-0.00}$	$9.02^{+0.00}_{-0.05}$	$0.19^{+0.00}_{-0.05}$	44.09
1290	27.42	2.50	$0.00^{+0.00}_{-0.00}$	$8.53^{+0.00}_{-0.10}$	$8.37^{+0.05}_{-0.12}$	$-0.19^{+0.05}_{-0.01}$	99.67
1294	26.39	2.50	$0.00^{+0.00}_{-0.00}$	$8.43^{+0.00}_{-0.00}$	$8.69^{+0.03}_{-0.00}$	$0.25^{+0.03}_{-0.00}$	25.24
1295	26.12	1.80	$0.20^{+0.04}_{-0.04}$	$8.95^{+0.10}_{-0.10}$	$9.85^{+0.06}_{-0.07}$	$0.70^{+0.21}_{-0.17}$	1.06
1296	26.90	2.05	$0.08^{+0.06}_{-0.02}$	$8.53^{+0.10}_{-0.21}$	$8.72^{+0.18}_{-0.19}$	$0.16^{+0.27}_{-0.10}$	1.75
1328	26.75	2.50	$0.00^{+0.00}_{-0.00}$	$8.53^{+0.10}_{-0.00}$	$8.64^{+0.11}_{-0.00}$	$0.09^{+0.00}_{-0.01}$	128.10
1352	25.32	2.60	$0.36^{+0.04}_{-0.06}$	$6.97^{+0.31}_{-0.52}$	$9.25^{+0.05}_{-0.25}$	$2.29^{+0.28}_{-0.40}$	13.81
1362	27.45	2.90	$0.02^{+0.00}_{-0.00}$	$9.05^{+0.11}_{-0.09}$	$9.30^{+0.25}_{-0.22}$	$-0.04^{+0.00}_{-0.02}$	75.31
1437	26.91	2.75	$0.02^{+0.02}_{-0.06}$	$8.64^{+0.42}_{-0.10}$	$8.83^{+0.25}_{-0.13}$	$0.14^{+0.09}_{-0.24}$	18.69
1474	25.86	2.30	$0.10^{+0.02}_{-0.04}$	$8.64^{+0.10}_{-0.10}$	$9.42^{+0.08}_{-0.10}$	$0.73^{+0.13}_{-0.15}$	1.14
1499	27.51	1.35	$0.42^{+0.42}_{-0.56}$	$6.04^{+0.94}_{-4.26}$	$7.97^{+inf}_{-0.27}$	$1.96^{+inf}_{-0.35}$	143.24
1501	27.77	1.75	$0.08^{+0.08}_{-0.90}$	$7.18^{+2.08}_{-3.12}$	$7.12^{+inf}_{-0.16}$	$-0.05^{+0.17}_{-0.17}$	57.46
1503	26.68	1.20	$0.08^{+0.06}_{-0.04}$	$8.95^{+0.10}_{-0.10}$	$8.83^{+0.05}_{-0.04}$	$-0.32^{+0.24}_{-0.18}$	17.13
1516	26.10	2.35	$0.10^{+0.06}_{-0.10}$	$8.01^{+0.94}_{-0.31}$	$8.70^{+0.54}_{-0.21}$	$0.71^{+0.19}_{-0.48}$	0.30
1519	26.00	2.15	$0.00^{+0.00}_{-0.00}$	$9.05^{+0.00}_{-0.00}$	$9.58^{+0.06}_{-0.04}$	$0.24^{+0.04}_{-0.17}$	1.77
1525	26.79	2.20	$0.00^{+0.00}_{-0.00}$	$8.74^{+0.00}_{-0.10}$	$8.81^{+0.12}_{-0.21}$	$-0.02^{+0.07}_{-0.07}$	17.29
1528	27.17	2.60	$0.00^{+0.00}_{-0.00}$	$8.95^{+0.00}_{-0.00}$	$9.07^{+0.04}_{-0.03}$	$-0.08^{+0.04}_{-0.03}$	18.81
1531	26.91	2.30	$0.18^{+0.06}_{-0.06}$	$8.22^{+0.31}_{-0.31}$	$8.83^{+0.18}_{-0.20}$	$0.63^{+0.19}_{-0.17}$	0.98
1535	25.30	2.60	$0.00^{+0.00}_{-0.00}$	$8.95^{+0.10}_{-0.00}$	$9.82^{+0.12}_{-0.02}$	$0.67^{+0.04}_{-0.05}$	1.10
1539	26.87	1.55	$0.16^{+0.04}_{-0.04}$	$8.22^{+0.21}_{-0.21}$	$8.42^{+0.12}_{-0.13}$	$0.22^{+0.23}_{-0.16}$	43.78
1556	26.67	2.75	$0.02^{+0.02}_{-0.02}$	$9.16^{+0.00}_{-0.00}$	$9.79^{+0.02}_{-0.02}$	$0.23^{+0.05}_{-0.07}$	2.67
1592	27.10	2.90	$0.02^{+0.02}_{-0.02}$	$8.84^{+0.10}_{-0.10}$	$9.08^{+0.08}_{-0.16}$	$0.10^{+0.06}_{-0.06}$	14.24
1606	26.80	2.50	$0.00^{+0.00}_{-0.00}$	$8.95^{+0.00}_{-0.00}$	$9.19^{+0.00}_{-0.03}$	$0.04^{+0.00}_{-0.03}$	27.28
1610	26.39	2.65	$0.02^{+0.02}_{-0.02}$	$9.16^{+0.10}_{-0.00}$	$9.88^{+0.21}_{-0.04}$	$0.32^{+0.11}_{-0.05}$	1.01
1611	26.41	2.15	$0.00^{+0.00}_{-0.04}$	$9.05^{+0.10}_{-0.00}$	$9.43^{+0.11}_{-0.04}$	$0.09^{+0.11}_{-0.15}$	0.88
1621	24.88	1.30	$0.10^{+0.10}_{-0.04}$	$8.64^{+0.10}_{-0.31}$	$9.30^{+0.04}_{-0.13}$	$0.61^{+0.40}_{-0.17}$	3.17
1654	25.27	2.10	$0.28^{+0.06}_{-0.02}$	$8.64^{+0.10}_{-0.21}$	$10.17^{+0.08}_{-0.09}$	$1.48^{+0.20}_{-0.08}$	7.61
1662	26.19	2.40	$0.02^{+0.02}_{-0.04}$	$8.22^{+0.11}_{-0.10}$	$8.59^{+0.12}_{-0.12}$	$0.38^{+0.18}_{-0.18}$	0.54
1700	27.17	1.45	$0.00^{+0.00}_{-0.00}$	$8.64^{+0.00}_{-0.10}$	$8.22^{+0.03}_{-0.15}$	$-0.47^{+0.03}_{-0.06}$	12.12
1709	26.40	2.50	$0.00^{+0.00}_{-0.02}$	$8.74^{+0.10}_{-0.00}$	$9.04^{+0.06}_{-0.07}$	$0.21^{+0.02}_{-0.08}$	4.91
1734	27.50	2.70	$0.00^{+0.00}_{-0.00}$	$9.05^{+0.00}_{-0.10}$	$9.15^{+0.03}_{-0.23}$	$-0.19^{+0.03}_{-0.02}$	137.18
1747	27.05	2.40	$0.06^{+0.06}_{-0.14}$	$8.32^{+1.04}_{-0.31}$	$8.49^{+0.79}_{-0.24}$	$0.17^{+0.24}_{-0.40}$	0.45
1777	25.01	2.75	$0.08^{+0.04}_{-0.04}$	$8.84^{+0.21}_{-0.21}$	$10.11^{+0.16}_{-0.25}$	$1.13^{+0.11}_{-0.13}$	1.46
1903	26.74	2.65	$0.46^{+0.12}_{-0.02}$	$6.24^{+1.14}_{-0.62}$	$9.03^{+0.36}_{-0.36}$	$2.80^{+0.99}_{-0.52}$	0.32
2006	26.89	1.95	$0.16^{+0.04}_{-0.06}$	$8.74^{+0.21}_{-0.10}$	$9.19^{+0.22}_{-0.20}$	$0.36^{+0.25}_{-0.27}$	23.46
2060	27.76	2.90	$0.08^{+0.04}_{-0.12}$	$8.53^{+1.14}_{-0.21}$	$8.65^{+0.62}_{-0.18}$	$0.09^{+0.17}_{-0.57}$	3.82

Table B.5: Best-fit parameters for Sawicki et al. (2007) HDF catalog, -700 Myr e-folding exponential SFR.

ID	$\mathcal{R}_{VI}$	$z_{phot}$	$E(B-V)$	$\log(\text{Age}/\text{yr})$	$\log(M_*/M_\odot)$	$\log(\text{SFR}/(M_\odot/\text{yr}))$	$\chi^2$
2066	27.12	2.75	$0.00^{+0.00}_{-0.00}$	$8.95^{+0.10}_{-0.00}$	$9.12^{+0.18}_{-0.00}$	$-0.03^{+0.02}_{-0.00}$	45.08
2073	27.80	2.05	$0.00^{+0.00}_{-0.00}$	$8.64^{+0.10}_{-0.00}$	$8.22^{+0.16}_{-0.02}$	$-0.47^{+0.04}_{-0.02}$	15.68
2079	26.98	2.45	$0.12^{+0.22}_{-0.04}$	$8.64^{+0.21}_{-0.10}$	$9.09^{+0.16}_{-0.06}$	$0.40^{+0.10}_{-0.17}$	9.43
2095	26.55	2.65	$0.00^{+0.00}_{-0.04}$	$8.64^{+0.10}_{-0.10}$	$8.88^{+0.13}_{-0.14}$	$0.19^{+0.02}_{-0.17}$	14.12
2106	25.88	2.60	$0.00^{+0.00}_{-0.04}$	$8.74^{+0.10}_{-0.10}$	$9.28^{+0.07}_{-0.17}$	$0.45^{+0.03}_{-0.12}$	2.28
2111	26.57	2.50	$0.00^{+0.00}_{-0.00}$	$8.84^{+0.00}_{-0.00}$	$9.15^{+0.02}_{-0.00}$	$0.17^{+0.02}_{-0.00}$	107.16
2169	27.89	2.70	$0.10^{+0.10}_{-0.10}$	$6.76^{+1.66}_{-0.58}$	$7.21^{+0.16}_{-0.82}$	$0.45^{+0.78}_{-0.39}$	31.38
2171	25.55	2.65	$0.00^{+0.00}_{-0.00}$	$8.74^{+0.00}_{-0.00}$	$9.42^{+0.05}_{-0.02}$	$0.59^{+0.05}_{-0.02}$	11.30
2188	27.32	2.20	$0.00^{+0.00}_{-0.00}$	$8.64^{+0.00}_{-0.00}$	$8.47^{+0.04}_{-0.07}$	$-0.22^{+0.04}_{-0.07}$	43.15
2206	26.56	2.50	$0.00^{+0.00}_{-0.00}$	$8.74^{+0.00}_{-0.10}$	$8.98^{+0.00}_{-0.14}$	$0.15^{+0.02}_{-0.00}$	63.78
2208	26.58	2.50	$0.08^{+0.06}_{-0.02}$	$8.74^{+0.10}_{-0.21}$	$9.26^{+0.08}_{-0.23}$	$0.43^{+0.18}_{-0.08}$	1.71
2221	27.94	1.70	$0.14^{+0.14}_{-0.18}$	$7.39^{+2.29}_{-1.04}$	$7.36^{+0.47}_{-0.71}$	$-0.00^{+0.40}_{-2.83}$	0.09
2228	25.75	1.80	$0.28^{+0.06}_{-0.02}$	$8.64^{+0.00}_{-0.21}$	$9.82^{+0.18}_{-0.13}$	$1.13^{+0.25}_{-0.14}$	11.70
2255	27.25	1.80	$0.00^{+0.00}_{-0.09}$	$9.16^{+0.00}_{-0.00}$	$9.16^{+0.10}_{-0.00}$	$-0.39^{+0.00}_{-0.00}$	35.59
2260	26.10	2.90	$0.14^{+0.02}_{-0.02}$	$8.84^{+0.10}_{-0.10}$	$9.94^{+0.07}_{-0.08}$	$0.96^{+0.09}_{-0.08}$	6.20
2282	24.63	2.60	$0.03^{+0.02}_{-0.00}$	$8.74^{+0.00}_{-0.10}$	$9.85^{+0.04}_{-0.19}$	$1.03^{+0.08}_{-0.03}$	1.73
2300	26.66	2.75	$0.12^{+0.06}_{-0.04}$	$8.74^{+0.21}_{-0.21}$	$9.45^{+0.19}_{-0.19}$	$0.62^{+0.18}_{-0.13}$	1.04
2306	25.42	2.70	$0.10^{+0.04}_{-0.04}$	$8.74^{+0.21}_{-0.21}$	$9.86^{+0.18}_{-0.21}$	$1.03^{+0.13}_{-0.15}$	0.54
2342	27.85	1.85	$0.00^{+0.00}_{-0.02}$	$9.05^{+0.00}_{-0.10}$	$8.72^{+0.05}_{-0.06}$	$-0.62^{+0.05}_{-0.29}$	17.82
2366	26.44	2.30	$0.26^{+0.00}_{-0.04}$	$9.05^{+0.10}_{-0.10}$	$10.36^{+0.16}_{-0.16}$	$1.03^{+0.06}_{-0.18}$	8.42
2404	27.76	2.00	$0.10^{+0.02}_{-0.04}$	$8.64^{+0.21}_{-0.10}$	$8.54^{+0.30}_{-0.15}$	$-0.15^{+0.20}_{-0.21}$	5.23
2409	26.90	2.20	$0.08^{+0.04}_{-0.02}$	$8.95^{+0.10}_{-0.10}$	$9.34^{+0.13}_{-0.17}$	$0.19^{+0.20}_{-0.06}$	0.65
2490	27.03	2.50	$0.00^{+0.00}_{-0.02}$	$8.84^{+0.00}_{-0.00}$	$8.96^{+0.04}_{-0.00}$	$-0.02^{+0.04}_{-0.10}$	69.66
2501	25.98	2.45	$0.04^{+0.02}_{-0.04}$	$8.74^{+0.10}_{-0.10}$	$9.34^{+0.09}_{-0.19}$	$0.51^{+0.10}_{-0.13}$	2.40
2560	26.37	2.05	$0.12^{+0.02}_{-0.04}$	$8.64^{+0.10}_{-0.10}$	$9.19^{+0.19}_{-0.15}$	$0.50^{+0.15}_{-0.18}$	0.64
2616	25.58	2.85	$0.14^{+0.02}_{-0.06}$	$8.74^{+0.31}_{-0.10}$	$10.00^{+0.21}_{-0.09}$	$1.17^{+0.09}_{-0.21}$	1.27
2625	26.65	2.25	$0.12^{+0.04}_{-0.08}$	$8.22^{+0.62}_{-0.21}$	$8.71^{+0.37}_{-0.14}$	$0.50^{+0.15}_{-0.31}$	0.76
2702	25.73	2.70	$0.06^{+0.04}_{-0.02}$	$8.74^{+0.10}_{-0.21}$	$9.58^{+0.09}_{-0.23}$	$0.75^{+0.13}_{-0.10}$	3.07
2710	25.05	2.40	$0.06^{+0.04}_{-0.00}$	$8.84^{+0.00}_{-0.10}$	$9.91^{+0.08}_{-0.08}$	$0.93^{+0.17}_{-0.04}$	5.68
2808	27.75	2.70	$0.28^{+0.12}_{-0.10}$	$6.66^{+1.56}_{-0.44}$	$7.92^{+0.39}_{-0.39}$	$1.26^{+0.80}_{-0.25}$	5.83
2832	26.69	2.90	$0.00^{+0.00}_{-0.02}$	$9.05^{+0.04}_{-0.00}$	$9.52^{+0.04}_{-0.05}$	$0.18^{+0.04}_{-0.05}$	40.00
2835	27.68	2.90	$0.00^{+0.00}_{-0.04}$	$8.95^{+0.21}_{-0.10}$	$8.95^{+0.19}_{-0.18}$	$-0.20^{+0.02}_{-0.13}$	7.80
2848	27.80	2.05	$0.00^{+0.00}_{-0.00}$	$8.53^{+0.21}_{-0.10}$	$8.10^{+0.56}_{-0.18}$	$-0.45^{+0.32}_{-0.06}$	21.17
2849	25.59	2.80	$0.06^{+0.02}_{-0.02}$	$8.95^{+0.10}_{-0.10}$	$9.98^{+0.14}_{-0.15}$	$0.83^{+0.09}_{-0.06}$	2.39
2853	25.22	2.50	$0.06^{+0.04}_{-0.02}$	$8.64^{+0.10}_{-0.00}$	$9.59^{+0.10}_{-0.13}$	$0.90^{+0.12}_{-0.08}$	1.45
2876	25.81	2.40	$0.00^{+0.00}_{-0.00}$	$8.53^{+0.00}_{-0.00}$	$9.01^{+0.03}_{-0.03}$	$0.45^{+0.03}_{-0.03}$	18.22
2894	27.17	2.80	$0.00^{+0.00}_{-0.10}$	$8.74^{+0.42}_{-0.10}$	$8.82^{+0.36}_{-0.16}$	$-0.01^{+0.05}_{-0.22}$	4.62
2967	26.80	1.65	$0.12^{+0.04}_{-0.04}$	$8.84^{+0.10}_{-0.10}$	$9.07^{+0.13}_{-0.14}$	$0.09^{+0.17}_{-0.25}$	13.05
3025	26.97	2.90	$0.02^{+0.02}_{-0.04}$	$8.64^{+0.21}_{-0.10}$	$8.85^{+0.12}_{-0.13}$	$0.17^{+0.09}_{-0.13}$	4.88
3036	27.56	2.70	$0.00^{+0.00}_{-0.00}$	$8.74^{+0.10}_{-0.00}$	$8.63^{+0.15}_{-0.02}$	$-0.20^{+0.03}_{-0.02}$	7.32
3042	27.21	1.25	$0.24^{+0.24}_{-0.04}$	$6.87^{+0.10}_{-0.56}$	$7.39^{+0.14}_{-0.41}$	$0.53^{+1.26}_{-0.11}$	10.62
3048	24.74	2.20	$0.16^{+0.04}_{-0.02}$	$8.64^{+0.03}_{-0.10}$	$10.03^{+0.07}_{-0.12}$	$1.34^{+0.12}_{-0.13}$	1.76
3083	25.65	2.05	$0.12^{+0.04}_{-0.02}$	$8.74^{+0.10}_{-0.10}$	$9.60^{+0.11}_{-0.05}$	$0.77^{+0.19}_{-0.11}$	3.85
3087	26.46	2.80	$0.06^{+0.06}_{-0.06}$	$8.22^{+0.62}_{-0.42}$	$8.74^{+0.33}_{-0.25}$	$0.53^{+0.24}_{-0.31}$	1.41
3111	24.61	2.35	$0.00^{+0.00}_{-0.04}$	$8.74^{+0.10}_{-0.00}$	$9.72^{+0.07}_{-0.08}$	$0.89^{+0.04}_{-0.18}$	3.98
3115	25.41	2.10	$0.20^{+0.04}_{-0.02}$	$8.32^{+0.21}_{-0.21}$	$9.51^{+0.14}_{-0.11}$	$1.19^{+0.19}_{-0.11}$	13.38
3134	25.09	2.55	$0.12^{+0.06}_{-0.06}$	$8.74^{+0.10}_{-0.10}$	$10.02^{+0.16}_{-0.04}$	$1.19^{+0.11}_{-0.12}$	7.63
3176	25.86	2.30	$0.10^{+0.04}_{-0.04}$	$8.53^{+0.10}_{-0.10}$	$9.30^{+0.04}_{-0.15}$	$0.74^{+0.12}_{-0.11}$	7.99
3189	26.24	2.05	$0.00^{+0.00}_{-0.02}$	$8.84^{+0.10}_{-0.00}$	$9.10^{+0.07}_{-0.02}$	$0.12^{+0.04}_{-0.08}$	28.72
3201	27.16	1.55	$0.32^{+0.10}_{-0.06}$	$7.60^{+0.52}_{-0.73}$	$8.28^{+0.28}_{-0.57}$	$0.72^{+0.32}_{-0.34}$	3.84
3250	27.14	2.65	$0.02^{+0.02}_{-0.08}$	$8.22^{+0.62}_{-0.21}$	$8.27^{+0.35}_{-0.16}$	$0.07^{+0.12}_{-0.31}$	0.88
3255	26.74	2.90	$0.04^{+0.00}_{-0.02}$	$8.95^{+0.10}_{-0.00}$	$9.44^{+0.08}_{-0.00}$	$0.29^{+0.00}_{-0.09}$	58.64
3256	26.90	2.05	$0.36^{+0.08}_{-0.08}$	$6.56^{+0.16}_{-0.94}$	$8.29^{+0.23}_{-0.29}$	$1.74^{+0.82}_{-0.24}$	0.21
3263	27.57	2.05	$0.24^{+0.04}_{-0.02}$	$8.53^{+0.10}_{-0.21}$	$8.97^{+0.10}_{-0.16}$	$0.41^{+0.16}_{-0.14}$	11.23
3264	23.66	2.35	$0.20^{+0.04}_{-0.04}$	$8.43^{+0.21}_{-0.21}$	$10.44^{+0.13}_{-0.09}$	$2.00^{+0.17}_{-0.15}$	7.82
3269	26.81	2.65	$0.00^{+0.00}_{-0.06}$	$8.53^{+0.31}_{-0.00}$	$8.66^{+0.21}_{-0.04}$	$0.10^{+0.05}_{-0.21}$	0.08
3373	24.31	2.10	$0.18^{+0.04}_{-0.06}$	$8.32^{+0.42}_{-0.10}$	$9.89^{+0.34}_{-0.10}$	$1.57^{+0.16}_{-0.25}$	3.81